REGIOSELECTIVE FLUORINATION AND AMINATION METHODOLOGIES USING SELECTFLUOR

by
Joseph N. Capilato

A dissertation submitted to Johns Hopkins University in conformity with the requirements for the degree of Doctor of Philosophy

Baltimore, Maryland

July 2021

Abstract

Organofluorine compounds have become ubiquitous over the last century due to their advantageous properties in pharmaceuticals, materials, refrigerants, agrochemicals and other areas. Recently, the synthesis of fluorine-containing compounds has been facilitated by the commercialization of products such as Selectfluor and NFSI. These reagents can participate in both one- and two-electron fluorination chemistry (analogous to fluorine gas, albeit with reduced reactivity). While numerous fluorination methods have been reported using N−F reagents such as these, most share a common problem—regioselectivity. For instance, most radical fluorination methods rely on activated C−H bonds, such as benzylic or allylic C−H bonds, to demonstrate site-selectivity. On the other hand, in the case of nonactivated aliphatic C−H bonds, radical fluorination is seldom used due to the lack of selectivity. Our group has begun to investigate this issue over the last few years and we have identified several viable solutions. In this dissertation, regioselective fluorination and amination methodologies are investigated using commercially available Selectfluor reagent. A variety of directing groups are shown to interact with Selectfluor, including carbonyls, sulfonyls, and ketals—allowing site-selective fluorination of complex substrates. New amination reactions are also demonstrated with the multifaceted Selectfluor reagent, including aminofluorination of unactivated alkenes and arene C–H amination of alkoxybenzenes. Reaction mechanisms are explored using computational chemistry, spectroscopic techniques and a variety of other methods. Future studies in our group aim to discover new directing groups in order to further expand the utility of these reactions.

Advisor: Professor Thomas Lectka

Reader: Professor Rebekka Klausen

Reader: Professor John Toscano

For my Family & Friends

Acknowledgments

The research described in this dissertation would not have been possible without the countless people who have helped me throughout this journey. I first need to acknowledge Professor Thomas Lectka, who welcomed me into his group in 2016 despite having a full lab at the time and already agreeing to take three other students that year. Over the last five years, Prof. Lectka has taught me innumerable important lessons and his continual guidance has enabled me to grow as a scientist and a person. It was inspiring to witness his passion for chemistry and his knack for conceiving and executing interesting projects. I am also grateful for the level of creative freedom he gave me in my research, all the while keeping me focused.

Beyond my advisor, I would also like to thank my other committee mentors, Professors Rebekka Klausen and John Toscano. Not only did they provide useful comments during my department and graduate board oral examinations, but they also offered helpful advice throughout my time at JHU. I am also appreciative of the two external members of my committee—Dana Ferraris and Laurence Carroll—for their time and valuable comments.

Next, I would like to acknowledge all my colleagues in the Lectka lab who I have worked with over the years. When I joined the group in 2016, the senior group members Desta Bume, Max Holl, Liangyu Guan and Cody Pitts were immensely helpful to myself and the other new graduate students. They passed on information that was vital to my success in the group, including proper bench chemistry technique, tips for writing manuscripts and the publication process, computational chemistry guidelines, and many other lessons. The three graduate students who joined the group in the same year as me,

Stefan Harry, Mohammad Kazim and Fereshte Ghorbani, were also essential to my research achievements at JHU. They were always available to teach, talk or listen whenever needed, and it has been a pleasure to work alongside them. In addition to the graduate student lab members, I have also worked with numerous undergraduate students during my time in the Lectka group. I am fortunate to have had the opportunity to train and work with Louis Hoffenberg, Rayyan Jokhai and Wei Hao Lee. Not only did they contribute to several projects, but they also provided me with a chance to mentor younger scientists, which is an experience that I will always cherish.

I also must acknowledge everyone who has helped me in the chemistry department at JHU. In particular, Drs. Joel Tang, Ananya Majumdar and Jonathan Catazaro (NMR), Dr. Maxime Siegler (crystallography) and Dr. Phil Mortimer (mass spectrometry) assisted me with data acquisition on many occasions. Boris Steinberg and numerous administrative staff (Lauren McGhee, John Kidwell, Meghan Carter, Joe Russell) were also helpful during my time at JHU. Other chemistry labs on the Homewood campus, especially those in NCB such as the Tovar, Greenberg and Goldberg groups, facilitated my research on numerous occasions by generously providing chemicals.

Before I arrived at JHU, I got my start in research as an undergraduate and graduate student working with Professor Lark Perez at Rowan University. I am very thankful to Prof. Perez for taking me into his group and the many lessons he taught me about organic chemistry and medicinal chemistry. His ability to make chemistry research exciting and fun is what ultimately motivated me to pursue a PhD in chemistry. I am also appreciative of my high school teachers—namely Lawrence Frockowiak (biology) and Daria Hall (chemistry)—for getting me interested in science before college. My positive experience

in their class undoubtedly played a role in the decision to study biochemistry during my bachelor's degree.

Finally, I would like to acknowledge the continuous support I have received from my family and friends during the course of my graduate education. In particular, my mother Patricia and my father Joseph have been vital to every part of this journey, and I could not have done this without their help. The rest of my family (and several family friends) were also supportive of me during this time, and have thus aided this work. I am thankful for my friends both in Baltimore and back home, including Josh, Joe, Nick and Nate who visited me on several occasions during my time here. To all my family and friends—thank you for your constant support—this work is dedicated to you.

Publications Drawing Upon This Dissertation

1. Bume, D. D.; Pitts, C. R.; Ghorbani, F.; Harry, S. A.; **Capilato, J. N.**; Siegler, M. A.; Lectka, T. "Ketones as Directing Groups in Photocatalytic sp^3 C-H Fluorination" *Chem. Sci.* **2017**, *8*, 6918-6923.

2. **Capilato, J. N.**; Bume, D. D.; Lee, W. H.; Hoffenberg, L. E. S.; Jokhai, R. T.; Lectka, T. "Fluorofunctionalization of C=C Bonds with Selectfluor: Synthesis of β-Fluoropiperazines through a Substrate-Guided Reactivity Switch" *J. Org. Chem.* **2018***, 83,* 14234–14244.

3. **Capilato, J. N.**; Pitts, C. R.; Rowshanpour, R.; Dudding, T.; Lectka, T. "Site-Selective Photochemical Fluorination of Ketals: Unanticipated Outcomes in Selectivity and Stability" *J. Org. Chem.* **2020**, *85*, 2855-2864.

4. Ghorbani, F.; Harry, S. A.; **Capilato, J. N.**; Pitts, C.; Joram, J.; Peters, G.; Tovar, J.; Smajlagic, I.; Siegler, M.; Dudding, T.; Lectka, T. "Carbonyl-Directed Aliphatic Fluorination: A Special Type of Hydrogen Atom Transfer Beats Out Norrish II" *J. Am. Chem. Soc.* **2020**, *142*, 14710–14724.

5. **Capilato, J. N.**; Siegler, M.; Rowshanpour, R.; Dudding, T.; Lectka, T. "Cooperative Noncovalent Interactions Lead to a Highly Diastereoselective Sulfonyl-Directed

Fluorination of Steroidal α,β-Unsaturated Hydrazones" *J. Org. Chem.* **2021**, *86*, 1300–1307.

6. **Capilato, J. N.**; Lectka, T. "Arene Amination Instead of Fluorination: Substitution Pattern Governs the Reactivity of Dialkoxybenzenes with Selectfluor" *J. Org. Chem*. **2021**, *86*, 5771–5777.

7. **Capilato, J. N.**; Siegler, M.; Lectka, T. "Spectroscopic and Crystallographic Characterization of the N^+–C–H···O Interaction" *manuscript in preparation*

Table of Contents

Chapter 1: Introduction

Chapter 2: Ketones as Directing Groups in Photocatalytic sp^3 C–H Fluorination

Chapter 3: Aminofluorination of Unactivated Alkenes and Fluoro-rearrangement of Activated Alkenes

List of Tables

List of Figures

List of Schemes

List of Abbreviations

Å	Angstroms
Ac	acetyl
Ac_2O	acetic anhydride
AcOH	acetic acid
$AgNO_3$	silver nitrate
BDE	bond dissociation energy
BEt_3	triethylborane
BF_4	tetrafluoroborate
Bz	benzoyl
Cbz	carboxybenzyl
$CDCl_3$	deuterated chloroform
CFL	compact fluorescent lamp
CH_2Cl_2	dichloromethane
CPET	concerted proton-coupled electron transfer
$CuBr_2$	copper (ii) bromide
D_2	deuterium gas
DABCO	diazabicyclooctane
DAST	diethylaminosulfur trifluoride
DFT	density functional theory

DHEA	dehydroepiandrosterone
DI	deionized
DIPEA	diisopropylethylamine
DMAP	*N*,*N*-dimethylaminopyridine
EAS	electrophilic aromatic substitution
equiv.	equivalents
ESI	electrospray ionization
ET	electron transfer
ET/PT	electron transfer/proton transfer
Et_2O	diethylether
Et_3N	triethylamine
EtOAc	ethyl acetate
FGI	functional group interconversion
g	gram
GLP	G9a-like protein
h	hour(s)
H_2O	water
H_2SO_4	sulfuric acid
HAT	hydrogen atom transfer
HCl	hydrogen chloride

HNO_3	nitric acid
HPLC	high-performance liquid chromatography
HRMS	high-resolution mass spectrometry
hν	light
Hz	Hertz
IRC	intrinsic reaction coordinate
K_2CO_3	potassium carbonate
kcal	kilocalorie
KIE	kinetic isotope effect
kJ/mol	kilojoule per mole
KOH	potassium hydroxide
LED	light-emitting diode
Me	methyl
MeCN	acetonitrile
MeOH	methanol
MEP	molecular electrostatic potential
$MgSO_4$	magnesium sulfate
MHz	megahertz
mL	milliliter
mmol	millimole(s)

MS-CPET	multisite concerted proton-coupled electron transfer
$Na_2S_2O_3$	sodium thiosulfate
Na_2SO_4	sodium sulfate
$NaBH_4$	sodium borohydride
$NaHCO_3$	sodium bicarbonate
NaOH	sodium hydroxide
NBO	natural bond order
NFSI	*N*-fluorobenzenesulfonimide
NHS	*N*-hydroxysuccinimide
nm	nanometer
NMR	nuclear magnetic resonance
OEt	ethoxy
OMe	methoxy
ox.	oxidation
p-TsOH	para-toluenesulfonic acid
PCET	proton-coupled electron transfer
Pd/C	palladium on carbon
Ph	phenyl
PhCOF	benzoyl fluoride
PPh_3	triphenylphosphine

PT	proton transfer
rt	room temperature
SET	single electron transfer
SF	Selectfluor
SiO_2	silicone dioxide
S_N1	unimolecular nucleophilic substitution
S_N2	bimolecular nucleophilic substitution
SRD	Selectfluor radical dication
THF	tetrahydrofuran
TMS	tetramethylsilane
TMSCl	trimethylsilyl chloride
TS	transition state
TsCl	tosyl chloride
UV	ultraviolet
UV-Vis	ultraviolet-visible light
V	volts

Chapter 1

Introduction

1.1 Development of Radical Fluorination Methodologies in the Lectka Lab.

Despite a growing list of applications for fluorine-containing organic molecules, synthetic fluorination methodologies still have a number of issues to address. While in recent years reactivity has been greatly improved through the discovery and commercialization of new fluorination reagents, the issue of selectivity remains a problem that discourages widespread use of this fundamental reaction.[1] Our laboratory has contributed several practical fluorination methods throughout the past decade, focusing on Selectfluor as our preferred fluorination reagent. For example, some of our first work in this area involved metal-catalyzed radical fluorinations, employing both copper and iron catalysts.[2] Although these reactions were indeed useful and represented an improved fluorination procedure from existing work, the clear limitation of these methods was regioselectivity. Accordingly, the substrate scope was generally limited to symmetrical molecules and compounds that contained activated C–H bonds (such as benzylic or allylic C–H bonds). Shortly after disclosing these metal-catalyzed fluorinations, we explored photochemical means to catalyze an analogous metal-free reaction. Our group contributed a few methods to this area,[3] which had similarly high efficiency as the metal-catalyzed reactions, though regioselectivity remained an unsolved problem.

More recently, our group has shifted focus towards addressing this issue involving fluorination regioselectivity, and we have added several innovative methods to the literature. Two interesting and related examples involve the photochemical ring opening

of cyclopropanols and aryl cyclopropanes – both of which result in a site-selective fluorination but produce fundamentally different products.[4] After these works, we found a more practical approach towards regioselective fluorination that employs a directing group strategy. Utilizing rigid polycyclic compounds (such as steroids and other terpenoids) our group demonstrated that the enone carbonyl group can direct fluorination on complex substrates where regioselectivity would otherwise be problematic.[5] This surprising result led us to investigate carbonyl groups other than enones, and we soon learned that ketones can also act as directing groups in the reaction, albeit under modified conditions.[6]

1.2 Arrangement of Chapters.

The subsequent chapters of this dissertation consist of the author's previously published research papers in chronological order. The last chapter, "Experimental Details," contains the supporting information for these publications.

1.3 Brief Summary.

When I joined Prof. Lectka's research group in 2016, they had recently discovered and published a novel enone-directed aliphatic fluorination of steroids. The next logical step was to explore other directing groups in the reaction, starting with other types of carbonyls. Together with six coauthors, I contributed to the expansion of this method to accommodate ketone carbonyl groups (discussed in Chapter 2). Importantly, the success of this chemistry required a modified approach; we employed a visible-light protocol, in contrast to the harsher UV-light conditions of the enone-directed fluorination. In Chapter

3, Selectfluor is utilized for a fundamentally different transformation—an amination, or more specifically, an aminofluorination of alkenes. Next, Chapter 4 details the serendipitous discovery of a regioselective sp^3 fluorination of structurally complex acetonides. In Chapter 5, using a variety of techniques we investigated the reaction mechanism for carbonyl-directed fluorination with Selectfluor. Significantly, we found that our initial mechanistic hypothesis was incorrect, and instead a coordinated hydrogen atom transfer was involved in the reaction. We further explored and expanded upon these noncovalent interactions in Chapter 6, where a sulfonyl-directed stereoselective fluorination is discussed. In Chapter 7, a regioselective arene C–H amination of alkoxybenzenes with Selectfluor is presented. Lastly, nonclassical N^+–C–H hydrogen bond interactions are examined in Chapter 8, with relevance to Selectfluor reactivity. Moving forward, our laboratory aims to further expand this chemistry via the discovery of novel directing groups and application towards diverse functionalizations.

1.4 References.

[1] Campbell, M.; Ritter, T. Late-Stage Fluorination: From Fundamentals to Application. *Org. Process Res. Dev.*, 2014, **18**, 474-480.

[2] (a) Bloom, S.; Pitts, C. R.; Miller, D.; Haselton, N.; Holl, M. G.; Urheim, E.; Lectka, T. A Polycomponent Metal-Catalyzed Aliphatic, Allylic, and Benzylic Fluorination. *Angew. Chem. Int. Ed.* **2012**, *51*, 10580-10583; (b) Bloom, S.; Pitts, C. R.; Woltornist, R.; Griswold, A.; Holl, M. G.; Lectka, T. Iron(II)-Catalyzed Benzylic Fluorination. *Org. Lett.* **2013**, *15*, 1722-1724; (c) Bloom, S.; Sharber, S. A.; Holl, M. G.; Knippel, J. L.; Lectka, T. Metal-Catalyzed Benzylic Fluorination as a Synthetic Equivalent to 1,4-Conjugate Addition of Fluoride. *J. Org. Chem.* **2013**, *78*, 11082-11086.

[3] (a) Bloom, S.; Knippel, J. L.; Lectka, T. A Photocatalyzed Aliphatic Fluorination. *Chem. Sci.* **2014**, *5*, 1175-1178; (b) Bloom, S.; McCann, M.; Lectka, T. Photocatalyzed Benzylic Fluorination: Shedding "Light" on the Involvement of Electron Transfer. *Org. Lett.* **2014**, *16*, 6338-6341; (c) Bume, D. D.; Pitts, C. R.; Jokhai, R. T.; Lectka, T. Direct, Visible Light-Sensitized Benzylic C-H Fluorination of Peptides using Dibenzosuberenone: Selectivity for Phenylalanine-Like-Residues. *Tetrahedron.* **2016**, *72*, 6031-6036.

[4] (a) Bloom, S.; Bume, D. D.; Pitts, C. R.; Lectka, T. Site-Selective Approach to β-Fluorination: Photocatalyzed Ring Opening of Cyclopropanols. *Chem. Eur. J.* **2015**, *21*, 8060-8063; (b) Pitts, C. R.; Ling, B.; Snyder, J. A.; Bragg, A. E.; Lectka, T. Aminofluorination of Cyclopropanes: A Multifold Approach through a Common, Catalytically Generated Intermediate. *J. Am. Chem. Soc.* **2016**, *138*, 6598-6609.

[5] Pitts, C. R.; Bume, D. D.; Harry, S. A.; Siegler, M. A.; Lectka, T. Multiple Enone-Directed Reactivity Modes Lead to the Selective Photochemical Fluorination of Polycyclic Terpenoid Derivatives. *J. Am. Chem. Soc.* **2017**, *139*, 2208-2211.

[6] Bume, D. D.; Pitts, C. R.; Ghorbani, F.; Harry, S. A.; Capilato, J. N.; Siegler, M. A.; Lectka, T. Ketones as Directing Groups in Photocatalytic sp^3 C-H Fluorination. *Chem. Sci.* **2017**, *8*, 6918-6923.

Chapter 2

Ketones as Directing Groups in Photocatalytic sp^3 C–H Fluorination

2.1 Introduction.

Innate selectivity in aliphatic C–H bond fluorination is achieved when most other C–H bonds are either sterically hindered or electronically deactivated. These factors allow very little control and versatility with respect to radical fluorination of intricate substrates, especially at sites near electron-withdrawing groups such as ketones. Consider the fluorination of 2-dodecanone (Figure 2.1). Using existing methods, the reaction will result

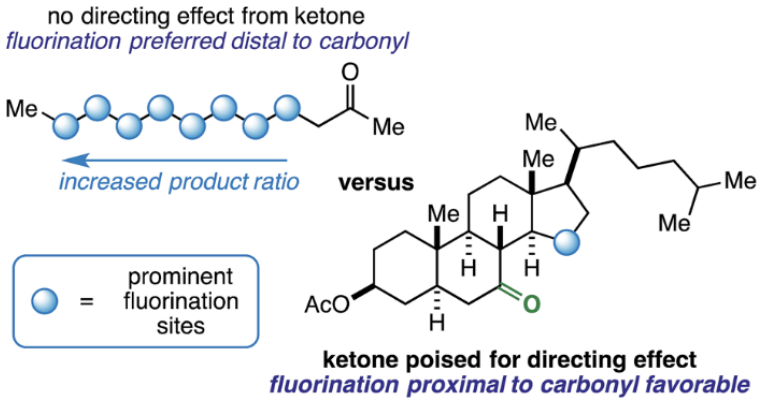

Figure 2.1. Linear aliphatic ketones versus rigid ketones poised for directing effect.

in a complicated mixture of fluorinated isomers with the relative product ratio increasing the farther the site is from the ketone – a well-documented manifestation of the "polar effect".[1] What if the desired site of fluorination is in proximity to the carbonyl (beyond the α-position accessible through enolate chemistry[2])? Under the right conditions, it is possible that the role of a ketone can be switched from a deactivator to an activator (i.e. directing

group) on rigid molecular skeletons where the ketone oxygen atom is properly poised.[3] Herein, we report the ability of ketones to function as directing groups under visible light-sensitized fluorination conditions, thus allowing greater control over regioselectivity in radical-based fluorination.

Considering the prominent role of fluorine in medicinal chemistry,[4] surprisingly few directed sp^3 C–H fluorination reactions have been developed beyond extant benzylic[5] or allylic fluorination methods.[6] Several aliphatic fluorination methods have been reported recently using transition metal catalysts,[7] radical initiators,[8] organic molecule catalysts,[9] and photosensitizers,[10] but these methods generally are geared toward small, symmetrical molecules or those with more activated or accessible C–H bonds. With respect to more biologically relevant molecules, selective β-fluorination of amino acid derivatives has been achieved through palladium catalysis using a chelating auxiliary ligand in a three-step ligand installation-fluorination-ligand removal process.[11-13] In our laboratory, we have recently developed an enone-directed photochemical fluorination of polycyclic terpenoid derivatives through direct 300 nm photolysis.[14] Unfortunately, under the same reaction conditions (using ultraviolet light), we found that ketones afford highly unselective fluorination and are not optimal directing groups; thus, a different approach was necessary.

We imagined that a milder procedure that employs visible light sensitization could allow the necessary balance between reactivity and selectivity to bring the more general and important concept of a ketone-directed reaction to fruition (Figure 2.2).

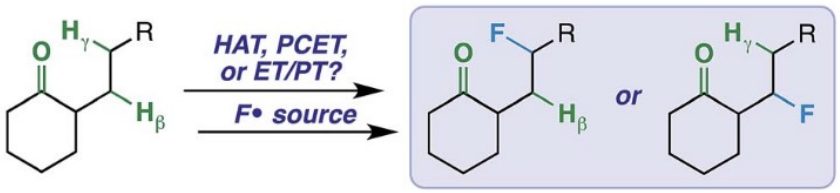

Figure 2.2 Possible designs for a ketone-directed aliphatic fluorination.

Accordingly, we report a visible light-sensitized ketone-directed C–H fluorination method using catalytic benzil (10 mol%), Selectfluor (as a putative atomic source of fluorine[15]), and cool white LED's.[16] Under these mild conditions, predictably selective β- or γ-fluorination can be achieved based on proximity of the hydrogen atom to the ketone. Both cyclic and exocyclic ketones are demonstrated to direct fluorination effectively on a variety of mono-, di-, tri-, and tetracyclic systems (such as steroidal ketones) in up to 85% yield. In accord with most excited-state ketone hydrogen atom transfer (HAT) chemistry, we found that structural rigidity plays an important role in attaining both desired reactivity and selectivity.[17] However, we report initial findings that an electron transfer mechanism (either concerted PCET or stepwise ET/PT) is more likely operative.

2.2 Reaction Optimization.

In order to establish an optimal photosensitizer, we began by screening a variety of compounds with a steroidal ketone test substrate (**1**) poised for γ-hydrogen atom transfer, Selectfluor, and a cool white LED source. Note that the LED source, with a sharp absorbance cut-off at ca. 400 nm by UV-vis analysis, was used instead of a compact fluorescent light (CFL) source, as the latter has a minor absorbance in the ultraviolet region.

Accordingly, we focused primarily on putative sensitizers that possess absorbances above 400 nm; this measure was taken to avoid undesirable reactivity from direct excitation of the substrate and/or fluorine source (corroborated by control experiments that show no reaction in the absence of a sensitizer or light). Although a number of compounds effected the fluorination reaction to form **2** (Table 2.1), we found the overall best results (82% yield) using a catalytic amount of benzil—a well-established triplet sensitizer that is commercially available, extremely cost-effective, and easy to handle.[18,19]

Table 2.1. Screening for visible light sensitizers

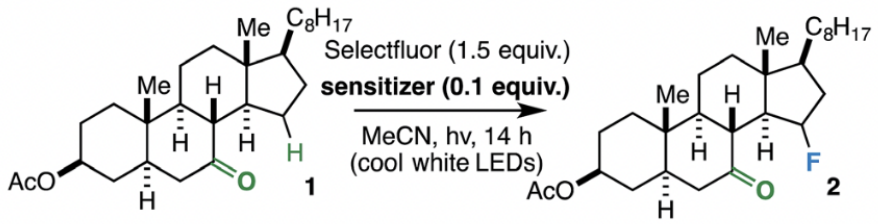

Entry	Sensitizer	^{19}F NMR yield (%)
1	—	0
2	Benzophenone	Trace
3	9-Fluorenone	Trace
4	Xanthone	Trace
5	9,10-Phenanthrenequinone	54
6	Benzil	73[a]
7	**Benzil**	**82**

[a] Reaction with 2.0 equiv. Selectfluor.

It is important to note that the use of other N–F reagents as putative sources of atomic fluorine, i.e. NFSI and N-fluoropyridinium tetrafluoroborate, do not result in the desired fluorinated product **2**. Although NFSI can also react with alkyl radicals, Selectfluor has

been shown to react at a faster rate and may be more likely to participate in electron transfer processes (discussed below).[15a,24] Additionally, no fluorination reaction was observed upon stirring all three components in the dark at room temperature or running the photochemical reaction under ambient air. Heating the reaction mixture to reflux in the dark also did not afford **2**, but trace unidentified tertiary fluorides were observed in the ^{19}F NMR spectrum of the crude reaction mixture. Finally, a slight decrease in product yield was observed when using Selectfluor in greater than 1.5 equiv. (Table 2.1, entry 6); this is a function of a decrease in selectivity, as greater quantities of other fluorinated isomers were observed by ^{19}F NMR analysis of the crude reaction mixture.

2.3 Exploration of Substrate Scope.

With an optimized protocol in hand, we focused our efforts on evaluation of the substrate scope with respect to a variety of common ring systems (Table 2.2). Menthone contains two tertiary carbon sites, but we observe strictly compound **3** in 55% yield under fluorination conditions, consistent with the notion of ketone involvement (note that although a putative 6-membered transition state from one of the methyl groups can be imagined, we did not observe primary fluorides). Compounds **4** and **5** represent examples of benzylic fluorination through putative 5-membered transition states. It is important to note that ethylbenzene does not undergo benzylic fluorination under the same conditions, suggesting the ketone plays a necessary role. In addition, compound **4** demonstrates reaction compatibility with a boron-based functional group (pinacolborane) that is used widely in cross-coupling applications.[20]

Table 2.2 Substrate scope: mono-, di-, tri-, and exocyclic ketone directing groups for fluorination of cyclic and exocyclic sp^3 C–H sites

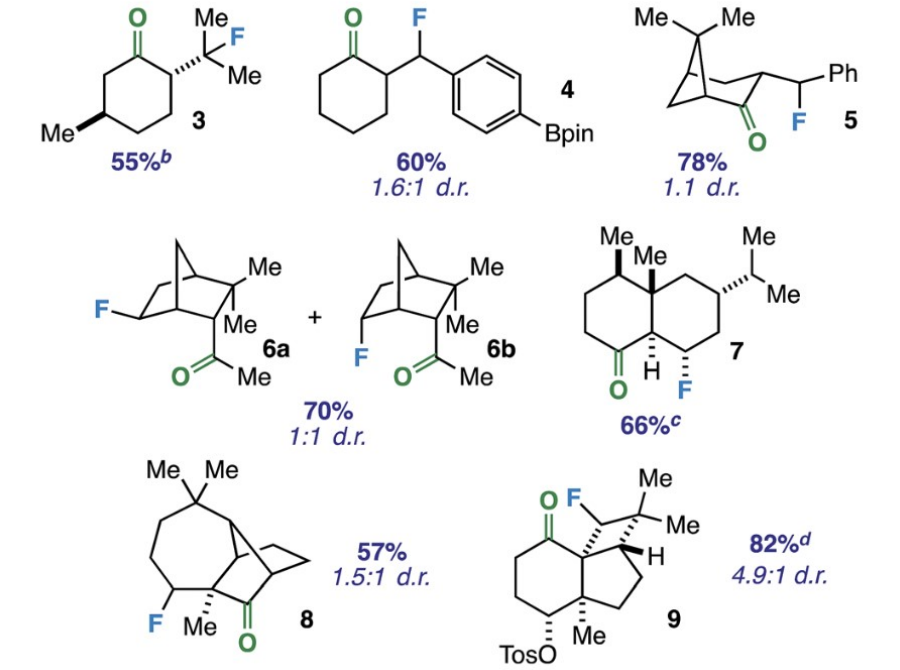

In these instances, the tertiary and benzylic C–H sites are arguably more activated toward fluorination. Thus, we examined substrates that should target specific secondary carbon sites. Employing an exocyclic ketone on a rigid norbornane scaffold, we were able to access a mixture of exo and endo fluorides (**6**) at the predicted site in 70% yield. Beyond bridged bicyclic systems, there are also opportunities for ketone- directed fluorination on certain decalone cores. For instance, compound **7** (derived from sesquiterpenoid valencene) was formed selectively in the presence of other tertiary carbon sites distal from the ketone. Subsequently, we examined directed fluorination on more complex tricyclic ring systems. For one, a longifolene-derived ketone provided selective fluorination of the most accessible carbon site on the cycloheptane ring (**8**). Remarkably, we were also able

to target a C–H bond on a strained cyclobutane ring to form fluorinated kobusone derivative **9**. What is more, this reaction proceeded smoothly in the presence of an oxidized sulfur-containing functional group (i.e. a tosylate).

Considering the prevalence and importance of biologically active steroidal ketones,[21] we surveyed the fluorination of ketones akin to cholesterol derivative **2** (Table 2.3).

Table 2.3 Substrate scope: steroidal ketone directing groups for predictable γ- or β-fluorination of sp^3 C–H sites

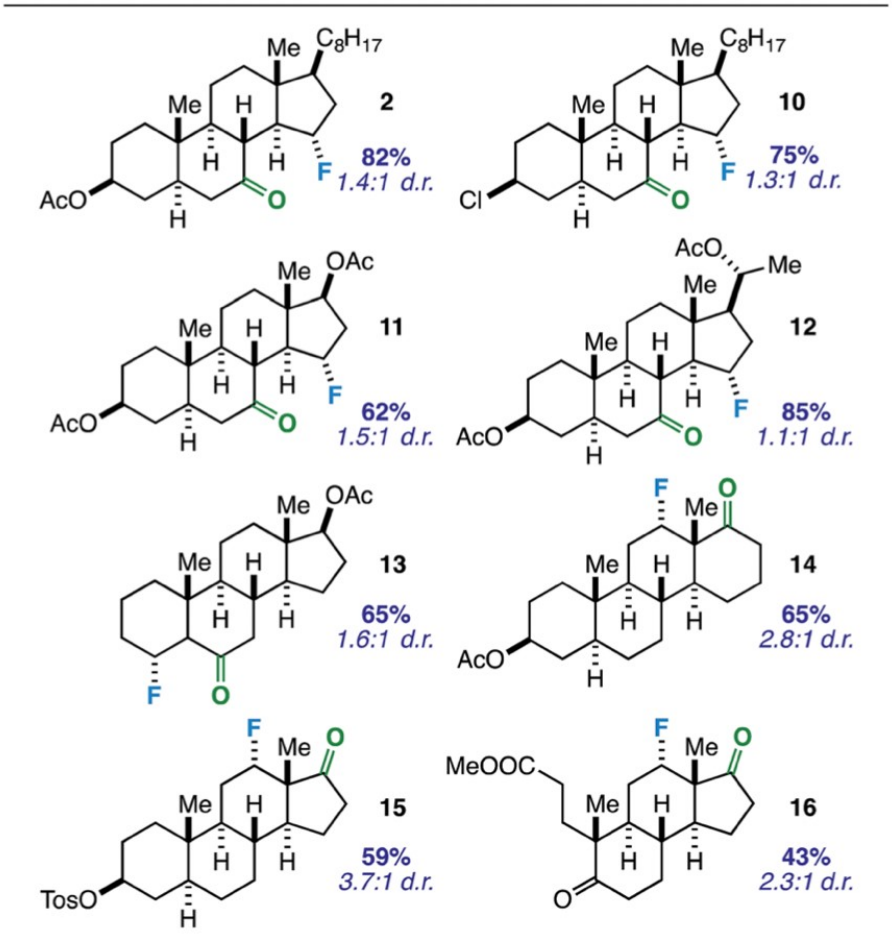

Compounds **10**–**12** represent cholesterol, testosterone, and progesterone derivatives with starting ketones at C7 also poised for C15 functionalization. Note that compound **10** also exhibits reaction tolerance of aliphatic chlorides. Selective g-fluorination was observed in each case (62–85% yield).

Subsequently, we applied the ketone-directed reaction to b-fluorination on the steroid core. Thus, a C6 steroidal ketone was found to fluorinate the C4 position through a putative 5- membered transition state to afford **13** in 65% yield. No evidence of degradation to the corresponding enone was observed following column chromatography on silica gel. In another instance, C12-fluorinated trans-androsterone derivative **14** (with an expanded D-ring) was also readily accessible. Recognizing that fluorinated trans-androsterone derivatives may be more desirable with the cyclopentane ring intact, we asked: will the cyclopentanone also access C12 fluorination through a 5-membered transition state? To our satisfaction, compound **15** was formed in 59% yield. We also examined a tricyclic secosteroid substrate (**16**) as another example of a cyclopentanone moiety directing fluorination to the adjacent cyclohexane ring.

Importantly, note that the virtue of the tetra- and tricyclic ring systems discussed thus far is their decreased conformational flexibility; this allows for selective, predictable fluorination in a somewhat paradoxical manner. That is, more complex polycyclic carbon frameworks, in general, promote selective C–H fluorination where it intuitively may inhibit it in other non-directed circumstances. Thus, this method appears to be best suited for late-stage fluorination of larger, more intricate structures.[22]

On another note, the ideal substrates for this reaction have a clear distinction over the preference for γ- vs. β-fluorination based on geometric constraints. However, how does the

reaction proceed when both 5- and 6-membered transition states are possible? Progesterone, with an acetyl group at C17, can act as a probe and also provide a real-world example of when this competitive fluorination could be of interest (i.e. to access different fluorinated bioactive steroids). Accordingly, we found that the free rotation of the s-bond between C17 and C20 allows fluorination of both C12 (17) and C16 (18) in a ratio of 1.0 : 3.1 (55% total yield, Scheme 2.1). Although the regioselectivity is modest, this may be an asset in a medicinal chemistry setting where multiple fluorinated regioisomers of similar steroids are desirable for biological testing.[23]

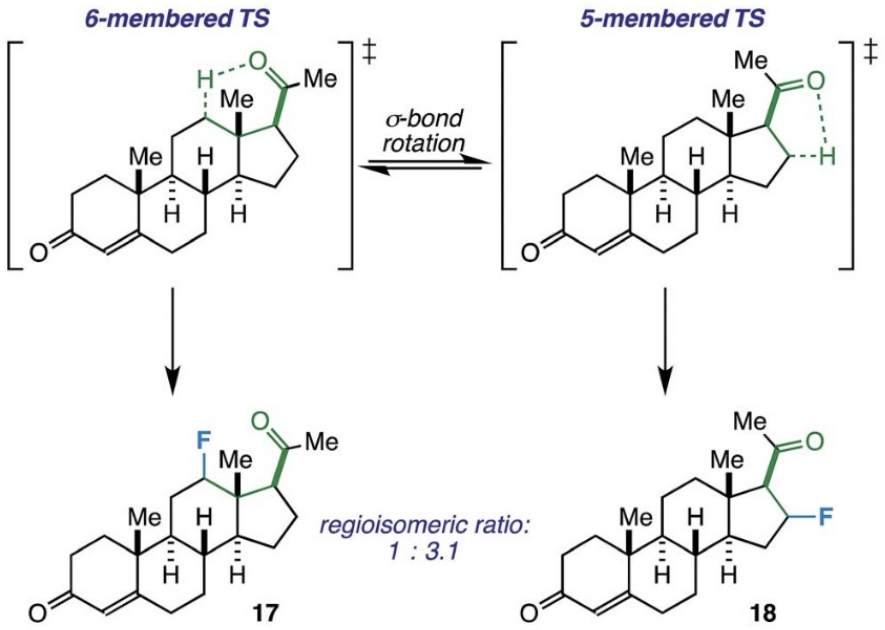

Scheme 2.1. Fluorinated progesterone product ratio from putative 5- vs. 6-membered transition states.

2.4 Mechanistic Studies.

At this point, we have demonstrated cyclic (5- and 6-membered rings) and exocyclic aliphatic ketones directing fluorination on either cyclic (4-, 5-, 6-, and 7-membered rings) or short, linear side-chain sites. How does the reaction hold up to linear aliphatic ketones? Using 2-heptanone as the substrate, we observed δ-, γ-, and β-fluorination in 2.3 : 1.3 : 1.0, respectively, in the ^{19}F NMR spectrum of the crude reaction mixture. This could indicate an indiscriminate radical chain mechanism instead of a directed reaction,[24,25] as it exhibits features of the so-called polar effect.[1] In order to expand on this result, we also ran the reaction with 2-decanone and 2-dodecanone. In each case, there was a large preference for fluorination at the penultimate carbon atom alongside multiple secondary fluoride isomers (Figure 2.1).

Thus, under the same reaction conditions, the rigid ketones afford selective β- or γ-fluorination and the conformationally flexible ketones do not. Perhaps the linear ketones (1) prefer intermolecular over intramolecular HAT and/or (2) promote cage escape of the N-centered radical derived from Selectfluor that is a key player in radical chain mechanisms.[24,25] Accordingly, we ran the reactions with the linear ketones under more dilute conditions to favor intramolecular HAT,[26] but observed the same product distributions by ^{19}F NMR. What is more, a HAT mechanism directed by a ketone would imply accessibility of the ketone triplet excited state. The reported triplet energy of benzil (53 kcal mol^{-1}),[27] which is the only chromophore present under our conditions, is not high enough to undergo triplet–triplet energy transfer with aliphatic ketones[28] (typically with triplet energies of 80 kcal mol^{-1}).[29] Therefore, the ketone triplet state should not be present

in any significant concentration, and a HAT mechanism seems unlikely for both flexible and rigid ketones.[30]

Conceivably, the benzil triplet state can promote the reaction instead by facilitating electron transfer from the substrate to Selectfluor;[31,32] this would result in formation of the well-established N-centered radical intermediate. As alternative ways to generate this intermediate, we subjected the linear ketones to our established copper(I)/Selectfluor[7a] and BEt_3/ Selectfluor[8] protocols and found nearly identical fluorinated product distributions in each case. Interestingly, when representative rigid cyclic ketones (e.g. starting ketones for compounds **2** and **11**) were also subjected to the BEt_3/Selectfluor protocol (in absence of light and a sensitizer), the same selectivity was observed as the visible light-sensitized reaction (Scheme 2.2). Thus, this putative N-centered radical intermediate is likely the key

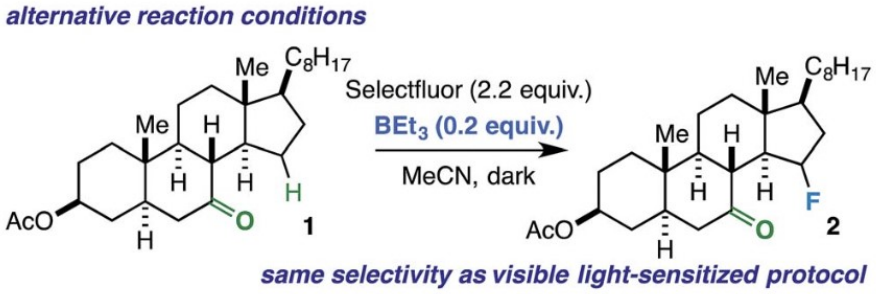

Scheme 2.2. Same selectivity observed using BEt_3/Selectfluor protocol as an alternative way to generate the N-centered radical intermediate from Selectfluor in the absence of light and benzil.

player in the mechanism for both flexible and rigid ketones. As this intermediate is known to be a powerful oxidant, it is possible that an electron transfer (ET) mechanism is operative whereby the ketone assists in proton transfer (PT) instead of HAT.[33] An electron transfer

mechanism is also consistent with our observation that the reaction is best suited for our relatively large substrates (with relatively low ionization potentials). Additionally, if the ketone is not properly poised to act as the intramolecular "base," then it is possible other reaction components could act as intermolecular bases (MeCN, the amine derived from Selectfluor, etc.), which can explain the loss of selectivity in conformationally flexible ketones versus rigid ketones. Lastly, at this time, it is unclear whether the mechanism is concerted (proton-coupled electron transfer, or PCET) or stepwise (electron transfer/proton transfer, or ET/PT)[34] and whether it involves a chain propagation or a closed cycle; we will explore these aspects in future studies.

2.5 Conclusion.

In summary, this visible light sensitization approach creates an opportunity to use ubiquitous ketones as directing groups in photochemical sp^3 C–H fluorination. In a somewhat paradoxical manner, the method is best suited for complex, polycyclic molecules (likely due to increased conformational rigidity); however, its utility as a directed reaction is also demonstrated to be more general. It allows easy access to fluorinated products that have not been synthesized previously in good yields and selectivity, and it represents a necessary leap forward in directing radical fluorination. Future studies will seek to elucidate the reaction mechanism by exploring the nature of putative electron transfer processes.

2.6 References.

[1] (a) C. Walling, Free Radicals in Solution, Wiley, New York, NY, 1957; (b) R. Bernardi, R. Galli and F. Minisci, J. Chem. Soc. B, 1968, 324–325; (c) F. Minisci, R. Galli and R. Bernardi, Chem. Commun., 1967, 903–904; (d) A. A. Zavitsas and J. A. Pinto, J. Am. Chem. Soc., 1972, 94, 7390–7396; (e) T. Newhouse and P. S. Baran, Angew. Chem., Int. Ed., 2011, 50, 3362–3374.

[2] For some examples: (a) D. H. Paull, M. T. Scerba, E. Alden- Danforth, L. R. Widger and T. Lectka, J. Am. Chem. Soc., 2008, 130, 17260–17261; (b) P. Kwiatkowski, T. D. Beeson, J. C. Conrad and D. W. C. MacMillan, J. Am. Chem. Soc., 2011, 133, 1738–1741; (c) J. Erb, D. H. Paull, L. Belding, T. Dudding and T. Lectka, J. Am. Chem. Soc., 2011, 133, 7536– 7546.

[3] (a) S. Ariel, V. Ramamurthy, J. R. Scheffer and J. Trotter, J. Am. Chem. Soc., 1983, 105, 6960–6962; (b) V. Ramamurthy and K. Venkatesan, Chem. Rev., 1987, 87, 433–481.

[4] S. Purser, P. R. Moore, S. Swallow and V. Gouverneur, Chem. Soc. Rev., 2008, 37, 320–330.

[5] (a) S. Bloom, C. R. Pitts, R. Woltornist, A. Griswold, M. G. Holl and T. Lectka, Org. Lett., 2013, 15, 1722–1724; (b) W. Liu and J. T. Groves, Angew. Chem., Int. Ed., 2013, 52, 6024–6027; (c) S. Bloom, S. A. Sharber, M. G. Holl, J. L. Knippel and T. Lectka, J. Org. Chem., 2013, 78, 11082– 11086; (d) J.-B. Xia, C. Zhu and C. Chen, J. Am. Chem. Soc., 2013, 135, 17494–17500; (e) S. Bloom, M. McCann and T. Lectka, Org. Lett., 2014, 16, 6338–6341; (f) D. Cantillo, O. de Frutos, J. A. Rincon, C. Mateos and O. C. Kappe, J. Org. Chem., 2014, 79, 8486–8490; (g) M. B. Nodwell, A. Bagai, S. D. Halperin, R. E. Martin, H. Knust and R. Britton, Chem. Commun., 2015, 51, 11783–11786; (h) D. D. Bume, C. R. Pitts, R. T. Jokhai and T. Lectka, Tetrahedron, 2016, 72, 6031–6036; (i) A. Koperniku, H. Liu and P. B. Hurley, Eur. J. Org. Chem., 2016, 2016, 871–886; (j) A. M. Hua, D. N. Mai, R. Martinez and R. D. Baxter, Org. Lett., 2017, 19, 2949–2952.

[6] M.-G. Braun and A. Doyle, J. Am. Chem. Soc., 2013, 135, 12990–12993.

[7] (a) S. Bloom, C. R. Pitts, D. Miller, N. Haselton, M. G. Holl, E. Urheim and T. Lectka, Angew. Chem., Int. Ed., 2012, 51, 10580–10583; (b) W. Liu, X. Huang, M. Cheng, R. J. Nielson, W. A. Goddard III

and J. T. Groves, Science, 2012, 337, 1322–1325; (c) J.-B. Xia, Y. Ma and C. Chen, Org. Chem. Front., 2014, 1, 468–472.

[8] (a) C. R. Pitts, B. Ling, R. Woltornist, R. Liu and T. Lectka, J. Org. Chem., 2014, 79, 8895–8899; (b) X. Zhang, S. Guo and P. Tang, Org. Chem. Front., 2015, 2, 806–810.

[9] Y. Amaoka, M. Nagamoto and M. Inoue, Org. Lett., 2013, 15, 2160–2163.

[10] For some examples: (a) S. Bloom, J. L. Knippel and T. Lectka, Chem. Sci., 2014, 5, 1175–1178; (b) C. W. Kee, K. F. Chin, M. W. Wong and C.-H. Tan, Chem. Commun., 2014, 50, 8211–8214; (c) S. D. Halperin, H. Fan, S. Chang, R. E. Martin and R. Britton, Angew. Chem., Int. Ed., 2014, 53, 4690–4693; (d) J.-B. Xia, C. Zhu and C. Chen, Chem. Commun., 2014, 50, 11701–11704; (e) J. G. West, T. A. Bedell and E. J. Sorensen, Angew. Chem., Int. Ed., 2016, 55, 8923–8927.

[11] For some of the pioneering examples of palladium catalysis in a directed sp^3 C–H fluorination application, see: (a) K. L. Hull, W. Q. Anani and M. S. Sanford, J. Am. Chem. Soc., 2006, 128, 7134–7135; (b) K. B. McMurtrey, J. M. Racowski and M. S. Sanford, Org. Lett., 2012, 14, 4094–4097.

[12] (a) R.-Y. Zhu, K. Tanaka, G.-C. Li, J. He, H.-Y. Fu, S.-H. Li and J.-Q. Yu, J. Am. Chem. Soc., 2015, 137, 7067–7070; (b) Q. Zhang, X.-S. Yin, K. Chen, S.-Q. Zhang and B.-F. Shi, J. Am. Chem. Soc., 2015, 137, 8219–8226; (c) J. Miao, K. Yang, M. Kurek and H. Ge, Org. Lett., 2015, 17, 3738–3741; (d) X. Lu, B. Xiao, R. Shang and L. Liu, Chin. Chem. Lett., 2016, 27, 305–311.

[13] Amidyl radical-based remote C–H fluorination reactions have also been reported, but with limited scope: (a) Z. Li, L. Song and C. Li, J. Am. Chem. Soc., 2013, 135, 4640–4643; (b) B. J. Groendyke, D. I. AbuSalim and S. P. Cook, J. Am. Chem. Soc., 2016, 138, 12771–12774.

[14] C. R. Pitts, D. D. Bume, S. A. Harry, M. A. Siegler and T. Lectka, J. Am. Chem. Soc., 2017, 139, 2208–2211.

[15] (a) M. Rueda-Becerril, C. C. Sazepin, J. C. T. Leung, T. Okbinoglu, P. Kennepohl, J.-F. Paquin and G. M. Sammis, J. Am. Chem. Soc., 2012, 134, 4026–4029; (b) J.-D. Yang, Y. Wang, X.-S. Xue and J.-P. Cheng, J. Org. Chem., 2017, 82, 4129–4135.

[16] For recent reviews on photosensitization, see: (a) J. Zhao, W. Wu, J. Sun and S. Guo, Chem. Soc. Rev., 2013, 42, 5323– 5351; (b) N. A. Romero and D. Nicewicz, Chem. Rev., 2016, 116, 10075–10166.

[17] For general information on excited-state ketone hydrogen atom abstraction, see: P. Wagner and B.-S. Park, in Organic Photochemistry, ed. A. Padwa, Marcel Dekker, Inc., New York, NY, 1991, vol. 11, ch. 4, pp. 227–366.

[18] (a) W. G. Herkstroeter, A. A. Lamola and G. S. Hammond, J. Am. Chem. Soc., 1964, 86, 4537–4540; (b) W. G. Herkstroeter and G. S. Hammond, J. Am. Chem. Soc., 1966, 88, 4769–4777.

[19] Both benzil and 9,10-phenanthrenequinone have more signi□cant absorptions in the LED emission region (>400 nm) than benzophenone, 9-fluorenone, and xanthone. Such overlap is key to their success (and a testament to their role) as photosensitizers in this reaction.

[20] N. Miyaura and A. Suzuki, Chem. Rev., 1995, 95, 2457–2483.

[21] Q. Michaudel, G. Journot, A. Regueiro-Ren, A. Goswami, Z. Guo, T. P. Tully, L. Zou, R. O. Ramabhadran, K. N. Houk and P. S. Baran, Angew. Chem., Int. Ed., 2014, 53, 12091–12096.

[22] C. N. Neumann and T. Ritter, Angew. Chem., Int. Ed., 2015, 54, 3216–3221.

[23] In medicinal chemistry, a “fluorine scan” is common practice in drug derivatization and for studying SAR's. Thus, access to different regioisomers may be desirable. See: E. P. Gillis, K. J. Eastman, M. D. Hill, D. J. Donnelly and N. A. Meanwell, J. Med. Chem., 2015, 58, 8315–8359.

[24] C. R. Pitts, S. Bloom, R. Woltornist, D. J. Auvenshine, L. R. Ryzhkov, M. A. Siegler and T. Lectka, J. Am. Chem. Soc., 2014, 136, 9780–9791.

[25] C. R. Pitts, B. Ling, J. A. Snyder, A. E. Bragg and T. Lectka, J. Am. Chem. Soc., 2016, 138, 6598–6609.

[26] Reactions were performed at 2-fold, 4-fold, and 8-fold dilutions from our standard concentration.

[27] T. R. Evans and P. E. Leermakers, J. Am. Chem. Soc., 1967, 89, 4380–4382.

[28] For general information on triplet–triplet energy transfer, see: N. J. Turro, in Modern Molecular Photochemistry, The Benjamin/Cummings Publishing Company, Inc., Menlo Park, CA, 1978, ch. 9, pp. 296–361.

[29] (a) W. M. Nau and J. C. Scaiano, J. Phys. Chem., 1996, 100, 11360–11367; (b) J. K. Agyin, L. D. Timberlake and H. Morrison, J. Am. Chem. Soc., 1997, 119, 7945–7953.

[30] In addition, one would expect to observe byproducts from Norrish II cleavage in linear and certain exocyclic ketones if the reaction goes through a HAT mechanism – such byproducts were not observed in any significant amount.

[31] Electron transfer may occur directly from the substrate to the benzil triplet state or to a benzil/Selectfluor exciplex. See:J.W.Kee,H.Shao,C.W.Kee,Y.Lu,H.S.Sooand C.-H. Tan, Catal. Sci. Technol., 2017, 7, 848–857.

[32] A. G. Griesbeck, N. Hoffmann and K.-D. Warzecha, Acc. Chem. Res., 2007, 40, 128–140.

[33] C.-C. Hsieh, C.-M. Jiang and P.-T. Chou, Acc. Chem. Res., 2010, 43, 1364–1374.

[34] (a) J. J. Warren, T. A. Tronic and J. M. Mayer, Chem. Rev., 2010, 110, 6961–7001; (b) D. R. Weinberg, C. J. Gagliardi, J. F. Hull, C. F. Murphy, C. A. Kent, B. C. Westlake, A. Paul, D. H. Ess, D. G. McCafferty and T. J. Meyer, Chem. Rev., 2012, 112, 4016–4093.

Chapter 3

Aminofluorination of Unactivated Alkenes and Fluoro-rearrangement of Activated Alkenes

3.1 Introduction.

The fluorofunctionalization of C=C bonds is an active and timely topic of study that complements the general renaissance in fluorination methodology. The goals are multifold and include the synthesis of biologically active fluorinated molecules,[1] chemical intermediates,[2] and pharmaceuticals.[3] From the standpoint of reactivity, mild and inexpensive conditions are desired.[4] The mechanistic aspects of fluoro- functionalization methods are significant as well, reactions involving an electrophilic fluorinating reagent are often expected to result in different regiochemical outcomes than reactions in which fluoride ion is the reagent.[5] Instead conceive of a situation in which the structure of the alkene substrate determines the regioselectivity of the reaction. This bespeaks a probable mechanistic "switch", in which the fluorinating agent plays a fundamentally different role. Such switch mechanisms have been of interest to our research group for a long time,[6] not least for the reason that they reveal basic reactivity patterns in fairly illuminating ways. Recently, we have employed Selectfluor (SF) in a variety of catalyzed and promoted fluorination reactions,[7] including a fluoroamination of arylcyclopropanes.[8] We discovered to our surprise that the DABCO moiety of Selectfluor itself was incorporated into the ring-opened products.

In this featured article, we report a fluorofunctionalization of alkenes that follows an unusual reactivity pattern. In the presence of UV light and a sensitizer, regioselective ammoniofluorination of monosubstituted alkenes is observed. The resulting products

reveal the fluorine to be placed in the secondary position, and the ammonium substituent in the primary. In dramatic contrast, several di- and trisubstituted alkenes, especially those that can rearrange through carbocationic manifolds, afford the less-substituted fluoride instead with no incorporation of the DABCO moiety (Figure 3.1).

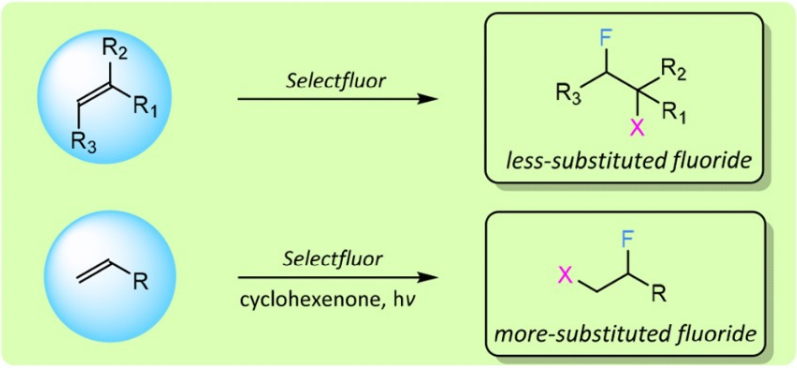

Figure 3.1. Switch in regioselectivity observed in the fluorination of alkenes.

The reaction of Selectfluor with alkenes was first reported shortly after the reagent was discovered.[9] Lal fluorinated styrene derivatives using Selectfluor in the presence of nucleophiles (no DABCO incorporation) and several reports have followed to describe the reaction of styrenyl alkenes in a similar manner.[10] Glycal enol ethers were also shown to react with Selectfluor to give fluorinated ammonium salts, which were then treated with various nucleophiles to displace the DABCO moiety.[11] In these two methods, regioselectivity arises due to the use of activated alkene substrates that form stabilized carbocations (i.e., a benzylic carbocation and an oxocarbenium ion). More recently, hydrofluorination,[12] phosphonofluorination,[13] and azidofluorination[14] of unactivated alkenes using Selectfluor have been described, relying upon radical conditions to form the more substituted fluoride product.

On the other hand, direct aminofluorination of alkenes is less explored, and the few existing methods have limited substrate scope and are less suitable for diverse synthetic transformations.[15] Tosyl-protected pent-4-en-1-amine derivatives have been utilized under both metal and metal-free conditions to bring about an intramolecular aminofluorination using fluoride sources.[16] Several N-arylpent-4-enamides were also shown to participate in a similar intramolecular reaction using Selectfluor and $AgNO_3$.[17] Additionally, styrenes have been employed as activated olefin substrates in palladium (the amine derived from N-fluorobenzenesulfonimide traps the carbocation after the initial fluoride addition)[18] and copper[19] catalyzed intermolecular aminofluorinations leading to sulfonamide derivatives. This reaction requires the use of [N-(p- toluenesulfonyl)imino] phenyliodinane in addition to two catalysts and a fluorine source. A metal-free aminofluorination of styrenyl alkenes has been recently developed as well, utilizing azoles to trap a benzylic cation.[20] To the best of our knowledge, the only reported method for intermolecular aminofluorination of unactivated alkenes produces fluorinated carbamates rather than amines, requires two fluorine sources and a preformed catalyst, and has somewhat limited substrate scope with regards to unactivated olefins.[21]

3.2 Optimization of Ammoniofluorination Conditions and Substrate Scope of the Reaction.

Given our recent work in the area of photochemical sp^3 C−H fluorinations,[22] we were intrigued by the idea of an analogous sp^2 fluorination. Initial attempts of fluorinating 5-methyl-1-hexene with Selectfluor in MeCN under UV-irradiation (using 300 nm light sources) led to a mixture of two products, the β-ammoniofluoride (compound **1a**) and a

tertiary fluoride that retained the olefin (compound **1b**, resulting from a photo- chemical sp^3 C–H fluorination at an activated tertiary site) in a ratio of approximately 1:1. In order to develop a regioselective fluorination protocol, we then screened different photo-sensitizers using 300 nm light sources (Table 3.1). As well, we briefly explored nonphotochemical conditions such as heat and BEt_3 (we have previously shown BEt_3 to

Table 3.1. Screening for Reaction Conditions.

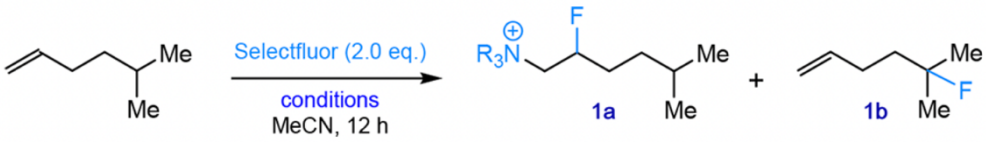

entry	conditions	% yields a	% yields b
1	*hν* (300 nm)	48	50
2	1,2,3,4,5-tetracyanobenzene, 0.1 equiv *hν* (300 nm)	79	15
3	80 °C (in dark)	80	18
4	rt (in dark)	<5	trace
5	2-cyclohexen-1-one, 1.0 equiv *hν* (300 nm)	**98**	<2
6	benzil, 0.1 equiv *hν* (LEDs)	70	12
7	5-dibenzosuberenone, 0.1 equiv *hν* (LEDs)	27	30
8	BEt_3, 0.2 equiv (in dark),	72	trace

effect the generation of the putative N-centered radical dication from Selectfluor that is important in electron transfer chemistry) to induce fluorination.[23] Gratifyingly, we found that the combination of cyclohexenone and 300 nm light to be the optimal conditions for a selective functionalization, resulting in the formation of the desired ammoniofluoride in excellent yield while affording only trace amounts of the tertiary fluoride byproduct.

Upon subjecting various alkenes to these optimized conditions, it became evident that monosubstituted alkenes work best (Table 3.2), whereas more substituted olefins tend to result in trace fluorination, a mixture of products, or both. We accordingly narrowed our focus to monosubstituted olefins and were pleased to observe that most perform well in the reaction, fluorinating regioselectively and in high yield.[24] Alkene substrates that include an alkyl or aryl substituent (compounds **1**–**5**) undergo ammoniofluorination in excellent yield.

Table 3.2. Substrate Scope of Monosubstituted Alkenes.

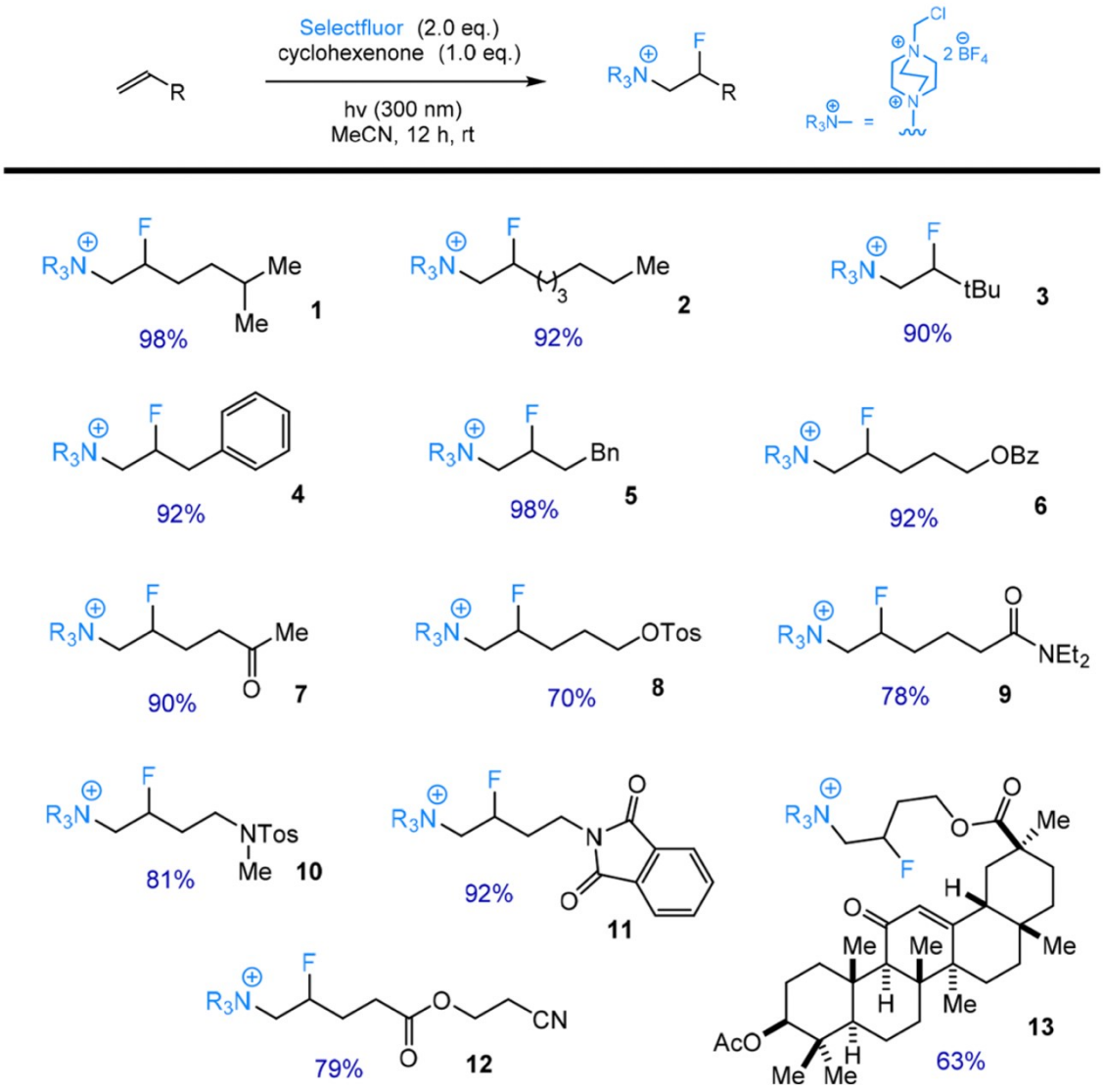

Oxygen-containing functional groups such as carbonyl, acetoxy, benzoyloxy, and sulfonyl were found to be compatible under our optimized reaction conditions (compounds **6**–**8**, **12**, and **13**). Moreover, several nitrogen-containing functional groups (namely, amido, phthalimido, sulfonamido, and cyano) were found to afford selectively ammoniofluorinated products in good yields (compounds **9**–**12**). Compound **13**, a derivative of the antiviral,[25] antifungal,[26] and antibacterial[27] drug enoxolone gives the desired ammoniofluoride product in good yield. This example demonstrates the reactivity of C=C bonds in the presence of many accessible sp^3 C–H bonds. It is worth noting that regioselectivity is not affected by the enone functional group at C11 even though it can direct fluorination to C1 under similar conditions.[28] Furthermore, compound **13** illustrates the potential to employ this method in a late-stage fluorination of a complex pharmaceutical target, making the reaction even more attractive to medicinal chemists.

3.3 Application of the Ammoniofluorination to the Synthesis of Fluoropiperazines.

We found that it is simple to isolate the Selectfluor-adducts after the ammoniofluorination but challenging to separate them from the unreacted Selectfluor and derived impurities, as has been previously shown in similar compounds.[26] Given that the Selectfluor moiety is not particularly useful or interesting as a substituent, we next turned our focus toward ways to derivatize the ammonium fluoride compounds. Adopting a previously reported procedure from the Ritter group,[29] the DABCO moiety of the Selectfluor-adduct was efficiently reduced with aqueous $Na_2S_2O_3$, providing easy access to β-fluoropiperazine derivatives (Table 3.3). Importantly, the Selectfluor impurities can

Table 3.3 One-Pot Synthesis of Fluoropiperazines from Alkenes

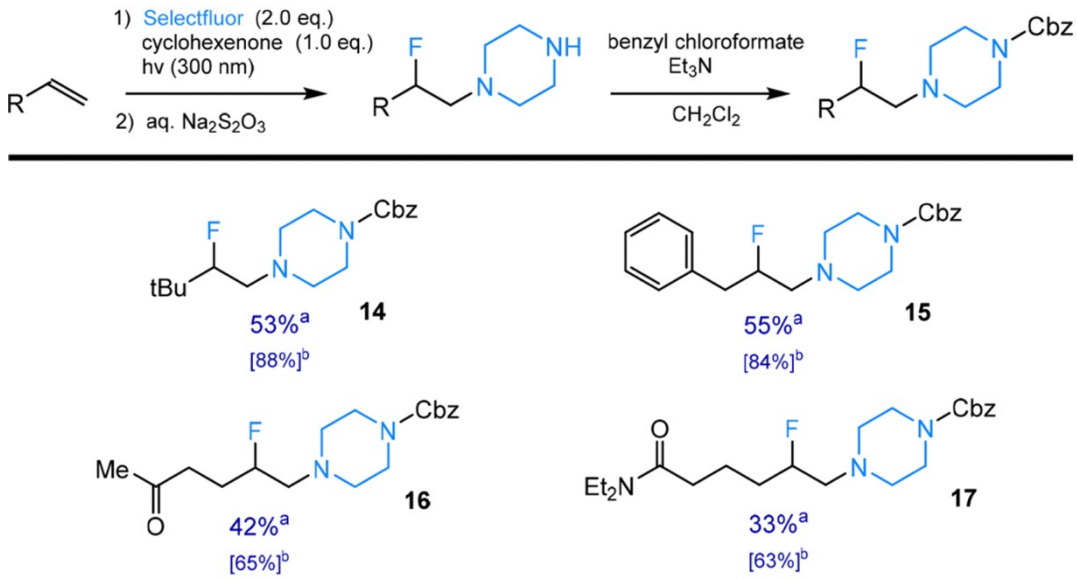

now be very easily separated from the desired product in an aqueous workup. The reduction can be performed in a one- pot fashion following the fluorination step; it works equally well on the isolated ammonium salts. For example, we demonstrated this approach on four alkenes and obtained the reduced products in good yields. We anticipate that a one- pot strategy to synthesize fluoropiperazines will be of great use to medicinal chemists, given the ubiquity of both piperazines and fluorine in pharmaceuticals.[30] The fluoropiperazine products were transformed into Cbz derivatives to facilitate chromatography (compounds **14**–**17**); however, they could also be isolated as the free secondary amines or instead alkylated or acylated with any appropriate electrophile.

On another front, we briefly explored nucleophilic displacement of the DABCO-adducts by treating the ammonium fluoride salts with various nucleophiles. Unfortunately, we found this to be a surprisingly reluctant reaction. Nucleophiles such as sodium thiophenolate, sodium azide, potassium thiocyanate, sodium hydroxide, and several others

were observed to give a mixture of products in low yield. Although we have previously reported the displacement of a Selectfluor- adduct with potassium thiocyanate, the ammonium group was on a secondary benzylic carbon and likely was displaced through a different mechanism (S_N1).[8] While we remain interested in the potential utility of this substitution reaction, further exploration in this area is beyond the scope of this work.

3.4. Reactivity Switch Observed in the Fluorination of Other Alkenes with Selectfluor.

In contrast to the reactivity of unactivated monosubstituted alkenes, we also report several new examples of alkenes reacting with SF to give the less substituted fluoride (Table 3.4). These products arise from a reactivity switch in which Selectfluor is reacting in a two-electron fashion with the olefin or instead via single electron transfer followed by rearrangement. Gibberellic acid, a plant hormone that is used in the agricultural industry,[31] undergoes a remarkably clean reaction with SF in high yield. The fluorogibberellin product (compound **18**) contains a $-CH_2F$ group as well as a ketone, which is the result of a Wagner-Meerwein rearrangement. A similar rearrangement has been reported on gibberellic acid using HCl;[32] however, under these conditions, the cyclohexene ring first aromatizes before the alkene reacts with the acid and ultimately rearranges. Therefore, this procedure is noteworthy as it allows modification of the 1,1-disubstituted alkene without disrupting the cyclohexene and lactone rings. Betulin, an abundant triterpene commonly extracted from birch bark,[33] is also known to undergo a Wagner-Meerwein rearrangement in the presence of strong acid[34] to form allobetulin. Upon treating betulin with SF, fluoroallobetulin (compound **19**) was obtained in good yield, possessing a $-CH_2F$ group consistent with SF behaving as a two-electron electrophilic source of fluorine.

Table 3.4 Examples of an Alkene Reacting Nonphotochemically with Selecfluor to Give the Less-Substituted Fluoride

substrate	*product*	*% yield*	*d.r.*
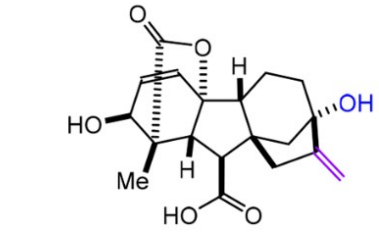 *gibberellic acid*	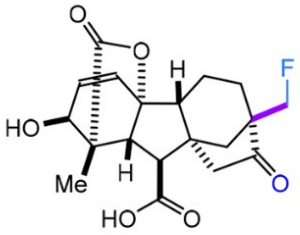 **18**	86[b]	n/a
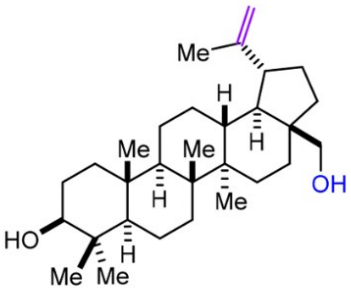 *betulin*	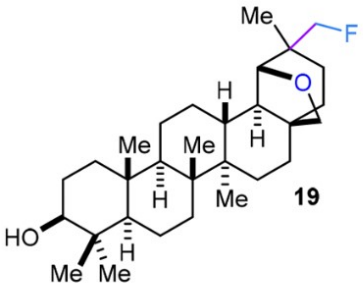 **19**	51[c]	6.7 : 1
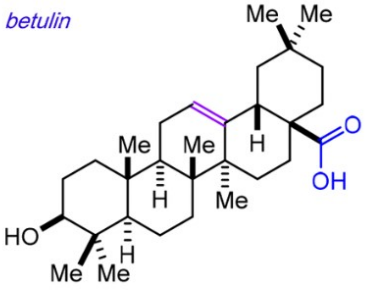 *oleanolic acid*	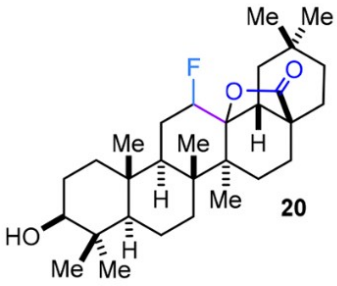 **20**	79[c]	9 : 1

Because many betulin derivatives are known to be biologically active (for example, possessing anticancer and anti- HIV activity), a fluorinated analogue could be of interest as well.[35] Oleanolic acid, another anticancer terpenoid,[36] provides an additional example of an alkene that reacts with SF to give the less substituted fluoride. This substrate, however, is unique due to the fact that it contains a trisubstituted C=C bond (the previous two examples being 1,1-disubstituted alkenes) that undergoes a lactonization (rather than a Wagner-Meerwein rearrangement) when treated with strong acid.[37] In the presence of

Selectfluor, a fluorolactonization occurs in high yield to afford compound **20**. A common trait of these three substrates is that the reactive alkene can be thought of as "activated." Each molecule contains some feature that stabilizes the carbocation resulting after fluorination (e.g., a potential to rearrange, an intramolecular nucleophile, etc.). This seems to be a pivotal factor that determines if Selectfluor by itself will react with an alkene and if it will do so regioselectively. Ultimately, these counterexamples provide evidence that the simple reaction between SF and a C=C bond is limited in scope, and therefore, methods involving fluorofunctionalization of unactivated alkenes are necessary.

3.5 Mechanistic Studies and Considerations.

Although gibberellic acid reacts with Selectfluor in the absence of light or additives, we subjected this substrate to a reaction with SF under the ammoniofluorination conditions (hν 300 nm, cyclohexenone, MeCN) as a control experiment. To our surprise, the primary fluoride still formed in high yield whereas no ammoniofluoride was observed. We also treated several unactivated alkenes with SF in the dark and observed only trace or no fluorination. The results of these controls are consistent with the notion that the structure of the alkene governs the mechanism by which it reacts with SF, and the reaction conditions are therefore of lesser importance.

We next performed a series of intermolecular competition experiments in which both types of alkenes (i.e., unactivated and activated) were present in the same vial and were subjected to the ammoniofluorination conditions. While the overall selectivity was consistent with our prediction, (the activated alkene fluorinates preferentially), the degree of selectivity was a bit surprising. In an initial reaction containing 1 equiv of gibberellic

acid, 1 equiv of allyl benzene, 1 equiv cyclohexenone, and 1.5 equiv of Selectfluor, we observed a 95% yield of the primary fluoride derived from gibberellic acid and an 11% yield of the secondary ammoniofluoride of allyl benzene after 12 h. Peculiarly, the yield for the fluorination of gibberellic acid increased in the presence of light; however, some minor byproducts were observed. By changing the conditions (1.2 equiv of Selectfluor, 9 h) we noted a 75% yield of fluorinated gibberellic acid and only 4% of the allyl benzene fluoroammonium salt. Similarly, we looked at the analogous competition experiment with oleanolic acid and allyl benzene, which gave the fluorolactone of oleanolic acid in 30% yield (due to low solubility in MeCN at room temperature) but only trace amounts of the ammoniofluoride of allyl benzene. These results suggest that a putative two-electron reaction of Selectfluor with activated alkenes can be significantly faster than the one-electron reaction of Selectfluor with unactivated olefins, even if the activated substrates are more sterically hindered.

The reaction between SF and monsubstituted alkenes proceeds thermally, although the yields of desired products are often low and other fluorinated byproducts are observed as well. On the other hand, in the presence of cyclohexenone and 300 nm irradiation, the reaction is high yielding and very selective. These are conditions in which the Selectfluor radical dication (SRD) is expected to form. Attack of the SRD at the primary carbon of the alkene produces free radical 21, which is fluorinated by SF, thus regenerating the SRD to carry forward the chain (Figure 3.2a). In the case of the more electron rich di- and trisubstituted alkenes, a different scenario pertains. For example, fluorine can transfer to the primary carbon from SF as formal F^+, resulting in a carbocation that rearranges. Alternatively, single electron transfer (SET) from the alkene to SF results in the SRD and

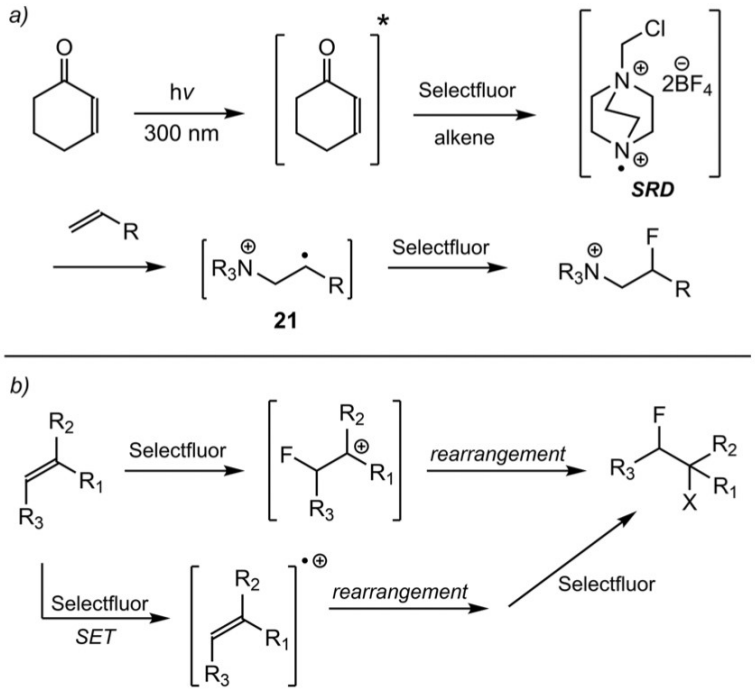

Figure 3.2 Mechanistic considerations for the reaction of Selectfluor with C=C bonds.

the substrate radical cation, which can rearrange through a carbocationic process before reacting with SF at the primary radical position (Figure 3.2b). As SF so commonly plays through SET chemistry,[38] this alternative must be taken seriously.

While the Selectfluor radical dication is known as an intermediate which typically reacts with sp^3 bonds,[39] it has been recently reported to engage in charge-transfer with arenes.[26] Even more recently, the SRD has been postulated in a proposed mechanism to undergo an addition to an olefin to give a radical similar to 21, which could go on to get trapped by a Cu(II)-CN species.[40] These works provide support for our proposed mechanism, but at this time we cannot definitively confirm any details without a more in-depth mechanistic study.

It is currently unclear what the exact role of cyclohexenone is in the ammoniofluorination; however, the enone triplet excited state is potentially involved.

Extant photochemistry involving the reaction of cyclic enones with alkenes is centered on the well-studied [2 + 2] photocycloaddition.[41] The original hypothesis for this reaction, which invoked the (n, π*) enone excited state as well as exciplex formation, is now understood to be inaccurate. Rather, it is the (π, π*) state of the enone that is involved in the cycloaddition and exciplexes are no longer described in the mechanism, as evidence for their involvement never materialized. Given the fact that this ammoniofluorination is generally high yielding (with respect to the alkene), we were surprised to observe a yield of only 35% recovered cyclohexenone after the reaction. Even less cyclohexenone is recovered (11%) when the enone is treated under the ammoniofluorination conditions without the alkene present. These findings prompted us to examine the byproducts formed during the reaction, and accordingly, we have observed evidence for the formation of [2 + 2] photocycloaddition products. Adducts of cyclohexenone and neohexene were detected in small quantities by ^{1}H NMR in addition to the photodimer of cyclohexenone, which has been previously reported to form in the presence of UV light.[42] On the other hand, we observed no trapped (fluorinated) 1,4-biradicals, intermediates that are known to be involved in [2 + 2] photocycloadditions. While [2 + 2] cycloadditions represent a minor competing reaction pathway cyclohexenone can participate in, the molecule must be playing a slightly different role in the ammoniofluorination mechanism. For instance, the enone could be acting as a photosensitizer, exciting the alkene which could then be oxidized by SF and ultimately give the SRD after loss of fluoride.[8] Another scenario that we envisioned involves the triplet excited enone directly oxidizing the alkene to form a radical anion/radical cation pair that could react with SF to give the SRD. Calculated energies of the involved species suggest that the sensitization route is considerably more

favorable, having a ΔG_{calc} value of −5.5 kcal while the other proposed path is significantly uphill (Figure 3.3a). Furthermore, the subsequent step to form the SRD from the excited alkene was likewise found to be energetically favorable (Figure 3.3b), providing a plausible means of initiation. Nevertheless, these energies should be viewed strictly qualitatively given the nature of charged open-shell species. It is of course still possible that cyclohexenone is playing a role other than sensitizer in this reaction, and for that reason we plan to explore this intriguing mechanism in future research efforts.

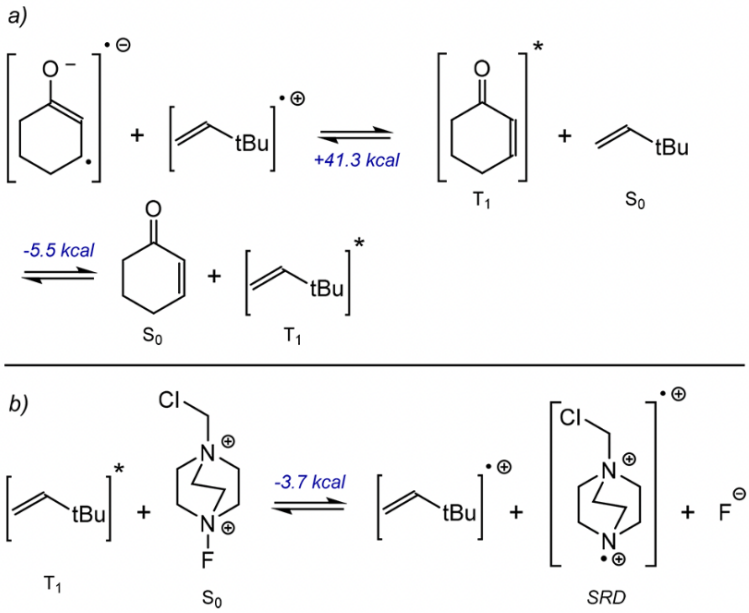

Figure 3. Calculated energies of intermediates at *ω*B97XD/6-311+G** (MeCN).

Figure 3.3. Calculated energies of intermediates at ωB97XD/6- 311+G** (MeCN).

3.6. Conclusion.

A one-pot method involving a novel photochemical ammoniofluorination furnishes β-fluoropiperazines from monosubstituted alkenes. In addition to being operationally simple

and cost-effective, the reaction is highly regioselective for the formation of the more substituted (secondary) fluoride. We contrasted this reactivity to several alkene-containing natural products which react with the same fluorinating reagent, Selectfluor, to give the less substituted fluoride. Further studies are required to complete our understanding of this reactivity switch, but the structure of the alkene and the overall compound seems to play a paramount role that outweighs the reaction conditions. We anticipate that the ammoniofluorination reaction will be of immediate use in the medicinal chemistry community and aim to further elucidate mechanistic details in future projects.

3.7 References.

[1] (a) Shah, P.; Westwell, A. D. The role of fluorine in medicinal chemistry. J. Enzyme Inhib. Med. Chem. 2007, 22, 527−540. (b) Hiyama, T.; Yamamoto, H. Biologically Active Organofluorine Compounds. Organofluorine Compounds 2000, 1, 137−182.

[2] (a) Gloria, C. Organic fluorinated intermediates: Production and Industrial Uses. J. Fluorine Chem. 1992, 58, 128. (b) Pathak, V. N.; Sareen, V.; Joshi, K. C. Fluorinated 1,3-diketones as reaction intermediates for synthesis of biologically active heterocycles. J. Fluorine Chem. 1985, 29, 202.

[3] (a) O'Hagan, D. Fluorine in health care: Organofluorine containing blockbuster drugs. J. Fluorine Chem. 2010, 131, 1071− 1081.(b)Wang,J.;Sańchez-Rosello,́M.;Aceña,J.L.;delPozo,C.; Sorochinsky, A. E.; Fustero, S.; Soloshonok, V. A.; Liu, H. Fluorine in Pharmaceutical Industry: Fluorine-Containing Drugs Introduced to the Market in the Last Decade (2001−2011). Chem. Rev. 2014, 114, 2432−2506.

[4] (a) Campbell, M. G.; Ritter, T. Late-Stage Fluorination: From Fundamentals to Application. Org. Process Res. Dev. 2014, 18, 474− 480. (b) Champagne, P. A.; Desroches, J.; Hamel, J.; Vandamme, M.; Paquin, J. Monofluorination of Organic Compounds: 10 Years of Innovation. Chem. Rev. 2015, 115, 9073−9174. (c) Chatalova- Sazepin, C.; Hemelaere, R.; Paquin, J.; Sammis, G. M. Recent Advances in Radical Fluorination. Synthesis 2015, 47, 2554−2569.

[5] (a) Zhao, H.; Gabbaï, F. P. Nucleophilic Fluorination Reactions Starting from Aqueous Fluoride Ion Solutions. Org. Lett. 2011, 13, 1444−1446. (b) Shamma, T.; Buchholz, H.; Prakash, G. K.; Olah, G. A. Electrophilic Fluorination of Aromatics with Selectfluor and Trifluoromethanesulfonic Acid. Isr. J. Chem. 1999, 39, 207−210.

[6] (a) Abraham, C. J.; Paull, D. H.; Bekele, T.; Scerba, M. T.; Dudding, T.; Lectka, T. A Surprising Mechanistic "Switch" in Lewis Acid Activation: A Bifunctional, Asymmetric Approach to α-Hydroxy Acid Derivatives. J. Am. Chem. Soc. 2008, 130, 17085−17094. (b) Wack, H.; Drury, W. J.; Taggi, A. E.; Ferraris, D.; Lectka, T. Nucleophilic Metal Complexes as Acylation Catalysts: Solvent- Dependent "Switch" Mechanisms Leading to the First Catalyzed Staudinger Reaction. Org. Lett. 1999, 1, 1985−1988.

[7] (a) Bume, D. D.; Harry, S. A.; Lectka, T.; Pitts, C. R. Catalyzed and Promoted Aliphatic Fluorination. J. Org. Chem. 2018, 83, 8803− 8814. (b) Bume, D. D.; Pitts, C. R.; Ghorbani, F.; Harry, S. A.; Capilato, J. N.; Siegler, M. A.; Lectka, T. Ketones as directing groups in photocatalytic sp3 C−H fluorination. Chem. Sci. 2017, 8, 6918− 6923. (c) Bloom, S.; Pitts, C. R.; Miller, D. C.; Haselton, N.; Holl, M. G.; Urheim, E.; Lectka, T. A Polycomponent Metal-Catalyzed Aliphatic, Allylic, and Benzylic Fluorination. Angew. Chem., Int. Ed. 2012, 51, 10580−10583.

[8] Pitts, C. R.; Ling, B.; Snyder, J. A.; Bragg, A. E.; Lectka, T. Aminofluorination of Cyclopropanes: A Multifold Approach through a Common, Catalytically Generated Intermediate. J. Am. Chem. Soc. 2016, 138, 6598−6609.

[9] Lal, G. S. Site-Selective Fluorination of Organic Compounds Using l-Alkyl-4-fluoro-l,4-diazabicyclo[2.2.2]octane Salts (Selectfluor Reagents). J. Org. Chem. 1993, 58, 2791−2796.

[10] (a) Luo, H.; Loh, T. Synthesis of aryl allylic fluorides by direct electrophilic fluorination of alkenes. Tetrahedron Lett. 2009, 50, 1554−1556. (b) Kumar, A.; Singh, T. V.; Venugopalan, P. Microwave assisted fluorofunctionalization of phenyl substituted alkenes using selectfluor. J. Fluorine Chem. 2013, 150, 72−77. (c) Yang, Q.; Mao, L.; Yang, B.; Yang, S. Metal-Free, Efficient Oxyfluorination of Olefins for the Synthesis of α-Fluoroketones. Org. Lett. 2014, 16, 3460−3463.

[11] Albert, M.; Dax, K.; Ortner, J. A novel direct route to 2-deoxy- 2-fluoro-aldoses and their corresponding derivatives. Tetrahedron 1998, 54, 4839−4848.

[12] Barker, T. J.; Boger, D. L. Fe(III)/NaBH4-Mediated Free Radical Hydrofluorination of Unactivated Alkenes. J. Am. Chem. Soc. 2012, 134, 13588−13591.

[13] Zhang, C.; Li, Z.; Zhu, L.; Yu, L.; Wang, Z.; Li, C. Silver- Catalyzed Radical Phosphonofluorination of Unactivated Alkenes. J. Am. Chem. Soc. 2013, 135, 14082−14085.

[14] Li, Z.; Zhang, C.; Zhu, L.; Liu, C.; Li, C. Transition-metal-free, room-temperature radical azidofluorination of unactivated alkenes in aqueous solution. Org. Chem. Front. 2014, 1, 100−104.

[15] Kong, W.; Merino, E.; Nevado, C. Divergent Reaction Mechanisms in the Aminofluorination of Alkenes. Chimia 2014, 68, 430−435.

[16] (a) Wang, Q.; Zhong, W.; Wei, X.; Ning, M.; Meng, X.; Li, Z. Metal-free intramolecular aminofluorination of alkenes mediated by PhI(OPiv)2/hydrogen fluoride−pyridine system. Org. Biomol. Chem. 2012, 10, 8566−8569. (b) Wu, T.; Yin, G.; Liu, G. Palladium- Catalyzed Intramolecular Aminofluorination of Unactivated Alkenes. J. Am. Chem. Soc. 2009, 131, 16354−16355.

[17] Li, Z.; Song, L.; Li, C. Silver-Catalyzed Radical Amino- fluorination of Unactivated Alkenes in Aqueous Media. J. Am. Chem. Soc. 2013, 135, 4640−4643.

[18] Qiu, S.; Xu, T.; Zhou, J.; Guo, Y.; Liu, G. Palladium-Catalyzed Intermolecular Aminofluorination of Styrenes. J. Am. Chem. Soc. 2010, 132, 2856−2857.

[19] Saavedra-Olavarria, J.; Arteaga, G. C.; Lopez, J. J.; Perez, E. G. Copper-catalyzed intermolecular and regioselective aminofluorination of styrenes: facile access to β-fluoro-N-protected phenethylamines. Chem. Commun. 2015, 51, 3379−3382.

[20] Zhang, Q.; Zheng, G.; Zhang, Q.; Li, Y.; Zhang, Q. Metal-Free Three-Component Regioselective Aminofluorination of Styrene Derivatives. J. Org. Chem. 2017, 82, 8258−8266.

[21] Lu, D.; Zhu, C.; Sears, J.; Xu, H. Iron(II)-Catalyzed Intermolecular Aminofluorination of Unfunctionalized Olefins Using Fluoride Ion. J. Am. Chem. Soc. 2016, 138, 11360−11367.

[22] (a) Bloom, S.; McCann, M.; Lectka, T. Photocatalyzed Benzylic Fluorination: Shedding “Light” on the Involvement of Electron Transfer. Org. Lett. 2014, 16, 6338−6341. (b) Pitts, C. R.; Bloom, M. S.;

Bume, D. D.; Zhang, Q. A.; Lectka, T. Unstrained C−C bond activation and directed fluorination through photocatalytically- generated radical cations. Chem. Sci. 2015, 6, 5225−5229.

[23] Pitts, C. R.; Ling, B.; Woltornist, R.; Liu, R.; Lectka, T. Triethylborane-Initiated Radical Chain Fluorination: A Synthetic Method Derived from Mechanistic Insight. J. Org. Chem. 2014, 79, 8895−8899.

[24] We found that styrene did not fluorinate regioselectively under the ammoniofluorination conditions, likely because it contains an activated olefin (a benzylic carbocation results after Selectfluor reacts with the alkene at the primary position.

[25] Badam, L.; Amagaya, S.; Pollard, B. In vitro antiviral activity of indigenous glycyrrhizin, licorice and glycyrrhizic acid (Sigma) on Japanese encephalitis virus. J. Community Dis. 1997, 29, 91−99.

[26] Guo, N.; Takechi, M.; Uno, C. Protective effect of glycyrrhizine in mice with systemic Candida albicans infection and its mechanism. J. Pharm. Pharmacol. 1991, 13, 380−383.

[27] (a) Fuji, H. Y.; Tian, J.; Luka, C. Effect of glycyrrhetinic acid on influenza virus and pathogenic bacteria. Bull. Chin. Mater. Med. 1986, 11, 238−241. (b) Salari, M. H.; Sohrabi, N.; Kadkhoda, Z.; Khalili, M. Antibacterial effects of enoxolone on periodontopathogenic and capnophilic bacteria isolated from specimens of periodontitis patients. Iran. Biomed. J. 2003, 7, 39−42.

[28] (a) Pitts, C. R.; Bume, D. D.; Harry, S. A.; Siegler, M. A.; Lectka, T. Multiple enone-directed reactivity modes lead to the selective photochemical fluorination of polycyclic terpenoid deriva- tives. J. Am. Chem. Soc. 2017, 139, 2208−2211. (b) Bume, D. D.; Harry, S. A.; Pitts, C. R.; Lectka, T. Sensitized Aliphatic Fluorination Directed by Terpenoidal Enones: A “Visible Light” Approach. J. Org. Chem. 2018, 83, 1565−1575.

[29] Boursalian, G. B.; Ham, W. S.; Mazzotti, A. R.; Ritter, T. Charge-transfer-directed radical substitution enables para-selective C−H functionalization. Nat. Chem. 2016, 8, 810−815.

[30] (a) Edgar, S. A.; Davis, D. C.; Frazier, J. A. The efficacy of some piperazine compounds in the elimination of helminths from experimentally-and naturally-infected poultry. Poult. Sci. 1957, 36, 495−510. (b) Ban, T. A.; Fujimori, M.; Petrie, W. M.; Ragheb, M.; Wilson, W. Systematic studies with amoxapine, a new antidepressant.

Int. Pharmacopsychiatry 2017, 17, 18−27. (c) Nicholson, A. N.; Stone, B. M.; Turner, C.; Mills, S. L. Central effects of cinnarizine: restricted use in aircrew. Aviat. Space Environ. Med. 2002, 73, 570−574. (d) Boolell, M.; Allen, M. J.; Ballard, S. A.; Gepi-Attee, S.; Muirhead, G. J.; Naylor, A. M.; Osterloh, I. H.; Gingell, C. Sildenafil: an orally active type 5 cyclic GMP-specific phosphodiesterase inhibitor for the treatment of penile erectile dysfunction. Int. J. Impot. Res. 1996, 8, 47−52.

[31] (a) Pharis, R. P.; King, R. W. Gibberellins and reproductive development in seed plants. Annu. Rev. Plant Physiol. 1985, 36, 517− 568. (b) Brian, P. W.; Elson, G. W.; Hemming, H. G.; Radley, M. J. The plant growth promoting properties of gibberellic acid, a metabolic product of the fungus Gibberella fugikuroi. J. Sci. Food Agric. 1954, 5, 602−612.

[32] (a) Huigens, R. W., III; Morrison, K. C.; Hicklin, R. W.; Flood, T. A.; Richter, M. F.; Hergenrother, P. J. A ring-distortion strategy to construct stereochemically complex and structurally diverse compounds from natural products. Nat. Chem. 2013, 5, 195−202. (b) Cross, B. E. Gibberellic Acid. Part I. J. Chem. Soc. 1954, 0, 4670− 4676.

[33] Hayek, E. W. H.; Jordis, U.; Moche, W.; Sauter, F. A Bicentennial of Betulin. Phytochemistry 1989, 28, 2229−2242.

[34] Li, T.; Wang, J.; Zheng, X. Simple synthesis of allobetulin, 28- oxyallobetulin and related biomarkers from betulin and betulinic acid catalysed by solid acids. J. Chem. Soc., Perkin Trans. 1 1998, 0, 3957−3966.

[35] (a) Jonnalagadda, S. C.; Suman, P.; Morgan, D. C.; Seay, J. N. Recent Developments on the Synthesis and Applications of Betulin and Betulinic Acid Derivatives as Therapeutic Agents. Stud. Nat. Prod. Chem. 2017, 53, 45−84. (b) Dehelean, C. A.; Soica, C.; Ledeti, I.; Aluas, M.; Zupko, I.; Galuscan, A.; Cinta-Pinzaru, S.; Munteanu, M. Study of the betulin enriched birch bark extracts effects on human carcinoma cells and ear inflammation. Chem. Cent. J. 2012, 6, 137.

[36] Ziberna, L.; Samec, D.; Mocan, A.; Nabavi, S. F.; Bishayee, A.; Farooqi, A. A.; Sureda, A.; Nabavi, S. M. Oleanolic Acid Alters Multiple Cell Signaling Pathways: Implication in Cancer Prevention and Therapy. Int. J. Mol. Sci. 2017, 18, 643−659.

[37] Pattnaik, B.; Lakshma Nayak, V.; Ramakrishna, S.; Venkata Mallavadhani, U. Synthesis of ring-C modified oleanolic acid derivatives and their cytotoxic evaluation. Bioorg. Chem. 2016, 68, 152−158.

[38] Nyffeler, P. T.; Duron, S. G.; Burkart, M. D.; Vincent, S. P.; Wong, C. Selectfluor: Mechanistic Insight and Applications. Angew. Chem., Int. Ed. 2005, 44, 192−212.

[39] (a) Kee, C. W.; Chin, K. F.; Wong, M. W.; Tan, C. Selective fluorination of alkyl C−H bonds via photocatalysis. Chem. Commun. 2014, 50, 8211−8214. (b) Michaudel, Q.; Thevenet, D.; Baran, P. S. Intermolecular Ritter-Type C−H Amination of Unactivated sp3 Carbons. J. Am. Chem. Soc. 2012, 134, 2547−2550.

[40] Gao, D.; Vinogradova, E. V.; Nimmagadda, S. K.; Medina, J. M.; Xiao, Y.; Suciu, R. M.; Cravatt, B. F.; Engle, K. M. Direct Access to Versatile Electrophiles via Catalytic Oxidative Cyanation of Alkenes. J. Am. Chem. Soc. 2018, 140, 8069−8073.

[41] (a) Schuster, D. I.; Lem, G.; Kaprinidis, N. A. New insights into an old mechanism:[2+ 2] photocycloaddition of enones to alkenes. Chem. Rev. 1993, 93, 3−22. (b) Maradyn, D. J.; Weedon, A. C. The photochemical cycloaddition reaction of 2-cyclohexenone with alkenes: trapping of triplet 1, 4-biradical intermediates with hydrogen selenide. Tetrahedron Lett. 1994, 35, 8107−8110.

[42] (a) Yang, J.; Dewal, M. B.; Shimizu, L. S. Self-assembling bisurea macrocycles used as an organic zeolite for a highly stereoselective photodimerization of 2-cyclohexenone. J. Am. Chem. Soc. 2006, 128, 8122−8123. (b) Cecil, J. C.; Dyer, C. W.; Fleming, S. A.; Jessop, T. C. Structural elucidation of a photocycloaddition dimer of cyclohexenone. Anal. Sci. 1999, 15, 895−897.

[43] Ginotra, S. K.; Friest, J. A.; Berkowitz, D. B. Halocarbocycliza- tion entry into the oxabicyclo [4.3. 1] decyl exomethylene-δ-lactone cores of linearifolin and zaluzanin A: exploiting combinatorial catalysis. Org. Lett. 2012, 14, 968−971.

[44] Stokes, B. J.; Opra, S. M.; Sigman, M. S. Palladium-catalyzed allylic cross-coupling reactions of primary and secondary homoallylic electrophiles. J. Am. Chem. Soc. 2012, 134, 11408.

[45] Fukuyama, T.; Nishitani, S.; Inouye, T.; Morimoto, K.; Ryu, I. Effective Acceleration of Atom Transfer Carbonylation of Alkyl Iodides by Metal Complexes. Application to the Synthesis of the Hinokinin Precursor and Dihydrocapsaicin. Org. Lett. 2006, 8, 1383− 1386.

[46] Lu, Z.; Zeng, X.; Hammond, G. B.; Xu, B. Widely Applicable Hydrofluorination of Alkenes via Bifunctional Activation of Hydrogen Fluoride. J. Am. Chem. Soc. 2017, 139, 18202−18205.

[47] Alamillo-Ferrer, C.; Curle, J. M.; Davidson, S. C.; Lucas, S. C. C.; Atkinson, S. J.; Campbell, M.; Kennedy, A. R.; Tomkinson, N. C. O. Alkene Oxyamination Using Malonoyl Peroxides: Preparation of Pyrrolidines and Isoxazolidines. J. Org. Chem. 2018, 83, 6728−6740.

Chapter 4:

Site-Selective Photochemical Fluorination of Ketals: Unanticipated Outcomes in Selectivity and Stability

4.1 Introduction

Although substantial progress has been made over the past decade in taming radical fluorination methods,[1] achieving regioselective sp^3 C−H fluorination on complex molecules remains a fundamental problem in the field. In light of the prominent role of fluorine in biology,[2] medicine,[3] and materials,[4] our group, among others, has begun to address this problem.[5] For instance, we have demonstrated that carbonyl groups can direct aliphatic fluorination in polycyclic enone- and ketone-containing substrates.[6] Moreover, we and others have shown that innate regioselective fluorination can be achieved when the substrate contains an activated C−H bond (e.g., at a benzylic or allylic site) or when bulky substituents provide a steric bias.[7] One type of activated site that surprisingly is less targeted in the world of radical fluorination is the α-ethereal C−H bond. Given our long-standing interest in expanding the utility of aliphatic fluorination, we have developed a site-selective photochemical approach to the synthesis of relatively stable and isolable α-fluoroketals and carbamates that presents interesting problems in chemical reactivity. The first issue concerns stability—why of a pair of closely related products was only one isolable? The question of why only select α-ethereal hydrogen atoms are targeted is addressed through computations. Finally, an interesting total regiochemical switch upon minor structural modification of a diketal is also analyzed.

The gem-oxyfunctionalized products are of synthetic interest—particularly in the case of more stable compounds in this class, such as Teflon AF (a unique polymer material)[8] and fluorinated carbohydrates[9] (including 2′-OMe,4′-F-rU—an important tool for studying nucleic acids).[10] Various synthetic methods have been developed to access α- fluoroethers that generally rely on nucleophilic or electrophilic fluorination functional group interconversion (FGI) strategies. For example, diethylaminosulfur trifluoride (DAST) and Selectfluor have been employed as nucleophilic and electrophilic sources of fluorine, respectively, in the synthesis of glycosyl fluorides.[11] These are the most commonly encountered type of fluorinated sugars in the literature due to the well- established reactivity at the anomeric position. Other positions have also been fluorinated utilizing the same nucleophilic and electrophilic sources of fluorine; however, they typically require specialized precursors and/or longer syntheses.[12] Only a few C−H functionalization methods are known to produce gem-oxyfluorides directly from their corresponding ethers, esters, or other oxygen-containing substrates. For one, Vincent and co-workers reported aliphatic α-fluorination of simple cyclic ethers using N-fluorobis(trifluoromethane-sulfonimide) (NFSI).[13] The Hamashima group has also described two examples of photochemical α-fluorination of esters in moderate yield that is directed by a phthalimide group tethered to the substrate.[14] Beyond photochemical approaches, the α-fluorination of ethers, esters, lactones, and carbonates has been accomplished electrochemically, albeit on only simple and symmetrical small molecules.[15] Despite these initial reports, a recent review on this topic echoes the fact that selective, radical C−H fluorination of carbohydrates is significantly underexplored compared to traditional approaches.[16] We believe the photochemical fluorination described herein represents a piece of this

expanding repertoire and opens new avenues toward the synthesis of novel fluorinated sugars and other carbohydrates.

4.2. Screening

The discovery of the reaction was tied to two serendipitous results. In 2017, we reported a peculiar instance of tandem site-selective sp^3 C−H fluorination/hydroxylation of a complex spiroketal that suggested a key intermediacy of an unstable α-fluoroether formed under our photochemical conditions (Figure 4.1).[17] More recently, we had an interest in studying the steroid desonide to probe the aptitude of rigid ketals in directing aliphatic fluorination using Selectfluor, visible light, and a photoinitiator—analogous to our carbonyl- directed work. Although the product was different from what we initially expected, we found that the fluorination is highly

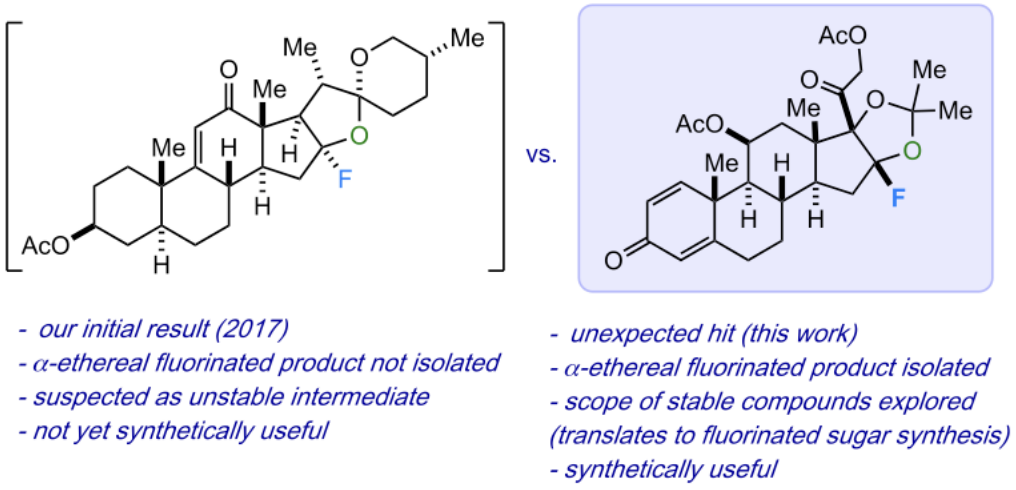

Figure 4.1. Serendipitous discovery of α-ethereal C−H fluorination on complex molecules.

regioselective and the product very stable and isolable. Shortly thereafter, we also discovered that regioselective fluorination of glucose diacetonide acetate to produce compound **1** can also be achieved under similar conditions, and we proceeded to screen for optimized conditions with this substrate (Table 4.1).

It was quickly determined that the reaction requires a photosensitizer (entries 1−3). Although the desired product was observed under 300 nm irradiation in the presence of catalytic 1,2,4,5-tetracyanobenzene (entry 4), we were also interested in exploring milder visible-light-mediated approaches. Accordingly, we screened several known visible light sensitizers in combination with compact fluorescent light (CFL) bulbs. We were pleased to find that benzil, 5-dibenzosuberenone, fluorenone, xanthone,[18] and benzophenone were all competent promoters of the reaction, with xanthone producing the highest yield of the

Table 4.1. Screening for Reaction Conditions.

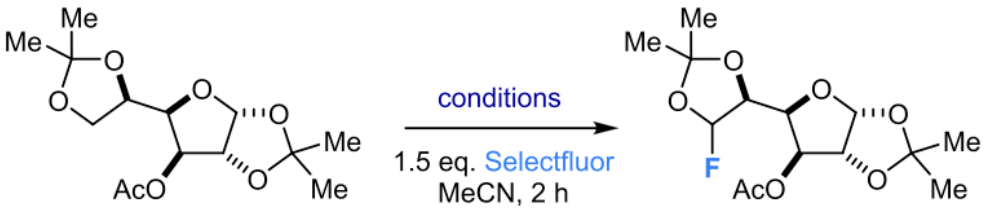

entry	conditions	% yield
1	dark (rt)	0%
2	dark (80 °C)	0%
3	hν (300 nm)	trace
4	hν (300 nm), w/ 1,2,4,5-tetracyanobenzene (0.1 eq.)	55%
5	hν (CFLs), w/ benzil (0.1 eq.)	72%
6	hν (CFLs), w/ benzil (0.1 eq.), NFSI instead of SF	0%
7	hν (CFLs), w/ 5-dibenzosuberenone (0.1 eq.)	44%
8	hν (CFLs), w/ fluorenone (0.1 eq.)	42%
9	hν (CFLs), w/ benzophenone (0.1 eq.)	59%
10	hν (CFLs), w/ xanthone (0.1 eq.)	**74%**

desired fluoride (Table 4.1, entries 5 and 7−10). Additionally, we explored NFSI as an alternative fluorine source, but the desired product was not observed, thereby hinting at the importance of Selectfluor as the fluorinating reagent in this transformation. Lastly, we found that short reaction times (around 2−3 h) work best, as the fluorination occurs fairly rapidly, and slight product decomposition was observed in some cases after longer periods of time.

4.3. Substrate Examples

In agreement with our previous site-selective photochemical fluorination methods, the reaction generally works best on complex polycyclic molecules (Table 4.2) – a paradoxical finding that we can rationalize as a consequence of the increased rigidity of the substrate and its ease of oxidation.[19] Sugar diacetonides are ideal substrates in the reaction due to their rigid nature, in addition to their abundance and ease of preparation.[20] Moreover, sugar acetonides possess a myriad of synthetic applications and are biologically active in certain contexts.[21] Diacetonide esters of glucose, galactose, fructose, and mannose undergo regioselective fluorination in good to excellent yields (54−91%) to provide compounds **1**, **2**, **3**, and **5**, respectively. Another sugar derivative that undergoes the site-selective fluorination in high yield is an acetonide derivative of vitamin C to give compound **4**.[22] Additionally, fluoride **8** was synthesized selectively from an adduct of glucose diacetonide and androstanediol. Such glycosteroids play important roles in medicine and biology;[23] however, their fluorinated counterparts are rare in the literature. In addition to our survey of monosaccharide substrates, aforementioned steroid **7** (a derivative of the allergy drug Nasacort)[24] formed with excellent regio- and stereoselectivity to give a single isomer of an

Table 4.2. Product Examples.

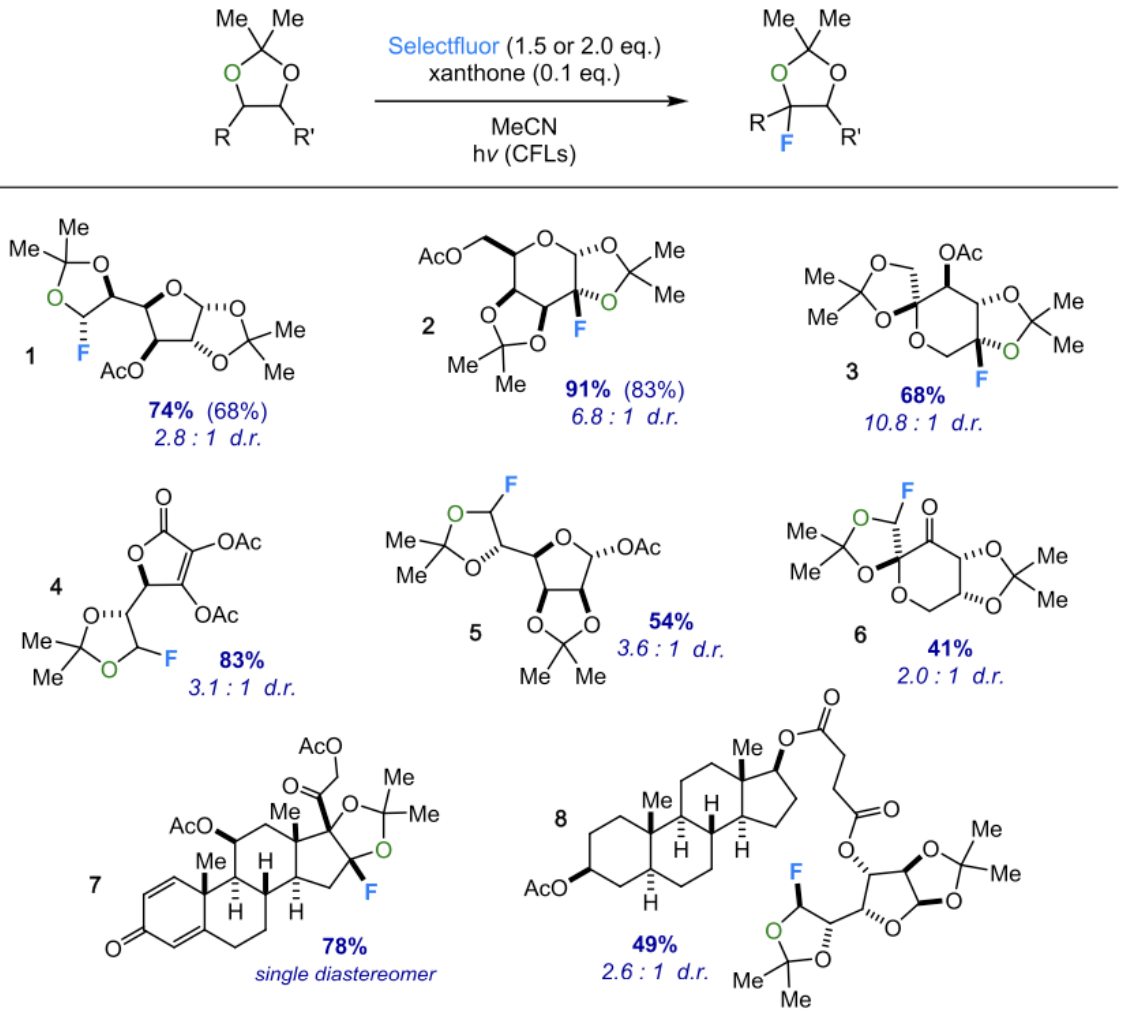

α-fluoroketal in high yield under optimized conditions. Significantly, we noted that the less-hindered (i.e., secondary) α-ethereal position is often favored but found an anomalous instance in compound **3**. Moreover, at a glance, it is not necessarily intuitive why certain tertiary α-ethereal positions are favored over others.

We next turned our attention to another class of important biomolecules, N-protected amino acids, to demonstrate fluorination of carbamates in a site-selective manner (Figure 4.2a). For example, N-carbobenzoxy-L-isoleucine (Z-Ile-OH) is a competent substrate in

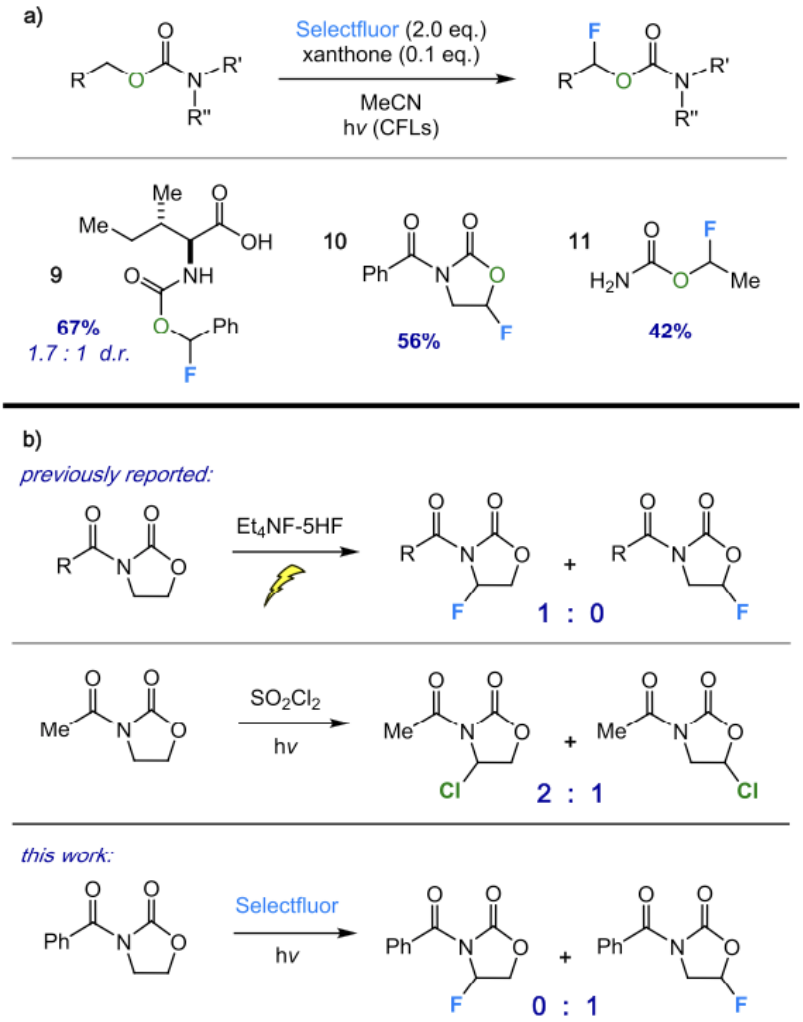

Figure 4.2. Application to carbamates.

the reaction, producing compound **9** selectively. Significantly, no fluorination was observed on the secondary or tertiary positions of the sec-butyl side chain found in isoleucine, even with 2.0 equiv of Selectfluor. Analogous oxazolidinones also work as substrates. They possess an array of biological activity[25] and are an important category of chiral auxiliaries in synthetic organic chemistry.[26] We synthesized compound **10** in good yield from 3-benzoyl-2-oxazolidinone (though enantioselective C−H fluorination of such

a compound remains an alluring goal). Only one similar gem- oxyfluorinated oxazolidinone can be found in the literature; however, the heterocycle was prepared in low yield from a fluorinated precursor rather than direct C−H functionalization of the oxazolidinone.[27] The regioselectivity of the reaction to form compound **10** is remarkable given the previously reported halogenations of oxazolidinones (Figure 2b). For example, electrochemical fluorination of N-acyl oxazolidinones gives exclusively the "other" regioisomer (α to nitrogen).[28] Moreover, photo- chemical chlorination of these substrates using sulfuryl chloride gives a 2:1 ratio of regioisomers, with the chloride α to nitrogen being favored.[29] Thus, our oxazolidinone fluorination is uniquely selective as it not only results in a single regioisomer, but the fluoride is geminal to oxygen rather than to nitrogen. One further example of the carbamate α- fluorination that we explored involves a much smaller molecule known as urethane (ethyl carbamate). Although this method seems to work best with larger, more complex substrates, this compound undergoes fluorination in moderate yield to give a molecule that, to our surprise, has not been previously prepared (compound **11**). Thus, the reaction can occur for both aliphatic and benzylic carbamates, as well as both cyclic and acyclic carbamates.

In addition to carbamates, we also found that both benzylic and aliphatic carbonate esters can partake in the site-selective fluorination; for example, both diethyl and dibenzyl carbonate were competent substrates in the reaction. Unfortunately, we observed that the yields were generally lower for these reactions, which we attributed to decreased stability of the gem-oxyfluorides relative to those of carbamates. Similarly, we found that ethers, such as N-acetylmorpholine, are also able to participate in the reaction, although the

resulting fluorides also seemed to be less stable and lower yielding than the ketals that we tested.

4.4. Site-Selectivity in Sugar Diacetonides.

We were intrigued by the observed regioselectivity of the fluorination of sugar diacetonides, as each substrate contains several distinct α-ethereal C−H bonds, yet excellent site-selectivity was observed in each case. Furthermore, the selectivity pattern exhibited in Table 2 is not particularly consistent with putative bond dissociation energies of α-ethereal C−H bonds. C−H bonds that are geminal to both oxygen atoms of an acetal, for instance, have bond dissociation energies (BDEs) that are ~23 kJ/mol lower than that of α-ethereal C−H bonds of acetonides.[30] In Table 2, the fluorination of galactose diactonide presents the most intriguing example, as one C− H bond is targeted among a host of ethereal bonds, three of which are fairly similar sterically and electronically (Figure 3, top).

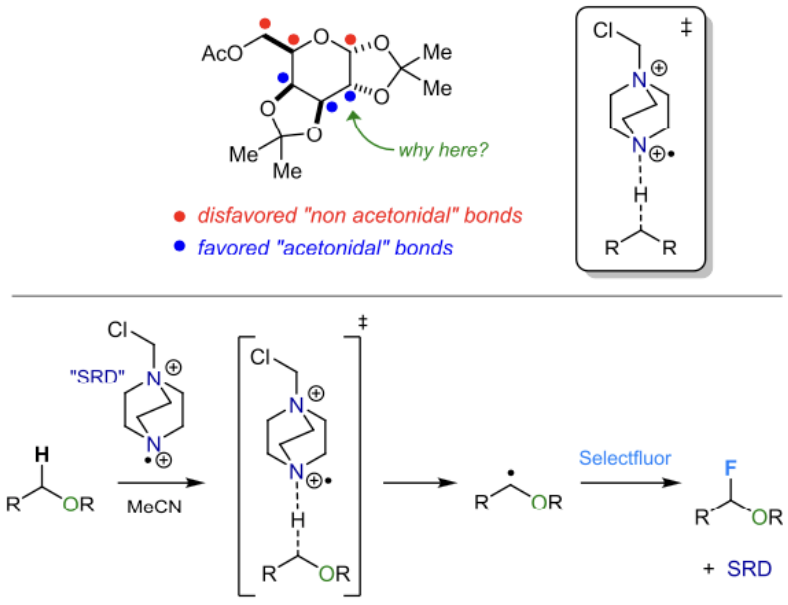

Figure 4.3. Possible functionalization sites in galactose diacetonide; hydrogen atom transfer through Selectfluor radical dication.

The radical dication derived from Selectfluor has been proposed to play a key role in hydrogen atom abstractions from alkanes and related classes of compounds (Figure 4.3, bottom).[31,32] In the case of ketal and carbamate substrates, a hydrogen atom geminal to oxygen is selectively abstracted to form a stabilized radical, which then is fluorinated by Selectfluor, thereby forming an α-ethereal fluoride and regenerating the Selectfluor radical dication to propagate a chain reaction. To better understand the basis of this reactivity, density functional theory (DFT) calculations were performed at the IEFPCM$_{(CH_3CN)}$UB3LYP/6-311++G(2d,2p)// UB3LYP/6-31G(d)[33] level using the Gaussian 09 software package.[34] Emerging from these computations was hydrogen atom transfer transition state TS_{C2} with a Gibbs free energy activation barrier ($\Delta G^{\ddagger}$) of 7.4 kcal mol^{-1} with respect to the separate reagents. Within this transition state, the reactive Selectfluor radical dication species is positioned for hydrogen atom transfer from carbon C(2), and there are minimal steric contacts; for example, the shortest C−H···H distance between the radical dication and the galactose diacetonide substrate was 2.38 Å, just inside the sum of the van der Waals radii of the two hydrogen atoms (Figure 4.4A).

Present in this transition state structure as well were stabilizing noncovalent interactions, clearly visible from the noncovalent interaction plot in Figure 4.4B (left-hand side). Short C−H···O contacts of 2.34 and 2.39 Å and natural bond order (NBO) charges (O = −0.644e, H = 0.307e, H = 0.296e) additionally corroborated the presence of favorable interactions, notably, with an underlying Coulombic charge component. Coupled with

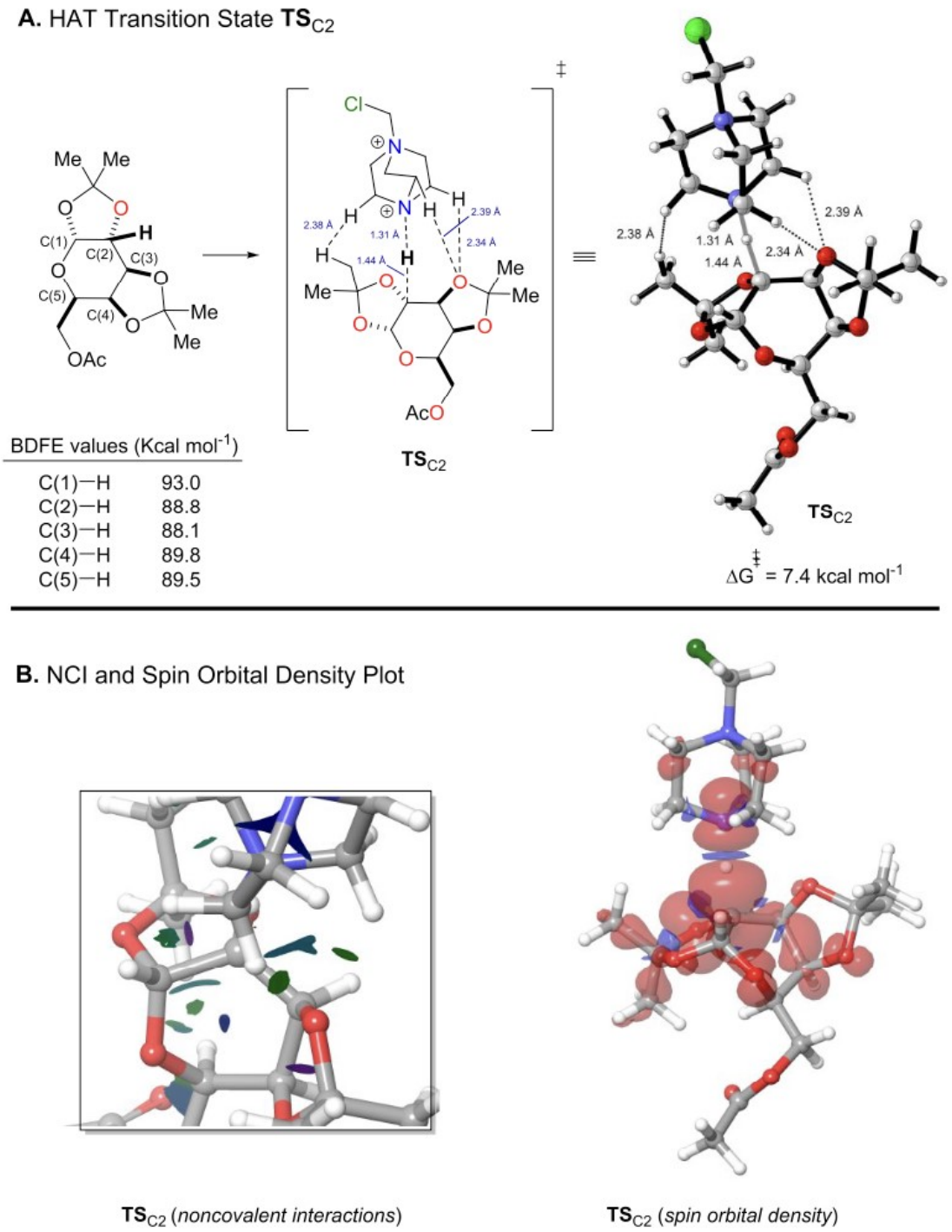

Figure 4.4. Computed transition state structure TSC2 for hydrogen atom transfer from galactose diacetonide.

these interactions was a stabilizing stereoelectronic anomeric effect, viz. unshared oxygen lone pair donation into an antibonding σ*-orbital of the exocyclic C(1)−O bond as supported by NBO analysis ($E_{n(O)\rightarrow C-O^*}$ = 9.16 kcal mol^{-1}). Last was a comparable distribution of spin density across the hydrogen atom transfer bond breaking and bond making subassembly with distances of 1.31 and 1.44 Å (Figure 4.4b, right-hand side). Significantly, we established the transition states in which hydrogen atom transfer occurs at the other α-ethereal positions (especially the sites α to two ether oxygen atoms and α to an acetate ester), that is, hydrogen atom transfer from C(1), C(3), C(4), or C(5) via TS_{C1} or TS_{C3-5} to be of higher energy ($\Delta G^{\ddagger}$ > 13 kcal mol^{-1}) than TS_{C2} (see SI for additional details and hydrogen atom transfer transition state structures TS_{C1} and $TS_{C3\text{-}5}$). In each case, a complex interplay of steric and electronic effects makes generalizations difficult. This selectivity is additionally remarkable as, based on the computed bond dissociation free energies of C(1)−H−C(5)−H, a lack of hydrogen atom transfer site-selectivity would be expected (Figure 4.4A).

4.5. Regioselectivity Switch.

An important trend that was noted in regard to regioselectivity was the general (although not strict) preference for fluorination at secondary positions over tertiary ones. For example, the glucose, mannose, ascorbic acid, and glycosteroid derivatives described above reacted with this selectivity pattern. Conversely, the fructose diacetonide ester fluorinates at a tertiary position of the ketal, although an enticing secondary position is available. We were astonished to discover that the regioselectivity of this fluorination could be switched by altering the substrate to include a ketone rather than an acetoxy group

(Figure 5a). This fructose diacetonide ketone derivative, better known as Shi's epoxidation diketal catalyst,[35] fluorinates in a site-selective fashion to give a secondary fluoride (compound 6). Given some of our recent work in the area, we attributed this selectivity switch to carbonyl direction, as the ketone is properly poised to direct fluorination to the β-position in a manner analogous to terpenoidal ketone-directed fluorination.[6] On the other hand, exceptionally good overlap between the forming radical of the hydrogen atom

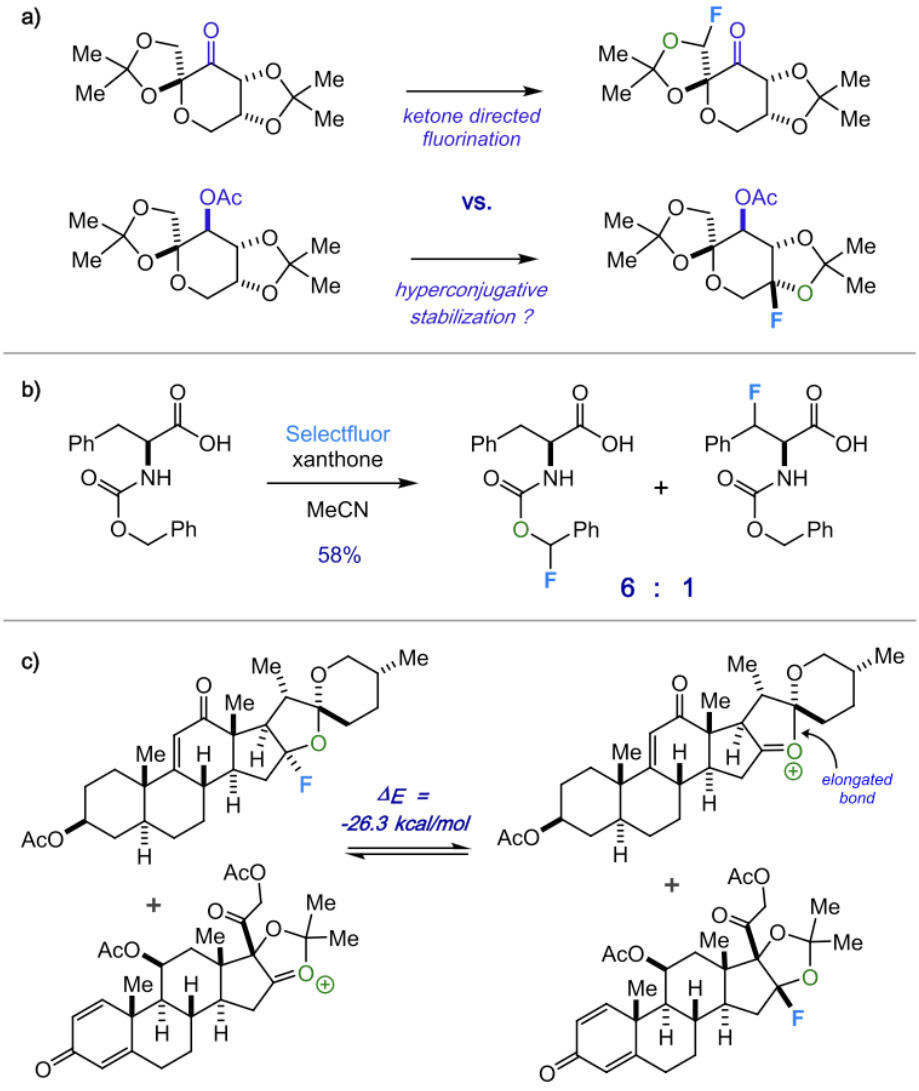

Figure 4.5. Regioselectivity and stability studies.

transfer C−H−N subarray and the endocyclic σ*(C−O) (which can be overcome only by carbonyl activation) could help explain this finding.[36]

Another area that we briefly explored was site-selectivity in the reaction of benzyl carbamates in the presence of other benzylic sites. N-Carbobenzoxy-L-phenyalanine (Z-Phe-OH) provides an ideal model substrate for this test. Fluorination of Z-Phe-OH under our reaction conditions produces a 6:1 regioisomeric ratio of products in 58% yield, with fluorination at the benzyl carbamate being greatly preferred over the normal benzylic position (Figure 5b). Although this observed selectivity is significant, we are currently investigating other ways to improve the regioselectivity to further expand the utility of this reaction.

4.6. Stability of Fluorinated Acetonides versus Spiroketals

As previously mentioned, our isolation of ketal **7** was unexpected given our prior result of a fluorinated spiroketal that was unstable and rearranged in situ. To gain some insight on this discrepancy, we considered an isodesmic relation between these two fluorides and their corresponding defluorinated oxocarbenium ions (Figure 5c). At the B3LYP/ 6-31+G** level of theory, we calculated the ΔE of the isodesmic reaction to be −26.3 kcal/mol. This energy difference is noteworthy and indicates a highly exothermic process in which the α-ethereal fluoride of the spiroketal is displaced to give a highly stabilized cation with an elongated (C−O) bond. Significantly, this result is consistent with our empirical findings that the fluorinated spiroketal was not isolable, whereas the fluorinated acetonide was straightforward to isolate.

In general, we found the α-ethereal fluorides of acetonide ketals and carbamates to be surprisingly stable, persisting through aqueous workup and silica gel chromatography. Beyond the synthesis of the fluorides themselves, we imagined that we could expand the scope of the reaction to derivatize the products into other useful compounds through defluorination. For example, we added 10 equiv of water into the reaction of sugar **1** after the fluorination transpired and allowed the mixture to stir overnight at room temperature. To our surprise, most of the fluoride remained intact, as determined by ^{19}F NMR. Whereas some precedent exists for the nucleophilic substitution of similar gem-oxyfluorides, the substrate scope is generally limited to simple molecules.[4,37]

4.7. Conclusion.

A site-selective photochemical fluorination was developed that accesses α-ethereal fluorides from ketals and carbamates using Selectfluor, catalytic xanthone, and visible light. The method appears to be best suited for rigid substrates such as steroids and sugar diacetonides and has also been demonstrated on simpler molecules, as well. Moreover, the gem-oxyfluoride products reported herein are notably stable and isolable. A DFT-computed transition state illuminated details on the origin of the site-selectivity of the reaction and presented a possible explanation for a regioselectivity switch that was observed in fructose derivatives. In all, developing this ability to target the α-ethereal C−H bond represents a promising approach to regioselective fluorination of complex molecules, which is complementary to the existing tactics: (1) relying on steric/electronic influences for serendipitous selectivity, (2) targeting benzylic/allylic C−H bonds, and (3) using enone or ketone-based (or other external) directing groups.

4.8. References.

[1] For some of the pioneering work in contemporary radical fluorination methodologies, see: (a) Rueda-Becerril, M.; Chatalova Sazepin, C.; Leung, J. C. T.; Okbinoglu, T.; Kennepohl, P.; Paquin, J.- F.; Sammis, G. M. Fluorine Transfer to Alkyl Radicals. J. Am. Chem. Soc. 2012, 134, 4026−4029. (b) Liu, W.; Huang, X.; Cheng, M.-J.; Nielsen, R. J.; Goddard, W. A., III; Groves, J. T. Oxidative Aliphatic C-H Fluorination with Fluoride Ion Catalyzed by a Manganese Porphyrin. Science 2012, 337, 1322−1325. (c) Bloom, S.; Pitts, C. R.; Miller, D.; Haselton, N.; Holl, M. G.; Urheim, E.; Lectka, T. A Polycomponent Metal-Catalyzed Aliphatic, Allylic, and Benzylic Fluorination. Angew. Chem., Int. Ed. 2012, 51, 10580−10583.

[2] Shah, P.; Westwell, A. D. The role of fluorine in medicinal chemistry. J. Enzyme Inhib. Med. Chem. 2007, 22, 527−540. (b) Hiyama, T.; Yamamoto, H. Biologically Active Organofluorine Compounds. Organofluorine Compounds 2000, 1, 137−182.

[3] O'Hagan, D. Fluorine in health care: Organofluorine containing blockbuster drugs. J. Fluorine Chem. 2010, 131, 1071−1081. (b)Wang,J.;Sańchez-Rosello,́M.;Aceña,J.L.;delPozo,C.; Sorochinsky, A. E.; Fustero, S.; Soloshonok, V. A.; Liu, H. Fluorine in Pharmaceutical Industry: Fluorine-Containing Drugs Introduced to the Market in the Last Decade (2001−2011). Chem. Rev. 2014, 114, 2432−2506.

[4] Ragni, R.; Punzi, A.; Babudri, F.; Farinola, G. M. Organic and Organometallic Fluorinated Materials for Electronics and Optoelec- tronics: A Survey on Recent Research. Eur. J. Org. Chem. 2018, 2018, 3500−3519.

[5] (a) Bume, D. D.; Harry, S. A.; Lectka, T.; Pitts, C. R. Catalyzed and Promoted Aliphatic Fluorination. J. Org. Chem. 2018, 83, 8803− 8814. (b) Miao, J.; Yang, K.; Kurek, M.; Ge, H. Palladium-Catalyzed Site-Selective Fluorination of Unactivated C(sp^3)−H Bonds. Org. Lett. 2015, 17, 3738−3741. (c) Yuan, Z.; Nodwell, M. B.; Yang, H.; Malik, N.;Merkens,H.;Beńard,F.;Martin,R.E.;Schaffer,P.;Britton,R. Site-Selective, Late-Stage C−H ^{18}F-Fluorination on Unprotected Peptides for Positron Emission Tomography Imaging. Angew. Chem., Int. Ed. 2018, 57, 12733−12736. (d) Wu, L.; Cao, X.; Chen, X.;

Fang, W.; Dolg, M. Visible-Light Photocatalysis of C(sp^3)-H Fluorination by the Uranyl Ion: Mechanistic Insights. Angew. Chem., Int. Ed. 2018, 57, 11812−11816.

[6] (a) Bume, D. D.; Pitts, C. R.; Ghorbani, F.; Harry, S. A.; Capilato, J. N.; Siegler, M. A.; Lectka, T. Ketones as Directing Groups in Photocatalytic sp^3 C-H Fluorination. Chem. Sci. 2017, 8, 6918− 6923. (b) Bume, D. D.; Harry, S. A.; Pitts, C. R.; Lectka, T. Sensitized Aliphatic Fluorination Directed by Terpenoidal Enones: A "Visible Light" Approach. J. Org. Chem. 2018, 83, 1565−1575.

[7] (a) Bloom, S.; Pitts, C. R.; Woltornist, R.; Griswold, A.; Holl, M. G.; Lectka, T. Iron(II)-Catalyzed Benzylic Fluorination. Org. Lett. 2013, 15, 1722−1724. (b) Liu, W.; Groves, J. T. Manganese-Catalyzed Oxidative Benzylic C-H Fluorination by Fluoride Ions. Angew. Chem., Int. Ed. 2013, 52, 6024−6027. (c) Bloom, S.; Knippel, J. L.; Holl, M. G.; Barber, R.; Lectka, T. A Cooperative Allylic Fluorination: Combination of Nucleophilic and Electrophilic Fluorine Sources. Tetrahedron Lett. 2014, 55, 4576−4580. (d) Bume, D. D.; Pitts, C. R.; Jokhai, R. T.; Lectka, T. Direct, Visible Light-Sensitized Benzylic C-H Fluorination of Peptides using Dibenzosuberenone: Selectivity for Phenylalanine-Like-Residues. Tetrahedron 2016, 72, 6031−6036. (e) Danahy, K. E.; Cooper, J. C.; Van Humbeck, J. F. Benzylic Fluorination of Aza-Heterocycles Induced by Single-Electron Transfer to Selectfluor. Angew. Chem., Int. Ed. 2018, 57, 5134−5138.

[8] Lowry, J. H.; Mendlowitz, J. S.; Subramanian, N. S. Optical characteristics of Teflon AF® fluoroplastic materials. Opt. Eng. 1992, 31, 1982−1985.

[9] Sharma, M.; Bernacki, R. J.; Korytnyk, W. Fluorinated Analogs of Cell-Surface Carbohydrates as Potential Chemotherapeutic Agents. Fluorinated Carbohydrates, ACS Symposium Series; American Chemical Society: Washington, DC, 1988; Vol. 374, pp 191−206.

[10] Malek-Adamian, E.; Patrascu, M. B.; Jana, S. K.; Martínez- Montero, S.; Moitessier, N.; Damha, M. J. Adjusting the structure of 2′-modified nucleosides and oligonucleotides via C4′-α-F or C4′-α- OMe substitution: synthesis and conformational analysis. J. Org. Chem. 2018, 83 (17), 9839−9849.

[11] Hein, M.; Miethchen, R. Fluorinated Carbohydrates. Advances in Organic Syntheses; Bentham Science Publishers, 2012; Vol. 2, pp 381−429.

[12] (a) Burton, A.; Wyatt, P.; Boons, G. J. Preparation of fluorinated galactosyl nucleoside diphosphates to study the mecha- nism of the enzyme galactopyranose mutase. J. Chem. Soc., Perkin Trans. 1 1997, 1, 2375−2382. (b) Akiyama, Y.; Hiramatsu, C.; Fukuhara, T.; Hara, S. Selective introduction of a fluorine atom into carbohydrates and a nucleoside by ring-opening fluorination reaction of epoxides. J. Fluorine Chem. 2006, 127, 920−923.

[13] Beniazza,R.;Abadie,B.;Remisse,L.;Jardel,D.;Lastećoueѐres, D.; Vincent, J. Light-promoted metal-free cross dehydrogenative couplings on ethers mediated by NFSI: reactivity and mechanistic studies. Chem. Commun. 2017, 53, 12708−12711.

[14] Egami, H.; Masuda, S.; Kawato, Y.; Hamashima, Y. Photo- fluorination of Aliphatic C−H Bonds Promoted by the Phthalimide Group. Org. Lett. 2018, 20, 1367−1370.

[15] Hasegawa, M.; Ishii, H.; Cao, Y.; Fuchigami, T. Regioselective Anodic Monofluorination of Ethers, Lactones, Carbonates, and Esters Using Ionic Liquid Fluoride Salts. J. Electrochem. Soc. 2006, 153, D162−D166.

[16] Uhrig, M. L.; Lantaño, B.; Postigo, A. Synthetic strategies for fluorination of carbohydrates. Org. Biomol. Chem. 2019, 17, 5173− 5189.

[17] Pitts, C. R.; Siegler, M. A.; Lectka, T. An Intermolecular Aliphatic C-F—H-C Interaction in the Presence of 'Stronger' Hydrogen Bond Acceptors: Crystallographic, Computational, and IR Studies. J. Org. Chem. 2017, 82, 3996−4000.

[18] Xia, J.-B.; Zhu, C.; Chen, C. Visible Light-Promoted Metal-Free C−H Activation: Diarylketone-Catalyzed Selective Benzylic Mono- and Difluorination. J. Am. Chem. Soc. 2013, 135, 17494−17500.

[19] Pitts, C. R.; Bume, D. D.; Harry, S. A.; Siegler, M. A.; Lectka, T. Multiple Enone-Directed Reactivity Modes Lead to the Selective Photochemical Fluorination of Polycyclic Terpenoid Derivatives. J. Am. Chem. Soc. 2017, 139, 2208−2211.

[20] Weymouth-Wilson, A. C.; Clarkson, R. A.; Jones, N. A.; Best, D.;Wilson,F.X.;Pino-GonzaĺEz,M.S.;Fleet,G.W.J.Largescale synthesis of the acetonides of l-glucuronolactone and of l-glucose: easy access to l-sugar chirons. Tetrahedron Lett. 2009, 50, 6307−6310.

[21] Movsisyan,L.D.;Schaf̈er,E.;Nguyen,A.;Ehrmann,F.R.; Schwab, A.; Rossolini, T.; Zimmerli, D.; Wagner, B.; Daff, H.; Heine, A.; Klebe, G.; Diederich, F. Sugar Acetonides are a Superior Motif for Addressing the Large, Solvent-Exposed Ribose-33 Pocket of tRNA- Guanine Transglycosylase. Chem. - Eur. J. 2018, 24, 9957−9967.

[22] Padayatty, S. J.; Katz, A.; Wang, Y.; Eck, P.; Kwon, O.; Lee, J. H.; Chen, S.; Corpe, C.; Dutta, A.; Dutta, S. K.; Levine, M. Vitamin C as an Antioxidant: Evaluation of Its Role in Disease Prevention. J. Am. Coll. Nutr. 2003, 22, 18−35.

[23] Ekholm, F. S.; Schneider, G.; Wölfling, J.; Leino, R. Synthesis of a Small Library of Estradiol-Based Glycosteroid Mimics Containing a Modified D-Ring. Eur. J. Org. Chem. 2011, 2011 (6), 1064−1077.

[24] Tano, Y.; Chandler, D.; Machemer, R. Treatment of Intraocular Proliferation with Intravitreal Injection of Triamcinolone Acetonide. Am. J. Ophthalmol. 1980, 90, 810−816.

[25] Diekema, D. J.; Jones, R. N. Oxazolidinone antibiotics. Lancet 2001, 358, 1975−1982.

[26] Heravi, M. M.; Zadsirjan, V. Oxazolidinones as chiral auxiliaries in asymmetric aldol reactions applied to total synthesis. Tetrahedron: Asymmetry 2013, 24, 1149−1188.

[27] Verniest, G.; Colpaert, F.; Van Hende, E.; De Kimpe, N. Synthesis and Reactivity of 1-Substituted 2-Fluoro- and 2,2- Difluoroaziridines. J. Org. Chem. 2007, 72, 8569−8572.

[28] Cao, Y.; Suzuki, K.; Tajima, T.; Fuchigami, T. Electrolytic partial fluorination of organic compounds. Part 78: Regioselective anodic fluorination of 2-oxazolidinones. Tetrahedron 2005, 61, 6854− 6859.

[29] Gaenzler, F. C.; Smith, M. B. A Dichlorination−Reductive- Dechlorination Route to N-Acetyl-2-Oxazolone. Synlett 2007, 2007, 1299−1301.

[30] Tumanov, V. E. Calculation of the C−H Bond Dissociation Energies in Linear and Cyclic Acetals and Thioacetals from Kinetic Data. Petroleum Chemistry 2005, 45, 350−363.

[31] (a) Pitts, C. R.; Bloom, S.; Woltornist, R.; Auvenshine, D. J.; Ryzhkov, L. R.; Siegler, M. A.; Lectka, T. Direct, Catalytic Monofluorination of sp^3 C-H Bonds: A Radical-Based Mechanism with Ionic Selectivity. J. Am. Chem. Soc. 2014, 136, 9780−9791. (b) Kee, C. W.; Chin, K. F.; Wong, M. W.; Tan, C. Selective fluorination of alkyl C−H bonds via photocatalysis. Chem. Commun. 2014, 50, 8211−8214.

[32] (a) Capilato, J. N.; Bume, D. D.; Lee, W. H.; Hoffenberg, L. E. S.; Jokhai, R. T.; Lectka, T. Fluorofunctionalization of C□C Bonds with Selectfluor: Synthesis of β-Fluoropiperazines through a Substrate-Guided Reactivity Switch. J. Org. Chem. 2018, 83, 14234−14244. (b) Pitts, C. R.; Ling, B.; Snyder, J. A.; Bragg, A. E.; Lectka, T. Aminofluorination of Cyclopropanes: A Multifold Approach through a Common, Catalytically Generated Intermediate. J. Am. Chem. Soc. 2016, 138, 6598−6609. (c) Bloom, S.; Bume, D. D.; Pitts, C. R.; Lectka, T. Site-Selective Approach to β-Fluorination: Photocatalyzed Ring Opening of Cyclopropanols. Chem. - Eur. J. 2015, 21, 8060−8063.

[33] (a) Becke, A. D. Density-functional thermochemistry. III. The role of exact exchange. J. Chem. Phys. 1993, 98, 5648−5652. (b) Francl, M. M.; Pietro, W. J.; Hehre, W. J.; Binkley, J. S.; Gordon, M. S.; DeFrees, D. J.; Pople, J. A. Self-consistent molecular orbital methods. XXIII. A polarization-type basis set for second-row elements. J. Chem. Phys. 1982, 77, 3654−3665. (c) Lee, C.; Yang, W.; Parr, R. G. Development of the Colle-Salvetti correlation-energy formula into a functional of the electron density. Phys. Rev. B: Condens. Matter Mater. Phys. 1988, 37, 785.

[34] Frisch, M. J.; Trucks, G. W.; Schlegel, H. B.; Scuseria, G. E.; Robb, M. A.; Cheeseman, J. R.; Scalmani, G.; Barone, V.; Mennucci, B.; Petersson, G. A.; Nakatsuji, H.; Caricato, M.; Li, X.; Hratchian, H. P.; Izmaylov, A. F.; Bloino, J.; Zheng, G.; Sonnenberg, J. L.; Hada, M.; Ehara, M.; Toyota, K.; Fukuda, R.; Hasegawa, J.; Ishida, M.; Nakajima, T.; Honda, Y.; Kitao, O.; Nakai, H.; Vreven, T.; Montgomery,J.A.,Jr.;Peralta,J.E.;Ogliaro,F.;Bearpark,M.; Heyd, J. J.; Brothers, E.; Kudin, K. N.; Staroverov, V. N.; Kobayashi, R.; Normand, J.; Raghavachari, K.; Rendell, A.; Burant, J. C.; Iyengar, S.S.;Tomasi,J.;Cossi,M.;Rega,N.;Millam,J.M.;Klene,M.;Knox, J. E.; Cross, J. B.; Bakken, V.; Adamo, C.; Jaramillo, J.; Gomperts, R.; Stratmann, R. E.; Yazyev, O.; Austin, A. J.; Cammi, R.; Pomelli, C.; Ochterski, J. W.; Martin, R. L.; Morokuma, K.; Zakrzewski, V. G.; Voth, G. A.; Salvador, P.; Dannenberg, J. J.; Dapprich, S.; Daniels, A. D.; Farkas, O.; Foresman, J. B.; Ortiz, J. V.; Cioslowski, J.; Fox, D. J. Gaussian 09, revision D.01; Gaussian, Inc.: Wallingford, CT, 2009.

[35] Wang, Z. X.; Tu, Y.; Frohn, M.; Zhang, J. R.; Shi, Y. An Efficient Catalytic Asymmetric Epoxidation Method. J. Am. Chem. Soc. 1997, 119, 11224−11235.

[36] Note that we were unsuccessful in isolating the fluorinated Shi catalyst derivative, as we found it to be inseparable from the starting material. Chromatography on silica gel, Florisil, and alumina led only to a 1:1 mixture of starting material and product, due to significant streaking which we believe is caused by hydration of the unusually reactive ketone (see SI).

[37] Rye, C. S.; Baell, J. B.; Street, I. Synthesis, reactivity and applications of 1-fluoroalkyl carboxylates: novel synthetic substrates for esterases and lipases. Tetrahedron 2007, 63, 3306−3311.

[38] Dolbier, W. R. Guide to Fluorine NMR for Organic Chemists, 2nd ed.; John Wiley & Sons, 2016; pp 66−68.

[39] Bantu, R.; Mereyala, H. B.; Nagarapu, L.; Kantevari, S. 3-O- Acyl triggered tandem Lewis acid catalyzed intramolecular cyclization of diacetone glucose derivatives to 5-O-acyl-3,6-anhydro-d-glucose. Tetrahedron Lett. 2011, 52, 4854−4856.

[40] Ch, R.; Tyagi, M.; Patil, P. R.; Ravindranathan Kartha, K. P. DABCO: an efficient promoter for the acetylation of carbohydrates and other substances under solvent-free conditions. Tetrahedron Lett. 2011, 52, 5841−5846.

[41] Zhang, P.; Ling, C. C. A mild acetolysis procedure for the regioselective removal of isopropylidene in di-O-isopropylidene- protected pyranoside systems. Carbohydr. Res. 2017, 445, 7−13.

[42] Matassini, C.; Mirabella, S.; Ferhati, X.; Faggi, C.; Robina, I.; Goti, A.; Moreno-Clavijo, E.; Moreno-Vargas, A. J.; Cardona, F. Polyhydroxyamino-Piperidine-Type Iminosugars and Pipecolic Acid Analogues from a D-Mannose-Derived Aldehyde. Eur. J. Org. Chem. 2014, 5419−5432.

[43] Tu, Y.; Wang, Z. X.; Shi, Y. An Efficient Asymmetric Epoxidation Method for trans-Olefins Mediated by a Fructose- Derived Ketone. J. Am. Chem. Soc. 1996, 118, 9806−9807.

[44] Theodoropoulos, D.; Craig, L. C. The Synthesis of Several Isoleucyl Peptides and Certain of Their Properties. J. Org. Chem. 1955, 20, 1169−1172.

[45] Li, B.; Wang, H.; Zhu, Q.; Shi, Z. Rhodium/Copper-Catalyzed Annulation of Benzimides with Internal Alkynes: Indenone Synthesis through Sequential C-H and C-N Cleavage. Angew. Chem., Int. Ed. 2012, 51, 3948−3952.

Chapter 5

Carbonyl-Directed Aliphatic Fluorination: A Special Type of Hydrogen Atom Transfer Beats Out Norrish II

5.1. Introduction

Putative single-electron transfer (SET) and hydrogen atom transfer (HAT) processes underpin much recent and remarkable synthetic chemistry.[1] The detailed mechanisms by which these reactions occur are generally much less well understood.[2] Under the umbrella of HAT, proton transfers play an additional role, giving rise to a spectrum of mechanistic scenarios: concerted proton-coupled electron transfer (CPET), sequential ET/PT, etc.[3] We recently reported that enone- containing rigid terpenoid derivatives, in which the carbonyl group is positioned to interact through potential five- or six- membered transition states with proximate C−H bonds, afforded alkyl fluorides regioselectively in moderate to high yields upon irradiation at 300 nm in the presence of Selectfluor (SF) (Scheme 5.1).[4]

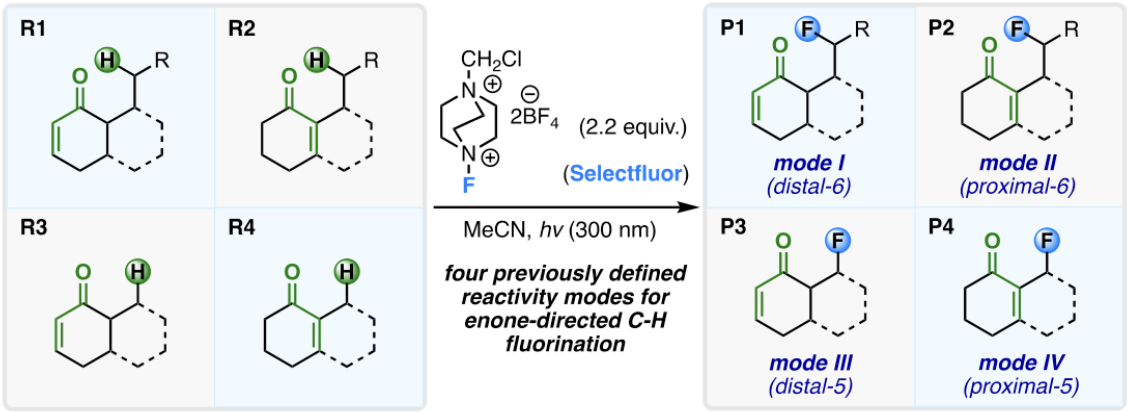

Scheme 5.1 Initial Discovery of Enone-Directed Fluorination Reactivity Modes, Classified Based on (1) Proximity of C=C Bonds to the Reactive Site and (2) Number of Bonds between the Carbonyl Oxygen Atom and the Abstracted Hydrogen Atom

We soon extended the scope of this work to include site- selective fluorination of substrates containing ketones, keto ethers, and benzylic positions activated by carbonyl groups (Figure 5.1).[5]

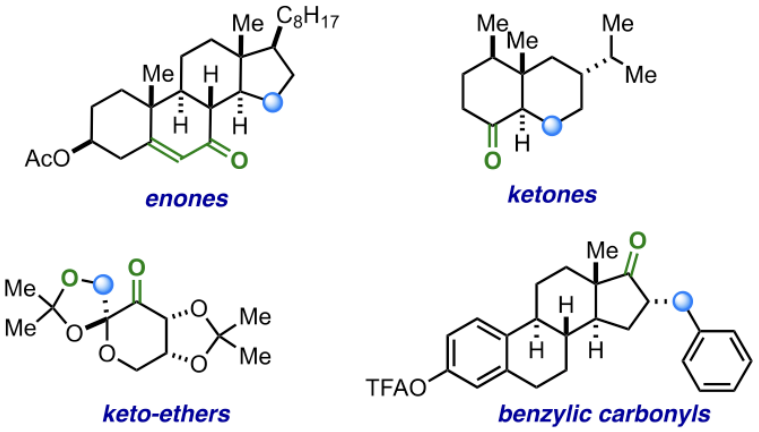

Figure 5.1 Expanded scope of study for carbonyl-directed fluorination in our recent work.

In each successive case, a proximate carbonyl group is poised to interact with a C−H bond through a five- or six-membered ring. On the other hand, how this remarkable transformation occurred was shrouded in mystery; aside from the fact that a proximate carbonyl group exerted a key directing effect, mechanistic details remained speculative.

We settled on five possible mechanistic hypotheses (Figure 2). Initially, our data seemed to comport with an interrupted Norrish II process involving intramolecular HAT (Scenario I). Electron transfer may play a pivotal role—in either sequential electron transfer−proton transfer (ET−PT, Scenario II) or PT−ET, which seems thermodynamically unreasonable but is included for the sake of completeness (Scenario III). Proton- coupled electron transfer, which may represent a point on the mechanistic continuum of HAT, must be

considered a serious alternative (PCET, Scenario IV). On the other hand, direct, rate-determining HAT remained a possibility, although this scenario begs the question of what precise role the carbonyl group plays in directing the reaction (Scenario V).

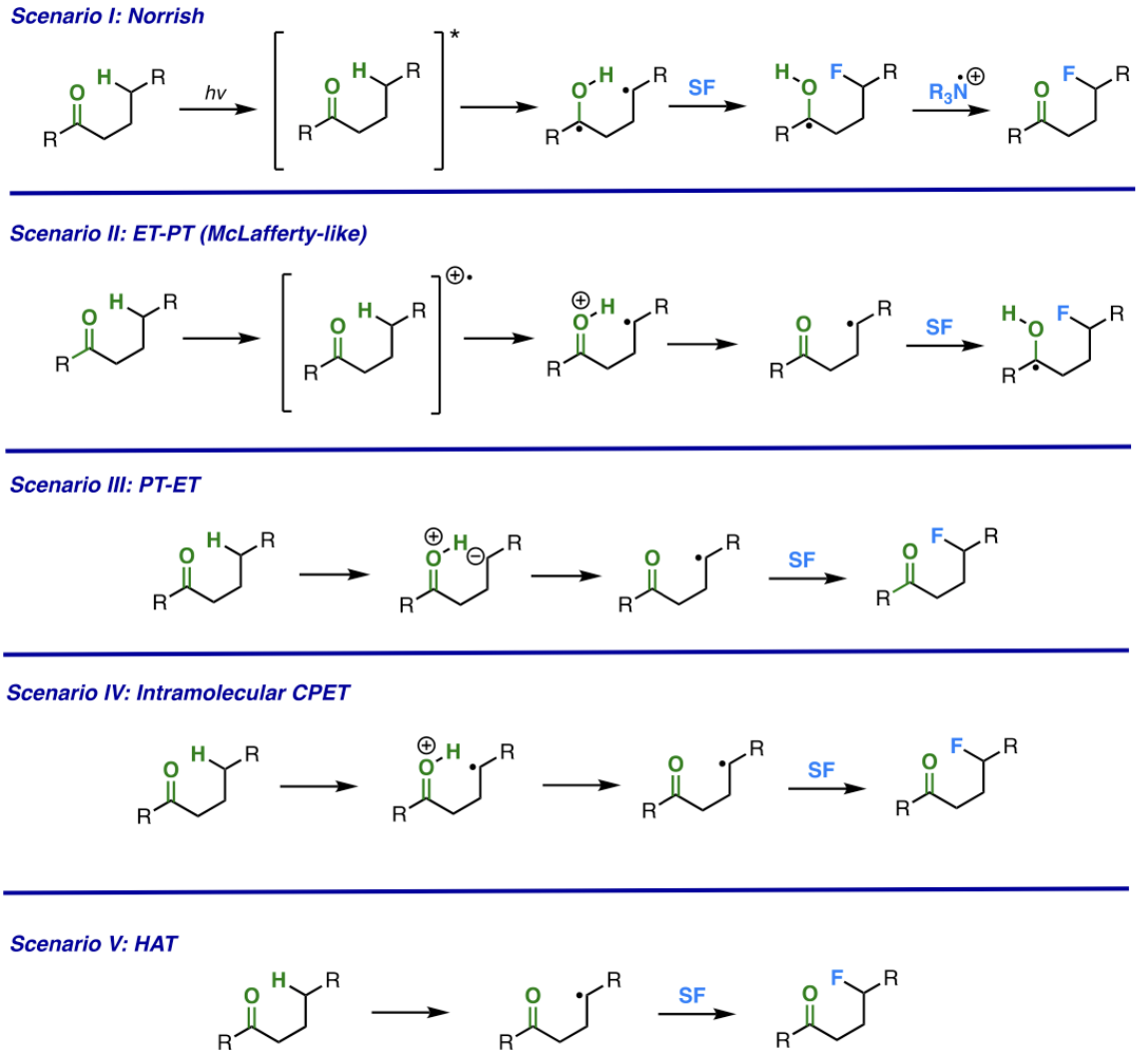

Figure 5.2 Five possible mechanistic hypotheses.

Given that the only chromophore present in the reaction mixture absorbing in the 300 nm region was the enone moiety of the substrate, we originally surmised that the main

viable initiation pathway following its excitation could be a Norrish type II intramolecular process.[6] This initial supposition turned out to be overly simplistic, if not incorrect, and was surprisingly clarified by the subsequent use of longer wavelength absorbing photoinitiators such as benzil, thereby obviating Norrish chemistry. After winding our way down a tortuous path, we found that the mechanism instead indicates intermolecular HAT chemistry at play, rather than classical intramolecular Norrish hydrogen atom abstraction. This HAT can also be thought of potentially as a limiting PCET termed multisite concerted proton-coupled electron transfer: MS-CPET.[7]

In this article, we wish to present our detailed mechanistic findings of this unusual and timely reaction. We also document the key role played by the remarkable chemical transformations of the photoinitiators (affecting the paradigm or supposition that such compounds often act as photocatalysts). Mechanistic clues accumulated along the way were bolstered by alternative initiation of the reaction through chemical (BEt_3/O_2) and electrochemical means. Our findings provide an interesting case of "directed" HAT in a general synthetic method and hopefully will prove to be of crucial importance for defining parameters for the development of related methods.

5.2. Background.

In earlier work, we developed a series of radical-based fluorination methods that highlight different potential mechanisms. For example, the Cu(I)-promoted fluorination of aliphatic substrates was shown (in at least some cases) most likely to proceed through a key HAT step.[8] Given the involvement of the putative Selectfluor radical dication (SRD) in published work and the present reaction, HAT became a logical mechanistic candidate,

although we were quite skeptical as this pathway generally leads to "scattershot" fluorination at a large number of sites within a complex molecule. On the other hand, the tandem C−C bond cleavage/fluorination of acetals (also involving SRD) must proceed through some sort of a SET process with no HAT involvement (Scheme 2).[9] The flexibility

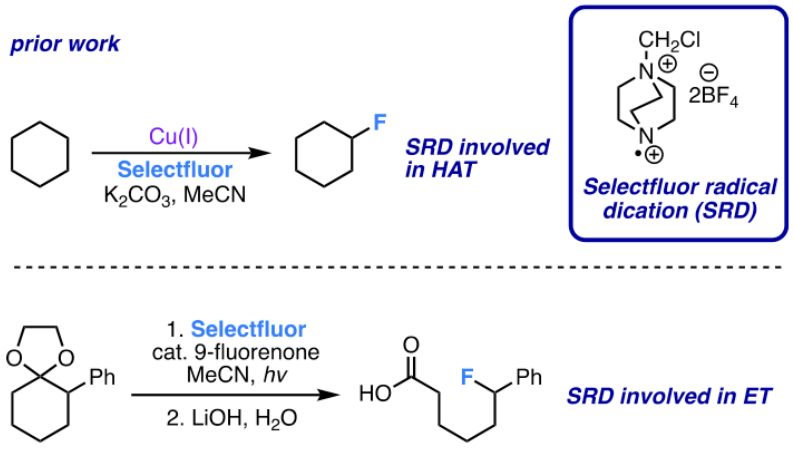

Scheme 5.2. Examples Where SRD Has Been Shown to Play a Significant Role in Both Hydrogen Atom Transfer (HAT) and Electron Transfer (ET)

of the SRD/SF pair to play different roles warned us about jumping to conclusions.[10] In the present work, we were once again intrigued by the possibility that SRD may play an imperative role.

In regard to PCET, recent work by Knowles and co-workers demonstrates its viability for a number of unique synthetic transformations.[11] Additionally, variants of the basic PCET system should be noted. For example, the subclass "MS-CPET" (multiple-site concerted proton−electron transfer) has only recently been explored for C−H activation. To our knowledge, Mayer and co-workers described the first mechanistic account in 2019,

whereby the carboxylate of fluorenyl-benzoate facilitates rapid cleavage of a benzylic C−H bond in the presence of a weak one-electron oxidant (Figure 5.3).[12] For our purposes, this

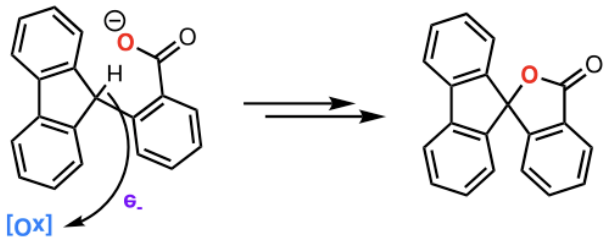

Figure 5.3 Mayer's multiple-site concerted proton−electron transfer (MS-CPET) system.

precedent is important as it parallels, at least superficially, the present findings in several ways. In Mayer's case, a carboxylate acts as an internal base through a six-membered ring transition state. The oxidant, in analogy to SRD, is an amine radical cation. We bear in mind what Mayer and co-workers have stated: "MS-CPET reactivity is increasingly proposed in biological and synthetic contexts, and some reactions typically described as HAT more resemble MS-CPET. Despite that HAT and MS-CPET reactions 'look different', we argue here that these reactions lie on a reactivity continuum and that they are governed by many of the same key parameters."[13] In our case as well, strict HAT or PCET may represent points on this reactivity continuum.

5.3. Mechanistic Experiments.

Our initial intuition for enone-directed fluorination led us to believe the observed selectivity was due to a Norrish-type pathway. As such, we proposed that intramolecular HAT may occur first, and the resulting carbon radical could then be intercepted through

fluorination by Selectfluor (SF) before either cleavage or Yang cyclization could occur (Figure 2, Scenario I). For example, direct irradiation of compound **1** in acetonitrile with 300 nm light in the presence of SF produces the directed fluorinated product **2** in 70% yield (Scheme 5.3).[4]

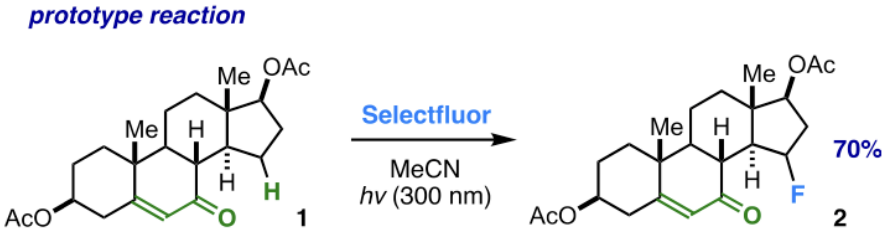

Scheme 5.3. Typical Example of Enone-Directed Fluorination through 300 nm Irradiation

In the absence of SF, the above conditions produce a small quantity of unidentifiable products. Reactions conducted in the dark and under 400 nm irradiation (using blue LEDs) only result in recovered starting material. Additionally, the UV−vis spectra of Selectfluor in MeCN at various concentrations showed no absorption bands above 300 nm (Figure 5.4). These experiments potentially implicate a role for the Norrish reaction in initiation (albeit it has an even more questionable role in chain propagation/fluorination).

There are other conceivable pathways for initiation, such as triplet−triplet energy transfer from the substrate to SF or electron transfer from the excited substrate to SF that can generate SRD[14] (although N−F bond activation in SF has been reported to occur at 400 nm with blue LEDs, as stated we see no absorption in the UV−vis spectrum in this range).[15] These alternatives are not mutually exclusive and may run parallel to each other; as all the hypotheses involve SRD, very complex hybrid mechanisms are possible. Thus direct

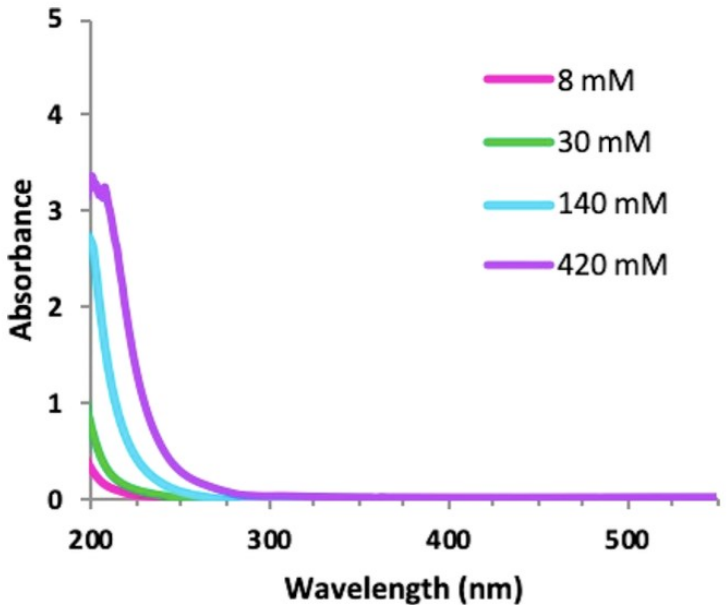

Figure 5.4. UV−vis spectra of Selectfluor in MeCN at various concentrations.

photolysis, at least from a mechanistic standpoint, appears to be anything but direct. In contrast to enones, the direct photolysis of rigid, optimally configured ketones produces a generally lower yield of desired fluorinated products along with other nondirected fluorinated species. Decomposition of ketone substrates into a number of fluorinated products competes with the desired process. For example, α-cleavage of the O–C–C bond gives rise to evident acyl fluoride byproducts by ^{19}F NMR.[16] Enones do not seem to be quite as susceptible to these types of cleavage processes.

The unsuccessful utilization of ketones (and poor yields of certain products obtained from enones) prompted us to turn to visible light/near-UV photosensitization with the goal of increasing yields and improving conditions. Paradoxically, we also sought to clarify (or simplify) the mechanism through the addition of a photo-sensitizer. Table 1 shows a range

of photosensitizers that we screened for both enones and ketones (reactivity was similar to both; steroid **1** is shown as a model substrate).

Table 5.1. Scope of Sensitizers Screened under 400 nm Irradiation

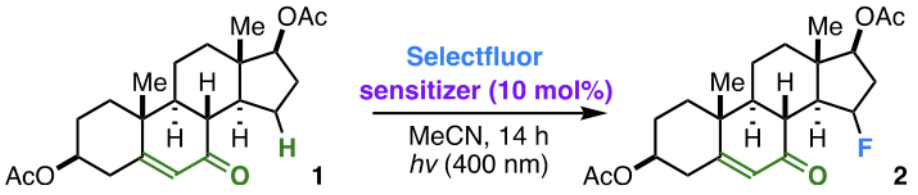

entry	sensitizer	^{19}F NMR yield (%)
1	–	0
2	2-bromo-9-fluorenone	43
3	9-fluorenone	47
4	dibenzosuberenone	55
5	9,10-phenanthrenequinone	64
6	4,4-difluorobenzil	67
7	2,7-dichloro-9-fluorenone	71
8	2-chlorothioxanthone	73
9	methylbenzoylformate	89
10	benzil	94

A trend stands out: carbonyl-containing sensitizers (such as benzil) work most effectively in the reaction. Benzil itself increases the yield considerably (from 70% to 94%) over direct photolysis. One other important fact related to the mechanism was immediately noted—a photosensitized approach utilizing 400 nm light (with a narrow 10 nm spectral dispersion) conclusively rules out a Norrish-type pathway at play in this case. Due to the ketone/enone absorbance below 350 nm and >20 kcal/mol triplet energy gap between benzil and ketone/ enone substrates, triplet sensitization is virtually prohibited.[17] In this case, it is not feasible to form the photoexcited substrate through direct excitation or

triplet−triplet energy transfer. Thus, the photosensitizers are playing a very different initiation role. When a directing carbonyl group is not present (control **3**) fluorination still results, although it qualifies as "scattershot," resulting in a multitude of fluorinated products, none of which is produced in useful quantities. A mixture of a known substrate **4** plus hydrocarbon **3** produces product **5** exclusively, even though **4** is expected to have a higher ionization potential (Scheme 5.4; competition). Moreover, hydrocarbon **3** fails to

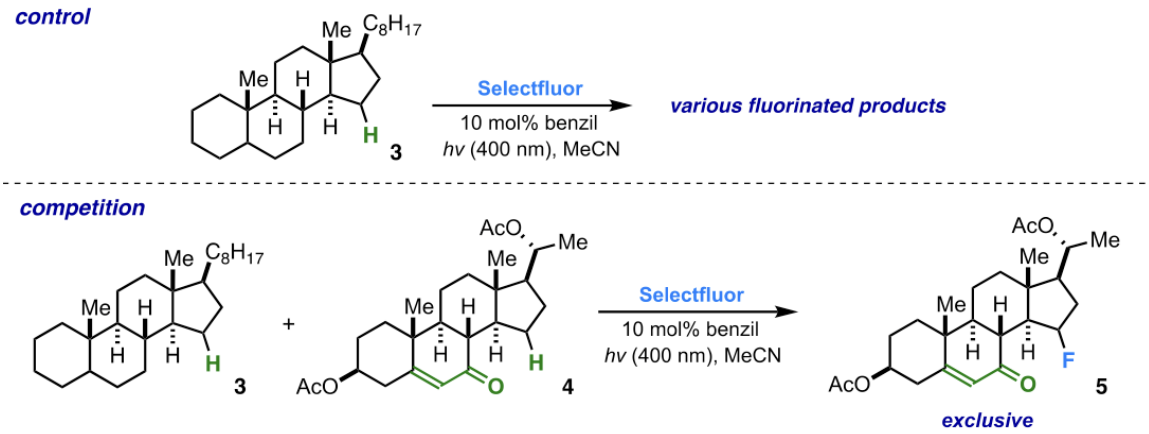

Scheme 5.4. Control and Intermolecular Competition Experiments

fluorinate under 300 nm irradiation (Scheme 5.4; control). The chemical (and photochemical) behavior of benzil has been well documented over the past 150 years (e.g., as a hydrogen atom abstractor, oxygen scavenger, organic reagent, and a triplet− triplet energy transfer facilitator).[18]

Our first thought turned to the possibility that photoexcited benzil acts through HAT (Scheme 5.4).[19] Photoexcited carbonyl-containing species are proposed to be competent hydrogen atom abstractors in a variety of settings.[20] In our case, this concept was unlikely for two reasons: (1) the energetics are not favorable (it would be a fairly endothermic

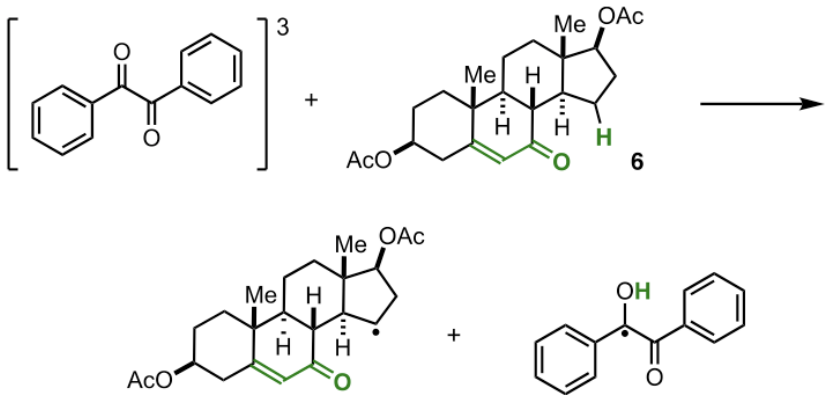

Scheme 5.5. Concept of Benzil Acting through Putative HAT

process for the steroid substrates) and (2) benzil in any event is not expected to be a selective hydrogen atom abstractor. The calculated abstraction energy for steroid 1 is uphill by almost 12 kcal/mol (IEFPCM(CH_3CN)UωB97X-D/6-311++G-(2d,2p)); in known cases where benzil engages in HAT, the hydrogen atom donor is fairly activated, as in cumene and isopropyl alcohol.[21] Furthermore, if the other photosensitizers of differing shapes, sizes, and electronic properties operate through HAT, it seems highly unlikely that they would afford the exact same site-selectivity as well. As can be seen in Table 1, along with direct photolysis, various other carbonyl photosensitizers afford identical selectivity. On the other hand, Bunbury and Wang have irradiated benzil in cyclohexane solution, observing in the process both cleavage products and products resulting from H-abstraction.[18a,b] In our case, in a control experiment involving benzil irradiated with steroid **6** at 400 nm, we do not observe the cleavage byproducts consistent with benzil acting as an abstractor, which should include benzaldehyde.

Appropriately, multifaceted benzil seems to take on yet another role in the present reaction. For example, we note the generation of significant quantities of benzoyl fluoride

in all successful fluorination reaction mixtures with SF as reagent. As a control, a mixture of benzil and SF (no substrate) in MeCN was irradiated by a 400 nm LED lamp and generated benzoyl fluoride in 44% yield when performed in a glovebox and 34% under normal reaction conditions. In contrast, benzoyl fluoride is not generated in the dark. As suggested in Scheme 5.6, the formation of benzoyl fluoride may logically be correlated to

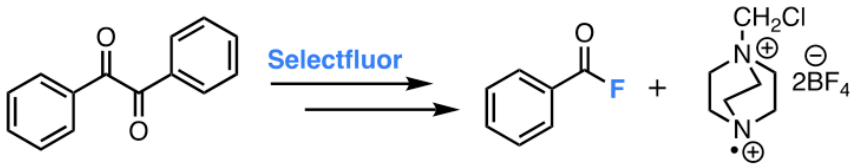

Scheme 5.6. Formation of Benzoyl Fluoride under Irradiation

the generation of SRD. However, the question remains as to how benzoyl fluoride is formed.

The α-cleavage of benzil is a conceivable pathway in which the reaction could be initiated. One can imagine the resultant benzoyl radicals reacting quickly with SF to produce PhCOF and SRD, thus initiating the reaction, as this process is predicted to be highly exothermic. The excitation and intersystem crossing of benzil to the T_n state may promote an energetically feasible homolysis—albeit one that has only been observed in laser pulse studies involving two-photon excitation.[18e,f] In fact, evidence for direct α-cleavage (Norrish I) of benzil under more normal chemical conditions is scant. Nevertheless, assuming that direct cleavage occurs under our conditions of photoexcitation, a simple synthetic probe to observe cross products would provide incontrovertible proof.

Accordingly, we irradiated a mixture of 4,4′-dimethylbenzil and benzil in acetonitrile with 400 nm light and found no detectable cross products (Scheme 5.7). The same result

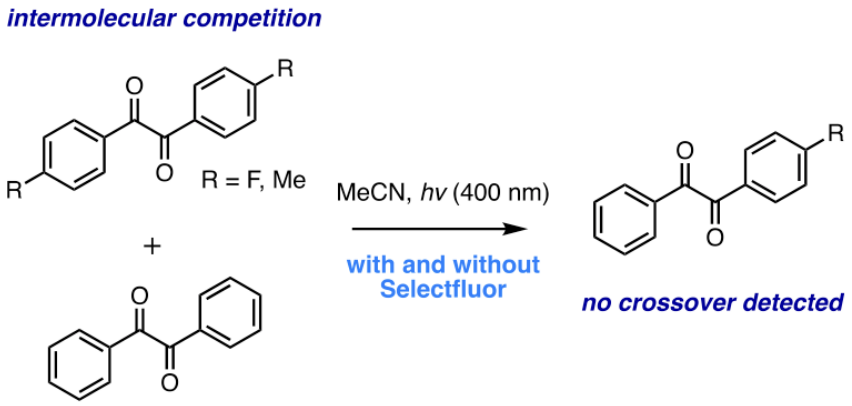

Scheme 5.7. Crossover Experiment to Probe Possible Direct α-Cleavage of Benzil Derivatives in the Presence and Absence of Selectfluor

was obtained with 4,4′-difluorobenzil (both of these benzil derivatives work equally well in the reaction). In the presence of SF, recovered starting materials also showed no evidence of scrambling, suggesting that SF does not promote the process.

The results are consistent with direct cleavage not occurring to a significant extent, or else recombination of benzoyl radicals is happening faster than their diffusion. Even very prolonged irradiations produce no evidence of cross products, which along with precedent suggests that direct α-cleavage of benzil is simply not occurring under the usual fluorination conditions (400 nm irradiation). However, we conducted an intermolecular competitive kinetic isotope effect experiment and tracked the consumption of the benzil starting materials (due to the instability of benzoyl fluoride, we were not able to measure its formation with quantitative mass spectrometry). We found an enhancement of ^{13}C in

the starting material as the reaction proceeds. This suggests that cleavage may be occurring through a different pathway (Scheme 5.8).

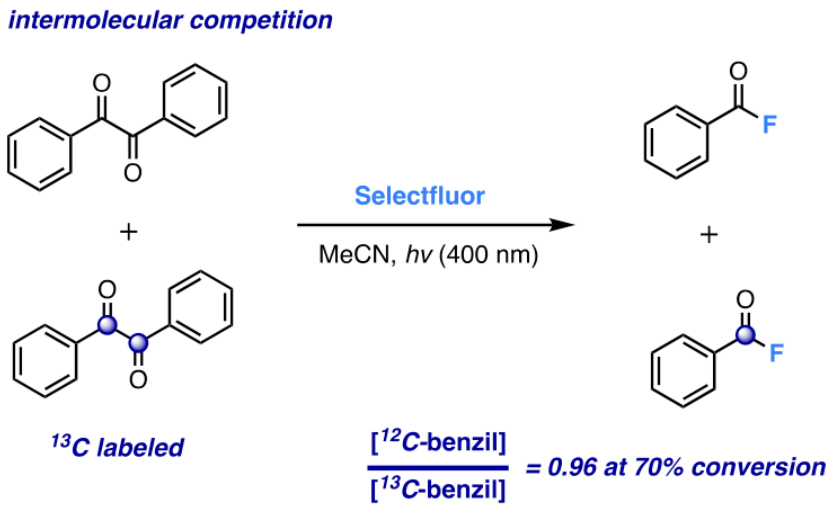

Scheme 5.8. Competitive Kinetic Isotope Effect (KIE) Experiment

Another conceivable route involves excited-state benzil abstracting a hydrogen atom from acetonitrile and subsequently cleaving to generate a benzoyl radical.[22] Although energetically uphill by most measures, it was simple enough to test this hypothesis. We conducted a KIE experiment employing acetonitrile-d_3; this experiment showed no change in rate when compared to acetonitrile (Scheme 5.9). Additionally, benzaldehyde is once again expected as a byproduct, yet none was detected.

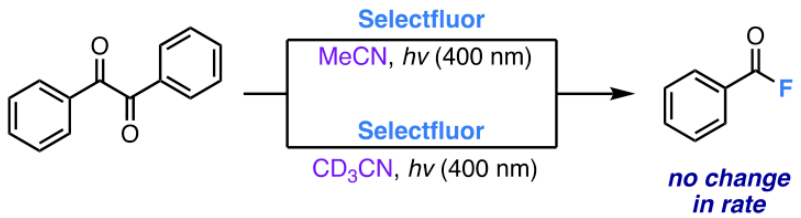

Scheme 5.9. KIE Experiment Probing Role of Solvent

One other illuminating piece of data was obtained by the use of 9-fluorenone as a photoinitiator. The reaction provides a slightly lower yield of fluorinated ketone/enone in comparison to the benzil-initiated reaction but still works moderately well. In the case of 9-fluorenone, hypothetical α-cleavage through a Norrish I fragmentation is expected to be less favorable than that of benzil as the resulting reactive intermediate consists of an aryl radical (Scheme 5.10). Nevertheless, purification of the reaction mixture led to the isolation of difluoride **7** (the structure was unambiguously assigned via single-crystal X-ray diffraction), evidently resulting from difluorination of an aryl-benzoyl radical, which should also be competent in generating SRD.

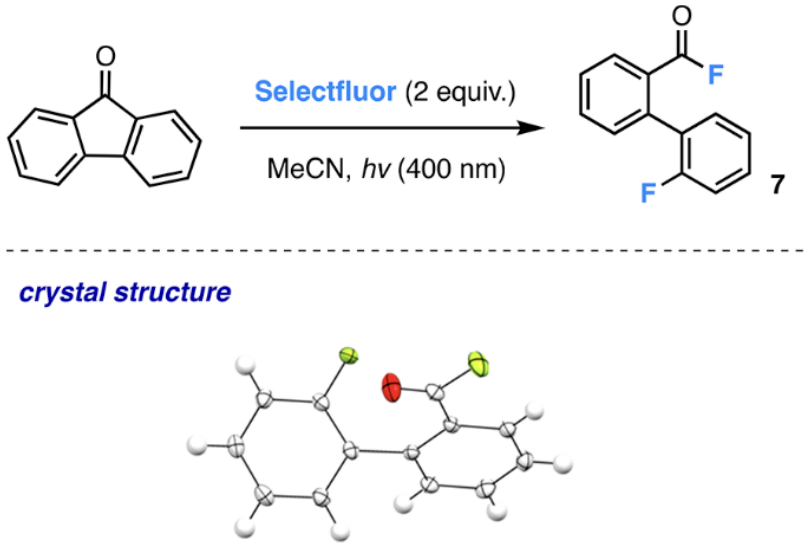

Scheme 5.10. α-Cleavage and Difluorination of 9-Fluorenone.

An attractive pathway for the production of benzoyl fluoride is suggested by Saltiel's classic reaction of ground-state triplet dioxygen with photoexcited benzil (Figure 5.5, left).[23] The resulting peroxyl radical intermediate (or perhaps transition state) cleaves to produce benzoyl radical and the daughter peroxy radical **8**. In order to determine whether

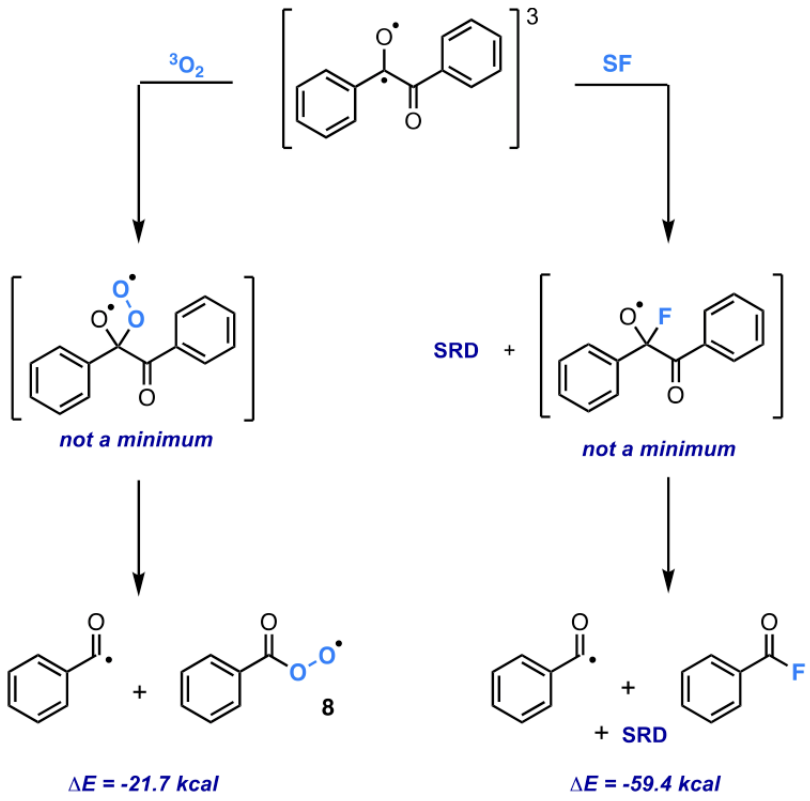

Figure 5.5. Analogy between Saltiel's experiments involving excited benzil and triplet dioxygen (left) and a plausible variant involving Selectfluor (right).

dioxygen was involved in our reaction, we conducted our original experiments under strict atmospheric regulation, whereby a reaction mixture containing benzil, substrate **1**, and SF in dioxygen-free acetonitrile (freeze–pump–thaw cycled) was prepared in a glovebox and then irradiated. The resultant crude mixture was found to have fluorinated in a comparable yield to the typical reaction conditions.

In addition, a fluorination reaction conducted under a pure dioxygen atmosphere failed to fluorinate either the steroid or benzil—suggesting that dioxygen was not only unnecessary for initiation but that too much retards the initiation step by quenching the

triplet-excited benzil either chemically or photochemically. Nevertheless, Saltiel's seminal experiments suggest a plausible analogy. In a more likely scenario, triplet benzil (drawn in a form emphasizing its diradical character) is trapped by Selectfluor (instead of dioxygen) and cleaves into benzoyl fluoride and benzoyl radical (Figure 5, right). This hypothesis is supported by DFT calculations ($\Delta E = -59.4$ kcal mol^{-1} for the formation of products [UωB97XD/6-311+G**-(MeCN)]). The calculated values for the fluorination of triplet benzil are considerably more exothermic than those calculated for the triplet oxygen reaction ($\Delta E = -21.7$ kcal mol^{-1}). Also in both cases, the presumed adducts (with $^3O_2$ and $F^\bullet$) are not stable minima and dissociate, suggesting a concerted route to products. Bear in mind that SF is an excellent radical trap and known to react extraordinarily rapidly with organic free radicals.[24]

A recent study by Tan and co-workers[25] addressed the interaction between photoexcited anthraquinone and Selectfluor using transient-absorption spectroscopy and DFT calculations. The authors propose that an anthraquinone−Selectfluor exciplex is responsible for initial HAT from their substrates, and this initiates a chain reaction. While we cannot rule out the formation of exciplexes in our system, it seems once again unlikely that HAT from excited-state benzil would be selective in any form.

Carbonyl- containing photopromoters that absorb in the region of irradiation are notable for their efficacy in the reaction, which we attribute to their propensity for α-cleavage in the presence of SF. Furthermore, a number of "noncarbonyl" photo-promoters work as well. Anthracene produces a good yield of product **5** with a CFL bulb, whereas perylene produces no product. Note that the triplet energies of both anthracene ($E_T \approx 42$ kcal/mol)

and perylene ($E_T \approx 35$ kcal/mol) are too low for sensitization to be viable and that both anthracene[26] and perylene[27] absorb within the region of the light source emission.

During the course of the reaction, anthracene is fluorinated (predominately in the 9-position) whereas perylene is not. One can imagine excited-state anthracene reacting with SF to liberate SRD and initiating a chain process (Scheme 5.11). A general rule of thumb is that any photopromoter that works well in the reaction is transformed itself by fluorination (presumably to produce SRD).

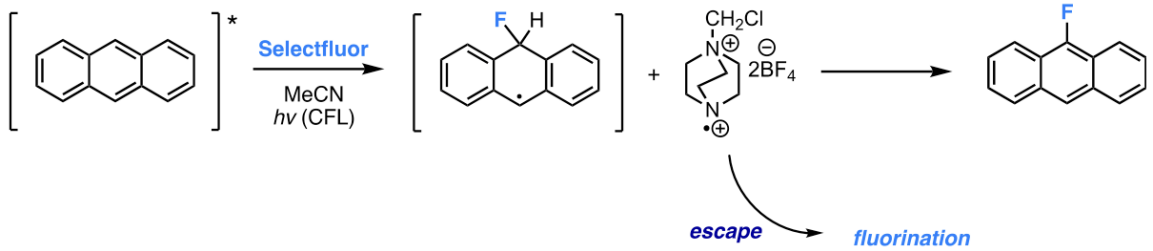

Scheme 5.11. Effecting the Fluorination Reaction with Noncarbonylic Photopromoters

To understand the intimate role that SRD plays within the mechanism, we sought methods for its generation by purely chemical means. N,N,N′,N′-Tetramethyl-p-phenylenediamine is an avid one- electron donor that generates the highly characteristic dye "Würster's Blue" in the process.[28] It reacts readily with SF, producing the colored dye immediately. Unfortunately, this reaction cannot be used to initiate a selective fluorination, as SRD itself is even more highly susceptible to one-electron reduction. The result is almost clean conversion of SF to amine **9** (Scheme 5.12).

We established in prior work that the production of ethyl radicals during the autoxidation[29] of triethylborane provides an adequate radical source to be fluorinated, thus

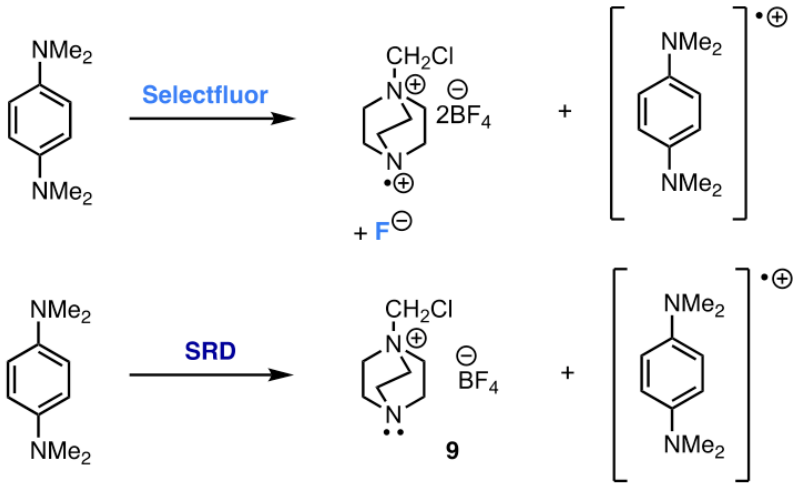

Scheme 5.12. Reactions of SF with N,N,N′,N′-Tetramethyl-p- phenylenediamine

generating SRD.[30] Under these strictly chemical conditions, fluorination of steroidal enones/ ketones is possible (albeit in lower yields) with identical reactivity patterns to those derived from direct and benzil-catalyzed photolysis (example in Scheme 5.13). Moreover,

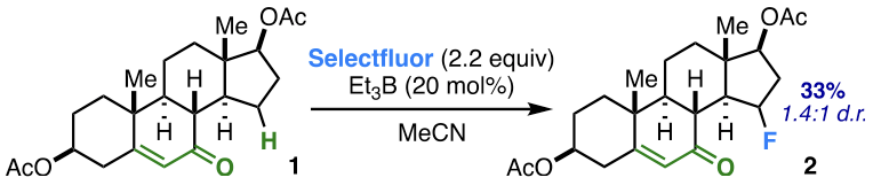

Scheme 5.13. Triethylborane Test in Which SRD Is Generated under Nonphotochemical Conditions.

the lower yields observed when using triethylborane are possibly attributed to maintaining a sufficient quantity of SRD at any one time, the necessary presence of dioxygen, and the vagaries of putative chain propagation in general. In particular, the reaction requires oxygen, but too much also inhibits the reaction.

Using cyclic voltammetry (CV), peak oxidation potentials of amine **9** (a direct precursor to SRD) and substrates 6 and 4 were found to lie between 1.9 and 2.4 V vs Ag/Ag^{+} (Figure 5.6). Unsurprisingly, the oxidations are irreversible at all scan rates probed, although peak

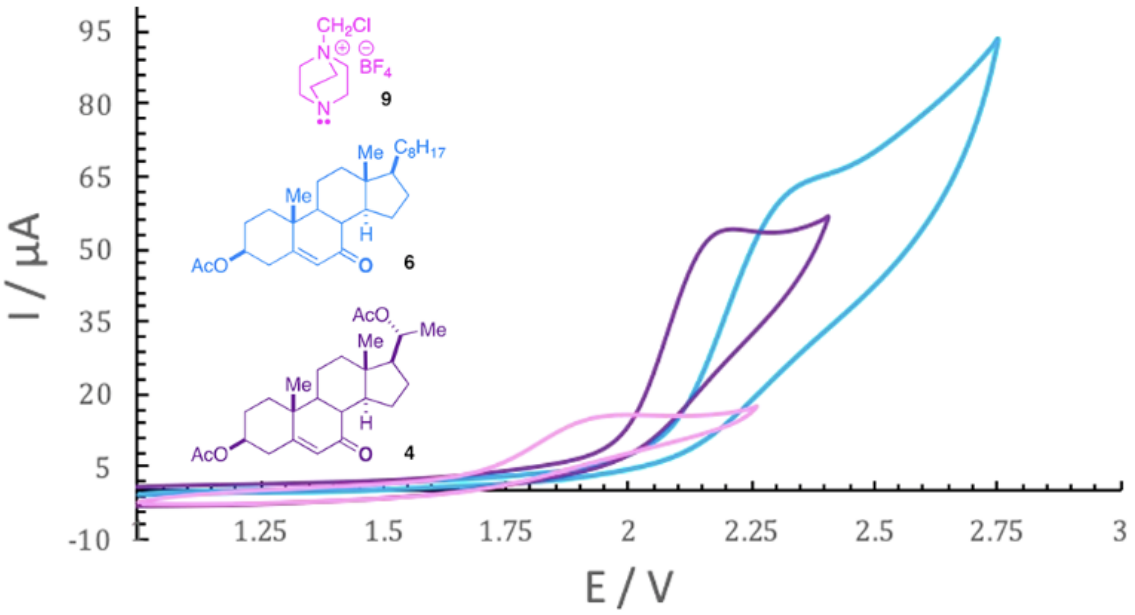

Figure 5.6. Cyclic voltammograms of compounds 9, 6, and 4 in dry and deoxygenated MeCN with 0.1 M TBAPF6 and a potential sweep rate of 100 mV/s (vs Fc/Fc+).

shapes change. We bore in mind that these outcomes are dependent on the electrochemical solution concentrations, but they provided a rough guide to voltage tuning for the performance of a bulk electrolysis.[31] Irreversible peak reduction of SF was also observed at −0.3 V; the presumably liberated SRD is quickly reduced itself (dry and deoxygenated MeCN with 0.1 M $TBAPF_6$ and a potential sweep rate of 100 mV/s (vs Fc/ Fc^{+})). We chose to conduct a bulk electrolysis experiment whereby substrate **4** and SF were mixed in

MeCN, and a potential of 1.8 V (approximate anodic potential of amine **9**, and out of range to oxidize compound **4**) was applied to the cell for 3 h (Scheme 5.14, left). Under these

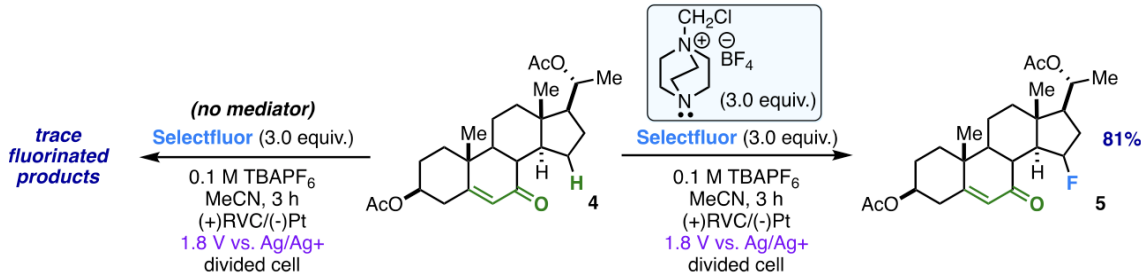

Scheme 5.14. Bulk Electrolysis Experiment Supporting the Involvement of SRD

conditions, product yields were very low (<3%). On the other hand, electrolysis in the presence of amine **9** resulted in an 81% yield of product, and once again, the exact same product distribution was observed as compared to the photolytic approach (Scheme 5.14, right). Amine promotor **9** proved absolutely necessary as a mediator—the optimal voltage for the reaction corresponds very roughly to its oxidation, suggesting that SRD is once again the indispensable actor. Direct oxidation of the steroid itself produced product (E = 2.3 V), albeit in only 10% yield, suggesting that a critical threshold of SRD as a chain carrier was not attained. Use of other fluorinating agents such as NFSI produced small amounts of various unselective fluorinated products. This experiment, besides its innate utility, cleared away a number of mechanistic ambiguities.

Reprising briefly the topic of direct photolysis, Scheme 15 provides one clue as to the lower yields observed; the substrate itself likely serves as the initiator. As mentioned, every successful photopromotor is itself fluorinated in order to liberate SRD. This may apply to direct photolysis as well—the minor acyl fluoride byproducts (highly characteristic by ^{19}F

NMR in the vicinity of +17 ppm) likely result from the cleavage of putative radical intermediate **10** (Scheme 5.15).

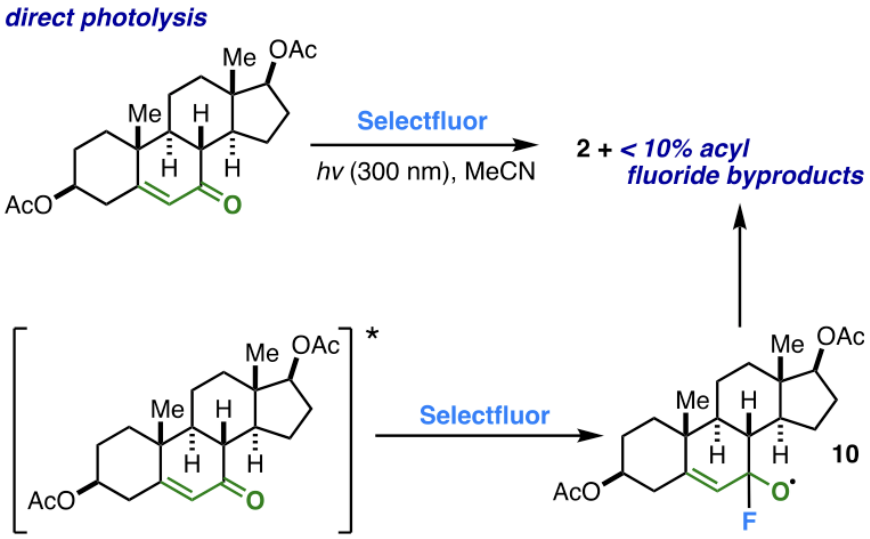

Scheme 5.15. Under 300 nm Irradiation in the Absence of a Sensitizer

In the absence of SF, unidentifiable products form but at a much lower rate than fluorinated byproducts when SF is present, suggesting that another pathway is at work. Consequently, yields are naturally lower as a bit of the substrate is sacrificed. The situation is most dramatic for ketones, whose propensity to fragment seems to be greater than that for enones.

Benzil, photoinitiation, borane initiation, and bulk electrolysis conclusively rule out Norrish II chemistry, as well as any other chemistry involving photoexcitation of the enone chromophore with the exception of direct excitation. If ET/PT were operative, the carbonyl lone pairs must act as an internal base to deprotonate intramolecularly an optimally poised C−H bond, yielding a protonated carbonyl and a secondary carbon radical. This step

(proton transfer) can happen sequentially or simultaneously with an electron transfer; consequently, there exist two reasonable pathways: electron transfer followed by proton transfer (ET−PT) or concerted transfer of the two particles (CPET). One other pathway (PT−ET) is high energy by any estimation and should be discounted.[32]

The enone activation process bears a resemblance to the gas-phase McLafferty rearrangement (Scheme 5.16). This venerable gas-phase reaction involves carbonyl-

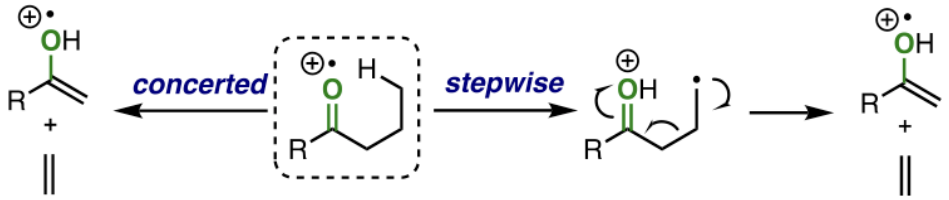

Scheme 5.16. Gas-Phase McLafferty Rearrangement

containing compounds possessing γ-hydrogens, similar to many of our substrates.[33] The (somewhat limited) mechanistic consensus advocates electron abstraction, followed by intramolecular HAT and then fragmentation (the present work could thus be considered a formal "interrupted" McLafferty reaction). Intramolecular isotope effects for these rearrangements are documented; these range over a wide spectrum of values.[34] However, intermolecular isotope effects for McLafferty reactions are not widely known. The McLafferty rearrangement would seem to be a candidate for PCET, but not much if anything is reported about this option. Djerassi and co-workers[35] have examined potential McLafferty rearrangements in keto steroids and found that only when the interacting carbonyl and C−H bonds can approach to within 1.5 Å is the rearrangement feasible (Figure 5.7). In more rigid steroidal ketones it does not occur, in contrast to the present chemistry.

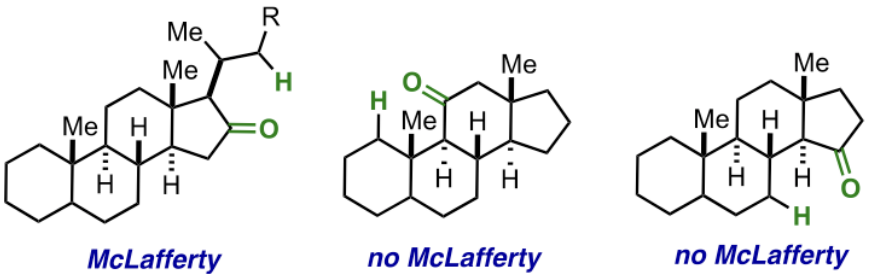

Figure 5.7. Examples of steroid cores that were or were not observed to undergo McLafferty rearrangements in gas-phase experiments.

This is an interesting fact that begs the question whether CPET or ET is involved in our system at all, as our geometric requirements are so different than typical McLafferty substrates. Granted, McLafferty chemistry is all gas phase, so the lack of correlation may not be taken as definitive.

One insightful calculation shows that CPET (to be more accurate: MS-PCET) is modestly exothermic for a typical steroidal substrate (Scheme 5.17). The precise number,

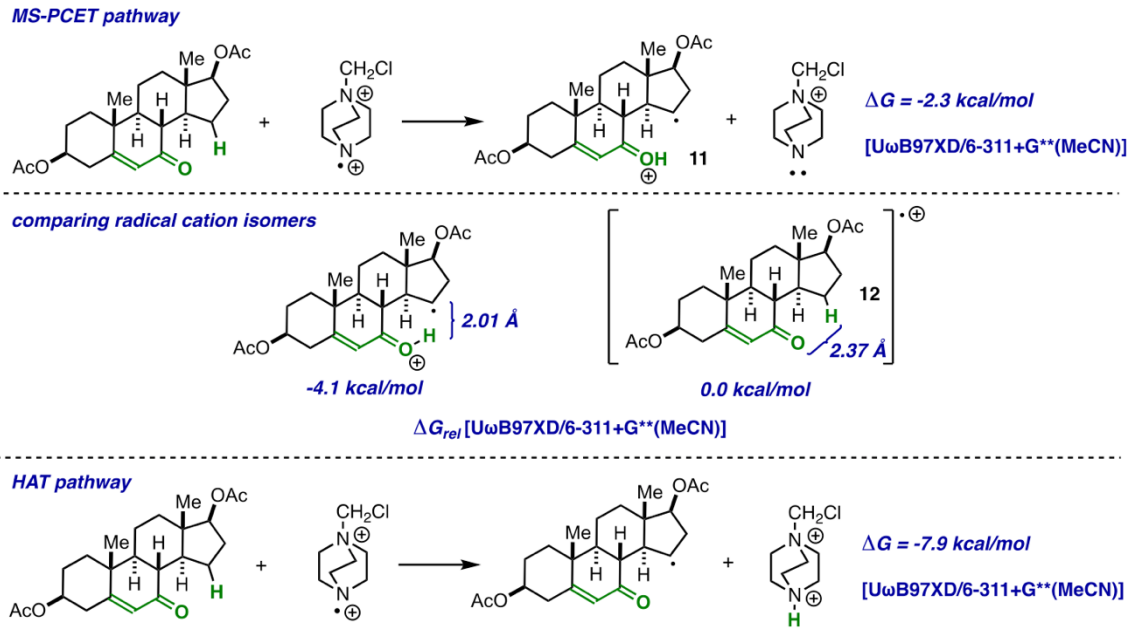

Scheme 5.17. Comparing Calculations of MS-PCET and HAT Mechanisms

of course, is to be best viewed as a ballpark figure. More interesting is the comparative energy of radical cation isomers that favor **11** by 2.3 kcal/mol. The structure of **11** reveals what could be characterized as a hydrogen-bonding contact between the radical center and the OH proton (2.01 Å).[36] A weaker interaction exists in computed radical cation **12** of 2.37 Å between C and O (Scheme 17). On the other hand, a straightforward HAT is exothermic by more than 7.9 kcal/mol.

Our efforts to discern between the two viable possibilities led us to use a mechanistic probe: an isotope effect experiment between 2-(pentadeuteroethyl)cyclohexanone and 2-ethyl-cyclohexanone). We observed a phenomenological kinetic isotope effect in a one-pot intermolecular competition reaction (KIE = 3.4) and also when comparing initial rates of reaction of each isotopomer separately (KIE = 3.7). Both results are large enough to encompass a primary effect (cleavage of the C−H bond) along with superimposing secondary effects (Scheme 5.18).[37] These numbers rule out an initial rate-limiting ET in ET−PT and argue against pre-equilibrium PT in PT−ET.

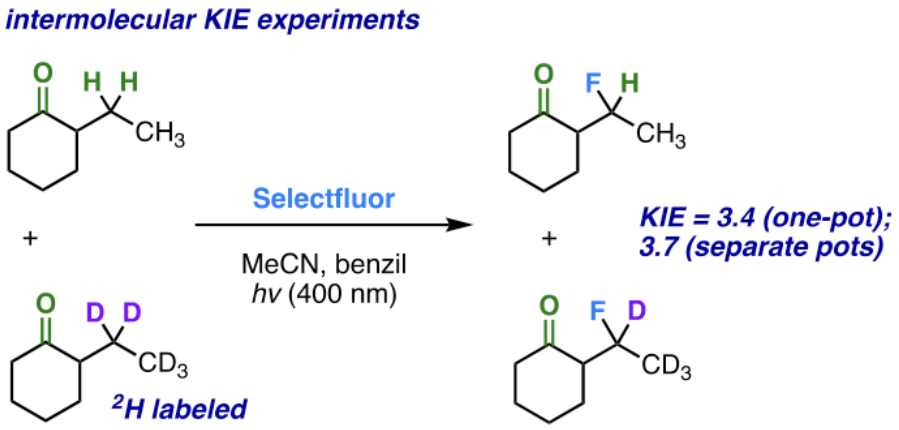

Scheme 5.18. Competitive Intermolecular Kinetic Isotope Effect Experiment

Although we observed a primary KIE, PT−ET (rate-limiting PT) is unreasonable; the rate-determining PT would be highly thermodynamically unfavorable due to the low acidity of the targeted C−H bond and the resulting instability of the zwitterion intermediate. One important experiment designed to distinguish MS-PCET and HAT from pre-equilibrium ET in ET/PT involves the use of SF derivatives possessing different oxidizing power. SF derivative 13-a has a more positive anodic peak potential (E_a = 2.14 V) and inflection-point potential (E_i = 1.88 V) compared to compound 9 (E_a = 1.99 V and E_i = 1.77 V) (Figure 5.8) and leads to a faster reaction (Scheme 5.19), which could be due to HAT, an enhanced electron transfer rate, or else fluorination. However, the observation of a KIE for proton transfer in the reaction militates against the fluorination step being rate-

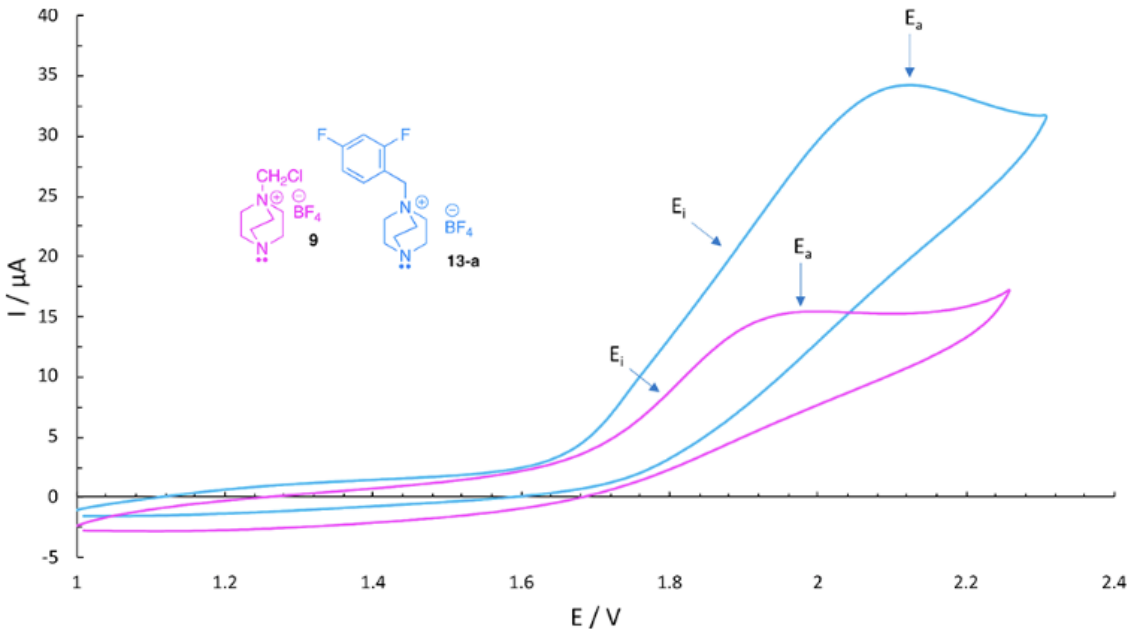

Figure 5.8. Cyclic voltammograms of compounds **9** and **13-a** in dry and deoxygenated MeCN with 0.1 M $TBAPF_6$ and a potential sweep rate of 100 mV/s (vs Fc/Fc^+).

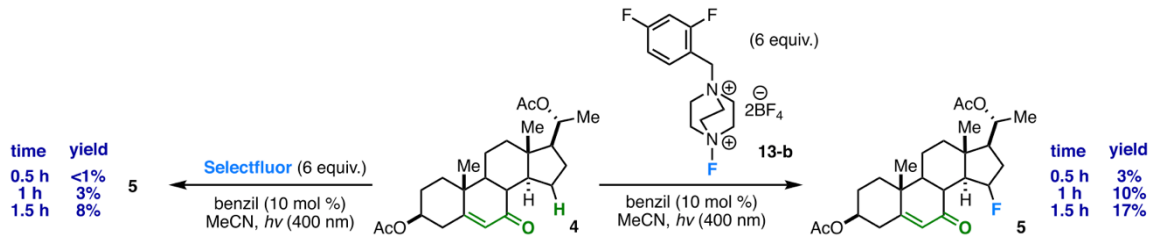

Scheme 5.19. Rate Comparative Studies for Compound 13-b vs SF; Monitored Initial Rate with Excess Fluorinating Reagent Present

determining; thus, this result supports the involvement of HAT or electron transfer in the rate-determining step. Congruent with this conclusion is our prior work that established a very fast rate for the reaction of SF with free radicals.[24a]

Considering the aforementioned results, we are left with viable pathways in the form of HAT and MS-PCET. The former, HAT through SRD, would seem to be disfavored based on calculated C−H bond dissociation energies (a factor of HAT capability).[38] DFT calculations on steroid **6** (ωB97XD/6-311++G** in MeCN) show numerous weaker C−H bonds in the presence of the targeted C−H bond in substrate **6** (Figure 5.9). However, this

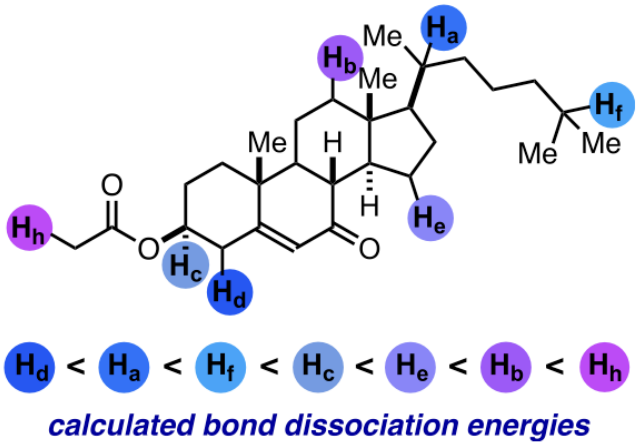

Figure 5.9. Relative calculated C−H bond dissociation energies (weakest to strongest from left to right).

analysis is naïve as it takes no account of steric and electronic factors. It is the transition-state energies that dictate the selectivity of HAT, not merely BDEs. Is it possible that SRD interacts with a proximate carbonyl group in a way to organize a lower energy transition state?

In order to address this issue, we undertook transition-state calculations on a model substrate. In less rigid systems (for example, entities containing a floppy side chain), the carbonyl is not adequately locked, and activation may occur at several sites simultaneously. In a simple probe, we observe product distribution in accordance with the "polar effect," a known HAT pathway (Scheme 5.20).[39]

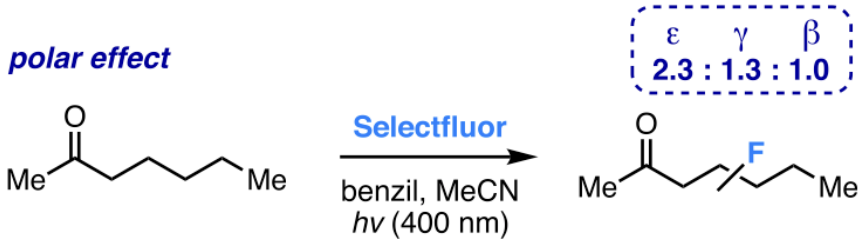

Scheme 5.20. Distribution of Fluorinated Products from Reactions Employing Nonrigid Carbonyl-Containing Substrates That Are Characteristic of the Established "Polar Effect"

In more rigid systems, however, if the carbonyl is indeed templating the approach of SRD to the targeted C−H bond, then it stands to reason that other HAT agents that do not possess this ability would afford "scattershot" fluorination if they were to afford anything

at all. A good example would be the free radical derived from NFSI; it is a known HAT agent[40] and contains no functional groups with particular affinity for carbonyl coordination. Scattershot fluorination is in fact the case; a variety of fluorinated products in low yield is observed in the reaction of NFSI and a model substrate. A similar result is obtained when N-fluoropyridinium triflate is used—small amounts of unselectively fluorinated products are observed (Figure 5.10).

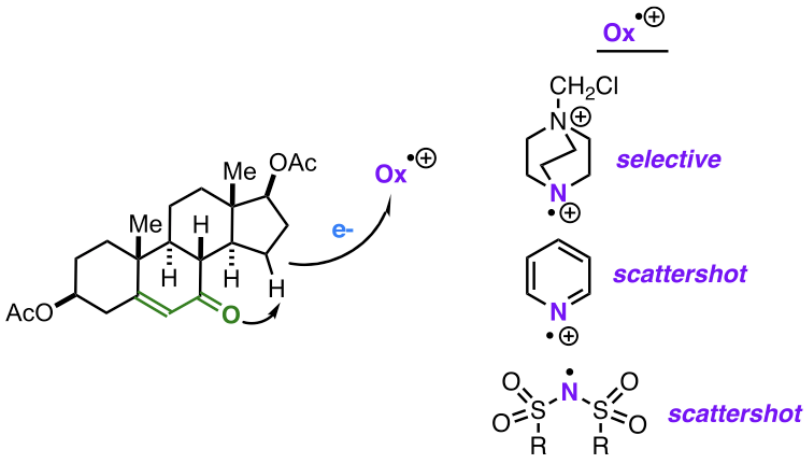

Figure 5.10. Product distribution classified as "selective" or "scatter- shot" in reactions involving presumed N-centered radical intermediates.

What about an outer-sphere PCET (MS-PCET)? Although the NFSI-derived free radical may not be sufficiently energetic to engage in PCET, using more reactive analogues of NFSI (e.g., the DesMarteau reagent)[41] produces a similar pattern of scattershot fluorination (Scheme 5.21). This is notable as the DesMarteau reagent should be energetically capable of engaging in MS-PCET. Once again, this consideration applies to N-fluoropyridinium. On the other hand, in a true MS-PCET system such as that of Mayer and co-workers, the desired event occurred in the presence of a wide variety of one-electron

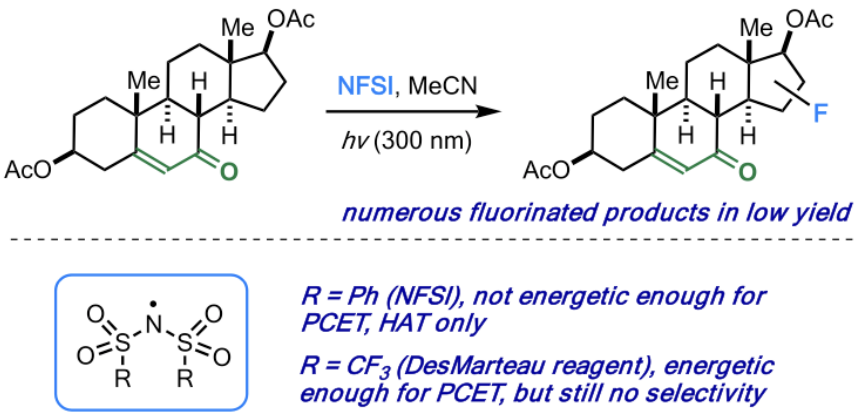

Scheme 5.21. Reactivity of NFSI Derivatives Differs from That of Selectfluor

oxidants as long as they possessed the correct potentials. In our case, it is clear that the nature of the reaction is not dependent on oxidation potential but on chemical structure. This would seem to be strong evidence for a very selective and special version of HAT or inner-sphere PCET.

After the critical HAT step, the substrate is left with a free radical (Scheme 5.22, compound **14**). The final step of the chain propagation is well established through prior studies: reaction between the resultant radical and Selectfluor to yield an alkyl fluoride and to regenerate SRD (Scheme 5.22, compound **15**).[29] To verify a chain process, we calibrated the quantum yield Φ of the standard reaction (SF, benzil, 400 nm LED, MeCN) against the photodecomposition of lime green potassium ferrioxalate, a well-established chemical actinometer, and found Φ = 18.

In the mechanistic study of the carbonyl- directed reaction, quantum calculations were always destined to play an important role. If our hypothesis of carbonyl-directed HAT is true, then the corresponding HAT transition states should be the lowest energy of all reasonable sites in the molecule. Sampling all chemically distinct hydrogen atoms at a

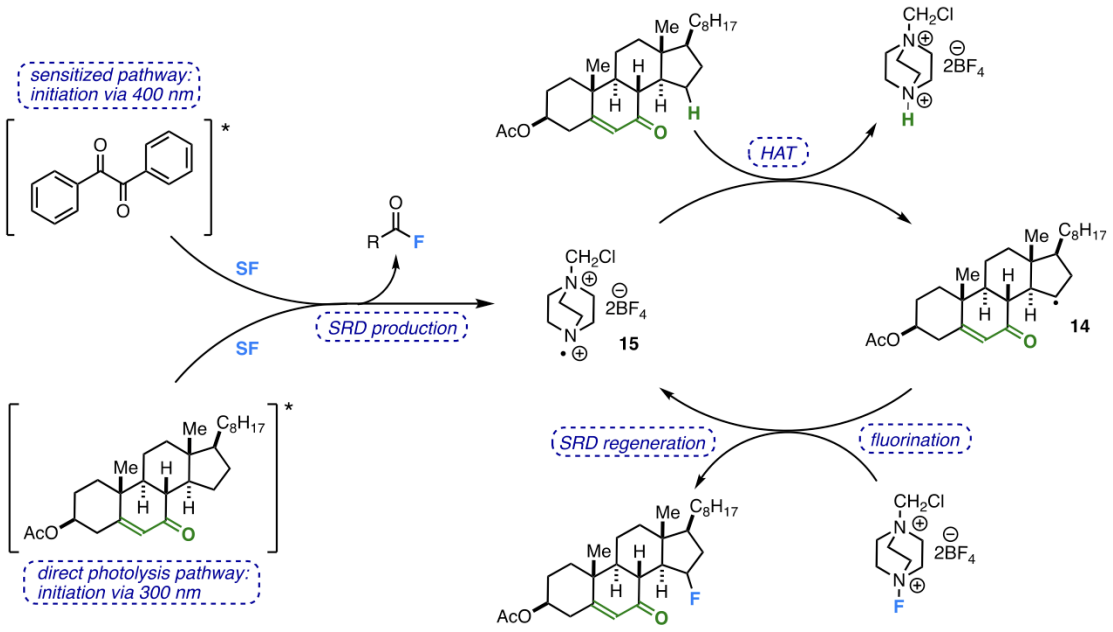

Scheme 5.22. Chain Propagation Mechanism at Play

sufficient level of theory is a tall order; however, we strove to be as comprehensive as possible. Additionally, each carbonyl- activated site is a methylene unit containing diastereotopic protons; it is quite possible that only one of those abstractions would be favored. Take, for example, model substrate **1** (Figure 5.11). Abstraction of the α proton is

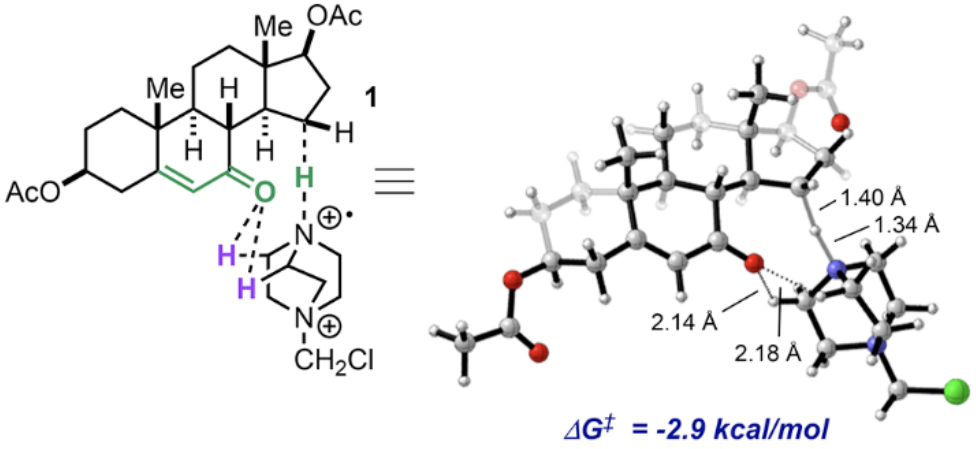

IEFPCM$_{(CH3CN)}$UωB97X-D/6-311++G(2d,2p)/UB3LYP/6-31G(d)

Figure 5.11. Comparing transition-state energies involving HAT from each of the diastereotopic protons at C15 of a prototypical enone- containing substrate.

favored by 2.9 kcal/mol over that of the β proton. Abstractions of protons from other logical sites are relatively disfavored (see the Supporting Information for structures). The reason is evident from both the geometry and energetics of the transition states—two key C–H···O–C hydrogen bonds anchor and stabilize the assembly in the correct orientation. This deduction was supported by second-order perturbation theory analysis of the Fock matrix in a natural bond orbital (NBO) basis for alpha and beta manifolds. These hydrogen bonds, involving slightly acidified protons on SRD, are calculated to be worth 4−5 kcal/ mol—more than enough to torque the system toward directed abstraction. The other stabilizing interaction exists between the transferring hydrogen atom and the carbonyl group. This is a weak H-bond in its own right and a contributing factor to the transition state stability as well. In the case of the lowest energy transition state, all three interactions are a bit tighter. The transferring hydrogen carries a calculated partial positive charge of 0.41, which is not unusual for HAT.[42] As for potential inner-sphere PCET, the theoretical criteria of Mayer and co-workers would seem to disfavor this possibility.[43]

Figure 5.12 shows an image of the computed spin orbital density of TS assembly TS-1 with its electrostatic potential superimposed. This distribution of spin tells an interesting story—namely, in this transition state, the cationic-radical nitrogen atom to which the hydrogen is being donated significantly lacks electron density—indicative of partial positive charge—while there is a larger degree of electron density at the transferring hydrogen atom, thus suggestive of negative charge buildup. The developing carbon-

centered radical, on the other hand, is essentially neutral. This spin orbital density and imbedded charge distribution are indicative of a three-electron, three-center transition state. Recollect that the lone pair of the distal carbonyl oxygen is directly pointed at the C−H bond undergoing homolytic cleavage; associated with this interaction is favorable Coulombic attraction between the cationic SRD species and the negatively charged carbonyl oxygen. Conversely, if this were a PCET mechanism, it would require the transferring hydrogen to be a part of a four- electron, three-center array more consistent with hydrogen bonding.[44] In this instance the carbonyl oxygen would need to have significant radical cationic character or at least positive charge buildup relative to the substrate.

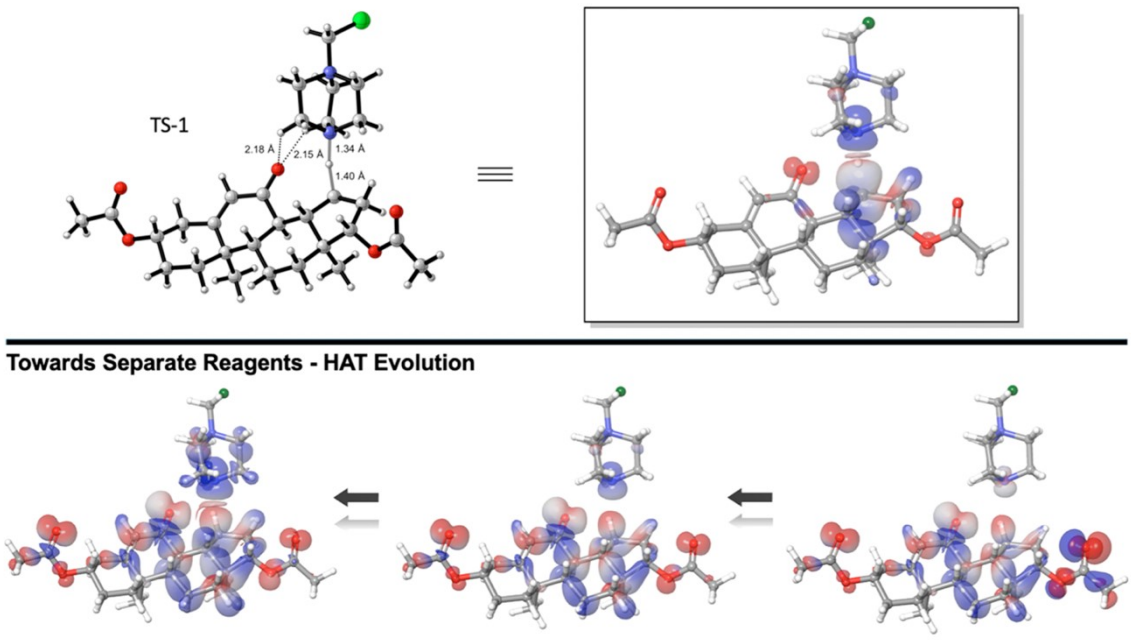

Figure 5.12. HAT transition state (top) and intrinsic reaction coordinate (IRC) derived evolution of HAT reaction coordinate (bottom) with molecular electrostatic potential (MEP) surfaces.

Figure 5.12 also depicts the evolution of the HAT reaction coordinate, with images of the spin orbital density with the electrostatic potential (blue positive, red negative) superimposed. Beginning at the bottom right is a precomplex wherein there is no orbital density indicative of HAT; instead it looks to be a scenario primed for PCET or at the least intramolecular hydrogen abstraction by the carbonyl oxygen (NBO analysis shows a very small donation of carbonyl oxygen lone pair electron density to the C−H bond involved in hydrogen abstraction of 2.3 kcal/mol). As one moves along the bottom of the figure toward the left-hand side, HAT orbital density emerges, and at the transition state (top of Figure 5.12) HAT type bonding is clearly visible, respectively.

The overall analysis holds for rigid ketones as well (Figure 5.13). Selective abstraction

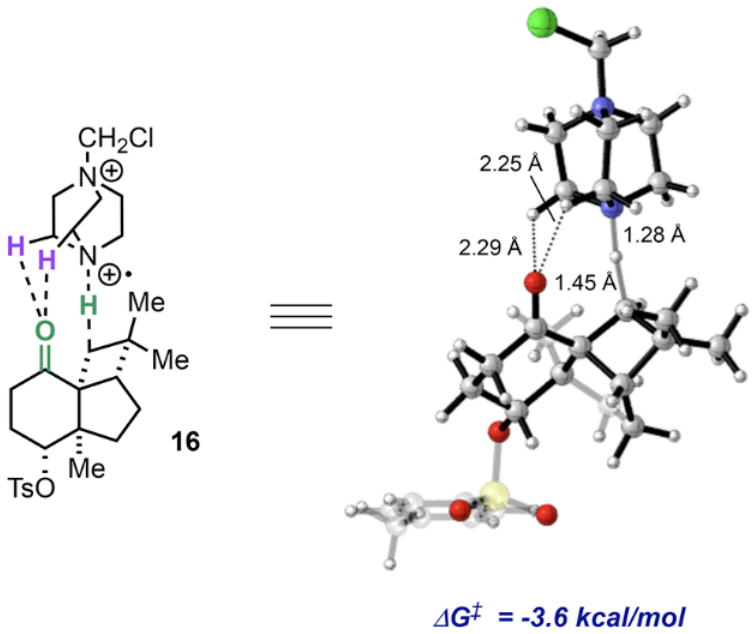

Figure 5.13. Comparing transition-state energies involving HAT from each of the diastereotopic protons of a rigid, nonsteroidal ketone- containing substrate.

from ketone **16** is unusual in that the calculated energies between diastereotopic transition states are sizable (3.6 kcal/mol). In the high-energy transition state, the anchoring effect of the two acidic C−H bonds on SRD is greatly attenuated; one of the contacts is severed completely.

Although the magnitude of the KIE in deuterated 2-ethylcyclohexanone indicates a primary isotope effect (Scheme 5.18), it occurred to us that substrate 1 would provide a way to affirm our computational predictions based on selective isotopic labeling. For a more compelling and less ambiguous case, we sought to make a specifically deuterated steroidal substrate optimally poised for fluorination (Scheme 5.23). For example, the unlabeled variant of **1** is predicted to fluorinate through preferential abstraction of the

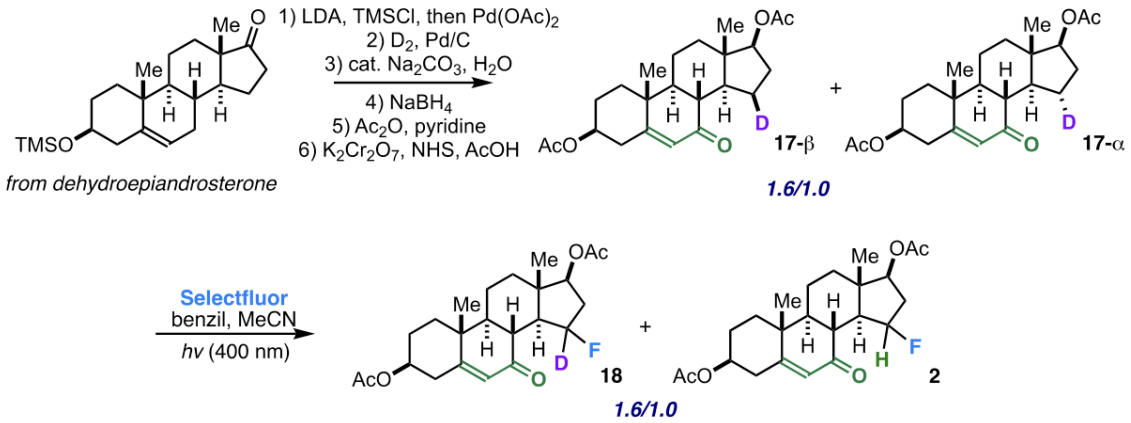

Scheme 5.23. Isotopic-Labeling Experiment Confirming Preferential Abstraction of the α-Hydrogen and Deuterium Atoms, Consistent with DFT-Predicted HAT Hypothesis.

β-C15 hydrogen atom. This prediction could be verified by a simple labeling experiment. In the event, we began the synthesis with dehydroepiandrosterone (DHEA). Enolization was followed by Pd(II)-catalyzed oxidation to form the enone. Reduction with D_2, followed by base-catalyzed exchange of the C16 hydrogen atoms, produced a mixture of

isotopomers in a 1.6/1 ratio. The synthesis is completed by stereospecific reduction of the ketone carbonyl, acetylation, and standard allylic oxidation with potassium dichromate, N-hydroxysuccinimide (NHS), and AcOH to produce the product as a mixture of βD/αD isomers of 1.6/1 (compound **17**). The assignment of isotopomers was made by ^{2}H NMR, with confirmation by ^{1}H NMR (see the Supporting Information). The use of benzene-d_6 as solvent greatly aids the assignment of diagnostic signals. Upon standard reaction conditions, remarkably, substrate **17** is converted to a 1.6/1 ratio of labeled isomeric products (compounds **18** and **2**). The result is exactly in line with what we would expect for preferential abstraction of the α-hydrogen and deuterium atoms. Preferential β-abstraction, on the other hand, would have yielded the opposite result.

5.4. Conclusion.

We have explored the mechanistic possibilities of our previously reported enone/ketone-directed site-selective sp^3 C−H fluorination of terpenoid derivatives. Our findings suggest intermolecular hydrogen atom transfer (HAT) chemistry is at play, rather than classical Norrish hydrogen atom abstraction as initially conceived. Isotope effect studies, detailed quantum computations, thermochemical experiments, and reactions with one-electron oxidants all point conclusively toward a special type of HAT mechanism in which SRD approaches the targeted C−H bond by coordinating to the proximate carbonyl group. This interesting form of HAT may mimic such venerable reactions as the Norrish II cleavage and the McLafferty reaction but in actuality is quite different. Finally, this principle of selective, directed HAT may be leveraged in the interaction of SRD and related radical cations with other functional groups in works to follow.

5.5. References.

[1] (a) Zhang, C.; Tang, C.; Jiao, N. Recent Advances in Copper- Catalyzed Dehydrogenative Functionalization via a Single Electron Transfer (SET) Process. Chem. Soc. Rev. 2012, 41, 3464−3484. (b) Yoon, C.; Mariano, P. Mechanistic and Synthetic Aspects of Amine-Enone Single Electron Transfer Photochemistry. Acc. Chem. Res. 1992, 25, 233−240. (c) Suess, A.; Ertem, M.; Cramer, C.; Stahl, S. Divergence Between Organometallic and Single-Electron-Transfer Mechanisms in Copper (II)-Mediated Aerobic C−H Oxidation. J. Am. Chem. Soc. 2013, 135, 9797−9804. (d) Lewis, F. Proton-Transfer Reactions of Photogenerated Radical Ion Pairs. Acc. Chem. Res. 1986, 19, 401−405. (e) Klein, E.; Lukeš, V. DFT/B3LYP Study of the Substituent Effect on the Reaction Enthalpies of the Individual Steps of Single Electron Transfer-Proton Transfer and Sequential Proton Loss Electron Transfer Mechanisms of Phenols Antioxidant Action. J. Phys. Chem. A 2006, 110, 12312−12320. (f) Liu, W.; Huang, X.; Cheng, M.-J.; Nielsen, R. J.; Goddard, W. A., III; Groves, J. T. Science 2012, 337, 1322−1325.

[2] (a) Warren, J.; Tronic, T.; Mayer, J. Thermochemistry of Proton-Coupled Electron Transfer Reagents and its Implications. Chem. Rev. 2010, 110, 6961−7001. (b) Hammes-Schiffer, S.; Stuchebrukhov, A. Theory of Coupled Electron and Proton Transfer Reactions. Chem. Rev. 2010, 110, 6939−6960.

[3] (a) Hammes-Schiffer, S.; Iordanova, N. Theoretical Studies of Proton-Coupled Electron Transfer Reactions. Biochim. Biophys. Acta, Bioenerg. 2004, 1655, 29−36. (b) Hammes-Schiffer, S. Comparison of Hydride, Hydrogen Atom, and Proton-Coupled Electron Transfer Reactions. ChemPhysChem 2002, 3, 33−42.

[4] Pitts, C.; Bume, D.; Harry, S.; Siegler, M.; Lectka, T. Multiple Enone-Directed Reactivity Modes Lead to the Selective Photo- chemical Fluorination of Polycyclic Terpenoid Derivatives. J. Am. Chem. Soc. 2017, 139, 2208−2211.

[5] (a) Bume, D. D.; Pitts, C. R.; Ghorbani, F.; Harry, S. A.; Capilato, J. N.; Siegler, M. A.; Lectka, T. Ketones as Directing Groups in Photocatalytic sp^3 C-H Fluorination. Chem. Sci. 2017, 8, 6918− 6923. (b) Bume, D. D.; Harry, S. A.; Pitts, C. R.; Lectka, T. Sensitized Aliphatic Fluorination Directed by

Terpenoidal Enones: A 'Visible Light' Approach. J. Org. Chem. 2018, 83, 1565−1575. (c) Bume, D. D.; Harry, S. A.; Lectka, T.; Pitts, C. R. Catalyzed and Promoted Aliphatic Fluorination. J. Org. Chem. 2018, 83, 8803−8814. (d) Capilato, J. N.; Pitts, C. R.; Rowshanpour, R.; Dudding, T.; Lectka, T. Site-Selective Photochemical Fluorination of Ketals: Unanticipated Outcomes in Selectivity and Stability. J. Org. Chem. 2020, 85, 2855−2864.

[6] (a) Norrish, R. G. W.; Bamford, C. H. Photo-decomposition of Aldehydes and Ketones. Nature 1937, 140, 195−196. (b) Sauers, R. R.; Edberg, L. A. Modeling of Norrish Type II Reactions by Semiempirical and ab Initio Methodology. J. Org. Chem. 1994, 59, 7061−7066. (c) Wagner, P. J. Type II Photoelimination and Photocyclization of Ketones. Acc. Chem. Res. 1971, 4, 168−177. (d) Turro, N. J.; Dalton, J. C.; Dawes, K.; Farrington, G.; Hautala, R.; Morton, D.; Niemczyk, M.; Schore, N. Molecular Photochemistry of Alkanones in Solution: alpha-Cleavage, Hydrogen Abstraction, Cycloaddition, and Sensitization Reactions. Acc. Chem. Res. 1972, 5, 92−101. (e) Ihmels, H.; Scheffer, J. R. The Norrish Type II Reaction in the Crystalline State: Toward a Better Understanding of the Geometric Requirements for γ-Hydrogen Atom Abstraction. Tetrahe- dron 1999, 55, 885−907.

[7] Miller, D.; Tarantino, K.; Knowles, R. Proton-Coupled Electron Transfer in Organic Synthesis: Fundamentals, Applications, and Opportunities. Top. Curr. Chem. 2016, 374, 30.

[8] Bloom, S.; Pitts, C. R.; Miller, D.; Haselton, N.; Holl, M. G.; Urheim, E.; Lectka, T. A Polycomponent Metal-Catalyzed Aliphatic, Allylic, and Benzylic Fluorination. Angew. Chem., Int. Ed. 2012, 51, 10580−10583.

[9] Pitts, C. R.; Bloom, M. S.; Bume, D. D.; Zhang, Q. A.; Lectka, T. Unstrained C−C Bond Activation and Directed Fluorination Through Photocatalytically-Generated Radical Cations. Chem. Sci. 2015, 6, 5225−5229. See also: Pitts, C. R.; Ling, B.; Snyder, J. A.; Bragg, A. E.; Lectka, T. Aminofluorination of Cyclopropanes: A Multifold Approach through a Common, Catalytically Generated Intermediate. J. Am. Chem. Soc. 2016, 138, 6598−6609.

[10] (a) Molnar, I.; Gilmour, R. Catalytic Difluorination of Olefins. J. Am. Chem. Soc. 2016, 138, 5004−5007. (b) Crossley, S.; Obradors, C.; Martinez, R.; Shenvi, R. Mn-, Fe-, and Co-Catalyzed Radical Hydrofunctionalizations of Olefins. Chem. Rev. 2016, 116, 8912−

9000.(c)Nyffeler,P.T.;Duroń,S.G.;Burkart,M.D.;Vincent,S.P.; Wong, C. H. Selectfluor: mechanistic insight and applications. Angew. Chem., Int. Ed. 2005, 44, 192−212. (d) Danahy, K. E.; Cooper, J. C.; Van Humbeck, J. F. Benzylic Fluorination of Aza-Heterocycles Induced by Single-Electron Transfer to Selectfluor. Angew. Chem., Int. Ed. 2018, 57, 5134−5138. (e) Kee, C. W.; Chin, K. F.; Wong, M. W.; Tan, C. H. Selective fluorination of alkyl C−H bonds via photocatalysis. Chem. Commun. 2014, 50, 8211−8214. (f) Amaoka, Y.; Nagatomo, M.; Inoue, M. Metal-free fluorination of C (sp^3)−H bonds using a catalytic N-oxyl radical. Org. Lett. 2013, 15, 2160−
2163. (g) Brunet, V.; O'Hagan, D. Angew. Chem., Int. Ed. 2008, 47, 1179−1182.

[11] (a) Tarantino, K.; Liu, P.; Knowles, R. Catalytic Ketyl-Olefin Cyclizations Enabled by Proton-Coupled Electron Transfer. J. Am. Chem. Soc. 2013, 135, 10022−10025. (b) Gentry, E.; Knowles, R. Synthetic Applications of Proton-Coupled Electron Transfer. Acc. Chem. Res. 2016, 49, 1546−1556. (c) Yayla, H. G.; Wang, H.; Tarantino, K. T.; Knowles, R. R.; Orbe, H. S. Catalytic Ring-Opening of Cyclic Alcohols Enabled by PCET Activation of Strong O−H Bonds. J. Am. Chem. Soc. 2016, 138, 10794−10797.

[12] (a) Markle, T. F.; Darcy, J. W.; Mayer, J. M. A New Strategy to Efficiently Cleave and Form C−H Bonds Using Proton-Coupled Electron Transfer. Sci. Adv. 2018, 4, 5776. (b) Darcy, J. W.; Kolmar, S. S.; Mayer, J. M. Transition State Asymmetry in C−H Bond Cleavage by Proton-Coupled Electron Transfer. J. Am. Chem. Soc. 2019, 141, 10777−10787.

[13] Darcy, J. W.; Koronkiewicz, B.; Parada, G.; Mayer, J. A Continuum of Proton-Coupled Electron Transfer Reactivity. Acc. Chem. Res. 2018, 51, 2391−2399.

[14] Kee, C. W.; Chin, K. F.; Wong, M. W.; Tan, C. H. Selective Fluorination of Alkyl C−H Bonds via Photocatalysis. Chem. Commun. 2014, 50, 8211−8214.

[15] Niu, L.; Liu, J.; Liang, X. A.; Wang, S.; Lei, A. Visible Light- Induced Direct α C−H Functionalization of Alcohols. Nat. Commun. 2019, 10, 467.

[16] Meanwell, M.; Lehmann, J.; Eichenberger, M.; Martin, R. E.; Britton, R. Synthesis of Acyl Fluorides via Photocatalytic Fluorination of Aldehydic C−H Bonds. Chem. Commun. 2018, 54, 9985−9988.

[17] (a) Herkstroeter, W. G.; Lamola, A. A.; Hammond, G. S. Mechanisms of Photochemical Reactions in Solution. XXVIII. Values of Triplet Excitation Energies of Selected Sensitizers. J. Am. Chem. Soc. 1964, 86, 4537−4540. (b) Schuster, D. I.; Dunn, D. A.; Heibel, G. E.; Brown, P. B.; Rao, J. M.; Woning, J.; Bonneau, R. Enone Photochemistry. Dynamic Properties of Triplet Excited States of Cyclic Conjugated Enones as Revealed by Transient Absorption Spectroscopy. J. Am. Chem. Soc. 1991, 113, 6245−6255. (c) Evans, T. R.; Leermakers, P. E. Emission Spectra and Excited-State Geometry of alpha-Diketones. J. Am. Chem. Soc. 1967, 89, 4380−4382.

[18] (a) Bunbury, D. L.; Chan, T. M. The Photolysis of 4- Hydroxybenzil and the Effect of Triethylamine on the Photolysis of Benzil and 4-Hydroxybenzil. Can. J. Chem. 1972, 50, 2499−2510. (b) Bunbury, D. L.; Wang, C. T. The Photolysis of Benzil in Cyclohexane Solution. Can. J. Chem. 1968, 46, 1473−1479. (c) Encinas, M. V.; Scaiano, J. C. Laser Photolysis Study of the Exciplex between Triplet Benzil and Triethylamine. J. Am. Chem. Soc. 1979, 101, 7740−7741. (d) Mohapatra, G. K. D.; Bhattacharya, J.; Bandopadhyay, J.; Bera, S. C. Flash Photolysis of Benzils. J. Photochem. 1987, 40, 47−58. (e) McGimpsey, W. G.; Scaiano, J. C. A Two-Photon Study of the "Reluctant" Norrish Type I Reaction of Benzil. J. Am. Chem. Soc. 1987, 109, 2179−2181. (f) Scaiano, J. C.; Johnston, L. J.; McGimpsey, W. G.; Weir, D. Photochemistry of Organic Reaction Intermediates: Novel Reaction Paths Induced by Two-Photon Laser Excitation. Acc. Chem. Res. 1988, 21, 22−29. (g) Mukai, M.; Yamauchi, S.; Hirota, N. Time-Resolved EPR Study on the Photochemical Reactions of Benzil. J. Phys. Chem. 1992, 96, 3305−3311. (h) Adam, W.; Oestrich, R. S. Two-Photon Cleavage of Benzil in the Laser-Jet: Intermolecular Reactions of Transient Benzoyl and tert-Butoxy Radicals in the Photolysis of tert-Butyl Peroxide Mixtures. J. Am. Chem. Soc. 1993, 115, 3455−3457. (i) Mukai, M.; Yamauchi, S.; Hirota, N. A Time-Resolved ERR Study of One- and Two-Photon Processes in the Photochemical Reactions of Benzil. J. Phys. Chem. 1989, 93, 4411−4413. (j) Kosa, C.; Lukać , I. Photophysical and Photochemical Properties of Benzil. Chem. Listy. 1996, 90, 287−294. (k) Furusawa, T.; Kawano, M.; Fujita, M. The Confined Cavity of a Coordination Cage Suppresses the Photo- cleavage of α-Diketones to Give Cyclization Products through Kinetically Unfavorable Pathways. Angew. Chem., Int. Ed. 2007, 46, 5717−5719. (l) Volman, D. H.; Hammond, G. S.; Gollnick, K. A Model for the Influence of Organized

Media on Photochemical Reactions. Advances in Photochemistry; Wiley: New York, 2009; Vol. 16, pp 85−87. (m) Simburger, H.; Kern, W.; Hummel, K.; Hagg, C. Photoreactions in Polymers Containing Benzil Units: A Comparative Study Under Excimer Laser and Hg-Lamp Irradiation. Polymer 2000, 41, 7883−7897 and references therein..

[19] Yang, Y.; Liu, L.; Chen, J.; Han, K. Hydrogen Bonding Tunes the Early Stage of Hydrogen-Atom Abstracting Reaction. Phys. Chem. Chem. Phys. 2014, 16, 17828.

[20] Leigh, W. J.; Lathioor, E. C.; St. Pierre, M. J. Photoinduced Hydrogen Abstraction from Phenols by Aromatic Ketones. A New Mechanism for Hydrogen Abstraction by Carbonyl n,π* and π,π* Triplets. J. Am. Chem. Soc. 1996, 118, 12339−12348.

[21] Zhang, X.; Ma, J.; Li, S.; Li, M. D.; Guan, X.; Lan, X.; Phillips, D. L.; Zhu, R. Ketyl Radical Formation via Proton-Coupled Electron Transfer in an Aqueous Solution versus Hydrogen Atom Transfer in Isopropanol after Photoexcitation of Aromatic Carbonyl Compounds. J. Org. Chem. 2016, 81, 5330−5336.

[22] Huggenberger, C.; Lipscher, J.; Fischer, H. Self-Termination of Benzoyl Radicals to Ground- and Excited-State Benzil. Symmetry Control of a Radical Combination. J. Phys. Chem. 1980, 84, 3467−3474.

[23] (a) Saltiel, J.; Curtis, H. C. Photooxidation of Benzil. Mol. Photochem. 1969, 1, 239−243. (b) Lukać,Ī.;Kośa,C.TheFormation of Dibenzoyl Peroxide by Photooxidation of Benzil in a Polymer Film. Macromol. Rapid Commun. 1994, 15, 929−934. (c) Cosa, G.; Scaiano, J. C. Photochemistry of Diketones: Observation of a Triplet State- Oxygen Adduct. J. Am. Chem. Soc. 2004, 126, 8636−8637.

[24] (a) Pitts, C. R.; Bloom, S.; Woltornist, R.; Auvenshine, D. J.; Ryzhkov, L. R.; Siegler, M. A.; Lectka, T. Direct, Catalytic Monofluorination of sp^3 C−H Bonds: A Radical-Based Mechanism with Ionic Selectivity. J. Am. Chem. Soc. 2014, 136, 9780−9791. (b) Rueda-Becerril, M.; Sazepin, C. C.; Leung, J. C. T.; Okbinoglu, T.; Kennepohl, P.; Paquin, J.-F.; Sammis, G. M. Fluorine Transfer to Alkyl Radicals. J. Am. Chem. Soc. 2012, 134, 4026−4029.

[25] Kee, J. W.; Shao, H.; Kee, C. W.; Lu, Y.; Soo, H. S.; Tan, C.-H. Mechanistic Insights for the Photoredox Organocatalytic Fluorination of Aliphatic Carbons by Anthraquinone Using Time-Resolved and DFT Studies. Catal. Sci. Technol. 2017, 7, 848.

[26] Padhye, M.; McGlynn, S.; Kasha, M. Lowest Triplet State of Anthracene. J. Chem. Phys. 1956, 24, 588.

[27] Parker, C.; Joyce, T. Formation Efficiency and Energy of the Perylene Triplet. Chem. Commun. 1966, 4, 108.

[28] Pearson, A. J.; Xiao, W. Fluorescent Photoinduced Electron Transfer (PET) Sensing Molecules with p-Phenylenediamine as Electron Donor. J. Org. Chem. 2003, 68, 5361−5368.

[29] (a) Zhang, Z. C.; Chung, T. M. Reaction Mechanism of Borane/Oxygen Radical Initiators during the Polymerization of Fluoromonomers. Macromolecules 2006, 39, 5187−5189. (b) Mirviss, S. B. Mechanism of the Oxidation of Trialkylboranes. J. Org. Chem. 1967, 32, 1713−171. (c) Szpera, R.; Moseley, D.; Smith, L.; Sterling, A.; Gouverneur, V. The Fluorination of C-H Bonds: Developments and Perspectives. Angew. Chem., Int. Ed. 2019, 58, 14824−14848. (d)Troyano,F.;Merkens,K.;Gomez-Suarez,A.Selectfluor®Radical Dication (TEDA2+.) − A Versatile Species in Modern Synthetic Organic Chemistry. Asian J. Org. Chem. 2020, 9, 992.

[30] Pitts, C. R.; Ling, B.; Woltornist, R.; Liu, R.; Lectka, T. Triethylborane-Initiated Radical Chain Fluorination: A Synthetic Method Derived from Mechanistic Insight. J. Org. Chem. 2014, 79, 8895−8899.

[31] Takahira, Y.; Chen, M.; Kawamata, Y.; Mykhailiuk, P.; Nakamura, H.; Peters, B. K.; Reisberg, S. H.; Li, C.; Chen, L.; Hoshikawa, T.; Shibuguchi, T.; Baran, P. S. Electrochemical C(sp3)− H Fluorination. Synlett 2019, 30, 1178−1782.

[32] (a) Weinberg, D. R.; Gagliardi, C. J.; Hull, J. F.; Murphy, C. F.; Kent, C. A.; Westlake, B. C.; Paul, A.; Ess, D. H.; McCafferty, D. G.; Meyer, T. Proton-Coupled Electron Transfer. Chem. Rev. 2012, 112, 4016−4093. (b) Warren, J.; Tronic, T.; Mayer, J. Thermochemistry of Proton-Coupled Electron Transfer Reagents and its Implications. Chem. Rev. 2010, 110, 6961−7001.

[33] (a) Williams, H.; Wilson, J. M.; Budzikiewicz, H.; Djerassi, C. Mass Spectrometry in Structural and Stereochemical Problems. XXIV. A Study of the Hydrogen Transfer Reactions Accompanying Fragmentation Processes of 11-Keto Steroids. Synthesis of Deuterated Androstan-11-ones. J. Am. Chem. Soc. 1963, 85, 2091−2105. (b) Djerassi, C.; Mutzenbecher, G. v.; Fajkos, J.; Williams, D. H.; Budzikiewicz, H. Mass Spectrometry in Structural and Stereochemical Problems. LXV. Synthesis and Fragmentation Behavior of 15-Keto Steroids. The Importance of Interatomic Distance in the McLafferty Rearrangement. J. Am. Chem. Soc. 1965, 87, 817.

[34] (a) Loos, J.; Schröder, D.; Schwarz, H. Diastereoselectivity in the McLafferty Rearrangement of Photoionized 3-Methyl Valeramide. J. Org. Chem. 2005, 70, 1073−1076. (b) Loos, J.; Schröder, D.; Schwarz, H.; Thissen, R.; Dutuit, O. Competitive Reactions and Diastereoselective CH Bond Activation in the McLafferty Rearrange- ment of Photoionized 3-Methyl Valeramide. Int. J. Mass Spectrom. 2005, 240, 121−137. (c) Loos, J.; Schröder, D.; Zummack, W.; Schwarz, H.; Thissen, R.; Dutuit, O. Dissociation Behavior of Ionized Valeramide: Part I. Experimental Studies. Int. J. Mass Spectrom. 2002, 214, 105−128.

[35] Djerassi,C.;Tökeś,L.MassSpectrometryinStructuraland Stereochemical Problems. XCIII. Further Observations on the Importance of Interatomic Distance in the McLafferty Rearrange- ment. Synthesis and Fragmentation Behavior of Deuterium-Labeled 12-Keto Steroids. J. Am. Chem. Soc. 1966, 88, 536−544.

[36] Hammerum, S. Alkyl Radicals as Hydrogen Bond Acceptors: Computational Evidence. J. Am. Chem. Soc. 2009, 131, 8627−8635.

[37] Simmons, E.; Hartwig, J. On the Interpretation of Deuterium Kinetic Isotope Effects in C-H Bond Functionalizations by Transition-Metal Complexes. Angew. Chem., Int. Ed. 2012, 51, 3066−3072.

[38] Jing,L.;Nash,J.;Kenttaṁaa,H.CorrelationofHydrogen- Atom Abstraction Reaction Efficiencies for Aryl Radicals with their Vertical Electron Affinities and the Vertical Ionization Energies of the Hydrogen-Atom Donors. J. Am. Chem. Soc. 2008, 130, 17697−17709.

[39] (a) Walling, C. Free Radicals in Solution; Wiley, New York, 1957. (b) Bernardi, R.; Galli, R.; Minisci, F. Polar and Steric Effects in Hydrogen Abstraction by Dialkylamine Cation Radicals. J. Chem.

Soc. B 1968, 324−325. (c) Minisci, F.; Galli, R.; Bernardi, R. Polar Effects in Radical Reactions: A New Selective Type of Radical Bromination. Chem. Commun. 1967, 903−904. (d) Zavitsas, A. A.; Pinto, J. A. The Meaning of the "Polar Effect" in Hydrogen Abstractions by Free Radicals. Reactions of the tert-Butoxy Radical. J. Am. Chem. Soc. 1972, 94, 7390−7396. (e) Newhouse, T.; Baran, P. If C-H Bonds Could Talk: Selective C-H Bond Oxidation. Angew. Chem., Int. Ed. 2011, 50, 3362−3374.

[40] Nodwell, M. B.; Bagai, A.; Halperin, S. D.; Martin, R. E.; Knust, H.; Britton, R. Direct Photocatalytic Fluorination of Benzylic C−H Bonds with N-Fluorobenzenesulfonimide. Chem. Commun. 2015, 51, 11783−11786.

[41] Singh, S.; DesMarteau, D.; Zuberi, S.; Witz, M.; Huang, H. N. N-Fluoroperfluoroalkylsulfonimides. Remarkable New Fluorination Reagents. J. Am. Chem. Soc. 1987, 109, 7194−7196.

[42] Tishchenko, O.; Truhlar, D. G.; Ceulemans, A.; Nguyen, M. A Unified Perspective on the Hydrogen Atom Transfer and Proton- Coupled Electron Transfer Mechanisms in Terms of Topographic Features of the Ground and Excited Potential Energy Surfaces as Exemplified by the Reaction between Phenol and Radicals. J. Am. Chem. Soc. 2008, 130, 7000−7010.

[43] Mayer, J. M. Simple Marcus-Theory-Type Model for Hydrogen-Atom Transfer/Proton-Coupled Electron Transfer. J. Phys. Chem. Lett. 2011, 2, 1481−1489.

[44] (a) Harcourt, R. D. Four-Electron Three-Center Bonding: One-Electron and Concerted Two-Electron Delocalizations into Bonding and Antibonding Molecular Orbitals. J. Phys. Chem. A 1999, 103, 4293−4297. (b) Klein, J.; Knizia, G. cPCET Versus HAT: A Direct Theoretical Method for Distinguishing X-H Bond-Activation Mechanisms. Angew. Chem., Int. Ed. 2018, 57, 11913−11917.

Chapter 6:

Cooperative Noncovalent Interactions Lead to a Highly Diastereoselective Sulfonyl-Directed Fluorination of Steroidal α,β-Unsaturated Hydrazones

6.1. Introduction.

Nonclassical hydrogen bonding, including C−H···n (n = lone pair) and C−H···π bonds, has been the subject of increased attention in recent years. Of particular interest is the ability of such interactions to affect the structure and behavior of biological molecules, including proteins, lipids, and nucleic acids.[1] For example, steroids, being principally hydrocarbon- based, may rely on C−H···π hydrogen bonds to form highly specific interactions with their corresponding receptor binding domains.[2] One well-studied example of this can be seen in the binding of cholesterol to the β2-adrenergic receptor.[3] Our laboratory, having experience in synthetic steroid chemistry,[4] was interested in the potential to borrow this clever recognition paradigm from nature in order to address the synthetically challenging topic of stereoselectivity. In this note, we report steroid hydrazones that engage in putative C−H··· N/ π interactions in the ground state. However, a complementary set of C−H···O hydrogen bonds dictates a highly diastereoselective and apparently contrasteric sulfonyl- directed fluorination in the transition state for the reaction with Selectfluor.

6.2. Synthesis and X-ray Crystal Structure of Steroid 2.

We began our studies with dehydroepiandrosterone (DHEA), an essential and abundant human steroid that is also utilized pharmaceutically under the name Prasterone.[5] We

reasoned that the oxidation of DHEA to the medicinally relevant enone[6] would provide a suitable handle to functionalize the steroid skeleton with an aromatic moiety that had the proper orientation to stack intramolecularly on either the α- or β-face of the steroid.[7] Thus, a concise synthesis of a diacetoxyenone derivative of DHEA was carried out according to our previously published protocol,[8] followed by the formation of the tosylhydrazone **1** (Scheme 6.1). While the hydrazone was successfully generated, we observed the partial

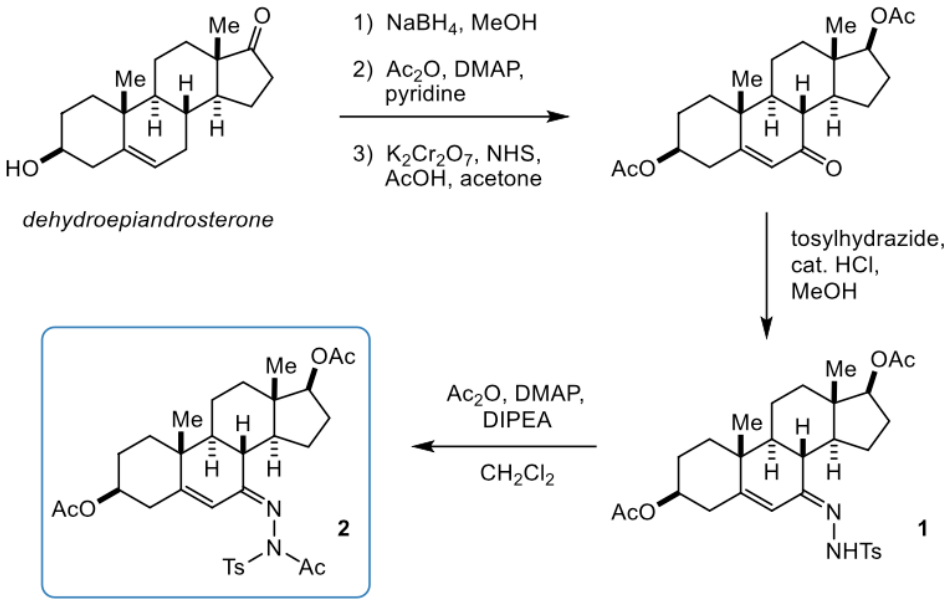

Scheme 6.1. Synthesis of Steroid Hydrazone **2** from DHEA

solvolysis of the acetoxy esters under these conditions, likely due to the use of acidic methanol. Accordingly, another cycle of acylation produced compound **2**, resulting from the unintentional (but serendipitous) acetylation of the sulfonamide to the sulfonimide. The ^{1}H NMR spectrum of **2** contained some peculiar features, which complicated our identification of the compound; therefore, we obtained single- crystal X-ray diffraction

data that allowed us to assign the structure unambiguously. Significantly, we observed two prominent intramolecular C−H interactions involving the vinylic C−H bond of the B-ring olefin: an apparently weak C− H···N hydrogen bond involving the hydrazino nitrogen atom and a C−H···π interaction involving the aromatic ring (Figure 6.1). This π-interaction occurs on the α-face of the steroid skeleton; the hydrazino moiety is oriented in such a

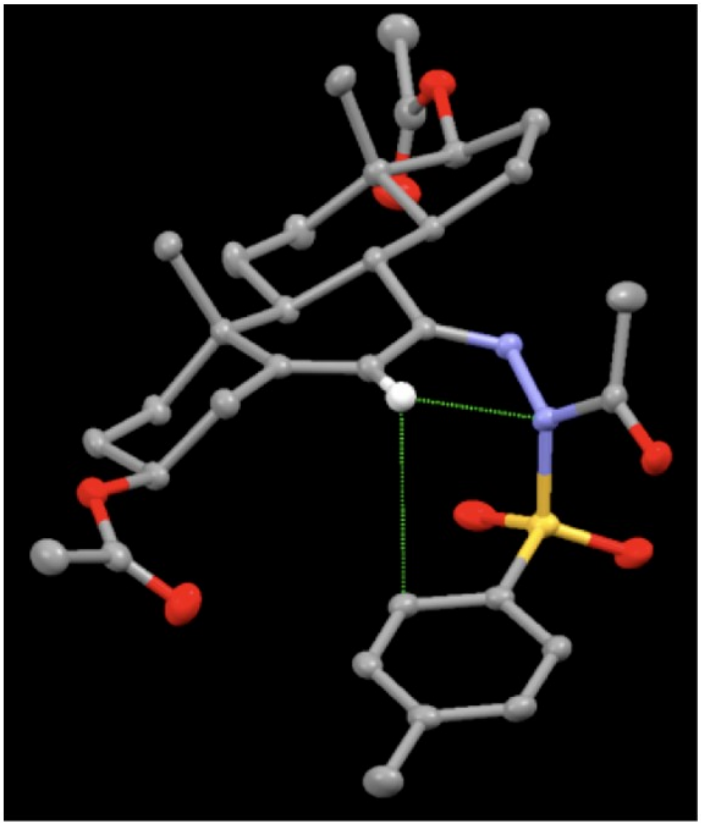

Figure 6.1. X-ray crystal structure of **2**.

fashion to enable both types of interactions, as the aryl ring adopts a quasi-slip-stacking (parallel-displaced) orientation below the B- ring of the tetracycle. A short distance of 2.49 Å was measured from the C6 hydrogen atom to the acceptor nitrogen atom[9] along with a

C−H···N bond angle of 94°. Furthermore, a distance of 3.11 Å was measured from the hydrogen atom to the closest carbon atom in the phenyl ring of the tosyl group (C−H···C bond angle of ca. 114°); corroborating this interaction is pyrimidization of the nitrogen atom. Although these C−H···N/ π bond angles are relatively small,[10] this can be attributed at least in part to the bifurcated and intramolecular nature of the interaction.

To better understand this unique intramolecular interaction, we resynthesized the steroidal hydrazone **1**, which was the originally intended target of this study. Performing the hydrazonation in neutral THF rather than acidic methanol allowed the straightforward isolation of 1 without the solvolysis of the acetoxy groups. Significantly, we observed a difference in the ^{1}H NMR of 1 compared to that of 2; the signal for the vinylic C−H bond of the B-ring olefin was abnormally broad and deshielded in steroid **2** (Figure 6.2).

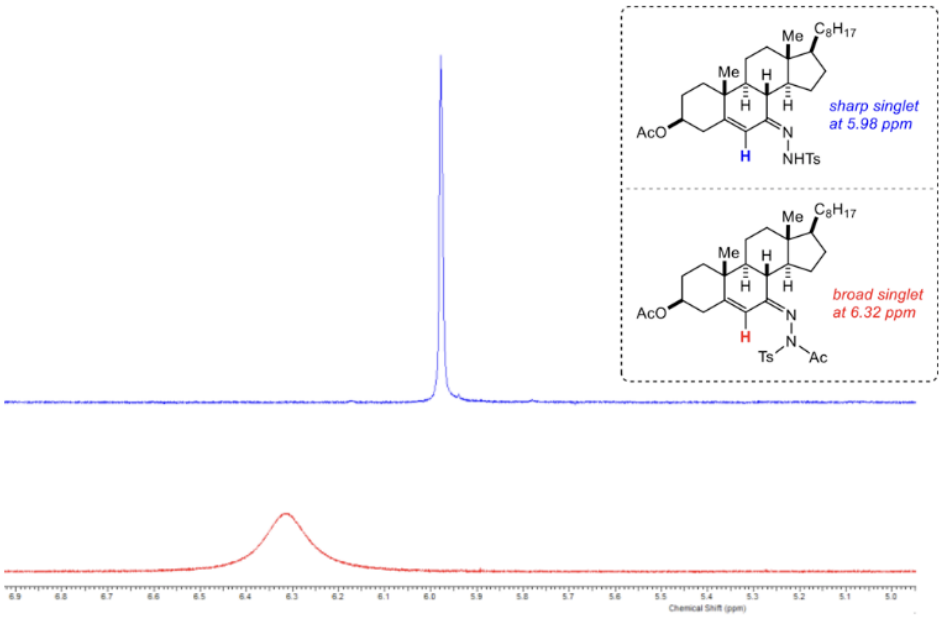

Figure 6.2. ^{1}H NMR comparison of vinylic C−H signals.

Given the crystal structure, we associate these spectroscopic features with the intramolecular C−H interactions in **2**. The ^{1}H NMR spectrum of 1 is analogous to both the starting material DHEA and the enone derivative in that this signal is a sharp singlet rather than a broad one[11] and is not unusually deshielded as it is in **2**.

6.3. Stereoselective Fluorination of Steroid 2.

Next, we shifted focus to search for interesting reactivity. Noting that the intramolecular interaction occurs on the α-face of the steroid, we recognized this as a potential means to selectively functionalize the less-hindered β-face. Contributing to this goal, the hydrazone moiety itself is nucleophilic at the α-position through its enamine tautomer,[12] meaning that potential functionalizations could benefit from being site- selective in addition to stereoselective. In the case of α,β- unsaturated hydrazone **2**, we anticipated the formation of a dienamine with a nucleophilic character at the C4 position of the steroid's A-ring. Surprisingly, such functionalizations of steroid imines are scant in the literature, although several examples have been reported using these precursors to access steroid lactams or amines by either a Beckman rearrangement or a reduction, respectively.[13]

Given our interest in the fluorination of steroids, we subjected cholesterol hydrazone **4** to a simple reaction with Selectfluor. A high-yield fluorination occurred that was both regio- and stereoselective, affording product **8** in a 76% yield (Scheme 6.2). The reaction proceeds under mild conditions —it is nonphotochemical and uncatalyzed —and occurs at room temperature in the dark. In regard to the site-selectivity, the fluorine atom was established to be at C6 (B-ring, α-position to the imine) rather than the initially proposed C4 position on the A-ring. This discrepancy is interesting as we first anticipated the

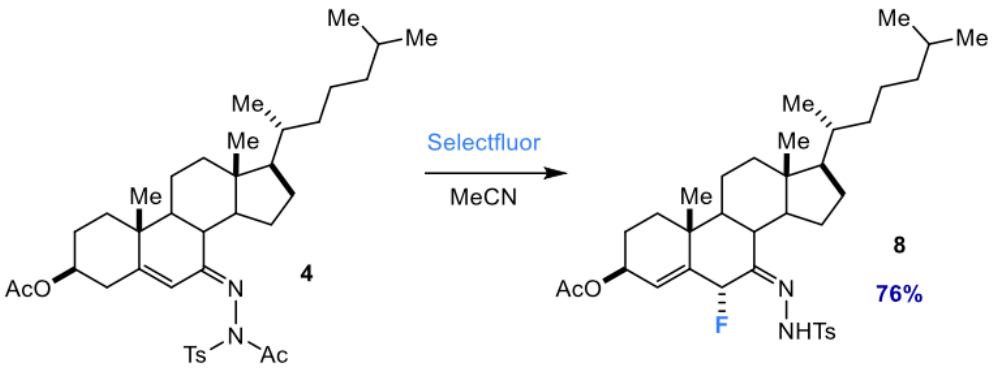

Scheme 6.2. Fluorination of Steroid Hydrazone **4**.

reaction of the dienamine intermediate at C4 to reestablish the α,β-unsaturated imine rather than the formation of the allylic ester. The facial selectivity of the fluorination is also counterintuitive at first glance; the reaction occurs on the α-face of the steroid rather than the putatively less-hindered β-face.

Another interesting feature of product **8** is the loss of the acetamide group, as the typically stable sulfonimide was cloven to the sulfonamide during fluorination. To gain insight into this unusual occurrence, we subjected hydrazone **4h** (which lacks the sulfonimide) to a fluorination under the same conditions. Surprisingly, the reaction did not take place with this derivative, further demonstrating the unique reactivity of steroid **4**. To follow up on this result, we synthesized an N- methyl analogue, **9**, to probe the necessity of the acetimide group (Figure S21).[14] This steroid was subjected to the fluorination and was found to undergo the reaction in identical regio- and stereoselectivities to the imide hydrazones, albeit in a lower yield (ca. 30%).[15]

To improve the synthetic utility of the fluorination, we considered methods to remove the hydrazone group under mild conditions, which would be necessary to make medicinally

relevant fluorosteroids.[16] While several options exist to accomplish this goal,[17] including Wolff−Kishner-type reactions, we stumbled across a simpler solution. We found that adding a small portion of additional Selectfluor to the reaction mixture after fluorination resulted in the apparent hydrolysis of the hydrazone products to the corresponding ketone in a one-pot fashion.[18] Synthetically, this becomes advantageous as one can toggle between fluorinated hydrazone or ketone products simply by controlling the stoichiometry of the Selectfluor.

We next sought to determine whether other steroids could participate in this unique C−H interaction and fluorination. Conveniently, the B-ring olefin found in DHEA is conserved across many naturally occurring steroids (Δ^5-steroids),[19] enabling synthesis of a variety of derivatives using analogous methods. A cholesterol hydrazone was prepared[20] (compound **4**) using the synthesis outlined for steroid **2** (Figure 6.3). This steroid engages in both the C−H interactions and the fluorination, delivering product **5** despite a substantial difference in the D-ring substituent. Along these lines, the spiroketal steroid diosgenin[21] was employed to synthesize a hydrazone analogue, **6**, that was found to undergo the C−H interactions and the fluorination, giving fluoride **7**.

Originally, we proposed that steric effects should control the stereoselectivity of the reaction. Given the observed C−H interactions described above, the tosylhydrazone moiety is positioned toward the α-face of the steroid, resulting in the β- face experiencing noticeably less steric hindrance. As noted, we found that the fluorination exclusively produced the α-fluoride product. Further complicating our analysis was the literature precedent for the fluorination of steroids at the same position (C6). Rozatian et al. reported a 43:57 mixture of diastereomers for C6 fluorination of a steroid enol ester using

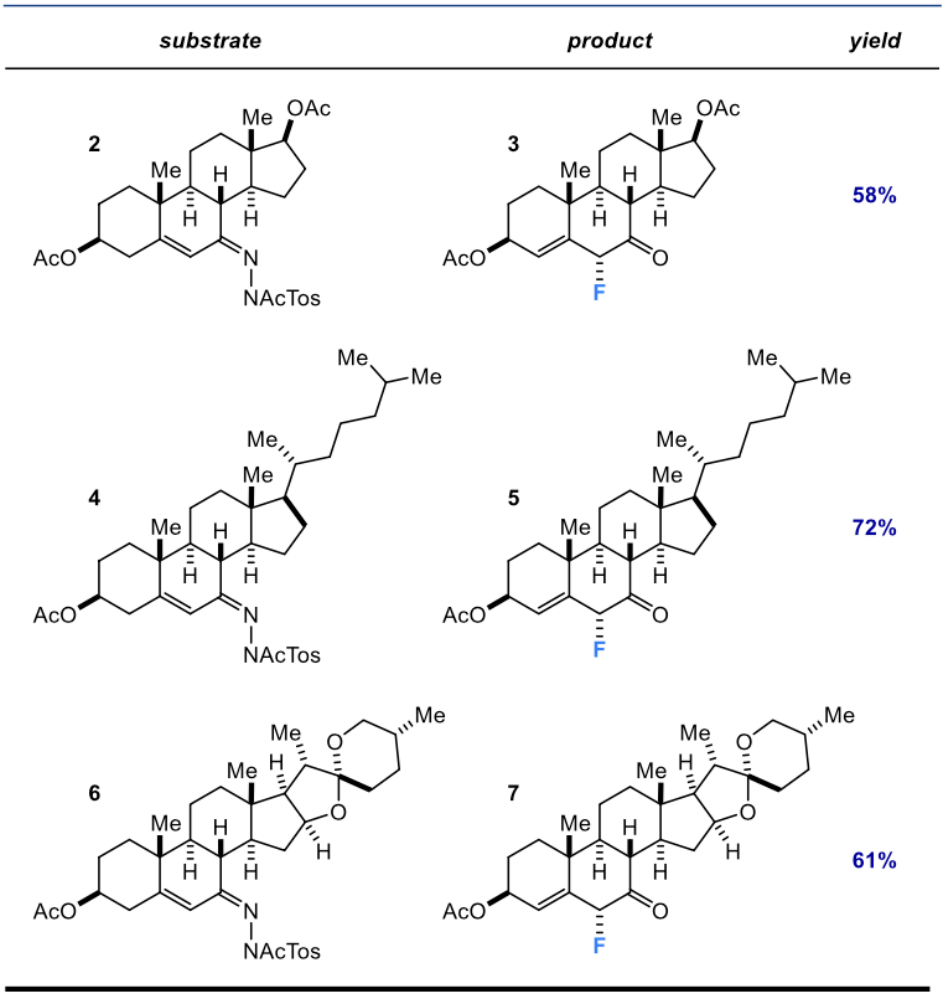

Figure 6.3. Product examples for hydrazone fluorination.

Selectfluor (Figure 6.4).[22] On the other hand, higher β-selectivity was observed using bulky boron complexing agents.[23] Moreover, the fluorination in these examples occurred distal (γ) to the enol to regenerate the conjugated enone, in contrast to our results.

6.4. A Sulfonyl Directing Group Identified in the Transition State for Fluorination.

To explain these observations, along with the finding that fluorination occurred on the more hindered face of the steroid, we propose that the sulfonylhydrazone moiety acts as a

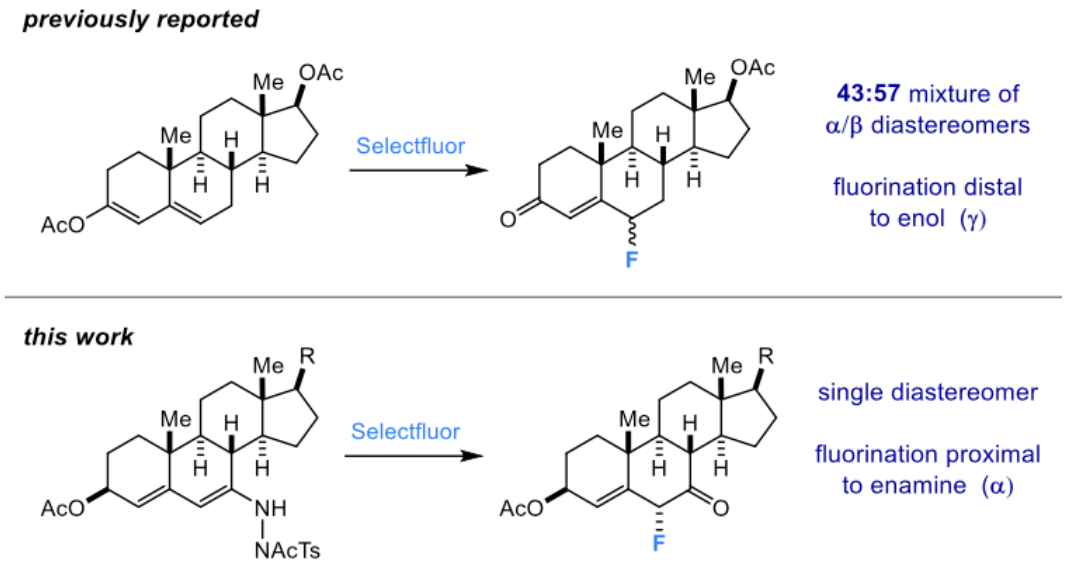

Figure 6.4. Literature precedent for fluorination at C6.

directing group. Recently, we reported the mechanistic study of a regioselective radical-based fluorination of steroids and other complex substrates. To our surprise, the selectivity of this reaction was driven by the ability of the Selectfluor-based radical cation to hydrogen bond to a carbonyl group on the substrate.[24] In the present reaction, we propose that the oxygen atoms of the sulfonyl group may be operating analogously to those carbonyls (acting as a hydrogen bond acceptor to the relatively acidic hydrogen atoms found in Selectfluor).

We turned to computational chemistry to examine the transition state for fluorination. The literature precedent for electronically similar enol esters suggests that a two-electron process may be occuring.[25] Couple this with our stereo- chemical data, which is difficult to reconcile with outer-sphere one-electron chemistry, and we chose to focus on the possibility of a concerted transition state, bearing in mind that the synchronicity of electron transfer could vary. Emerging from these calculations was a preferred α-fluorination

transition state α-TS1$_\alpha$ with a Gibbs free-energy activation barrier of 16.0 kcal/mol relative to the reacting components (Figure 6.5, calculated at ωb97xd/6-31G(d,p)//

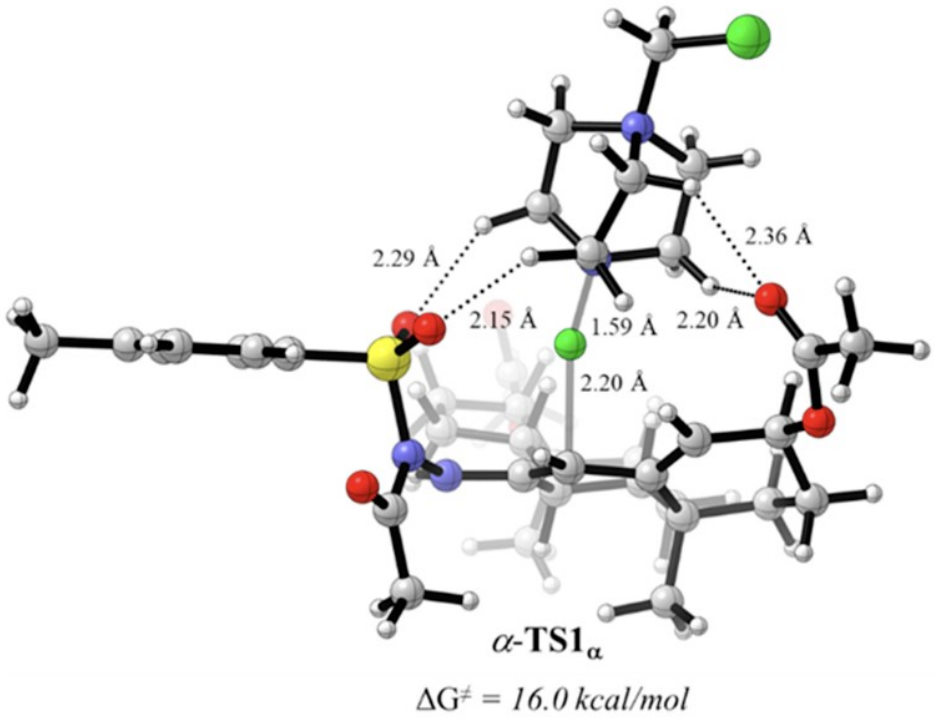

Figure 6.5. Computed transition state for the fluorination of **2**.

ωB97Xd/6-311+G(d,p) (MeCN)). Structurally, a hydrogen bond network defines the transition state, steering the fluorination to the α- face of the steroid substrate. Crucial to this network is a two- point hydrogen bond interaction with distances of 2.15 and 2.29 Å acting as a directing group tether between both sulfonyl oxygen atoms and two Selectfluor hydrogen atoms adjacent to the bridgehead nitrogen engaged in fluorine transfer. In addition, a pair of stabilizing hydrogen bonds with distances of 2.20 and 2.36 Å bridges the acetoxy carbonyl oxygen to the two hydrogen atoms of Selectfluor. A carbon−fluorine bond- forming distance of 2.20 Å and a nitrogen−fluoride bond- breaking distance of 1.59

Å were measured. Lastly, the role of Coulombic charge stabilization is notable as seen in the molecular electrostatic potential map (MEP) surface (Figure S29, left-hand side), wherein the electronegative sulfonyl and acetoxy group (red) reach out like guiding hands to direct Selectfluor (blue).

In contrast, the β-fluorination transition state α-TS1$_\beta$, with an activation barrier of 17.5 kcal/mol, was disfavored despite having bond-making and bond-breaking distances similar to those of α-TS1$_\alpha$ as well as a hydrogen bond network (Figure S29). Diving deeper into this structure nevertheless reveals the slippage of the anchoring and strongly directing sulfonyl group two-point hydrogen bond of α-TS1$_\alpha$.[26] Furthering the stereoselective preference, the sulfonyl groups are inherently oriented toward the α-face given the C−H···N/ π interaction, and this fact explains the apparent paradox of contrasteric reactivity. On the other hand, γ-fluorination of the enamine is uncompetitive, with relative Gibbs free activation barriers in excess of 24 kcal/mol. In this case, disrupting the stabilizing sulfonyl hydrogen bonding resulted in γ-fluorination being disfavored (see the Supporting Information for α- and β-face γ- fluorination transition states γ-TS1$_\alpha$ and γ-TS1$_\beta$, respectively).

Given the unique role of Selectfluor in this particular fluorination, we became interested in testing an alternative electrophilic fluorinating reagent in the reaction. We proposed that structurally distinct fluorinating reagents might deliver the same fluoride product, albeit without the stereoselectivity that is observed with Selectfluor. Steroid **2** was subjected to a reaction with N-fluorobenzenesulfonimide (NFSI); however, no fluorination occurred at room temperature, and NFSI only reacted upon heating. Several trace fluorinated products were formed, although none resembled the products obtained with Selectfluor. As NFSI is

often interchangeable with Selectfluor in simple electrophilic fluorinations,[27] this experiment high- lights the unique reactivity of Selectfluor in certain cases.

6.5. Conclusion.

We have developed a diastereoselective fluorination of steroid α,β-unsaturated hydrazones. Sulfonyl directing groups are shown to hydrogen bond to C−H atoms on the fluorination reagent in the transition state. In the ground state, however, these steroids experience an intra- molecular bifurcated C−H···N/π interaction. This work demonstrates once again the powerful cumulative effects of relatively weak interactions, such as C−H hydrogen bonds, on stereoselectivity.

6.6. References.

[1] (a) Desiraju, G. R.; Steiner, T. The Weak Hydrogen Bond In Structural Chemistry and Biology; Oxford University Press, Inc.: New York, NY, 2001. (b) Nishio, M.; Umezawa, Y.; Fantini, J.; Weiss, M. S.; Chakrabarti, P. CH−π hydrogen bonds in biological macro- molecules. Phys. Chem. Chem. Phys. 2014, 16, 12648−12683.

[2] Yeagle, P. L. The Structure of Biological Membranes, 2nd ed.; CRC Press: Boca Raton, FL, 2004.

[3] Hanson, M. A.; Cherezov, V.; Griffith, M. T.; Roth, C. B.; Jaakola, V. P.; Chien, E. Y.; Velasquez, J.; Kuhn, P.; Stevens, R. C. A Specific Cholesterol Binding Site Is Established by the 2.8 Å Structure of the Human β2-Adrenergic Receptor. Structure 2008, 16, 897−905.

[4] (a) Pitts, C. R.; Bume, D. D.; Harry, S. A.; Siegler, M. A.; Lectka, T. Multiple enone-directed reactivity modes lead to the selective photochemical fluorination of polycyclic terpenoid derivatives. J. Am. Chem. Soc. 2017, 139, 2208−2211. (b) Bume, D. D.; Harry, S. A.; Pitts, C. R.; Lectka, T. Sensitized aliphatic fluorination directed by terpenoidal enones: A “visible light” approach. J. Org. Chem. 2018,

83, 1565−1575. (c) Capilato, J. N.; Bume, D. D.; Lee, W. H.; Hoffenberg, L. E. S.; Jokhai, R. T.; Lectka, T. Fluorofunctionalization of C= C Bonds with Selectfluor: Synthesis of β-Fluoropiperazines through a Substrate-Guided Reactivity Switch. J. Org. Chem. 2018, 83, 14234− 14244. (d) Capilato, J. N.; Pitts, C. R.; Rowshanpour, R.; Dudding, T.; Lectka, T. Site-Selective Photochemical Fluorination of Ketals: Unanticipated Outcomes in Selectivity and Stability. J. Org. Chem. 2020, 85, 2855−2864.

[5] Eberling, P.; Koivisto, V. A. Physiological importance of dehydroepiandrosterone. Lancet 1994, 343, 1479−1481.

[6] (a) Numazawa, M.; Mutsumi, A.; Tachibana, M.; Hoshi, K. Synthesis of androst-5-en-7-ones and androsta-3, 5-dien-7-ones and their related 7-deoxy analogs as conformational and catalytic probes for the active site of aromatase. J. Med. Chem. 1994, 37, 2198−2205. (b) Arsenou, E. S.; Fousteris, M. A.; Koutsourea, A. I.; Papageorgiou, A.; Karayianni, V.; Mioglou, E.; Iakovidou, Z.; Mourelatos, D.; Nikolaropoulos, S. S. The allylic 7-ketone at the steroidal skeleton is crucial for the antileukemic potency of chlorambucil's active metabolite steroidal esters. Anti-Cancer Drugs 2004, 15, 983−990.

[7] Frisčič,T.;Lancaster,R.W.;Fabian,L.;Karamertzanis,P.G. Tunable recognition of the steroid α-face by adjacent π-electron density. Proc. Natl. Acad. Sci. U. S. A. 2010, 107, 13216−13221.

[8] Bume, D. D.; Pitts, C. R.; Ghorbani, F.; Harry, S. A.; Capilato, J. N.; Siegler, M. A.; Lectka, T. Ketones as directing groups in photocatalytic sp^3 C−H fluorination. Chem. Sci. 2017, 8, 6918−6923.

[9] It should be noted that the hydrogen atoms were placed at calculated positions; thus, the C_6−H distance was fixed. The C_6−N distance was measured to be 2.72 Å.

[10] Nishio, M.; Umezawa, Y.; Honda, K.; Tsuboyama, S.; Suezawa, H. CH/π hydrogen bonds in organic and organometallic chemistry. CrystEngComm 2009, 11, 1757−1788.

[11] Lam, Y. P.; Yeung, Y. Y. Metal-Free Allylic Oxidation of Steroids Using TBAI/TBHP Organocatalytic Protocol. Chem. - Asian J. 2018, 13, 2369−2372.

[12] Stork, G.; Brizzolara, A.; Landesman, H.; Szmuszkovicz, J.; Terrell, R. The enamine alkylation and acylation of carbonyl compounds. J. Am. Chem. Soc. 1963, 85, 207−222.

[13] (a) Charaschanya, M.; Aube, J. Reagent-controlled regiodi- vergent ring expansions of steroids. Nat. Commun. 2018, 9, 943. (b) Szendi, Z.; Dombi, G.; Vincze, I. Steroids, LIII: New routes to aminosteroids. Monatsh. Chem. 1996, 127, 1189−1196.

[14] Spectroscopic evidence of the C−H interaction was observed for this steroid; while the vinylic hydrogen atom was significantly deshielded compared to that of 4h (6.61 vs 5.98 ppm), the signal was sharp rather than broad (see the Supporting Information).

[15] To rationalize this finding, we propose that the electron- withdrawing imide moiety facilitates the tautomerization of the α,β- unsaturated hydrazone to the reactive conjugated dienamine.

[16] Jasem, Y. A.; Thiemann, T.; Gano, L.; Oliveira, M. C. Fluorinated steroids and their derivatives. J. Fluorine Chem. 2016, 185, 48−85.

[17] (a) Hutchins, R. O.; Milewski, C. A.; Maryanoff, B. E. Selective deoxygenation of ketones and aldehydes including hindered systems with sodium cyanoborohydride. J. Am. Chem. Soc. 1973, 95, 3662− 3668. (b) Caglioti, L.; Magi, M. The reaction of tosylhydrazones with lithium aluminium hydride. Tetrahedron 1963, 19, 1127−1131.

[18] Although we employed freshly dried or distilled solvent for the reaction, evidently a trace quantity of water was still present in the reaction. Given the typical acid-catalyzed mechanism for hydrazone hydrolysis, we propose that Selectfluor fluorinates the hydrazone nitrogen atom, initiating the hydrolysis.

[19] Salvador, J.A.R.; Sae Melo, M.L.; Campos Neves, A.S. Copper- catalysed allylic oxidation of Δ5-steroids by t-butyl hydroperoxide. Tetrahedron Lett. 1997, 38, 119−122.

[20] Mourelatos, C.; Kareli, D.; Dafa, E.; Argyraki, M.; Koutsourea, A.; Papakonstantinou, I.; Fousteris, M.; Pairas, G.; Nikolaropoulos, S.; Lialiaris, T. S. Cytogenetic and antineoplastic effects by newly synthesised steroidal alkylators in lymphocytic leukaemia P388 cells in vivo. Mutat. Res., Genet. Toxicol. Environ. Mutagen. 2012, 746, 1−6.

[21] Moalic,S.;Liagre,B.;Corbière,C.;Bianchi,A.;Daucą,M.; Bordji, K.; Beneytout, J. L. A plant steroid, diosgenin, induces apoptosis, cell cycle arrest and COX activity in osteosarcoma cells. FEBS Lett. 2001, 506, 225−230.

[22] Rozatian, N.; Harsanyi, A.; Murray, B. J.; Hampton, A. S.; Chin, E. J.; Cook, A. S.; Hodgson, D. R.; Sandford, G. Kinetics of electrophilic fluorination of steroids and epimerisation of fluoroste- roids. Chem. - Eur. J. 2020, 26, 12027−12035.

[23] Poss, A. J.; Shia, G. A. γ-Fluorination of Unsaturated Ketones with N-Fluorobenzenesulfonimide. Tetrahedron Lett. 1995, 36, 4721− 4724.

[24] Ghorbani, F.; Harry, S. A.; Capilato, J. N.; Pitts, C. R.; Joram, J.; Peters, G. N.; Tovar, J. D.; Smajlagic, I.; Siegler, M. A.; Dudding, T.; Lectka, T. Carbonyl-Directed Aliphatic Fluorination: A Special Type of Hydrogen Atom Transfer Beats Out Norrish II. J. Am. Chem. Soc. 2020, 142, 14710−14724.

[25] Wood, S. H.; Etridge, S.; Kennedy, A. R.; Percy, J. M.; Nelson, D. J. The Electrophilic Fluorination of Enol Esters Using SelectFluor: A Polar Two-Electron Process. Chem. - Eur. J. 2019, 25, 5574−5585.

[26] The sulfonyl two-point hydrogen bond in α-TS1$_\alpha$ is not present in α-TS1β. Instead, a bifurcated hydrogen bond arrangement with distances of 2.22 and 2.27 Å was observed, representing a potential source of destabilization and making α-TS1β disfavored (see the Supporting Information).

[27] Taylor, S. D.; Kotoris, C. C.; Hum, G. Recent advances in electrophilic fluorination. Tetrahedron 1999, 55, 12431−12477.

[28] Frisch, M. J.; Trucks, G. W.; Schlegel, H. B.; Scuseria, G. E.; Robb, M. A.; Cheeseman, J. R.; Scalmani, G.; Barone, V.; Mennucci, B.; Petersson, G. A.; Nakatsuji, H.; Caricato, M.; Li, X.; Hratchian, H. P.; Izmaylov, A. F.; Bloino, J.; Zhang, G.; Sonnenberg, J. L.; Hada, M.; Ehara, M.; Toyota, K.; Fukuda, R.; Hasegawa, J.; Ishida, M.; Nakajima, T.; Honda, Y.; Kitao, O.; Nakai, H.; Vreven, T.; Montgomery, J. A., Jr.; Peralta, J. E.; Ogliaro, F.; Bearpark, M.; Heyd, J. J.; Brothers, E.; Kudin, K. N.; Staroverov, V. N.; Kobayashi, R.; Normand, J.; Raghavachari, K.; Rendell, A.; Burant, J. C.; Iyengar, S. S.; Tomasi, J.; Cossi, M.; Rega, N.; Millam, J. M.; Klene, M.; Knox, J.e.; Cross, J. B.; Bakken, V.; Adamo, C.; Jaramillo, J.; Gomperts, R.; Stratmann, R. E.; Yazyev, O.; Austin, A. J.; Cammi, A. R.; Pomelli, C.; Ochterski, J. W.; Martin, R. L.; Morokuma, K.; Zakrzewski, V. G.; Voth, G. A.; Salvador, P.; Dannenberg, J. J.; Dapprich, S.; Daniels, A. D.; Farkas, Ö.; Foresman, J. B.; Ortiz, J. V.; Cioslowski, J.; Fox, D. J. Gaussian 09, rev. E.01; Gaussian, Inc.: Wallingford, CT, 2009.

[29] Chai, J.-D.; Head-Gordon, M. Long-range corrected hybrid density functionals with damped atom−atom dispersion corrections. Phys. Chem. Chem. Phys. 2008, 10, 6615−6620.

[30] (a) Gonzaĺez, C.; Schlegel, H. B. Reaction path following in mass-weighted internal coordinates. J. Phys. Chem. 1990, 94, 5523− 5527. (b) Fukui, K. The Path of Chemical Reactions − The IRC Approach. Acc. Chem. Res. 1981, 14, 363−368.

[31] Cancès, E.; Mennucci, B.; Tomasi, J. A New Integral Equation Formalism for the Polarizable Continuum Model: Theoretical Background and Applications to Isotropic and Anisotropic Dielectrics. J. Chem. Phys. 1997, 107, 3032−3041.

[32] Legault, C. Y. CYLview, ver. 1.0b; Universite de Sherbrooke: Quebec, Canada, 2009. http://www.cylview.org.

[33] Dennington, R.; Keith, T.; Millam, J. GaussView, ver. 5; Semichem, Inc.: Shawnee, KS, 2009.

[34] Schrödinger Release 2019-2: MacroModel; Schrödinger, LLC: New York, NY, 2019.

[35] Schrödinger Release 2019-2: Jaguar; Schrödinger, LLC: New York, NY, 2019.

Chapter 7:

Arene Amination Instead of Fluorination: Substitution Pattern Governs the Reactivity of Dialkoxybenzenes with Selectfluor

7.1. Introduction.

Electron-rich aromatic compounds are typically best-known for their ability to engage in electrophilic aromatic substitution (EAS) reactions with strong electrophiles.[1] This classic reaction paradigm and the complementary topic of directing group effects are fundamental concepts taught to every student of organic chemistry. Less appreciated is the dual ability of these electron-rich arenes to undergo single-electron oxidation to the corresponding radical cations.[2] Several groups have recently demonstrated the synthetic utility of this approach en route to compounds of biological or pharmaceutical interest.[3] Our laboratory has found a class of electron-rich arenes that can be predictably tuned to favor either an apparent two- electron or a sequential one-electron reactivity (i.e., EAS vs oxidation to the radical cation, respectively) under the same conditions.

Using Selectfluor as the key reagent in our studies, we found that dialkoxyarenes react based on their substitution patterns. At the onset, we reasoned that Selectfluor would be ideal for this study as it possesses the necessary dual reactivity; it is widely employed as both an electrophilic fluorination reagent and an oxidant.[4] Surprisingly, upon the reaction with Selectfluor, *meta*-dialkoxyarenes give exclusively the EAS fluoride product whereas *ortho*- and *para*-dialkoxyarenes predominantly form amination products, resulting from the putative single-electron oxidation of the electron-rich arene. We quickly recognized the

potential of this divergent reactivity to be useful as a synthetic method as well as a tool to better understand these archetypal reactions.

C−N bond-forming reactions are well-studied and widely employed throughout synthetic chemistry.[5] Methods that functionalize an unactivated carbon atom, as opposed to substitution chemistry involving amines and alkyl, acyl, or aryl halides, are particularly useful; however, they may suffer from a lack of regioselectivity.[6] Thus, the site-selective amination of electron-rich arenes is of practical utility, especially given the ubiquity of nitrogen-containing pharmaceuticals.[7] Typically, these valuable products are synthesized in a roundabout fashion from the electron-rich arene via either a halogenation− cross-coupling sequence or a nitration−reduction−substitution sequence.[8] Direct C−H to C−N bond formation between arenes and nitrogen heterocycles is more rare, although a few recent methods have been reported.[9] In this article, we disclose a remarkably simple and effective solution to this problem using only the coupling partners (the nitrogen heterocycle and electron-rich arene) and commercially available Selectfluor. Moreover, we reveal a mechanistic switch that occurs based on the substitution pattern of the electron-rich arene, allowing a user to toggle between the amination and fluorination products.

7.2. Substitution Pattern Governs the Reactivity of Dialkoxybenzenes with Selectfluor.

Our attention was drawn to this reactivity upon treating Selectfluor with veratrole (1,2-dimethoxybenzene) in acetonitrile at room temperature. Instead of the expected EAS product 1-fluoro-3,4-dimethoxybenzene, we isolated an amination product, an adduct of veratrole and the Selectfluor-derived amine, in a nearly quantitative yield (Figure 7.1,

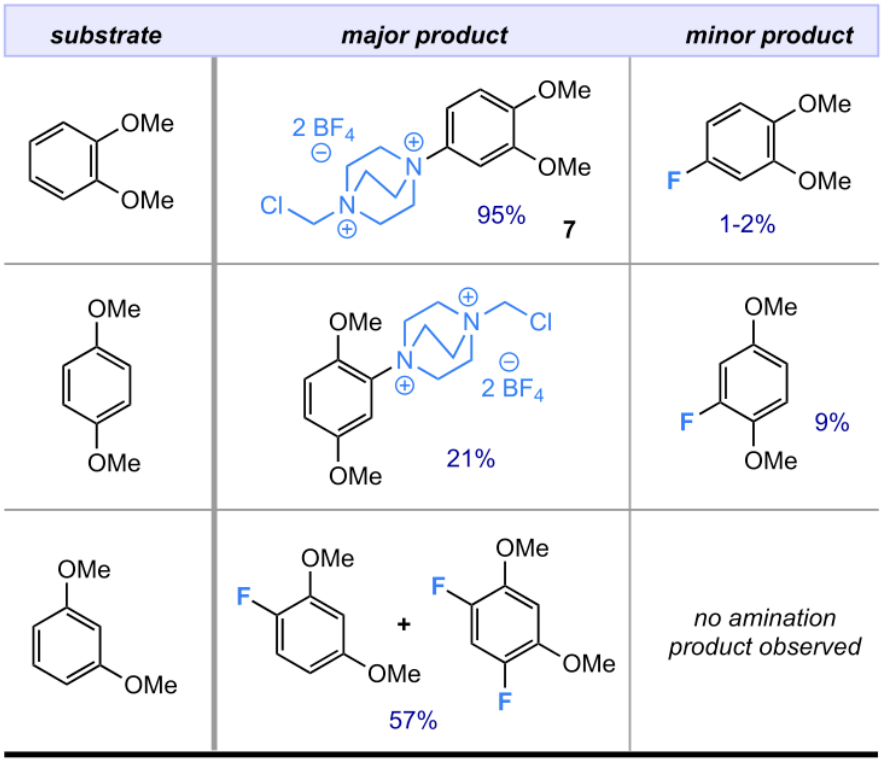

Figure 7.1. Divergent reactivity of dialkoxybenzenes with Selectfluor.

compound **7**). This came as a surprise given our knowledge of similar products being prepared using a dual- catalyst system, since no examples have been reported using Selectfluor alone.[10] Accordingly, several analogous arenes were tested to determine the generality of the reaction. Anisole afforded only the EAS fluorination product upon a reaction with Selectfluor,[11] suggesting the need for an increased electron-rich character to accomplish the amination. That idea, however, was contravened by the reaction of 1,3-dimethoxybenzene with Selectfluor, which exclusively formed the EAS aryl fluoride.[12] Further complicating the situation, 1,4- dimethoxybenzene predominately gave the amination product, although in lower yield than veratrole. Given the trend presented in Figure 1, it was not immediately obvious what might be causing the reactivity switch

between the fluorination and amination reactions. From both a steric and an electronic viewpoint, one would not predict a large difference between the three isomers of dimethoxybenzene in regard to fluorination versus amination.

7.3. Substrate Scope of the Reaction.

While the aryl−Selectfluor adducts are not high-demand compounds themselves, they can be easily transformed to medicinally relevant aryl piperazines using a one-pot process developed by the Ritter group (Figure 7.2, compounds **7** and **8**).[10] We found that other types of adducts can be formed in a high yield by performing the reaction in the presence of a variety of nitrogen heterocycles, thereby greatly increasing the synthetic utility of the reaction. As some veratrole−nitrogen heterocycle adducts are known to be medicinally active, such as the drug Domipizone,[13] these products demonstrate the simple and direct synthesis of pharmaceutically relevant veratrole adducts. Screening was performed using veratrole as a model electron- rich arene; many nitrogen heterocycles were found to be competent in the reaction, although the use of Selectfluor could be problematic with certain highly reactive heterocycles. Nevertheless, benzimidazole, benzotriazole, 5-tBu-tetrazole, and imidazole were found to work well in the reaction, providing compounds **1**−**4** in good yields. A dibrominated imidazole and 2-methylphthalimidobenzimidazole provided the desired aryl adducts in a higher yield than unsubstituted imidazole and benzimidazole (compounds **5** and **6**, respectively), a notable result given the prevalence of imidazole- and benzimidazole-containing pharmaceuticals that are substituted at the 2-position.[14]

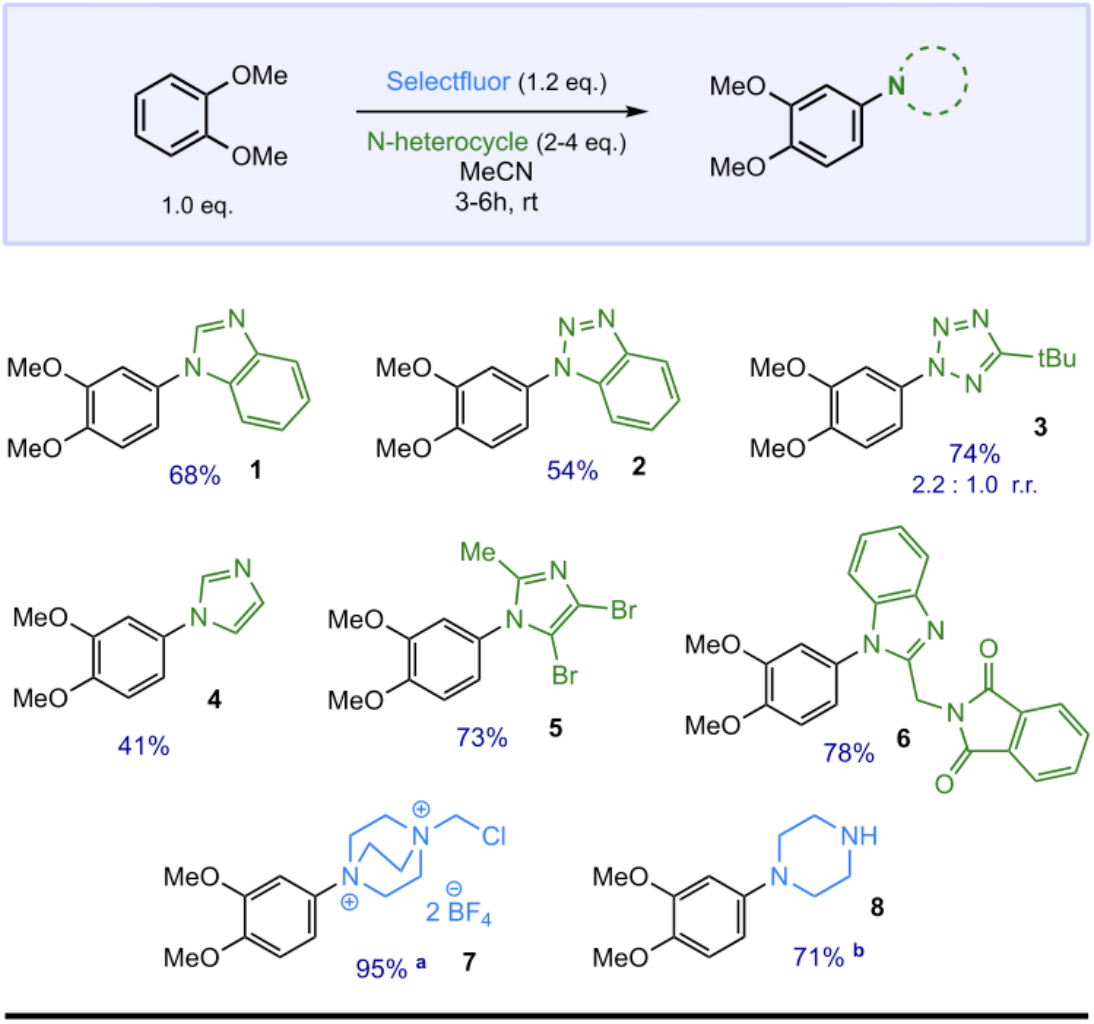

[a] no N-heterocycle was added; [b] $Na_2S_2O_3$ was added after formation of 7

Figure 7.2. Scope of nitrogen heterocycles.

Having established some representative examples for the substrate scope of the nitrogen heterocycles, we next shifted our focus to examining the substrate scope of the electron-rich arenes. Beyond 1,2-dialkoxybenzenes, we also demonstrate that their 1,4-substituted analogues can undergo the amination, albeit in slightly lower yields than their ortho-counterparts (Figure 7.3, compound **9**). Importantly, in this case we found that the amination reaction with benzimidazole was higher yielding than the amination without

benzimidazole (to form the aryl−Selectfluor adduct). Replacing one of the methoxy groups in veratrole with either a thiomethyl or a dimethylamino group proved to be detrimental to the desired amination. On the other hand, adding a third alkoxy group at the 3-position resulted in a productive reaction; the amination with benzimidazole had a slightly higher yield than that of veratrole (compound **10**). This allowed for the expeditious derivatization

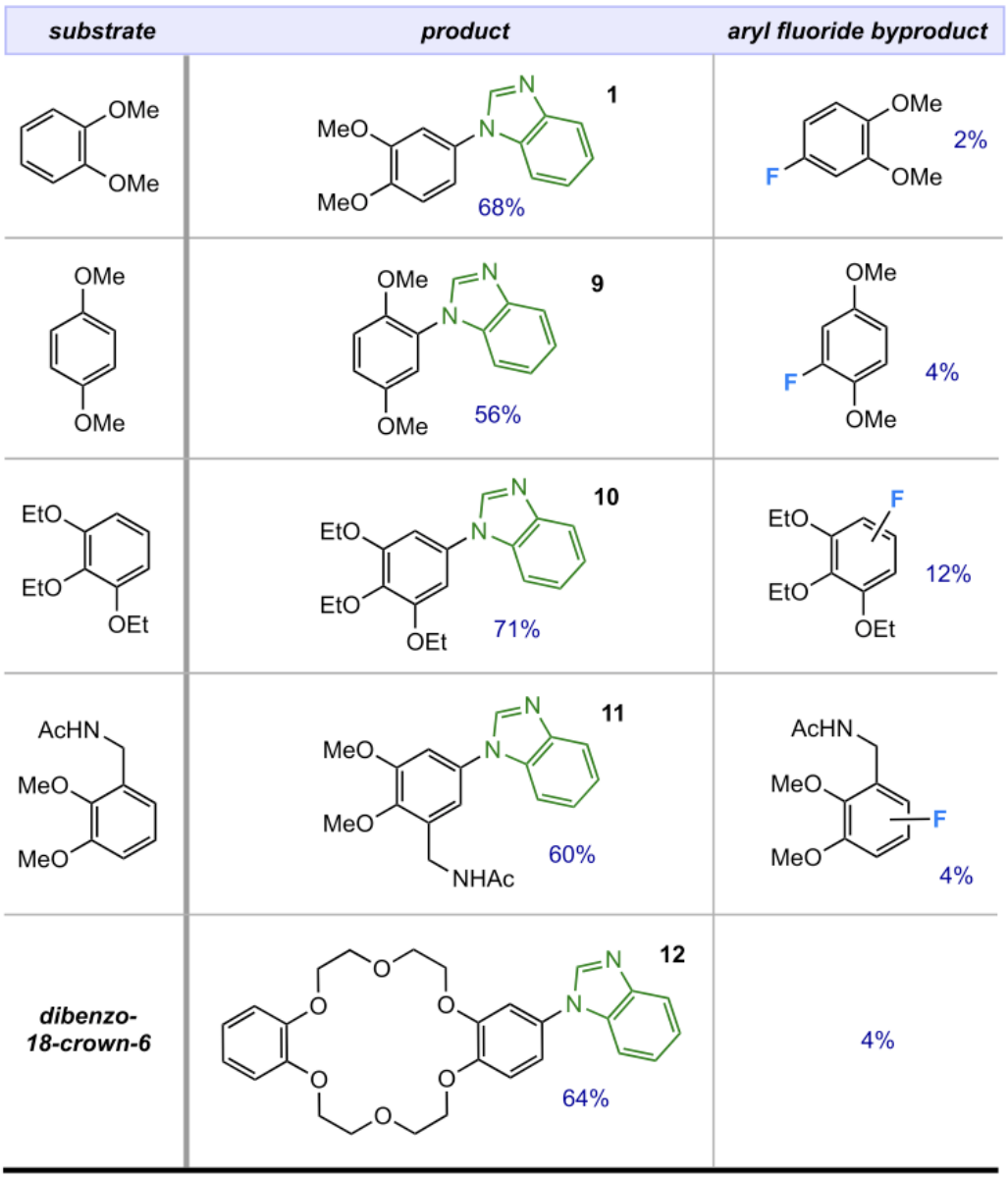

Figure 7.3. Substrate examples of alkoxyarenes.

of 1,2,3-trialkoxybenzene compounds that are common in biology and medicine.[15] Along those lines, an alkyl substituent was also tolerated at the 3-position, as an N-benzylacetamide derivative underwent amination in a good yield (compound **11**). The phase-transfer catalyst dibenzo-18-crown-6 was found to be similarly successful in the amination (compound **12**), allowing one-step access to new catalysts that could be useful in specialty applications. As illustrated in Figure 3, each of these examples gives a small amount of an aryl fluoride byproduct due to the use of Selectfluor; however, the desired amination product is easily separated from the fluoride impurity by column chromatography, as the aromatic amines are significantly more polar than the fluorides.

The aptitude of other electron-rich arenes to participate in the reaction proved difficult to predict, although we did find that other species beyond the examples presented in Figure 3 can undergo the amination reaction. Carbazole, for instance, can engage in the amination with Selectfluor, albeit in a moderately low yield. This finding came as a surprise to us given the large structural difference between carbazole and the alkoxybenzenes; however, to further complicate the analysis, the oxygen analogue of carbazole (dibenzofuran) was unsuccessful in the reaction. This is consistent with our earlier observation that the dimethylamino and thiomethyl analogues of veratrole did not undergo the amination. Together, these results demonstrate the discriminate nature of the reaction, as certain electron-rich arenes are not competent in the amination and instead undergo either fluorination or no reaction.

7.4. Application to Medicinal Chemistry.

To demonstrate the synthetic utility of this transformation, we propose an improved synthesis of a medicinally relevant compound (compound **13**, Figure 7.4). This

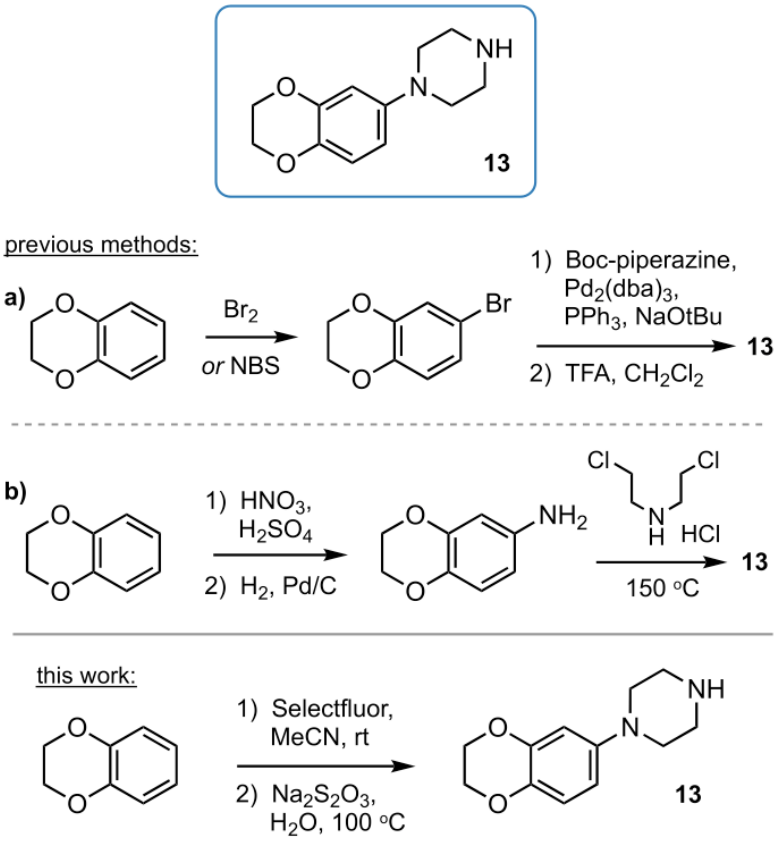

Figure 7.4. Application to medicinal chemistry.

commercially available benzodioxane derivative is employed as a precursor to dopamine D4 receptor ligands (via the N-benzylation of the piperazinyl secondary amine).[16] Additionally, **13** represents an analogue of eltoprazine, a drug useful for treating neurodegenerative disorders.[17] Two distinct methods have been utilized to synthesize **13** from 1,4-benzodioxane: (a) either a halogenation−cross-coupling sequence or (b) a nitration− reduction−substitution sequence, which provides the product in three steps.[18] On

the other hand, using our method, **13** can be accessed in two steps, both of which are operationally simpler than the steps in the previous syntheses. Notably, our approach avoids undesirable reactions from the previous methods, such as the Buchwald−Hartwig cross coupling amination or the nitration using concentrated nitric acid. As demonstrated by this example, the direct C−H to C−N bond formation featured in this reaction represents a powerful strategy toward the expeditious synthesis of nitrogen hetero- cycles that are of medicinal interest.

7.5. Mechanistic Studies.

To understand the reaction mechanism, we first sought to shed light on the divergent reactivity of the dialkoxybenzene regioisomers. Why would the ortho- and para-isomers undergo amination while the meta- isomer undergoes fluorination instead? We turned to computational chemistry to address this question, calculating the energy difference for the oxidation of the three dimethoxybenzene isomers using DFT (B3LYP/6-311++G** (MeCN)). Consistent with experimental results, the oxidation of the *meta*- isomer was the most energetically uphill (7 kJ/mol higher than the *ortho*-isomer and 35 kJ/mol higher than the *para*-isomer (Figure 7.5)). This energy difference is significant and coincides with the observation that in the present reaction the meta isomer may not undergo oxidation to its radical cation and the subsequent amination but could instead react with Selectfluor in a putative electrophilic aromatic halogenation. The oxidation of *para*-dialkoxy substrates is evidently more favorable than those of the ortho-substrates; however, the amination was higher-yielding for *ortho*-dialkoxyarenes. To rationalize this observation, we considered steric factors, which favor the ortho-substrates.

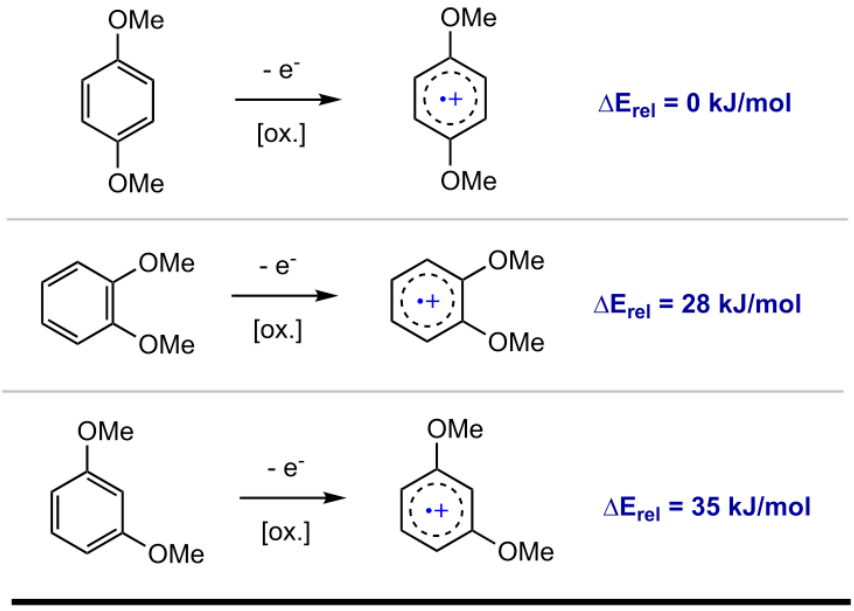

Figure 7.5. Energy of the arene oxidation calculated at B3LYP/6-311+ +G** (MeCN).

Next, we became interested in probing the relative reaction rates of the two competing reactions—amination vs fluorination. Thus, we subjected Selectfluor (1.0 equiv) to an intermolecular competition experiment with equimolar amounts of *ortho*- and *meta*-dimethoxybenzene (5.0 equiv each). A ratio of 1.0:3.5 was observed for the amination and fluoride products derived from the *ortho*- and *meta*-isomers, respectively (Figure 7.6).

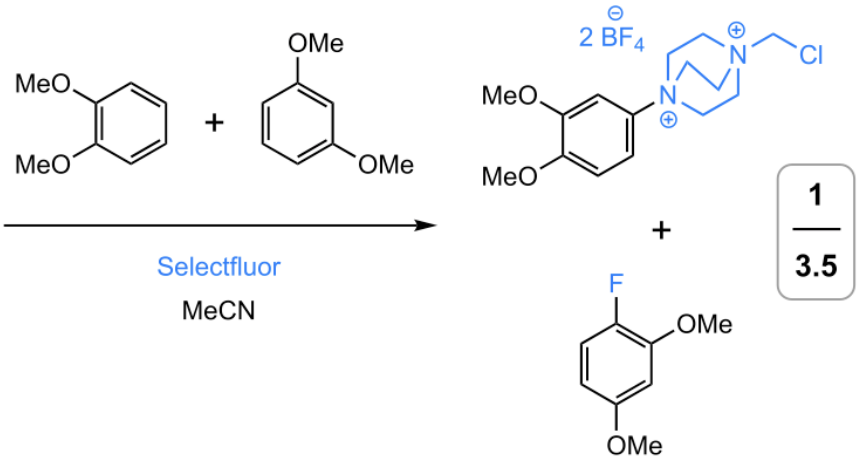

Figure 7.6. An intermolecular competition experiment.

From this experiment, it is apparent that the aryl fluorination is much faster than the amination. This finding further demonstrates the unusual behaviour of *ortho*-dialkoxybenzenes, which undergo amination in high yields despite the fact that fluorination is apparently faster.

Finally, we propose an initial mechanistic hypothesis for the amination reaction, relying on literature precedents and our own experience in working with Selectfluor. The reaction can begin with the oxidation of the electron-rich dialkoxyarene by Selectfluor to produce the corresponding arene radical cation, the Selectfluor-radical dication (SRD), and fluoride (Figure 7.7). The arene radical cation can be trapped by a nitrogen heterocycle via a nucleophilic addition to the allylic cation to form the 4-substituted adduct. This species

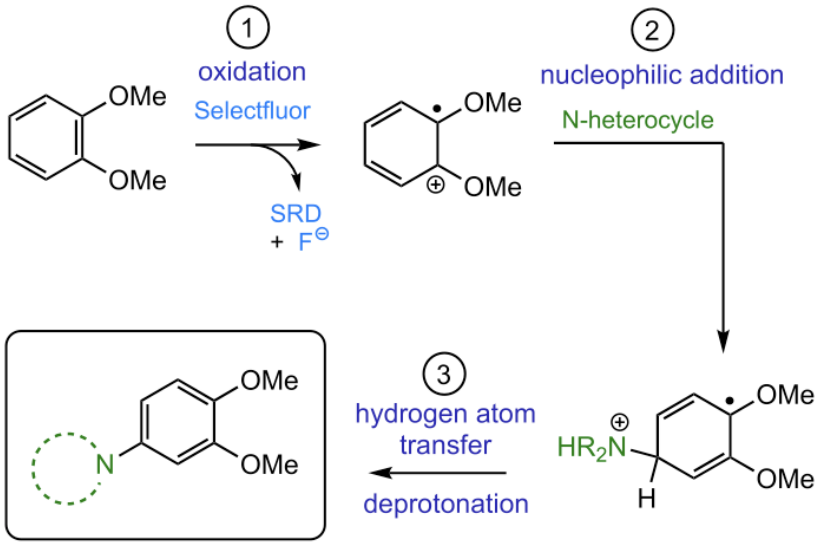

Figure 7.7. Proposed mechanism for arene amination.

could then undergo hydrogen atom transfer (HAT) to form the product. This HAT step is most likely accomplished with the SRD that was produced during the course of the reaction, as the Selectfluor-radical dication is known for its ability to abstract hydrogen atoms from a variety of substrates.[19] On the other hand, an alternate mechanism might involve a nucleophilic aromatic substitution of the Selectfluor−arene adduct with the nitrogen heterocycle. We ruled out this possibility by performing an experiment in which the Selectfluor−veratrole adduct was generated first and then benzimidazole was added after the Selectfluor was fully consumed. In this reaction, we observed no conversion of the Selectfluor−veratrole adduct to the benzimidazole−veratrole adduct, thereby disproving the nucleophilic aromatic substitution mechanism. An additional subtle mechanistic difference involves the oxidation of the radical produced from step two; in this case, the intermediate loses a proton to rearomatize instead of losing a hydrogen atom. Our group aims to investigate this distinction and elucidate further mechanistic details in a forthcoming study.

7.6. Conclusion.

In conclusion, the arene substitution pattern of dialkoxybenzenes was shown to govern the divergent reactivity with Selectfluor. Ortho- and para-isomers predominately give amination products, whereas the meta-isomer exclusively gives fluoride products. The amination pathway allows direct access to pharmaceutically important nitrogen heterocycles using a simple yet efficient set of conditions. DFT calculations illuminated details regarding the mechanistic switch, as the meta-isomer was revealed to be more

difficult to oxidize. Finally, an initial mechanism was proposed, involving oxidation, nucleophilic addition, hydrogen atom transfer, and rearomatization.

7.7. References.

[1] (a) Olah, G. A. Aromatic substitution. XXVIII. Mechanism of electrophilic aromatic substitutions. Acc. Chem. Res. 1971, 4, 240− 248. (b) Galabov, B.; Nalbantova, D.; Schleyer, P. v. R.; Schaefer, H. F. Electrophilic Aromatic Substitution: New Insights into an Old Class of Reactions. Acc. Chem. Res. 2016, 49, 1191−1199.

[2] (a) Jonsson, M.; Lind, J.; Reitberger, T.; Eriksen, T. E.; Merenyi, G. Redox chemistry of substituted benzenes: the one-electron reduction potentials of methoxy-substituted benzene radical cations. J. Phys. Chem. 1993, 97, 11278−11282. (b) Sarma, B. B.; Carmieli, R.; Collauto, A.; Efremenko, I.; Martin, J. M. L.; Neumann, R. Electron Transfer Oxidation of Benzene and Aerobic Oxidation to Phenol. ACS Catal. 2016, 6, 6403−6407.

[3] (a) Tay, N. E. S.; Nicewicz, D. A. Cation Radical Accelerated Nucleophilic Aromatic Substitution via Organic Photoredox Catalysis. J. Am. Chem. Soc. 2017, 139, 16100−16104. (b) Niu, L.; Liu, J.; Yi, H.; Wang, S.; Liang, X.; Singh, A. K.; Chiang, C.; Lei, A. Visible-Light- Induced External Oxidant-Free Oxidative Phosphonylation of C- (sp^2)−H Bonds. ACS Catal. 2017, 7, 7412−7416. (c) Venditto, N. J.; Nicewicz, D. A. Cation Radical-Accelerated Nucleophilic Aromatic Substitution for Amination of Alkoxyarenes. Org. Lett. 2020, 22, 4817−4822.

[4] (a) Nyffeler, P. T.; Durón, S. G.; Burkart, M. D.; Vincent, S. P.; Wong, C. H. Selectfluor: mechanistic insight and applications. Angew. Chem., Int. Ed. 2005, 44, 192−212. (b) Lal, G. S. Site-selective fluorination of organic compounds using 1-alkyl-4-fluoro-1,4- diazabicyclo[2.2.2]octane salts (selectfluor reagents). J. Org. Chem. 1993, 58, 2791−2796. (c) Yuan, J.; Zhu, J.; Li, B.; Yang, L.; Mao, P.; Zhang, S.; Li, Y.; Qu, L. Transition-metal free C3-amidation of quinoxalin-2(1H)-ones using Selectfluor as a mild oxidant. Org. Biomol. Chem. 2019, 17, 10178−10187.

[5] (a) Hili, R.; Yudin, A. K. Making carbon-nitrogen bonds in biological and chemical synthesis. Nat. Chem. Biol. 2006, 2, 284−287. (b) Park, Y.; Kim, Y.; Chang, S. Transition Metal-Catalyzed C−H Amination: Scope, Mechanism, and Applications. Chem. Rev. 2017, 117, 9247−9301.

[6] Michaudel, Q.; Thevenet, D.; Baran, P. S. Intermolecular Ritter- Type C−H Amination of Unactivated sp^3 Carbons. J. Am. Chem. Soc. 2012, 134, 2547−2550.

[7] Vitaku, E.; Smith, D. T.; Njardarson, J. T. Analysis of the Structural Diversity, Substitution Patterns, and Frequency of Nitrogen Heterocycles among U.S. FDA Approved Pharmaceuticals. J. Med. Chem. 2014, 57, 10257−10274.

[8] (a) Gerristma, D.; Brenstrum, T.; McNulty, J.; Capretta, A. Phospha-adamantanes as ligands for organopalladium chemistry: aminations of aryl halides. Tetrahedron Lett. 2004, 45, 8319−8321. (b) Chen, H.; Liu, P.; Li, H.; Zhang, H.; Daniel, S.; Zeng, Z. Fluorocarbon and Hydrocarbon N-Heterocyclic (C_5−C_7) Difluor- ooxymethylene-Bridged Liquid Crystals. Eur. J. Org. Chem. 2013, 2013 (33), 7517−7527.

[9] (a) Romero, N. A.; Margrey, K. A.; Tay, N. E.; Nicewicz, D. A. Site-selective arene C-H amination via photoredox catalysis. Science 2015, 349, 1326−1330. (b) Pandey, G.; Singh, D.; Laha, R. Selective C(sp^2)−H Functionalization of Arenes for Amination Reactions by Using Photoredox Catalysis. Asian J. Org. Chem. 2017, 6, 469−474. (c) Xie, L. Y.; Qu, J.; Peng, S.; Liu, K. J.; Wang, Z.; Ding, M. H.; Wang, Y.; Cao, Z.; He, W. M. Selectfluor-mediated regioselective nucleophilic functionalization of N-heterocycles under metal-and base-free conditions. Green Chem. 2018, 20, 760−764. (d) Huang, Y.; Lei, J.; Fu, X.; Xie, W.; Li, X. Synthesis of 1,2,3-triazole-substituted 6,7-dihydroindolizin-8(5H)-one derivatives mediated by Selectfluor. J. Chem. Res. 2019, 43, 179−183.

[10] Boursalian, G. B.; Ham, W. S.; Mazzotti, A. R.; Ritter, T. Charge-transfer-directed radical substitution enables para-selective C- H functionalization. Nat. Chem. 2016, 8, 810−815.

[11] Baudoux, J.; Cahard, D. Electrophilic Fluorination with N−F Reagents. Org. React. 2008, 69, 347−672.

[12] Bacci, J. P.; Kearney, A. M.; Van Vranken, D. L. Efficient Two- Step Synthesis of 9-Aryl-6-hydroxy-3H-xanthen-3-one Fluorophores. J. Org. Chem. 2005, 70, 9051−9053.

[13] Beyerle, R.; Bohn, H.; Just, M.; Martorana, P.; Nitz, R.-E.; Zoller, G. Tetrahydropyridazinone derivatives, process for their and their use. EP 0129791 A2, 1985.

[14] (a) Hassall, E.; Israel, D.; Shepherd, R.; Radke, M.; Dalväg, A.; Sköld, B.; Junghard, O.; Lundborg, P. Omeprazole for treatment of chronic erosive esophagitis in children: a multicenter study of efficacy, safety, tolerability and dose requirements. J. Pediatr. 2000, 137, 800− 807. (b) Daraji, D. G.; Prajapati, N. P.; Patel, H. D. Synthesis and Applications of 2-Substituted Imidazole and Its Derivatives: A Review. J. Heterocycl. Chem. 2019, 56, 2299−2317.

[15] (a) Woodward, R. B.; Bader, F. E.; Bickel, H.; Frey, A. J.; Kierstead, R. W. The total synthesis of reserpine. J. Am. Chem. Soc. 1956, 78, 2023−2025. (b) Slobodnick, A.; Shah, B.; Pillinger, M. H.; Krasnokutsky, S. Colchicine: old and new. Am. J. Med. 2015, 128, 461−470. (c) Darrell, J. H.; Garrod, L. P.; Waterworth, P. M. Trimethoprim: laboratory and clinical studies. J. Clin. Pathol. 1968, 21, 202−209.

[16] (a) Hodgetts, K. J.; Kieltyka, A.; Brodbeck, R.; Tran, J. N.; Wasley, J. W.; Thurkauf, A. 6-(4-Benzylpiperazin-1-yl) benzodioxanes as selective ligands at cloned primate dopamine D4 receptors. Bioorg. Med. Chem. 2001, 9, 3207−3213. (b) Kügler, F.; Sihver, W.; Ermert, J.; Hübner, H.; Gmeiner, P.; Prante, O.; Coenen, H. H. Evaluation of ^{18}F-labeled benzodioxine piperazine-based dopamine D4 receptor ligands: lipophilicity as a determinate of nonspecific binding. J. Med. Chem. 2011, 54, 8343−8352.

[17] Schipper, J.; Tulp, M. T. M.; Sijbesma, H. Neurochemical profile of eltoprazine. Drug Metab. Drug Interact. 1990, 8, 85−114.

[18] (a) Song, J.; Lee, H. E.; Kim, Y. J.; Kim, S. Y.; Kim, D. S.; Min, K. H. Discovery of small molecules that inhibit melanogenesis via regulation of tyrosinase expression. Bioorg. Med. Chem. Lett. 2012, 22, 6943−6946. (b) Tran, J. N.; Thurkauf, A.; 6-(4-Arylalkylpiperazin-1- yl) benzodioxane and 6-(4-arylalkylpiperazin-1-yl) chromane deriva- tives: dopamine receptor subtype specific ligands. US 6177566 B1, 2001.

[19] (a) Aguilar Troyano, F. J.; Merkens, K.; Gómez-Suárez, A. Selectfluor® Radical Dication (TEDA2+.)−A Versatile Species in Modern Synthetic Organic Chemistry. Asian J. Org. Chem. 2020, 9, 992−1007. (b) Zhao, H.; Jin, J. Visible Light-Promoted Aliphatic C− H Arylation Using Selectfluor as a Hydrogen Atom Transfer Reagent. Org. Lett. 2019, 21, 6179−6184. (c) Pitts, C. R.; Bloom, S.; Woltornist, R.; Auvenshine, D. J.; Ryzhkov, L. R.; Siegler, M. A.; Lectka, T. Direct, Catalytic Monofluorination of sp^3 C-H Bonds: A Radical-Based Mechanism with Ionic Selectivity. J. Am. Chem. Soc. 2014, 136, 9780−9791. (d) Ghorbani, F.; Harry, S. A.; Capilato, J. N.; Pitts, C.; Joram, J.; Peters, G.; Tovar, J.; Smajlagic, I.; Siegler, M.; Dudding, T.; Lectka, T. Carbonyl-Directed Aliphatic Fluorination: A Special Type of Hydrogen Atom Transfer Beats Out Norrish II. J. Am. Chem. Soc. 2020, 142, 14710−14724.

[20] Zhang, F.; Moses, J. E. Benzyne click chemistry with in situ generated aromatic azides. Org. Lett. 2009, 11, 1587−1590.

[21] Kantam, M. L.; Venkanna, G. T.; Sridhar, C.; Sreedhar, B.; Choudary, B. M. An efficient base-free N-arylation of imidazoles and amines with arylboronic acids using copper-exchanged fluorapatite. J. Org. Chem. 2006, 71, 9522−9524.

[22] Rajpurohit, S.; Sah, P. Synthesis and Antimicrobial Activity of Some Mannich Bases of Benzimidazolyl Substituted 1H-Isoindole- 1,3(2H) Diones. Asian J. Chem. 2005, 17 (2), 949−954.

[23] Tamboli, R. S.; Shidore, M. M.; Dash, R. C.; Kanhed, A. M.; Patel, N. R.; Shah, S. R.; Yadav, M. R. Improved Rapid and Green Synthesis of N-Aryl Piperazine Hydrochlorides Using Synergistic Coupling of Hydrated Task Specific Ionic Liquid ([BbIm] OH) and Microwave Irradiation. ChemistrySelect 2019, 4, 1138−1148.

[24] Ueda, T.; Mochida, T. Thermal Properties and Crystal Structures of Ionic Liquids from Ruthenium Sandwich Complexes with Trialkoxybenzene Ligands: Effects of Substituent Positions and Alkyl Chain Lengths. Organometallics 2015, 34, 1279−1286.

[25] Frisch, M. J.; Trucks, G. W.; Schlegel, H. B.; Scuseria, G. E.; Robb, M. A.; Cheeseman, J. R.; Scalmani, G.; Barone, V.; Mennucci, B.; Petersson, G. A.; Nakatsuji, H.; Caricato, M.; Li, X.; Hratchian, H. P.; Izmaylov, A. F.; Bloino, J.; Zhang, G.; Sonnenberg, J. L.; Hada, M.; Ehara, M.; Toyota, K.;

Fukuda, R.; Hasegawa, J.; Ishida, M.; Nakajima, T.; Honda, Y.; Kitao, O.; Nakai, H.; Vreven, T.; Montgomery, J. A., Jr.; Peralta, J. E.; Ogliaro, F.; Bearpark, M.; Heyd, J. J.; Brothers, E.; Kudin, K. N.; Staroverov, V. N.; Kobayashi, R.; Normand, J.; Raghavachari, K.; Rendell, A.; Burant, J. C.; Iyengar, S. S.; Tomasi, J.; Cossi, M.; Rega, N.; Millam, J. M.; Klene, M.; Knox, J. E.; Cross, J. B.; Bakken, V.; Adamo, C.; Jaramillo, J.; Gomperts, R.; Stratmann, R. E.; Yazyev, O.; Austin, A. J.; Cammi, A. R.; Pomelli, C.; Ochterski, J. W.; Martin, R. L.; Morokuma, K.; Zakrzewski, V. G.; Voth, G. A.; Salvador, P.; Dannenberg, J. J.; Dapprich, S.; Daniels, A. D.; Farkas, Ö.; Foresman, J. B.; Ortiz, J. V.; Cioslowski, J.; Fox, D. J. Gaussian 09, rev. E.01; Gaussian, Inc.: Wallingford, CT, 2009.

Chapter 8:

Spectroscopic and Crystallographic Characterization of the N^+–C–H···O Interaction

8.1 Introduction.

Being the weaker variant of classical hydrogen bonds, C–H···X interactions are frequently overlooked or dismissed as inconsequential. Nevertheless, the importance of these weak interactions has been well-documented in recent years. Nonclassical hydrogen bonding is now accepted to be an important player in the chemical repertoire of both small and large molecules. As C–H hydrogen atoms are less acidic than classical hydrogen bond donors (e.g. O–H and N–H hydrogen atoms), C–H···X bonds are an inherently weak interaction. Still, the hydrogen bond energy from these interactions is enough to influence chemical reactivity, molecular recognition and conformation—especially in the case of multiple C–H···X bonds acting in a cooperative sense.

Numerous types of C–H···X hydrogen bonds have been reported, employing different kinds of C–H hydrogen atoms (Figure 8.1). For instance, salicylaldehyde (2-hydroxybenzaldehyde) is known to experience an intramolecular C–H···O interaction involving its aldehydo hydrogen atom. Contributing to this hydrogen bond is the increased acidity of the acyl C–H hydrogen atom. Halogens have also been employed as hydrogen bond acceptors in C–H···X interactions in sugar derivatives. In this case, the axial hydrogen atom geminal to an acetoxy group is a more suitable hydrogen bond donor than that of a typical sp^3 C–H hydrogen atom; its increased acidity facilitates the C–H···X interaction. Besides heteroatom lone pairs, π bonds have also been reported to engage in

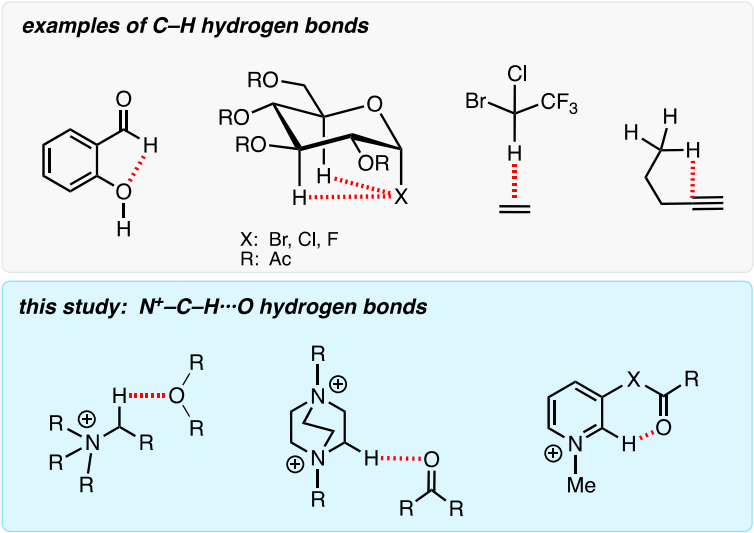

Figure 8.1. Various types of C–H hydrogen bonds.

nonclassical hydrogen bonds. Alkenes, alkynes and arenes are capable hydrogen bond acceptors; however, the relative acidity of the C–H hydrogen bond donor remains an important consideration in these cases.

With this in mind, N^+–C–H hydrogen atoms represent a favorable category of nonclassical hydrogen bond donors given their increased acidity over other types of C–H hydrogen atoms. Our group became interested in N^+–C–H···O interactions upon discovery of their involvement in a carbonyl-directed fluorination that was recently developed in our laboratory. In a reaction with Selectfluor, ketones and other carbonyl groups have been shown to direct aliphatic fluorination to β- or γ-carbon atoms, depending on the substrate (Scheme 8.1). Our group reported a mechanistic study on this reaction in which a key finding was the involvement of an N^+–C–H···O hydrogen bond in the transition state for hydrogen atom transfer (HAT). Participating in this nonclassical interaction is a hydrogen atom from the Selectfluor radical dication (SRD), and the carbonyl group of the substrate.

This mechanistic hypothesis was made in agreement with our computational data for DFT-calculated transition states of the reaction; however, we did not obtain physical evidence of an N^+–C–H···O interaction at the time.

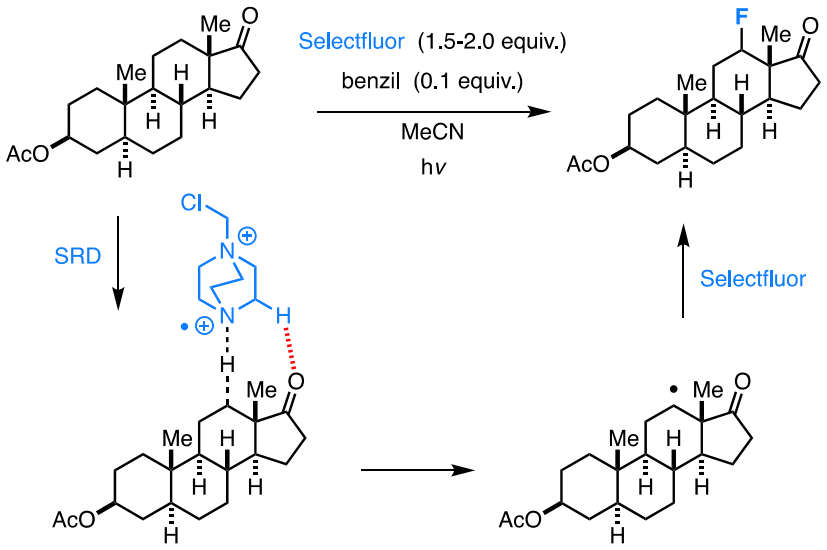

Scheme 8.1. Carbonyl-directed aliphatic fluorination with Selectfluor.

A recently published report investigated N^+–C–H···O hydrogen bonds in biological contexts—particularly, in protein-ligand complexes. The authors studied these interactions through computational chemistry as well as a survey of published protein crystal structures. Hydrogen bond parameters, such as distance and angle, were carefully examined. N^+–C–H···O distances less than 2.7 Å were considered as hydrogen bonds, whereas those less than 2.4 Å were regarded as being relatively stronger. While the hydrogen bond angle was less predictable, for 90% of their examples it was around 105-165°. Generally, the angles varied in a larger range than that of classical O–H···O hydrogen bonds, which show a greater preference for linearity. A significant finding from this study was that N^+–C–

H···O bonds have utility in medicinal chemistry, as these interactions were shown to affect the activity of a G9a-like protein (GLP) inhibitor. Although nonclassical hydrogen bonds are frequently overlooked, the application in drug design in addition to their role in synthetic methodology should result in a wider appreciation for these types of interactions.

8.2 Results and Discussion.

To provide further validation for our DFT-based model for carbonyl directed fluorination with Selectfluor, we synthesized a DABCO-ketosteroid adduct in hopes of observing an analogous type of N^+–C–H···O bond. In our mechanistic study, we proposed that the ketone on the substrate is involved in a N^+–C–H···O interaction with a hydrogen atom on the DABCO moiety of the SRD. To mimic this moment in the transition state, we devised a synthesis to incorporate a dicationic DABCO adjacent to a ketone on a representative steroid substrate. While the D-ring of the steroid is targeted instead of the C-ring in the below example, we have demonstrated in our synthetic method that all four steroidal rings can be regioselectively functionalized based on the particular substrate.

We started with dehydroepiandrosterone (DHEA), a biologically and medicinally important steroid that is commercially available (Scheme 8.2). Catalytic hydrogenation of the B-ring alkene with palladium was followed by α-bromination of the resulting ketosteroid with $CuBr_2$. The major diastereomer was isolated in pure form through recrystallization in methanol. DABCO was then employed in an S_N2 reaction with the bromosteroid, providing the monocation adduct in 58% yield. Lastly, protonation of the tertiary amine with HBr in methanol/acetone gave the dibromide salt **1**.

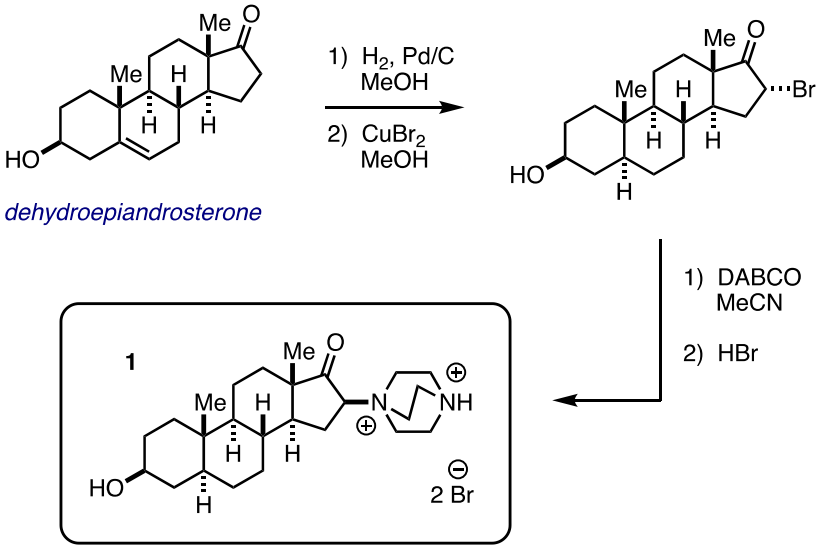

Scheme 8.2. Synthesis of compound **1** from DHEA.

Following the synthesis of compound **1**, recrystallization in methanol gave pure material that was suitable for NMR characterization. A subsequent smaller recrystallization using a solvent evaporation technique gave sizeable single crystals that were employed for X-ray crystallography. The crystal structure of **7** reveals an evident N^+–C–H···O hydrogen bond, involving the steroid ketone carbonyl and a hydrogen atom on the DABCO dication (Figure 8.2). Defining this interaction is a short hydrogen bond length of 2.36 Å along with a bond angle of 132°. Importantly, the DABCO bicycle is oriented in a fashion which facilitates hydrogen bonding—placing the hydrogen atom in the plane of the carbonyl. Rotation of the heterocycle relative to the steroid would have resulted in lengthening and weakening of the N^+–C–H···O interaction. The dicationic nature of the DABCO moiety is likely significant as it enables its C–H bonds to be unusually acidic. By analogy to **1**, other DABCO dications such as Selectfluor or SRD could engage in such hydrogen bond interactions with suitable substrates.

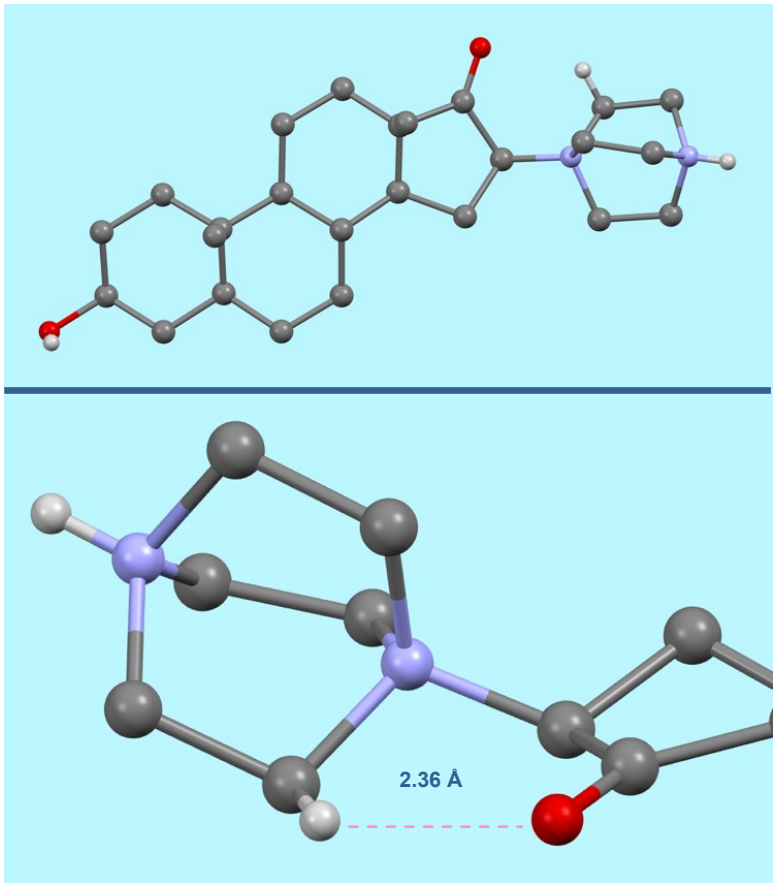

Figure 8.2. X-ray crystal structure of compound **1** (top); N^+–C–H···O hydrogen bond (bottom). Bromides and most hydrogen atoms are removed for clarity.

In addition to the N^+–C–H···O bond observed in compound **1**, several N^+–C–H···Br interactions were also identified in the crystal structure of the dibromide salt (Figure 8.3). Distances of 2.69, 2.82 and 2.85 Å were measured for interactions involving three different N^+–C–H hydrogen atoms and the two bromide anions. It is important to note that the counterions for Selectfluor are typically two tetrafluoroborate anions, in contrast to the dibromide salt **1**. As BF_4^- is a much weaker Lewis base than is bromide, this may

be significant in order to allow efficient coordination of the SRD or Selectfluor to the substrate.

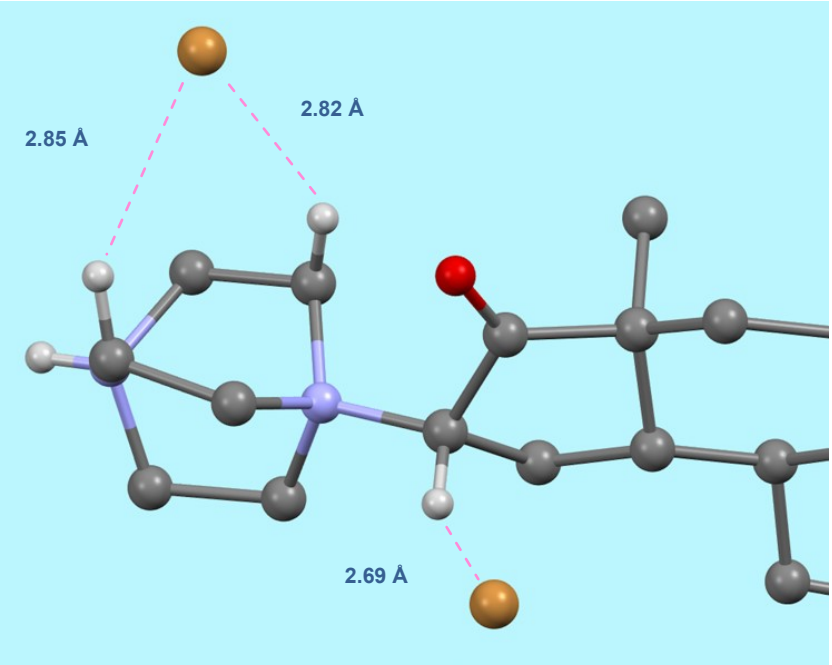

Figure 8.3. N^{+}–C–H···Br interactions observed in the crystal structure of compound **1**.

Next, we sought to corroborate our experimental results with computational chemistry. The optimized structure for compound **1** was calculated using Gaussian software (counterions were omitted for convenience); geometry optimizations were performed using the ωB97XD functional with a 6-311++G(d,p) basis set. Consistent with the X-ray crystal structure, a clear N^{+}–C–H···O hydrogen bond is present in the computed structure of **1** (Figure 8.4). The interaction appears somewhat stronger in this case—a distance of 2.15 Å was measured (slightly shorter than in the crystal structure). One possible explanation for this difference is the absence of bromide anions, which were seen to competitively

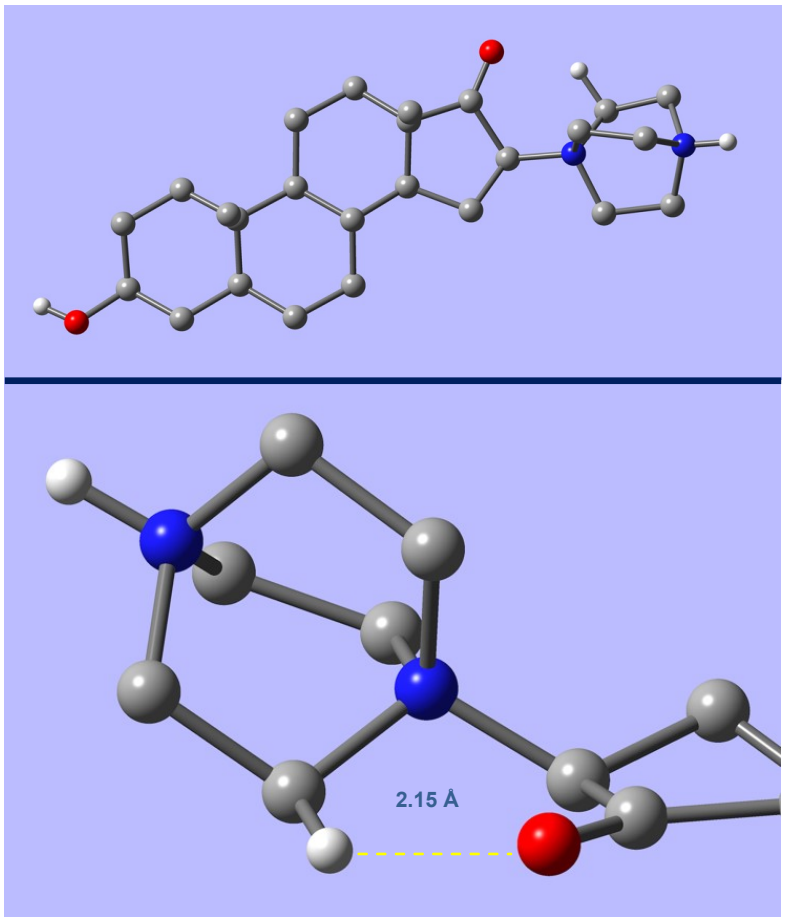

Figure 8.4. DFT-optimized structure of compound **1** at ωB97XD/6-311++G(d,p) (most hydrogen atoms are removed for clarity).

coordinate to the DABCO dication in the crystal structure. On the other hand, the overall geometry was highly consistent between the computed and observed structure. Notably, the orientation of the DABCO ring relative to the ketone carbonyl is virtually identical between these two structures, including the placement of the N^+–C–H hydrogen atom in the plane of the carbonyl.

N^+–C–H···O/N hydrogen bonds have not been studied spectroscopically to the best of our knowledge. To begin to address this issue, we performed ^{1}H NMR experiments that

provide further evidence of these interactions in Selectfluor-mediated functionalizations. Several hydrogen bond acceptors of varying strength were mixed with a solution of Selectfluor in CD_3CN, and the chemical shifts of the methylene groups were measured with NMR spectroscopy (Figure 8.5). Additionally, the chemical shift of the fluorine atom was recorded in order to rule out a halogen bond interaction that was recently proposed. The concentration of Selectfluor and the hydrogen bond acceptor was kept constant in each experiment (see details in Experimental Section). As expected, a noticeable deshielding effect was observed for the N^+–C–H signals as the strength of the hydrogen bond acceptor increased. Notably, the chemical shifts of the methylene N^+–C–H signals were affected to a greater extent than that of the fluorine atom. This trend is even more pronounced when one considers that fluorine is a much more sensitive nuclei than hydrogen in regard to changes in its NMR chemical shift in response to its electronic environment. Pyridine was the strongest hydrogen bond acceptor tested (excluding those which rapidly react with Selectfluor such as alkylamines). With pyridine as a hydrogen bond acceptor (50% v/v), we observed the ^1H methylene signals of Selectfluor to be deshielded by 0.64 ppm relative to the weakest hydrogen bond acceptor tested (acetonitrile). The ^{19}F signal, on the other hand, was altered to a lesser degree (0.15 ppm). This evidence disfavors the notion of halogen bonding in interactions of Selectfluor with Lewis bases, and instead, N^+–C–H$\cdots$X hydrogen bonds appear more likely.

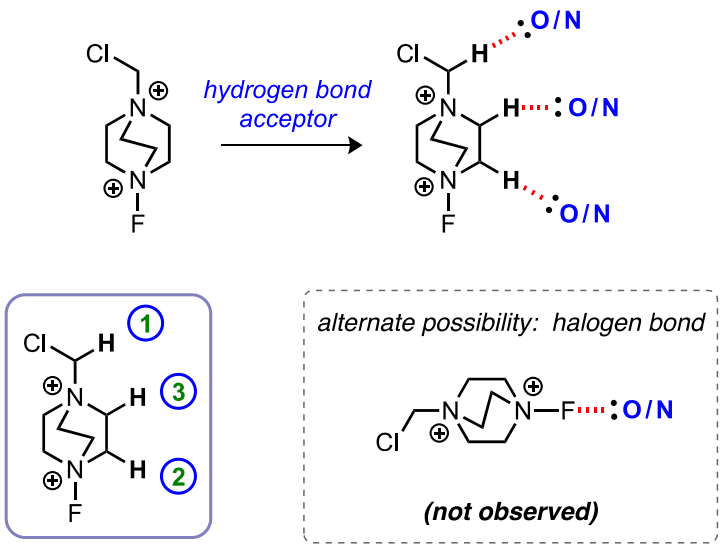

acceptor	H1	H2	H3	F
acetonitrile	5.32	4.74	4.30	48.50
diethylcarbonate	5.33	4.76	4.32	48.53
pyrazine	5.35	4.78	4.33	48.49
N,N-dimethylacetamide	5.44	4.83	4.39	48.45
pyridine	5.43	4.85	4.40	48.45
pyridine (1:1 w/ MeCN)	5.96	5.38	4.92	48.35

Figure 8.5. Effect of N^+–C–H hydrogen bonding on the ^1H NMR of Selectfluor.

To provide further spectroscopic evidence of N^+–C–H···O/N interactions with Selectfluor, we briefly investigated an intramolecular system. Dialkylation of DABCO with 2-(bromomethyl)pyridine occurred rapidly, providing dibromide salt **2**. The pyridinyl nitrogen atoms of **2** can be properly poised in this compound to engage in relatively strong N^+–C–H···N hydrogen bonds. In order to spectroscopically probe these intramolecular hydrogen bonds, we synthesized the dibenzyl analog **3**, which does not experience the hydrogen bond, as a reference compound. As anticipated, the presence of

the hydrogen bond acceptor (pyridine) was found to have a deshielding effect on the methylene N^+–C–H signals in the ^{1}H NMR (Figure 8.6). Notably, the DABCO hydrogen

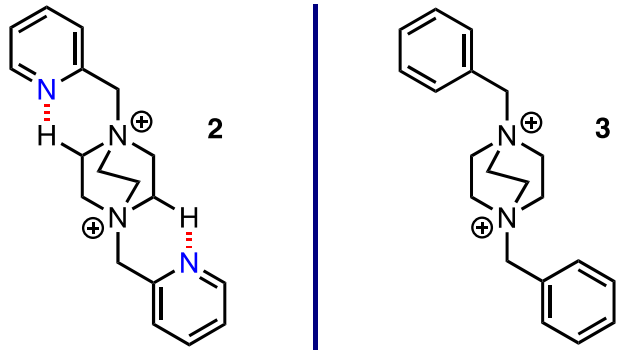

compound	H *(DABCO)*	H *(benzylic)*
2	4.14	4.88
3	3.91	4.77

Figure 8.6. Intramolecular N^+–C–H···N hydrogen bonding in a DABCO dication.

signal was deshielded more than twice as much as the benzylic signal, despite being farther away from the pyridine ring—suggesting the change in chemical shift is due to hydrogen bonding rather than an inductive effect. Further, the DABCO ^{1}H NMR signal is comprised of 12 hydrogen atoms, implying a stronger deshiedling effect on a per-hydrogen basis, since only two hydrogen atoms are engaged in the interaction in compound **2**. DFT-computed optimized structures supports the existence of these noncovalent bonds, as **2** adopts a conformation which enables a pair of relatively strong N^+–C–H···N hydrogen bonds with a short distance of 2.19 Å (Figure 8.7). Compound **3**, on the other hand, was observed to have a dissimilar conformation that is likely governed by sterics.

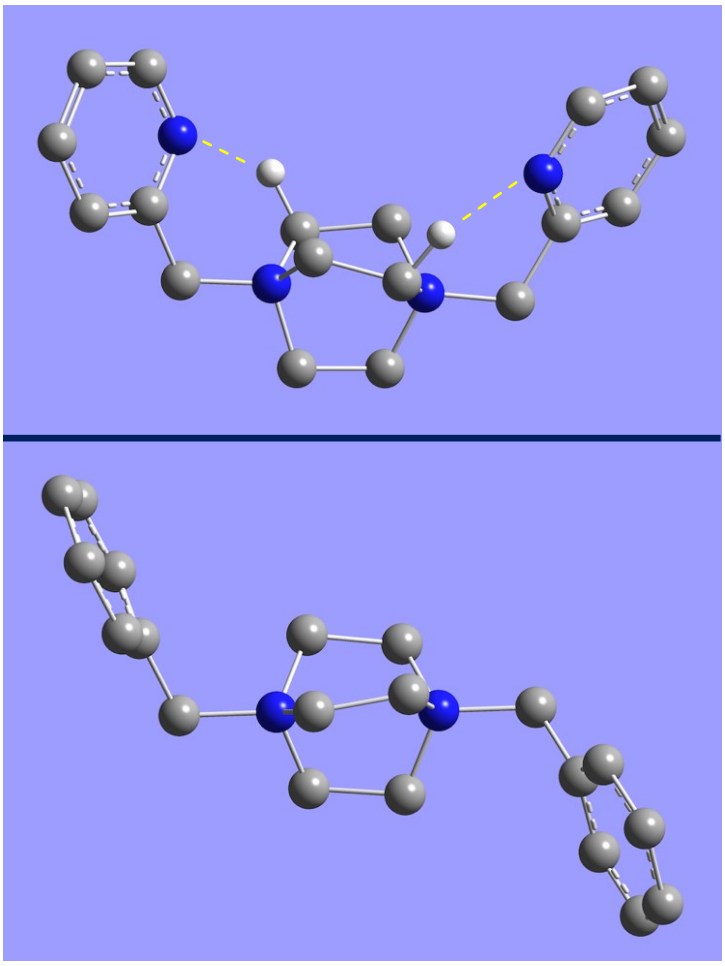

Figure 8.7. DFT-optimized structures of **2** (top) and **3** (bottom) computed at ωB97XD/6-311++G(d,p) (most hydrogen atoms are removed for clarity).

Next, we explored intramolecular N^+–C–H···O hydrogen bonds in pyridinium salts to demonstrate generality of these interactions beyond the DABCO salts previously highlighted. An advantage of this model system is that a single N^+–C–H hydrogen atom can be observed spectroscopically, in contrast to the 12 N^+–C–H hydrogen atoms found in DABCO dicationic salts. Synthesis of analogs of 3-hydroxy- and 3-aminopyridine containing various hydrogen bond acceptors was guided by computational chemistry.

Ester **4** was predicted to have the least productive N^+–C–H···O interaction, followed by carbamate **5** and amides **6-8** (see SI for computed structures). This trend was supported by ^{1}H NMR spectroscopy, which revealed a substantial deshielding effect for the N^+–C–H hydrogen atom as the strength of the hydrogen bond acceptor increased (Figure 8.8).

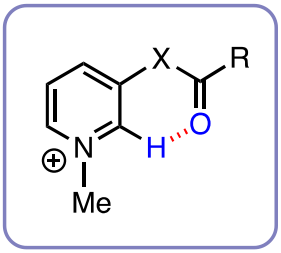

4: X = O; R = Me

5: X = O; R = NMe_2

6: X = NH; R = NO_2Ph

7: X = NH; R = OMePh

8: X = NH; R = $(OMe)_3Ph$

compound	H	N^+—Me	other Py H (avg. of 3)
4	8.67	4.33	8.32
5	8.83	4.36	8.33
6	9.54	4.34	8.36
7	9.63	4.32	8.36
8	9.64	4.33	8.38

Figure 8.8. Intramolecular N^+–C–H···O hydrogen bonding in pyridinium salts.

Notably, increased electron-donating ability of the 3-substituent resulted in deshielding of the adjacent N^+–C–H hydrogen atom, whereas this would be predicted to have the opposite effect in the absence of a hydrogen bond. In contrast to the hydrogen atom involved in the N^+–C–H···O bond, the chemical shifts of the N^+–Me and other three pyridine hydrogen atoms were not significantly affected by the 3-substituent. For instance, when comparing

the chemical shifts of compounds **4** and **7**, the hydrogen atom involved in the N^+–C–H···O bond was deshielded nearly one full ppm, whereas the N^+–Me and other pyridine hydrogen atoms (avg. of three) were altered by 0.01 and 0.04 ppm, respectively. Taken together, these data are consistent with the notion of an intramolecular N^+–C–H···O hydrogen bond occurring in these compounds.

The ^{1}H NMR trend in Figure 8.8 is in agreement with the observed hydrogen bond strength attained from DFT-computed optimized structures for compounds **4**-**8**. Pyridinium salt **7**, for instance, was found to experience a relatively strong intramolecular N^+–C–H···O hydrogen bond; the structure was computed at the ωb97xd/6-311++g(d,p) level of theory (Figure 8.9). A short distance of 2.06 Å was measured from the hydrogen

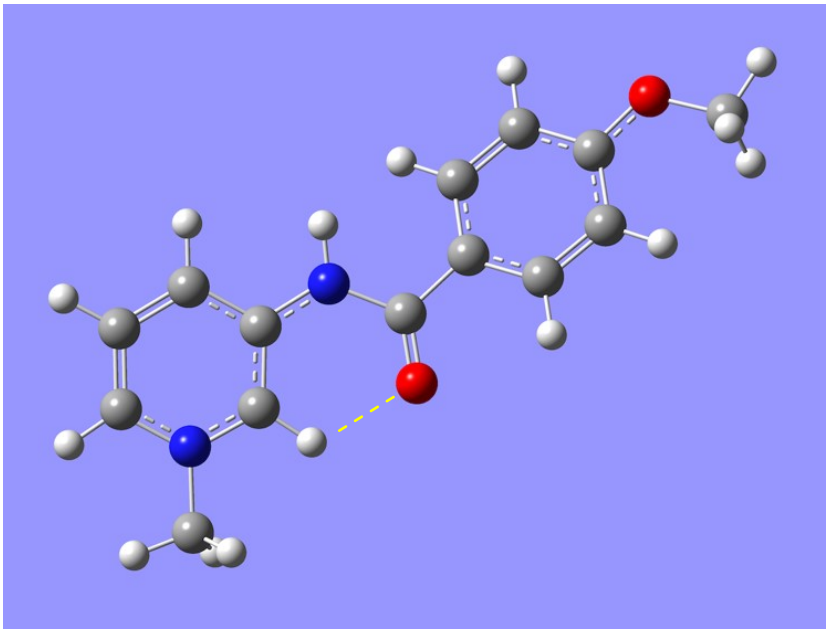

Figure 8.9. DFT-optimized structure of **7** (computed at ωB97XD/6-311++G(d,p)).

atom to the carbonyl oxygen atom. This close interaction is facilitated by the conformation of the amide—the carbonyl is planar to the pyridine ring and pointed towards the N^+–C–H hydrogen atom in order to minimize the distance and maximize the strength of the hydrogen bond.

In addition to NMR spectroscopy, we reasoned that these interactions could also be probed by IR spectroscopy. Unfortunately, the IR signals for the sp^2 hydrogen atoms were overlapped and indiscernible for compounds **4**-**8**. As a substitute, we turned to computational chemistry to analyze DFT-computed IR spectra. While the precise wavenumbers from the signals of the calculated spectra should not be considered infallible, the overall trend in regard to red or blue-shifting should yield valuable information. Notably, we found that increasing the strength of the hydrogen bond acceptor at the 3-position resulted in a red-shift of the N^+–C–H stretch (Figure 8.10). This trend is consistent

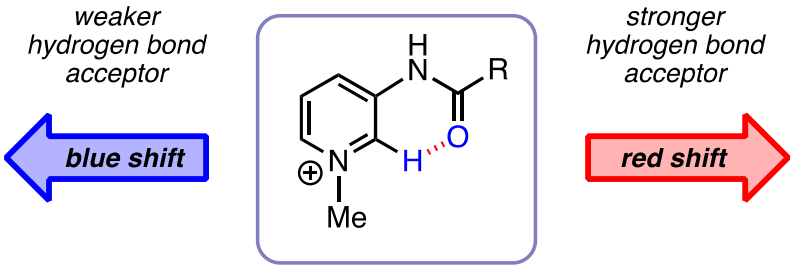

R	N^+–C–H stretch (cm^{-1})
4-NO_2Ph	3274.6
4-OMePh	3265.3

Figure 8.10. DFT-IR stretches for compounds **6** and **7** (computed at ωB97XD/6-311++G(d,p)).

with previously reported IR data involving N–H···F hydrogen bonds.

Next, we briefly investigated the relative hydrogen bond strength of an N^+–C–H···O interaction in contrast to the corresponding C–H···O interaction. Employing an intramolecular pyridinium model similar to compounds **4-8**, we found that the calculated energy of the N^+–C–H···O arrangement was 12.6 kcal lower than that of the analogous C–H···O conformation (Figure 8.11). This energy difference is significant and demonstrates the importance of the adjacent positive charge in increasing the acidity of the C–H hydrogen bond donor. A similar trend would be expected for sp^3 N^+–C–H···O vs. C–H···O systems, for instance, the DABCO dications discussed above.

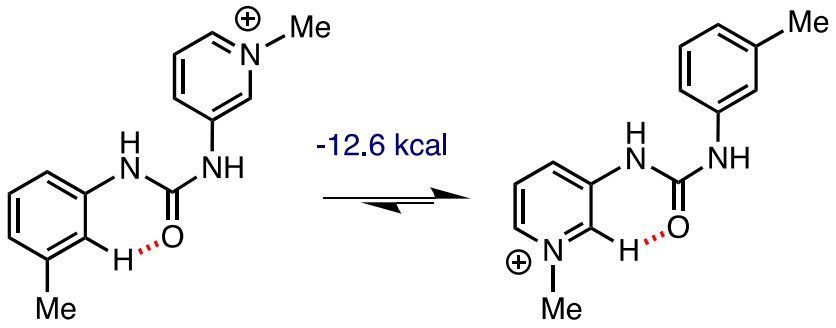

Figure 8.11. Relative hydrogen bond strength of N^+–C–H···O vs. C–H···O interactions.

Lastly, we performed a structure search using The Cambridge Crystallographic Data Centre (CCDC), probing for intramolecular ammonium C–H···O hydrogen bonds. Several published crystal structures were identified which possessed this motif (Figure 8.12), involving either a ketone, silyl ether or alcohol as the hydrogen bond acceptor. Distances and angles for each interaction were then measured using Mercury software. To our

surprise, the authors that published the crystal structures for **9-14** did not mention these hydrogen bond interactions in their manuscript. While those studies were geared towards other issues, this highlights the fact that nonclassical C–H···O/N interactions can in certain cases be overlooked or difficult to identify, particularly in the case of N^+–C–H···O hydrogen bonds.

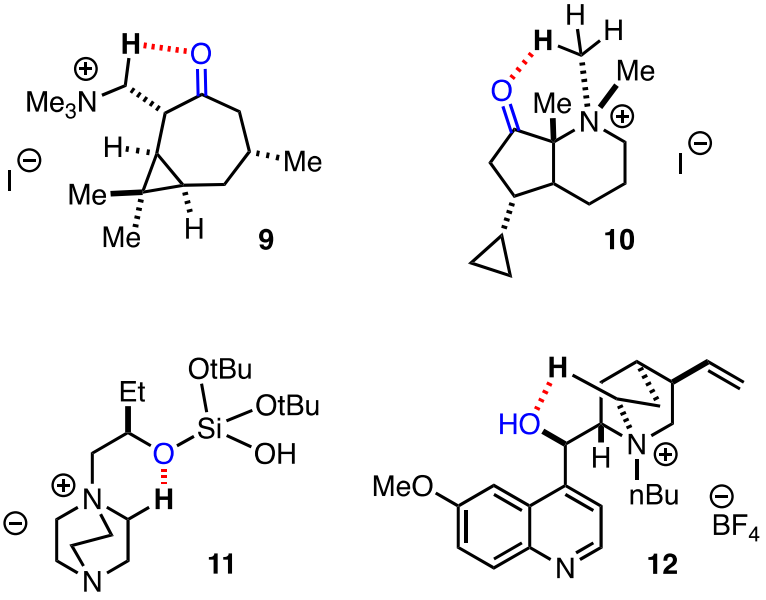

Figure 8.12. Intramolecular N^+–C–H···O hydrogen bonds observed in previously reported X-ray crystal structures (CCDC).

Bicyclic ketone **9** engages in an N^+–C–H···O bond with a hydrogen atom at its β-carbon (2.48 Å; 102°). As seen in the crystal structure, the $–CH_2NMe_3^+$ moiety is orientated in a fashion which amplifies the hydrogen bond interaction. Similarly, ketone **10** was found to have a N^+–C–H···O interaction involving one of the N-Me groups of the ammonium nitrogen atom (2.22 Å; 123°). Compound **11** demonstrates a silyl ether acting as a hydrogen bond acceptor in an N^+–C–H···O bond (2.46 Å; 123°). The hydrogen bond donor

portion of this molecule is particularly relevant to our carbonyl directed fluorination, since Selectfluor is also derived from DABCO. Additionally, butylated quinine **12** experiences an N^+–C–H···O bond, comprising the secondary alcohol and a hydrogen atom on the quinuclidine (2.48 Å; 109°). Notably, the alcohol group of **12** is rotated such that its lone pair is directly pointing towards the N^+–C–H hydrogen atom (Figure 8.13).

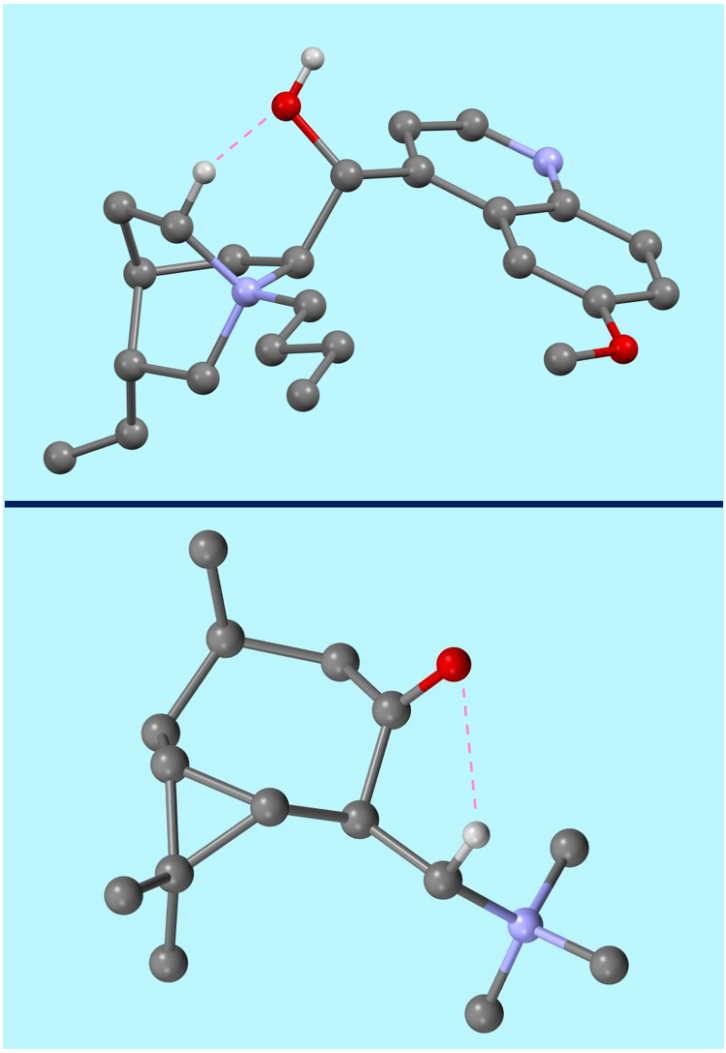

Figure 8.13. X-ray crystal structures of compound **12** (top) and **9** (bottom).

Having established precedent for intramolecular N^+–C–H···O bonds in previously reported crystal structures, we narrowed our search onto DABCO dication salts, which should have similar hydrogen bond donor acidity relative to Selectfluor or the SRD. Accordingly, compound **13** was identified, which exhibits two distinct hydrogen bond interactions—a carboxylic acid and a carboxylate simultaneously coordinate to the methylene core of the DABCO dication (Figure 8.14). The distance and angle of these hydrogen bonds were similar, with the shortest one being 2.35 Å and 120°.

A similar type of interaction was observed in the crystal structure of Selectfluor, wherein the chlorine atom engages in an N^+–C–H···Cl bond with hydrogen atoms on the adjacent DABCO ring. The distance and angle (2.72 Å; 105°) of this weak interaction were comparable to that of reported C–H···Cl hydrogen bonds. Consistent with prediction, the N^+–C–H···Cl interaction in **14** appears weaker than the N^+–C–H···O bond in **13**.

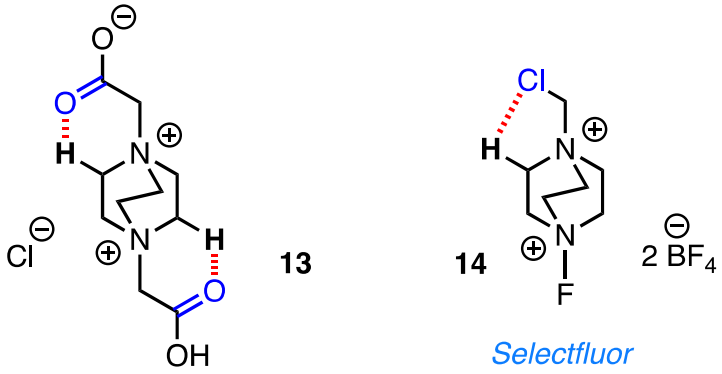

Figure 8.14. Intramolecular N^+–C–H···X hydrogen bonds in DABCO salts.

8.3 Conclusion.

The importance of noncovalent interactions has been well-demonstrated in recent years, yet N^+–C–H···O and N hydrogen bonds remain underappreciated. In this article, we have exhibited crystallographic, spectroscopic and computational evidence for these weak interactions, with relevance to Selectfluor chemistry. Further studies of this nature should facilitate the discovery of new synthetic methods and modes of recognition, and lead to a greater understanding of weak nonclassical interactions.

Chapter 9:

Experimental Section

9.1 General Methods.

Unless otherwise stated, all reactions were carried out under strictly anhydrous conditions and N_2 atmosphere. All solvents were dried and distilled by standard methods. All ^{1}H spectra were acquired on a 400 MHz NMR spectrometer in $CDCl_3$, ^{19}F spectra were acquired on a 300 MHz NMR spectrometer in CD_3CN or $CDCl_3$, and ^{13}C NMR spectra were acquired on a 400 MHz NMR spectrometer in $CDCl_3$. The ^{1}H, ^{13}C, and ^{19}F NMR chemical shifts are given in parts per million (δ) with respect to an internal tetramethylsilane (TMS, δ = 0.00 ppm) standard and/or 3-chlorobenzotrifluoride (δ = −64.2 ppm relative to $CFCl_3$). NMR data are reported in the following format: chemical shift (integration, multiplicity (s = singlet, d = doublet, t = triplet, q = quartet, m = multiplet), coupling constants (Hz)). IR data were obtained using an ATR-IR instrument. Spectral data were processed with Bruker software. Photochemical reactions were run in front of a 72-LED work light (Designers Edge L1923). HPLC purification (if necessary) was conducted on a Teledyne Isco CombiFlash EZ Prep system using a Dynamax-60A SiO_2 column and HPLC grade EtOAc and hexanes. The Gaussian '09 package was used for all calculations.

9.2 Experimental Details for Chapter 2.

General Fluorination Procedure. Selectfluor (133 mg, 0.38 mmol), benzil (5.0 mg, 0.025 mmol), and the substrate (0.25 mmol) were added to an oven-dried μω vial equipped with a stir bar; the vial was then sealed with a cap w/ septum using a crimper and

evacuated/refilled with N_2 multiple times. Anhydrous CH_3CN (4 mL) was added, and the reaction mixture was irradiated with a cool white LED work light while stirring. After 14 h, a 0.3 mL aliquot was taken for ^{19}F NMR yield determination, and the rest of the reaction mixture was transferred to a separatory funnel, diluted with H_2O, and extracted into CH_2Cl_2. The combined organic layers were washed with H_2O and brine, then dried with $MgSO_4$, filtered through Celite, and concentrated. The crude reaction mixture was purified via gradient column chromatography on silica gel eluting with EtOAc:hexanes.

Synthesis of Starting Materials.

3β-Acetoxy-5α-cholestan-7-one

Cholesteryl acetate (4.0 g, 9.3 mmol) was dissolved in a mixture of acetone (475 mL) and acetic acid (50 mL) in a round-bottom flask equipped with a stir bar and reflux condenser under N_2. The reaction mixture was treated with *N*-hydroxysuccinimide (10.7 g, 93.0 mmol) and $K_2Cr_2O_7$ (11.0 g, 37.2 mmol), and then the reaction mixture was stirred at 40 °C for 48 h. The reaction mixture was cooled to rt, quenched with 10% aqueous sodium metabisulfite solution, filtered through Celite, and extracted into Et_2O. The combined organic layers were washed with saturated $NaHCO_3$ and brine, and then dried with $MgSO_4$ and concentrated. The crude residue was recrystallized in MeOH to provide 3β-acetoxy-cholest-5-en-7-one (3.28 g, 80%).

A balloon filled with hydrogen was placed over a round-bottom flask containing a solution of 3β-acetoxy-cholest-5-en-7-one (1.20 g, 2.7 mmol) and 10% Pd/C (147 mg) in MeOH (45 mL) and EtOAc (15 mL). The reaction was then stirred at rt for 3 h. The catalyst was removed by filtration through Celite, and the filtrate was concentrated. The crude

residue was recrystallized using MeOH/EtOAc to obtain 3β-acetoxy-5α-cholestan- 7-one (1.09 g, 90%).

White solid; m.p. 189-191 oC. ^{1}H NMR (400 MHz, $CDCl_3$): δ 4.70-4.62 (m, 1H), 2.35-2.29 (m, 2H), 2.22-2.14 (m, 1H), 2.03-1.95 (m, 2H), 2.01 (s, 3H), 1.92-1.83 (m, 2H), 1.77 (dt, *J* = 13.4, 3.5 Hz, 1H), 1.69-1.61 (m, 1H), 1.60-1.46 (m, 6H), 1.42-1.21 (m, 5H), 1.19-0.95 (m, 9H), 1.08 (s, 3H), 0.89 (d, *J* = 6.5 Hz, 3H), 0.85 (d, *J* = 6.7 Hz, 3H), 0.84 (d, *J* = 6.6 Hz, 3H), 0.63 (s, 3H); ^{13}C{^{1}H} NMR (100 MHz, $CDCl_3$): δ 211.5, 170.4, 72.8, 55.02, 55.00, 49.96, 48.9, 46.5, 45.9, 42.5, 39.5, 38.7, 36.1, 36.0, 35.8, 35.7, 33.9, 28.4, 28.0, 27.1, 25.0, 23.8, 22.8, 22.6, 21.8, 21.3, 18.8, 12.1, 11.7; υ_{max} (ATR-IR): 1728, 1706 cm^{-1}; λ_{max} (CH_3CN): 293 nm; HRMS (ESI) m/z $C_{29}H_{48}O_3Na^+$: calc 467.349566, observed 467.349739.

2-(4-(4,4,5,5-Tetramethyl-1,3,2-dioxaborolan-2-yl)benzyl)cyclohexan-1-one

To a flame-dried three-neck round-bottom flask equipped with a stir bar and reflux condenser under N_2 was added LiBr (0.24 g, 3.0 mmol), diisopropylamine (0.45 mL, 3.2 mmol), and THF (15 mL). The reaction mixture was cooled to -20 °C, and then slowly treated with n-BuLi (2.0 mL, 3.2 mmol, 1.6 M in hexanes) and stirred for 30 min. The reaction mixture was cooled to -78 °C, and then cyclohexanone (0.29 mL, 2.8 mmol) was added dropwise and stirred for an additional 30 min. Subsequently, 4-bromomethylphenylboronic acid pinacol ester (1.00 g, 3.4 mmol) dissolved in THF (2.0 mL) was added dropwise, the reaction mixture was slowly warmed to rt, and stirred for 12 h. Then the reaction was quenched with 1.0 M HCl, extracted into Et_2O, the combined organic layers were dried over $MgSO_4$, filtered through Celite, and concentrated. The crude

residue was purified via column chromatography on silica gel eluting with EtOAc:hexanes to provide 2-(4-(4,4,5,5-tetramethyl-1,3,2-dioxaborolan-2- yl)benzyl)cyclohexan-1-one (0.79 g, 90 %).

White solid; m.p. 78-80 oC. ^{1}H NMR (400 MHz, $CDCl_3$): δ 7.74 (d, *J* = 8.0 Hz, 2H), 7.18 (d, *J* = 7.9 Hz, 2H), 3.25 (dd, *J* = 13.7, 4.6 Hz, 1H), 2.59-2.51 (m, 1H), 2.46-2.39 (m, 2H), 2.35-2.27 (m, 2H), 2.08-1.96 (m, 2H), 1.83-1.77 (m, 1H), 1.72-1.49 (m, 2H), 1.38-1.28 (m, 1H), 1.34 (s, 12H); ^{13}C{^{1}H} NMR (100 MHz, $CDCl_3$): δ 211.8, 143.6, 134.6, 128.4, 83.4, 52.1, 41.9, 35.5, 33.2, 27.8, 24.8, 24.7, 24.7; υ_{max} (ATR-IR): 1710 cm^{-1}; λ_{max} (CH_3CN): 296 nm; HRMS (ESI) m/z $C_{19}H_{26}BO_3Na^+$: calc 337.194546, observed 337.194437.

3-Benzylbicyclo[3.1.1]heptan-2-one

To a flame-dried three-neck round-bottom equipped with a stir bar and reflux condenser under N_2 was added LiBr (0.48 g, 5.5 mmol), diisopropylamine (0.80 mL, 5.7 mmol), and THF (17 mL). The reaction mixture was cooled to -20 °C, and then slowly treated with n-BuLi (3.60 mL, 5.7 mmol, 1.6 M in hexanes) and stirred for 30 min. The reaction mixture was cooled to -78 °C, and then (1R)-(+)-nopinone (0.70 mL, 5.0 mmol) dissolved in THF (2.0 mL) was added dropwise and stirred for an additional 30 min. Subsequently, benzyl bromide (0.90 mL, 7.5 mmol) dissolved in THF (2.0 mL) was added dropwise, the reaction mixture was slowly warmed to rt, and stirred for 12 h. The reaction was then quenched with 1.0 M HCl, extracted into Et_2O, the combined organic layers were dried over $MgSO_4$, filtered through Celite, and concentrated. The crude residue was purified via column chromatography on silica gel eluting with EtOAc:hexanes to provide 3-benzylbicyclo[3.1.1]heptan-2-one (0.91 g, 80 %).

Colorless oil. ^{1}H NMR (400 MHz, $CDCl_3$): δ 7.34-7.27 (m, 2H), 7.25-7.19 (m, 3H), 3.40-3.35 (m, 1H), 2.78-2.60 (m, 3H), 2.55-2.47 (m, 1H), 2.22-2.16 (m, 1H), 2.01-1.92 (m, 1H), 1.77 (dt, J = 14.1, 3.4 Hz, 1H), 1.31 (d, J = 10.5 Hz, 1H), 1.32 (s, 3H), 0.89 (s, 3H); ^{13}C{^{1}H} NMR (100 MHz, $CDCl_3$): δ 214.8, 139.5, 129.1, 128.3, 126.2, 58.2, 45.0, 41.7, 40.9, 40.5, 27.3, 25.7, 25.5, 22.0; υ_{max} (ATR-IR): 1706 cm^{-1}; λ_{max} (CH_3CN): 295 nm; HRMS (ESI) m/z $C_{14}H_{16}ONa^{+}$: calc 251.141420, observed 251.140246.

Acetylnorcamphane

A mixture of cyclopentadiene (1.19 g, 17.8 mmol) and mesityl oxide (8.76 g, 89.0 mmol) was heated to 160 °C in an autoclave for 14 h. The reaction mixture was then slowly cooled to rt, the starting materials were distilled off, and the remaining residue was purified via column chromatography eluting with EtOAc:hexanes to provide 2- acetyl-3,3-dimethylbicyclo[2.2.1]hept-5-ene (0.30 g, 10%).

A balloon filled with hydrogen was placed over a round-bottom flask containing a solution of 2-acetyl-3,3-dimethylbicyclo[2.2.1]hept-5-ene (0.30 g, 1.83 mmol) and 10% Pd/C (73 mg) in MeOH (20 mL) and EtOAc (5 mL). The reaction mixture was then stirred at rt for 14 h. The catalyst was removed by filtration through Celite, and the filtrate was concentrated. The crude residue was purified via column chromatography eluting with EtOAc:hexanes to provide acetylnorcamphane (0.28 g, 92%). The endo- and exo-isomers were purified via HPLC.

Colorless oil. ^{1}H NMR (400 MHz, $CDCl_3$): δ 2.42-2.39 (m, 1H), 2.37-2.35 (m, 1H), 2.06 (s, 3H), 1.94-1.86 (m, 1H), 1.81-1.79 (m, 1H), 1.66-1.56 (m, 2H), 1.40-1.31 (m, 1H), 1.29-1.18 (m, 2H), 1.16 (s, 3H), 0.98 (s, 3H); ^{13}C{^{1}H} NMR (100 MHz, $CDCl_3$): δ 210.3, 63.8,

49.8, 41.3, 38.2, 37.4, 32.4, 31.7, 24.5, 23.1, 21.4; υ_{max} (ATR-IR): 1700 cm^{-1}; λ_{max} (CH_3CN): 291 nm.

Nootkat-1-one

To a flame-dried round-bottom flask equipped with a stir bar was dissolved valencene (3.70 g, 18.0 mmol) and PtO_2 (100 mg, 0.44 mmol) in MeOH. The resulting solution was exposed to H_2 via balloon and stirred for 2 h. The catalyst was then removed by filtration through Celite, the filtrate was concentrated, and the crude residue was purified via column chromatography eluting with EtOAc:hexanes to provide dihydrovalencene (3.34 g, 90%).

The dihydrovalencene (1.00 g, 4.85 mmol) was dissolved in Et_2O (40 mL) using a 250 mL three-neck round-bottom flask equipped with a stir bar and condenser. After cooling the solution to 0 oC, aqueous 60-70% HNO_3 (25 mL) was added drop wise over 20 min, and the reaction mixture was stirred for additional 5 min. At this point, $NaNO_2$ (0.69 g, 2.0 mmol) was added, and the reaction mixture was slowly warmed to rt over 2 h. The reaction mixture was then transferred to a separatory funnel containing 40 mL of cold water. The aqueous layer was removed without agitation, and then the Et_2O layer was washed with cold H_2O, 1.0 M NaOH, and then H_2O. The combined organic layers were dried over Na_2SO_4, filtered through Celite, and concentrated. The crude residue (1.00 g) was dissolved in AcOH (40 mL) and diluted with H_2O (4 mL) in a round-bottom flask equipped with a stir bar and a condenser. The resulting reaction mixture was treated with Zn dust in portions over 20 min at rt, and was then heated to reflux for 4 h. Upon cooling to rt, the mixture was diluted with EtOAc, filtered through Celite (to remove residual Zn and related byproducts). The organic layer was washed with H_2O, dried over MgSO4, filtered through Celite, and

concentrated. The crude residue was purified via silica gel column chromatography eluting with EtOAc:hexanes to provide nootkat-1-one (0.30 g, 49%).

Colorless oil. ^{1}H NMR (400 MHz, $CDCl_3$): δ 2.42-2.23 (m, 2H), 2.07 (dd, J = 12.2, 3.2 Hz, 1H), 1.88-1.59 (m, 6H), 1.50-1.32 (m, 2H), 1.27-1.14 (m, 1H), 0.89-0.80 (m, 11H), 0.62 (s, 3H); ^{13}C{^{1}H} NMR (100 MHz, $CDCl_3$): δ 212.9, 58.0, 42.8, 42.2, 41.8, 41.2, 38.1, 32.8, 31.4, 28.2, 20.6, 19.9, 19.4, 14.4, 12.0; υ_{max} (ATR-IR): 1713 cm^{-1}; λ_{max} (CH_3CN): 292 nm; HRMS (ESI) m/z $C_{15}H_{26}ONa^{+}$: calc 245.187587, observed 245.187501.

(+)-Longicamphenylone

To a flame-dried three-neck round-bottom flask equipped with a stir bar was added (+)-longifolene (mixture of isomers, 1.00 g, 4.9 mmol) and DCM (25 mL). The solution was then cooled to -78 °C, purged with oxygen for 5 min, and then a stream of ozone gas was bubbled through the solution for 10 min (excess ozone was quenched by bubbling through a saturated aqueous $NaSO_3$). Subsequently, the solution was purged with oxygen for 5 min, warmed to rt under N_2, diluted with aqueous 50% AcOH (12 mL), and then treated with a Zn dust (0.50 g, 7.4 mmol). After stirring the reaction mixture for 2 h, residual Zn was filtered off, extracted into DCM, and successively washed with H_2O and saturated $NaHCO_3$. The organic layer was dried over $MgSO_4$, filtered through Celite and concentrated. The crude residue was purified via column chromatography on silica gel eluting with EtOAc:hexanes to afford (+)-longicamphenylone.

White solid; m.p. 49-50. ^{1}H NMR (400 MHz, $CDCl_3$): δ 2.52 (dm, J = 5.4 Hz, 1H), 2.42-2.40 (m, 1H), 1.97-1.86 (m, 2H), 1.78-1.72 (m, 1H), 1.68-1.63 (m, 2H), 1.56-1.38 (m, 4H), 1.24-1.17 (m, 1H), 1.10-1.06 (m, 1H), 1.01 (s, 3H), 0.95 (s, 3H), 0.90 (s, 3H); ^{13}C{^{1}H}

NMR (100 MHz, $CDCl_3$): δ 225.6, 60.6, 51.1, 48.6, 43.1, 42.9, 40.2, 36.7, 33.5, 29.1, 25.3, 25.2, 20.1; υ_{max} (ATR-IR): 1745 cm^{-1}; λ_{max} (CH_3CN): 290 nm; HRMS (ESI) m/z $(C_{14}H_{22}O_2)_2Na^+$: calc 467.322572, observed 467.313270.

5α-Tosyl-15-norpanasinsan-8-one

To a flame-dried three-neck round-bottom flask equipped with a stir bar was added (-)-caryophyllene oxide (5.00 g, 22.7 mmol) and DCM (120 mL). The solution was then cooled to -78 °C, purged with oxygen for 5 min, and then a stream of ozone gas was bubbled through the solution for 20 min (excess ozone was quenched by bubbling through a saturated aqueous $NaSO_3$). Subsequently, the solution was purged with oxygen for 5 min, warmed to rt under N_2, diluted with aqueous 50% AcOH (60 mL), and then treated with a Zn dust (2.23 g, 34.1 mmol). After stirring the reaction mixture for 2 h, residual Zn was filtered off, extracted into DCM, and successively washed with H_2O and saturated $NaHCO_3$. The organic layer was dried over $MgSO_4$, filtered through Celite and concentrated to afford kobusone (5.00 g, 99%) that was used without further purification. A solution of kobusone (1.00 g, 4.5 mmol) and KOH (12.00 g, 213.9 mmol) in EtOH (120 mL) was heated to reflux for 4 h. Then, the reaction mixture was diluted with H_2O (150 mL), extracted into Et_2O, dried over MgSO4, filtered through Celite and concentrated. The residue was purified via column chromatography on silica gel eluting with EtOAc:hexanes to provide 5α-hydroxy-15-norpanasinsan-8-one (0.8 g, 80%).

To a flame-dried round-bottom equipped with a stir bar under N_2 was added 5α-hydroxy-15-norpanasinsan-8-one (0.80 g, 3.6 mmol) and pyridine (20 mL). The reaction mixture was treated with TosCl (1.16 g, 6.1 mmol), and stirred at rt for 20 h. Then, the

reaction was quenched with water, diluted with EtOAc, washed successively with 1.0 M HCl, H_2O, saturated $NaHCO_3$, and brine. The organic layer was dried over $MgSO_4$, filtered through Celite, and the filtrate was concentrated. The crude residue was purified via column chromatography on silica gel eluting with EtOAc:hexanes to provide 5α- tosyl-15-norpanasinsan-8-one (0.70 g, 52%).

Viscous oil. ^{1}H NMR (400 MHz, $CDCl_3$): δ 7.83-7.79 (m, 2H), 7.36-7.33 (m, 2H), 4.72 (dd, *J* = 12.1, 4.4 Hz, 1H), 2.53-2.44 (m, 2H), 2.45 (s, 3H), 2.34-2.25 (m, 2H), 2.13-2.07 (m, 1H), 2.03-1.92 (m, 1H), 1.89-1.66 (m, 3H), 1.59-1.50 (m, 1H), 1.32 (d, *J* = 12.3 Hz, 1H), 0.96 (s, 3H), 0.84 (s, 3H), 0.83 (s, 3H); $^{13}C\{^1H\}$ NMR (100 MHz, $CDCl_3$): δ 209.8, 144.8, 134.2, 129.8, 127.6, 80.6, 58.6, 54.4, 52.6, 37.0, 35.7, 33.1, 31.1, 29.6, 27.6, 24.9, 24.4, 21.6, 12.7; υ_{max} (ATR-IR): 1699 cm^{-1}; λ_{max} (CH_3CN): 294 nm; HRMS (ESI) m/z $(C_{21}H_{28}O_4S)_2Na^+$: calc 775.330881, observed 775.330542.

3β-Chloro-5α-cholestan-7-one

Cholesteryl chloride (5.00 g, 12.3 mmol) was dissolved in a mixture of acetone (300 mL) and acetic acid (30 mL) in a round-bottom flask equipped with a stir bar and reflux condenser under N_2. The reaction mixture was treated with *N*-hydroxysuccinimide (11.2 g, 114 mmol) and $K_2Cr_2O_7$ (14.5 g, 49.3 mmol), and then the reaction mixture was stirred at 40 °C for 48 h. The reaction mixture was cooled to rt, quenched with 10% aqueous sodium metabisulfite solution, filtered through Celite, and extracted into Et_2O. The combined organic layers were washed with saturated $NaHCO_3$ and brine, and then dried over $MgSO_4$ and concentrated. The crude residue was recrystallized in MeOH to provide 3β-chloro-cholest-5-en-7-one (3.28 g, 80%).

A balloon filled with hydrogen was placed over a round-bottom flask containing a solution of 3β-chloro-cholest-5-en-7-one (1.00 g, 2.39 mmol) and 10% Pd/C (80 mg) in MeOH (30 mL) and EtOAc (20 mL). The reaction mixture was then stirred at rt for 3 h. The catalyst was removed by filtration through Celite, and the filtrate was concentrated. The crude residue was recrystallized using MeOH to obtain 3β-chloro-5α-cholestan-7- one (1.00 g, 99%).

White solid; m.p. 128-130 oC. ^{1}H NMR (400 MHz, $CDCl_3$): δ 3.85-3.77 (m, 1H), 2.37-2.30 (m, 2H), 2.22-2.13 (m, 1H), 2.11-1.95 (m, 3H), 1.91-1.73 (m, 5H), 1.57-1.46 (m, 4H), 1.40-1.28 (m, 4H), 1.26-1.19 (m, 1H), 1.16-1.06 (m, 6H), 1.1 (s, 3H), 1.05-0.96 (m, 3H), 0.89 (d, J = 6.6 Hz, 3H), 0.853 (d, J = 6.6 Hz, 3H), 0.848 (d, J = 6.6 Hz, 3H), 0.64 (s, 3H); ^{13}C{^{1}H} NMR (100 MHz, $CDCl_3$): δ 211.3, 58.6, 55.0, 54.98, 50.0, 48.8, 48.3, 45.7, 42.5, 39.4, 39.2, 38.6, 37.7, 36.1, 35.8, 35.6, 32.7, 28.4, 28.0, 24.9, 23.7, 22.8, 22.5, 21.7, 18.8, 12.0, 11.7; υ_{max} (ATR-IR): 1699 cm^{-1}; λ_{max} (CH_3CN): 292 nm; HRMS (ESI) m/z $(C_{27}H_{45}ClO)_2Na^+$: calc 863.621009, observed 863.620294.

3,17-Diacetoxy-androstan-7-one

To a flame-dried round-bottom equipped with a stir bar under N_2 was added prasterone (4.00 g, 13.9 mmol) and MeOH (75 mL). The reaction mixture was treated with $NaBH_4$ (0.53 g, 13.9 mmol) in portions over 10 min, and then stirred for an additional 2 h. The resulting white precipitate was collected by filtration and dried to provide 5- androstenediol (3.50 g, 87%).

The 5-androstenediol from the previous step (3.10 g, 10.7 mmol), p-TsOH•H_2O (60 mg, 0.30 mmol), and acetic anhydride (4.6 mL) were dissolved in pyridine (6.0 mL) under N_2.

After stirring for 1 h, the reaction mixture was heated to 95 °C and stirred for an additional 3.5 h. The reaction mixture was then cooled to rt and diluted with H_2O (150 mL). The white precipitate was collected by filtration, washed with H_2O, and dried to provide androstenediol-3,17-diacetate (3.52 g, 85%).

Androstenediol-3,17-diacetate (1.93 g, 5.2 mmol) was dissolved in a mixture of acetone (200 mL) and acetic acid (20 mL) in a round-bottom flask equipped with a stir bar and reflux condenser under N_2. The reaction mixture was treated with *N*-hydroxysuccinimide (5.93 g, 52 mmol) and $K_2Cr_2O_7$ (6.06 g, 21 mmol), and then the reaction mixture was stirred at 40 °C for 48 h. The reaction mixture was cooled to rt, quenched with 10% aqueous sodium metabisulfite solution, filtered through Celite, and extracted into Et_2O. The combined organic layers were washed with saturated $NaHCO_3$ and brine, and then dried over $MgSO_4$ and concentrated. The crude residue was recrystallized in MeOH to provide 3β,17β-diacetoxyandrost-5-ene-7-one (1.64 g, 82%).

A balloon filled with hydrogen was placed over a round-bottom flask containing a solution of 3β,17β-diacetoxyandrost-5-ene-7-one (1.00 g, 2.57 mmol) and 10% Pd/C (140 mg) in MeOH (40 mL) and EtOAc (10 mL). The reaction mixture was then stirred at rt for 3 h. The catalyst was removed by filtration through Celite, and the filtrate was concentrated. The crude residue was recrystallized using MeOH to afford 3,17-diacetoxy-androstan-7-one (0.70 g, 70%).

White solid; m.p. 189-191 oC. ^{1}H NMR (400 MHz, $CDCl_3$): δ 4.69-4.58 (m, 2H), 2.38-2.28 (m, 2H), 2.26-2.13 (m, 2H), 2.06-1.96 (m, 1H), 2.01 (s, 3H), 2.00 (s, 3H), 1.90-1.85 (m, 1H), 1.80-1.40 (m, 10H), 1.26-1.17 (m, 1H), 1.14-1.01 (m, 3H), 1.08 (s, 3H), 0.76 (s, 3H); ^{13}C{^{1}H} NMR (100 MHz, $CDCl_3$): δ 210.5, 170.9, 170.3, 81.9, 72.5, 54.8, 49.5, 46.0,

45.5, 43.7, 42.5, 35.8, 35.72, 35.70, 33.7, 27.4, 27.0, 24.5, 21.24, 21.20, 21.0, 12.0, 11.6; υ_{max} (ATR-IR): 1724, 1706 cm^{-1}; λ_{max} (CH_3CN): 292 nm; HRMS (ESI) m/z $C_{23}H_{34}O_5Na^+$: calc 413.229845, observed 413.230264.

3β,20α-Diacetoxy-5α-pregnan-7-one

To a flame-dried round-bottom flask equipped with a stir bar under N_2 was added pregnenolone (4.00 g, 12.6 mmol) and MeOH (80 mL). The reaction mixture was treated with $NaBH_4$ (0.96 g, 25.3 mmol) in portions over 10 min, and then stirred for an additional 2 h. The resulting white precipitate was collected by filtration and dried to provide pregn-5-ene-3β,20α-diol (3.00 g, 75%).

The pregn-5-ene-3β,20α-diol from the previous step (2.50 g, 7.9 mmol), p-TsOH•H_2O (48 mg, 0.24 mmol), and acetic anhydride (4 mL) were dissolved in pyridine (5 mL) under N_2. After stirring for 1 h, the reaction mixture was heated to 95 °C and stirred for an additional 4 h. The reaction mixture was then cooled to rt and diluted with H_2O (130 mL). The white precipitate was collected by filtration, washed with H_2O, and dried to provide pregn-5-en-3β,20α-diyl diacetate (2.40 g, 76%).

Pregn-5-en-3β,20α-diyl diacetate (2.40 g, 5.0 mmol) was dissolved in a mixture of acetone (300 mL) and acetic acid (30 mL) in a round-bottom flask equipped with a stir bar and reflux condenser under N_2. The reaction mixture was treated with *N*-hydroxysuccinimide (6.90 g, 60 mmol) and $K_2Cr_2O_7$ (7.06 g, 24 mmol), and then the reaction mixture was stirred at 40 °C for 48 h. The reaction mixture was cooled to rt, quenched with 10% aqueous sodium metabisulfite solution, filtered through Celite, and extracted into Et_2O. The combined organic layers were washed with saturated aqueous

$NaHCO_3$ and brine, and then dried over $MgSO_4$ and concentrated. The crude residue was recrystallized in MeOH to provide 3β,20α-diacetoxypregn-5-en-7-one (1.56 g, 75%).

A balloon filled with hydrogen was placed over a round-bottom flask containing a solution of 3β,20α-diacetoxypregn-5-en-7-one (0.80 g, 1.9 mmol) and 10% Pd/C (140 mg) in MeOH (40 mL) and EtOAc (10 mL). The reaction mixture was then stirred at rt for 3 h. The catalyst was removed by filtration through Celite, and the filtrate was concentrated. The crude residue was purified via column chromatography eluting with EtOAc:hexanes to provide 3β,20α-diacetoxy-5α-pregnan-7-one (0.60 g, 76%).

White solid; m.p. 149-150 oC. ^{1}H NMR (400 MHz, $CDCl_3$): δ 4.87-4.79 (m, 1H), 4.71-4.63 (m, 1H), 2.37-2.23 (m, 3H), 2.07-2.04 (m, 1H), 2.01 (s, 3H), 2.00 (s, 3H), 1.93-1.86 (m, 1H), 1.82-1.75 (m, 3H), 1.68-1.42 (m, 8H), 1.25-1.00 (m, 5H), 1.14 (d, J = 6.1 Hz, 3H), 1.08 (s, 3H), 0.61 (s, 3H); ^{13}C{^{1}H} NMR (100 MHz, $CDCl_3$): δ 211.1, 170.4, 170.3, 72.7, 72.6, 54.9, 53.9, 49.7, 48.3, 46.3, 45.7, 42.3, 38.1, 35.9, 35.8, 33.8, 27.1, 25.6, 24.9, 21.7, 21.5, 21.3, 19.9, 12.5, 11.7; υ_{max} (ATR-IR): 1729, 1708 cm^{-1}; λ_{max} (CH_3CN): 292 nm; HRMS (ESI) m/z $C_{25}H_{38}O_5Na^+$: calc 441.261145, observed 441.261728.

17β-Acetoxy-5α-androstan-6-one

To a flame-dried round-bottom equipped with a stir bar under N_2 was added prasterone (5.00 g, 17.3 mmol) and pyridine (70 mL). The reaction mixture was treated with TosCl (5.00 g, 26.2 mmol), and stirred at rt for 20 h. The reaction was then quenched with H_2O, diluted with EtOAc, washed successively with 1.0 M HCl, H_2O, saturated $NaHCO_3$, and brine. The organic layer was dried over $MgSO_4$, filtered through Celite, and the filtrate was

concentrated. The crude residue was purified via column chromatography eluting with EtOAc:hexanes to provide 3β-tosyloxyandrost-5-ene-17-one (5.60 g, 74%).

The 3β-tosyloxyandrost-5-ene-17-one (4.50 g, 10.0 mmol) was dissolved in MeOH (65 mL), and reaction mixture was treated with $NaBH_4$ (0.76 g, 20.0 mmol) in portions over 10 min, and then stirred for an additional 2 h. The resulting white precipitate was collected by filtration and dried to provide 3β-tosyloxyandrost-5-ene-17β-ol (4.30 g, 75%).

The 3β-tosyloxyandrost-5-ene-17β-ol from the previous step (4.30 g, 9.0 mmol), p-TsOH•H_2O (60 mg, 0.30 mmol), and acetic anhydride (30 mL) were dissolved in pyridine (30 mL) under N_2. After stirring for 1 h, the reaction mixture was heated to 95 °C and stirred for an additional 4 h. The reaction mixture was then cooled to rt and diluted with H_2O (150 mL). The white precipitate was collected by filtration, washed with H_2O, and dried over $MgSO_4$ to provide 17β-acetoxy-3β-p-tolylsulphonyloxyandrost- 5-ene (4.25 g, 87%).

The 17β-acetoxy-3β-p-tolylsulphonyloxyandrost-5-ene (4.25 g, 8.7 mmol) was dissolved in Et_2O (85 mL) using 500 mL three-neck round-bottom flask equipped with a stir bar and condenser. After cooling the solution to 0 oC, aqueous 60-70% HNO_3 (64 mL) was added dropwise over 20 min, and the reaction mixture was stirred for additional 5 min. At this point, $NaNO_2$ (0.90 g, 13.1 mmol) was added, and the reaction mixture was slowly warmed to rt over 2 h. The reaction mixture was then transferred to a separatory funnel containing 60 mL of cold water. The aqueous layer was removed without agitation, and the Et_2O layer was washed with cold H_2O, 1.0 M NaOH, and then H_2O. The combined organic layers were dried over Na_2SO_4, filtered through Celite, and concentrated. The crude residue (3.65 g) was dissolved in AcOH (70 mL) and diluted with H_2O (7 mL) in a round-bottom

flask equipped with a stir bar and a condenser. The resulting reaction mixture was treated with Zn dust in portions over 30 min at rt, and was then heated to reflux for 4 h. Upon cooling to rt, the mixture was diluted with EtOAc, filtered through Celite (to remove residual Zn and related byproducts). The organic layer was washed with H_2O, dried over $MgSO_4$, filtered through Celite, and concentrated. The crude residue was purified via column chromatography eluting with EtOAc:hexanes to provide 17β-acetoxy-5α-androst-2-en-6-one (0.90 g, 39%).

A balloon filled with hydrogen was placed over a round-bottom flask containing a solution of 17β-acetoxy-5α-androst-2-en-6-one (0.65 g, 2.0 mmol) and 10% Pd/C (100 mg) in MeOH (32 mL) and EtOAc (8 mL). The reaction mixture was then stirred at rt for 14 h. The catalyst was removed by filtration through Celite, and the filtrate was concentrated. The crude residue was purified via column chromatography eluting with EtOAc:hexanes to provide 17β-acetoxy-5α-androstan-6-one (0.40 g, 60%).

White solid; m.p. 124-126 oC. ^{1}H NMR (400 MHz, $CDCl_3$): δ 4.63-4.58 (m, 1H), 2.27 (dd, *J* = 13.0, 4.5 Hz, 1H), 2.20-2.10 (m, 2H), 2.02 (s, 3H), 1.96 (td, *J* = 12.7, 1.2 Hz, 1H), 1.86-1.65 (m, 5H), 1.60-1.33 (m, 6H), 1.31-1.19 (m, 5H), 1.17-1.07 (m, 2H), 0.76 (s, 3H), 0.71 (s, 3H); ^{13}C{^{1}H} NMR (100 MHz, $CDCl_3$): δ 212.0, 171.0, 82.3, 58.8, 54.2, 51.2, 46.2, 43.0, 41.7, 38.1, 37.6, 36.5, 27.3, 25.1, 23.2, 21.3, 21.1, 20.6, 20.4, 13.0, 12.0; υ_{max} (ATR-IR): 1734, 1710 cm^{-1}; λ_{max} (CH_3CN): 291 nm; HRMS (ESI) m/z $C_{21}H_{32}O_3Na^+$: calc 355.224366, observed 355.224678.

3β-Acetoxy-D-homo-5α-androstan-17a-one

Prasterone acetate (5.00 g, 15.1 mmol) was dissolved in EtOH (150 mL) and treated with KCN (31.5 g, 484 mmol) while stirring. The reaction mixture was cooled to 0 °C and AcOH (35 mL) was added dropwise; the reaction mixture was stirred for 1 h. The reaction mixture was stirred at rt for an additional 2 h and then quenched with H_2O. The white precipitate was collected by filtration, washed with H_2O, washed with 2% aqueous AcOH, and then dried over $MgSO_4$. The crude residue (4.80 g, 12.4 mmol), PtO_2 (1.00 g), and AcOH (150 mL) were shaken under H_2 at 40 psi in a Parr apparatus for 48 h. The solution was filtered through Celite, concentrated, and diluted with water (80 mL). Neutral impurities were removed by extracting into Et_2O. The aqueous layer was then transferred to a round-bottom flask, along with AcOH (10 mL), and cooled to 0 °C. Then, $NaNO_2$ (2.40 g, 34.8 mmol) dissolved in water (8 mL) was added to the reaction mixture, which was then stirred for 2 h at 0 °C. The reaction mixture was warmed to rt and stirred for additional 16 h. The precipitated white solid was collected via filtration, washed with H_2O, and dried. The crude residue was purified via column chromatography eluting with EtOAc:hexanes to provide 3β-acetoxy-D-homo-5α-androstan-17a-one (2.40 g, 56%).

White solid; m.p. 118-120 °C. ^{1}H NMR (400 MHz, $CDCl_3$): δ 4.70-4.61 (m, 1H), 2.59 (td, J = 14.0, 6.7 Hz, 1H), 2.17 (dm, J = 14.1 Hz, 1H), 2.06-1.95 (m, 1H), 1.99 (s, 3H), 1.89-1.69 (m, 5H), 1.65-1.50 (m, 3H), 1.48-1.27 (m, 6H), 1.25-1.09 (m, 4H), 1.06 (s, 3H), 1.02-0.94 (m, 1H), 0.87-0.74 (m, 1H), 0.79 (s, 3H), 0.68-0.61 (m, 1H); ^{13}C{^{1}H} NMR (100 MHz, $CDCl_3$): δ 216.4, 170.6, 73.5, 53.2, 51.4, 48.3, 43.9, 37.1, 36.4, 35.6, 35.1, 33.8, 32.4, 31.2, 28.4, 27.3, 25.9, 22.9, 21.4, 19.9, 16.9, 12.1; υ_{max} (ATR-IR): 1732, 1701 cm^{-1}; λ_{max} (CH_3CN): 293 nm; HRMS (ESI) m/z $C_{22}H_{34}O_3Na^+$: calc 369.240016, observed 369.240001.

3β-Tosyloxy-5α-androstan-17-one

To a flame-dried round-bottom equipped with a stir bar under N_2 was added prasterone (5.00 g, 17.3 mmol) and pyridine (70 mL). The reaction mixture was treated with tosyl chloride (5.00 g, 26.2 mmol), and stirred at rt for 20 h. The reaction was then quenched with H_2O, diluted with EtOAc, washed successively with 1.0 M HCl, H_2O, saturated $NaHCO_3$, and brine. The organic layer was dried over $MgSO_4$, filtered through Celite, and the filtrate was concentrated. The crude residue was purified via column chromatography on silica gel eluting with EtOAc:hexanes to provide 3β-tosyloxyandrost- 5-ene-17-one (5.60 g, 74%).

A balloon filled with hydrogen was placed over a round-bottom flask containing a solution of 3β-tosyloxyandrost-5-ene-17-one (0.65 g, 1.5 mmol) and 10% Pd/C (80 mg) in MeOH (24 mL) and EtOAc (6 mL). The reaction mixture was then stirred at rt for 3 h. The catalyst was removed by filtration through Celite, and the filtrate was concentrated. The crude residue was purified via column chromatography eluting with EtOAc:hexanes to provide 3β-tosyloxy-5α-androstan-17-one (0.60 g, 90%).

White solid; m.p. 157-158 oC. ^{1}H NMR (400 MHz, $CDCl_3$): δ 7.78 (d, *J* = 8.3 Hz, 2H), 7.32 (d, *J* = 8.0 Hz, 2H), 4.44-4.36 (m, 1H), 2.45-2.38 (m, 1H), 2.43 (s, 3H), 2.09-2.00 (m, 1H), 1.93-1.87 (m, 1H), 1.79-1.71 (m, 3H), 1.68-1.44 (m, 7H), 1.33-1.17 (m, 5H), 1.13-1.05 (m, 1H), 0.98-0.87 (m, 2H), 0.83 (s, 3H), 0.80 (s, 3H), 0.67-0.60 (m, 1H); ^{13}C{^{1}H} NMR (100 MHz, $CDCl_3$): δ 221, 144.3, 134.7, 129.7, 127.6, 82.1, 54.1, 51.3, 47.7, 44.8, 36.7, 35.8, 35.3, 34.9, 34.8, 31.4, 30.7, 28.3, 28.1, 21.7, 21.6, 20.4, 13.8, 12.1; υ_{max} (ATR-

IR): 1734 cm^{-1}; λ_{max} (CH_3CN): 298 nm; HRMS (ESI) m/z $C_{26}H_{36}O_4SNa^+$: calc 467.222651, observed 467.222407.

Methyl 5,17-dioxo-A-nor-3,4-seco-androstan-3-oate

To an oven-dried round-bottom flask equipped with a stir bar under N_2 was added prasterone (8.50 g, 29.5 mmol), aluminum isopropoxide (17.20 g, 84.0 mmol), cyclohexanone (14 mL) and dry toluene (45 mL). The mixture was refluxed for 12 h and then cooled to rt, quenched with H_2O, diluted with EtOAc and filtered through Celite. The organic layer was separated, washed with brine, dried over Na_2SO_4 and concentrated to provide testosterone. The crude residue was purified via column chromatography on silica gel eluting with EtOAc:hexanes (4.67 g, 55%).

To a round-bottom flask containing testosterone (4.70 g, 16.3 mmol) was added isopropanol (65 mL) followed by Na_2CO_3 (2.00 g, 18.8 mmol). A preheated solution of $NaIO_4$ (19.2 g, 89.7 mmol) and $KMnO_4$ (0.13 g, 0.82 mmol) in H_2O (54 mL) was added dropwise over 30 min using an addition funnel. The mixture was refluxed for 4 h, and was then cooled to rt. The reaction mixture was concentrated and then was acidified with 1.0 M HCl, extracted into DCM, washed with brine, dried over Na_2SO_4, filtered through Celite, and concentrated to provide 5-oxo-A-nor-3,5-seco-17β-hydroxy-androstan-3-oic acid that was used without a purification in the next step.

The 5-oxo-A-nor-3,5-seco-17β-hydroxy-androstan-3-oic from the previous step (884 mg, 2.9 mmol) was dissolved in acetone (29 mL) and the mixture was cooled to 0 °C. Jones reagent (4.4 mmol) was then added dropwise, the mixture was warmed to rt, and stirred for 1 h. The reaction mixture was quenched with H_2O, extracted into DCM, washed

with brine, dried over Na_2SO_4, filtered through Celite, and concentrated to provide A-nor-3,5-seco-5,17-diketo-androstan-3-oic acid, which was used without purification in the next step.

To an oven-dried round-bottom flask was added the crude product from the previous step (0.21 g, 0.69 mmol), K_2CO_3 (0.19 g, 1.4 mmol), and dry DMF (2.3 mL). The reaction mixture was stirred for 30 min at rt. Iodomethane (0.05 mL, 0.82 mmol) was then added, and the reaction mixture was stirred for 14 h. At this point, the reaction mixture was quenched with H_2O, extracted into Et_2O, washed with brine, dried over Na_2SO_4, filtered through Celite, and concentrated. The residue was purified via column chromatography on silica gel eluting with EtOAc:hexanes to provide methyl 5,17-dioxo- A-nor-3,4-seco-androstan-3-oate (73 mg, 33%).

Colorless oil. ^{1}H NMR (400 MHz, $CDCl_3$): δ 3.60 (s, 3H), 2.58-2.40 (m, 2H), 2.30-2.22 (m, 2H), 2.16-1.93 (m, 5H), 1.61-1.49 (m, 4H), 1.32-1.20 (m, 4H), 1.09 (s, 3H), 0.88 (s, 3H); ^{13}C{^{1}H} NMR (100 MHz, $CDCl_3$): δ 219.7, 213.6, 174.0, 51.4, 50.6, 50.3, 47.7, 47.4, 37.6, 35.5, 34.3, 30.9, 29.8, 29.4, 29.0, 21.7, 20.6, 20.3, 13.6; υ_{max} (ATR-IR): 1740, 1736, 1702 cm^{-1}; λ_{max} (CH_3CN): 293 nm; HRMS (ESI) m/z $C_{19}H_{28}O_4Na^+$: calc 343.187980, observed 343.187631.

Fluorinated Product Characterization Data

Table 2. Compound 3.

The reaction was run according to the general procedure, and the product yield was determined by ^{19}F NMR analysis. Spectral data match the literature for this compound.

Table 2. Compound 4.

The reaction was run according to the general procedure, and the minor diastereomer was isolated.

White solid; m.p. 94-95 °C. ^{1}H NMR (400 MHz, $CDCl_3$): 7.81 (2H, d, J = 7.6 Hz), 7.31 (2H, d, J = 8.2 Hz), 6.11 (1H, dd, J = 46.6, 3.9 Hz), 2.72-2.60 (1H, m), 2.50-2.44 (1H, m), 2.33-2.24 (1H, m), 2.09-2.00 (2H, m), 1.95-1.88 (1H, m), 1.78-1.66 (2H, m), 1.61- 1.49 (1H, m), 1.34 (12H, s); ^{13}C{^{1}H} NMR (100 MHz, $CDCl_3$): 209.1 (d, J = 2.2 Hz), 142.3, 142.1, 134.75, 134.74, 124.7, 124.6, 90.5 (d, J = 175.1 Hz), 83.8, 56.2 (d, J = 22.9 Hz), 42.2, 27.0, 26.24, 26.18, 24.85, 24.84, 24.5; ^{19}F NMR (282 MHz, $CDCl_3$): -193.7 (1F, dd, J = 46.5, 24.1 Hz); υ_{max} (ATR-IR): 1710 cm^{-1}; HRMS (ESI) m/z $C_{19}H_{26}BFO_3Na^+$: calc 355.185124, observed 355.184717.

Table 2. Compound 5.

The reaction was run according to the general procedure, and the product was isolated as a mixture of diastereomers.

Colorless oil. ^{1}H NMR (400 MHz, $CDCl_3$): 7.41-7.27 (5H, m), 6.19 (1H, dd, J = 44.4, 5.5 Hz), 3.45-3.32 (1H, m), 2.51-2.47 (1H, m), 2.23-1.97 (4H, m), 1.28 (3H, s), 0.95 (3H, s), 0.40 (1H, d, J = 10.7 Hz); ^{13}C{^{1}H} NMR (100 MHz, $CDCl_3$): 210.8 (d, J = 10.0 Hz), 137.7, 137.5, 128.4, 128.3, 126.2, 126.1, 94.2 (d, J = 175.8 Hz), 58.3 (d, J = 2.9 Hz), 49.5 (d, J = 23.6 Hz), 40.6, 39.9, 25.8, 23.8, 22.7 (d, J = 2.2 Hz), 22.0; ^{19}F NMR (282 MHz, $CDCl_3$): -185.0 (1F, dd, J = 44.2, 14.9 Hz), -192.4 (dd, J = 47.6, 41.3 Hz); υ_{max} (ATR- IR): 1706 cm^{-1}; HRMS (ESI) m/z $C_{16}H_{19}FONa^+$: calc 269.131215, observed 269.130823.

Table 2. Compound 6a and 6b.

The reaction was run according to the general procedure, and product was isolated as a mixture of diastereomers.

Colorless oil. ^{1}H NMR (400 MHz, $CDCl_3$): 5.67-4.81 (1H, m), 2.66-2.16 (3H, m), 2.13-1.89 (4H, m), 1.68-1.31 (3H, m), 1.26-1.24 (3H, m), 0.95-0.90 (3H, m); ^{13}C{^{1}H} NMR (100 MHz, $CDCl_3$): 209.8, 209.67, 209.66, 93.9, 92.2, 92.1, 90.5, 71.72, 61.70, 60.9, 60.8, 55.1, 54.9, 48.89, 48.88, 47.8, 47.6, 35.0, 33.81, 33.80, 33.5, 32.5, 32.3, 32.07, 32.06, 32.0, 22.7, 22.2; ^{19}F NMR (282 MHz, $CDCl_3$): -167.6 (1F, dddd, J = 55.6, 41.3, 22.9, 8.0 Hz), -168.33 (1F, ddddd, J = 55.6, 41.3, 15.5, 10.3, 5.2 Hz); υ_{max} (ATR-IR): 1703 cm^{-1}.

Table 2. Compound 7.

The reaction was run according to the general procedure, and the major diastereomer was isolated. Regiochemical assignment was made on the basis of 1) chemical shift in the ^{19}F NMR spectrum that indicates a secondary fluoride on a cyclohexane ring and 2) identification of $^{2}J_{CF}$- and $^{3}J_{CF}$-coupling to distinguishable peaks in the ^{13}C NMR spectrum, i.e. C4a, C6, C7, and C8a *vide infra*. Stereochemical assignment was made on the basis of 1) chemical shift and splitting in the ^{19}F NMR spectrum that indicates F_{eq} on a cyclohexane ring and 2) identification of the two distinct *trans* diaxial $^{3}J_{HH}$-coupling constants (11.1 and 10.3 Hz) in the ^{1}H NMR spectrum.

Viscous oil. ^{1}H NMR (400 MHz, $CDCl_3$): 4.96 (1H, dddd, J = 48.1, 11.1, 10.3, 5.3 Hz), 2.45 (1H, td, J = 13.2, 7.3 Hz), 2.37-2.30 (2H, m), 2.21-2.14 (1H, m), 1.95-1.89 (1H, m), 1.87-1.78 (1H, m), 1.71-1.60 (2H, m), 1.55-1.43 (1H, m), 1.40-1.30 (1H, m), 1.13 (1H, m), 0.97-0.92 (1H, m), 0.90-0.86 (9H, m), 0.63 (3H, s); ^{13}C{^{1}H} NMR (100 MHz, $CDCl_3$):

209.4, 87.5 (d, J = 170.3 Hz, C8), 62.5 (d, J = 15.8 Hz, C8a), 44.0 (d, J = 7.4 Hz, C4a), 42.8 (d, J = 1.1 Hz), 41.8, 41.3 (d, J = 1.8 Hz), 36.5 (d, J = 10.3 Hz, C6), 34.8 (d, J = 18.1 Hz, C7), 32.4 (d, J = 1.1 Hz), 32.0, 19.9, 19.3, 14.4, 13.1; ^{19}F NMR (282 MHz, $CDCl_3$): -177.0 (1F, dm, J = 48.2 Hz); υ_{max} (ATR-IR): 1720 cm^{-1}; HRMS (ESI) m/z $C_{15}H_{25}FONa^+$: calc 263.178165, observed 263.177975.

Table 2. Compound 8.

The reaction was run according to the general procedure, and the major diastereomer was isolated. Regiochemical assignment was made on the basis of 1) chemical shift and $^2J_{HF}$-coupling in the ^{19}F NMR spectrum that indicates a secondary fluoride and 2) identification of $^2J_{CF}$- and $^3J_{CF}$-coupling to distinguishable peaks in the ^{13}C NMR spectrum, i.e. C4, C6, and C9 (carbonyl carbon) *vide infra*. Stereochemistry was not assigned.

White solid; m.p. 64-67 °C. ^{1}H NMR (400 MHz, $CDCl_3$): 4.53 (1H, dm, J = 46.3 Hz), 2.63 (1H, dm, J = 5.3 Hz), 2.29 (1H, br s), 2.00-1.85 (3H, m), 1.83-1.77 (1H, ddd, J = 12.4, 9.1, 3.2 Hz), 1.70 (1H, br s), 1.68-1.60 (1H, m), 1.48-1.42 (1H, m), 1.25 (3H, s), 1.20-1.07 (2H, m), 1.04 (3H, s), 0.97 (3H, s); ^{13}C{^{1}H} NMR (100 MHz, $CDCl_3$): 219.0 (d, J = 2.6 Hz), 99.8 (d, J = 180.6 Hz), 60.2, 51.9, 51.2 (d, J = 15.8 Hz), 42.6 (d, J = 5.9 Hz), 33.3, 31.9, 30.6, 28.6, 27.7 (d, J = 23.6 Hz), 26.0, 24.7 (d, J = 1.8 Hz), 22.4 (d, J = 1.8 Hz); ^{19}F NMR (282 MHz, $CDCl_3$): -181.9 (1F, dm, J = 47.0 Hz);

υ_{max} (ATR-IR): 1741 cm^{-1}; HRMS (ESI) m/z $C_{14}H_{21}FONa^+$: calc 247.146865, observed 247.146615.

Table 2. Compound 9.

The reaction was run according to the general procedure, and the major diastereomer was isolated. Regiochemical assignment was made on the basis of 1) chemical shift and $^{2}J_{HF}$-coupling in the ^{19}F NMR spectrum as well as the large, diagnostic $^{1}J_{CF}$-coupling in the ^{13}C NMR spectrum that indicate a secondary fluoride on a cyclobutane ring and 2) identification of $^{2}J_{CF}$- and $^{3}J_{CF}$-coupling to distinguishable peaks in the ^{13}C NMR spectrum *vide infra*. Stereochemistry was not assigned.

Viscous oil. ^{1}H NMR (400 MHz, $CDCl_3$): 7.82-7.78 (2H, m), 7.37-7.33 (2H, m), 4.51 (1H, dd, J = 53.0, 0.9 Hz), 4.39 (1H, dd, J = 10.9, 6.3 Hz), 2.48-2.45 (1H, m), 2.46 (3H, s), 2.44-2.35 (2H, m), 2.13-2.01 (2H, m), 1.92-1.87 (1H, m), 1.64-1.47 (2H, m), 1.36- 1.30 (1H, m), 1.23-1.22 (6H, m), 0.95 (3H, d, J = 0.8 Hz); ^{13}C{^{1}H} NMR (100 MHz, $CDCl_3$): 206.8 (d, J = 1.1 Hz), 145.1, 134.0, 129.9, 127.7, 93.3 (d, J = 233.7 Hz), 79.3 (d, J = 1.8 Hz), 65.2 (d, J = 20.6 Hz), 50.2 (d, J = 1.5 Hz), 49.1 (d, J = 10.0 Hz), 39.5 (d, J = 22.1 Hz), 37.7, 37.3, 25.8, 23.1, 22.4, 21.7, 21.6 (d, J = 9.2 Hz), 13.9; ^{19}F NMR (282 MHz, $CDCl_3$): -192.7 (1F, dd, J = 53.4, 7.5 Hz); υ_{max} (ATR-IR): 1706 cm^{-1}; HRMS (ESI) m/z $C_{21}H_{27}FO_4SNa^{+}$: calc 417.150629, observed 417.149999.

Table 3. Compound 2.

The reaction was run according to the general procedure, and the major diastereomer was isolated. Regiochemical assignment was made on the basis of 1) chemical shift in the ^{19}F NMR spectrum that indicates a secondary fluoride, 2) $^{2}J_{HF}$- coupling in the ^{1}H and ^{19}F NMR spectra that indicates cyclopentane ring fluorination (54.9 Hz), and 3) identification of $^{2}J_{CF}$- and $^{3}J_{CF}$-coupling to distinguishable peaks in the ^{13}C NMR spectrum, i.e. C13, C14, and C16 *vide infra*. Stereochemical assignment was made on the basis of 1) a larger

$^{3}J_{HH}$-coupling constant assigned to the triplet (8.5 Hz) than the doublet (2.5 Hz) in the ^{1}H NMR spectrum, indicative of two protons *trans* to the C15 proton and 2) analogy to X-ray crystal structure of compound 12.

White solid; m.p. 119-120 °C. ^{1}H NMR (400 MHz, $CDCl_3$): 4.78 (1H, dtd, J = 54.9, 8.5, 2.5 Hz), 4.71-4.63 (1H, m), 2.55 (1H, t, J = 11.3 Hz), 2.35 (1H, t, J = 13.1 Hz), 2.18-2.04 (2H, m), 2.02 (3H, s), 1.98-1.75 (5H, m), 1.71-1.60 (2H, m), 1.58-1.42 (6H, m), 1.39- 1.29 (3H, m), 1.27-1.12 (5H, m), 1.11-1.09 (4H, m), 1.07-0.99 (1H, m), 0.91 (3H, d, J = 6.6 Hz), 0.86 (3H, d, J = 6.6 Hz), 0.85 (3H, d, J = 6.7 Hz), 0.68 (3H, s); ^{13}C{^{1}H} NMR (100 MHz, $CDCl_3$): 209.3, 170.4, 95.2 (d, J = 179.9 Hz, C15), 72.6, 54.8, 54.4 (d, J = 17.3 Hz, C14), 52.6, 48.7, 46.1, 45.8, 44.0 (d, J = 5.9 Hz, C13), 39.4, 38.6, 37.7, 37.4, 36.0, 35.9 (d, J = 19.2 Hz, C16), 34.9, 33.7, 28.0, 27.1, 23.7, 22.8, 22.5, 21.5, 21.3, 18.5, 13.2, 11.7; ^{19}F NMR (282 MHz, $CDCl_3$): -166.8 (1F, dm, J = 55.6 Hz); υ_{max} (ATR-IR): 1736, 1716 cm^{-1}; HRMS (ESI) m/z $C_{29}H_{47}FO_3Na^{+}$: calc 485.340145, observed 485.340635.

Table 3. Compound 10.

The reaction was run according to the general procedure, and the major diastereomer was isolated. Regiochemical assignment was made on the basis of 1) chemical shift in the ^{19}F NMR spectrum that indicates a secondary fluoride, 2) $^{2}J_{HF}$- coupling in the ^{1}H and ^{19}F NMR spectra that indicates cyclopentane ring fluorination (>50 Hz), and 3) identification of $^{2}J_{CF}$- and $^{3}J_{CF}$-coupling to distinguishable peaks in the ^{13}C NMR spectrum, i.e. C13, C14, and C17 *vide infra*. Stereochemical assignment was made on the basis of 1) a larger $^{3}J_{HH}$-coupling constant assigned to the triplet (8.7 Hz) than the doublet (2.2 Hz) in the ^{1}H

NMR spectrum, indicative of two protons *trans* to the C15 proton and 2) analogy to X-ray crystal structure of compound 12.

White solid; m.p. 107-109 °C. ^{1}H NMR (400 MHz, $CDCl_3$): 4.75 (1H, dtd, J = 55.1, 8.7, 2.2 Hz), 3.86-3.78 (1H, m), 2.56 (1H, t, J = 11.2 Hz), 2.37 (1H, t, J = 13.3 Hz), 2.17-2.03 (3H, m), 1.98-1.68 (7H, m), 1.63-1.42 (5H, m), 1.38-1.12 (8H, m), 1.11 (3H, s), 1.08- 1.01 (2H, m), 0.91 (3H, d, J = 6.6 Hz), 0.86 (3H, d, J = 6.7 Hz), 0.85 (3H, d, J = 6.6 Hz), 0.68 (3H, s); ^{13}C{^{1}H} NMR (100 MHz, $CDCl_3$): 209.1, 95.2 (d, J = 180.2 Hz, C15), 58.4, 54.9, 54.3 (d, J = 16.6 Hz, C14), 52.6, 48.8, 47.9, 45.7, 44.0 (d, J = 5.9 Hz, C13), 39.4, 39.1, 38.6, 37.7, 37.5 (d, J = 24.7 Hz, C16), 36.0, 35.9, 34.9, 32.6, 28.0, 23.7, 22.8, 22.5, 21.4, 18.5, 13.2, 11.7; ^{19}F NMR (282 MHz, $CDCl_3$): -168.7 (1F, dm, J = 55.1 Hz); υ_{max} (ATR-IR): 1717 cm^{-1}; HRMS (ESI) m/z $C_{27}H_{44}ClFONa^{+}$: calc 461.295670, observed 461.295693.

Table 3. Compound 11.

The reaction was run according to the general procedure, and the major diastereomer was isolated. Regiochemical assignment was made on the basis of 1) chemical shift in the ^{19}F NMR spectrum that indicates a secondary fluoride, 2) $^{2}J_{HF}$- coupling in the ^{1}H and ^{19}F NMR spectra that indicates cyclopentane ring fluorination (>50 Hz), and 3) identification of $^{2}J_{CF}$- and $^{3}J_{CF}$-coupling to distinguishable peaks in the ^{13}C NMR spectrum, i.e. C13, C14, and C17 *vide infra*. Stereochemical assignment was made on the basis of 1) a larger $^{3}J_{HH}$-coupling constant assigned to the triplet (8.9 Hz) than the doublet (3.0 Hz) in the ^{1}H NMR spectrum, indicative of two protons *trans* to the C15 proton and 2) analogy to X-ray crystal structure of compound **12**.

White solid; m.p. 159-160.5 °C. ^{1}H NMR (400 MHz, $CDCl_3$): 4.87 (1H, t, *J* = 8.9 Hz), 4.86 (1H, dtd, *J* = 53.9, 8.9, 3.0 Hz), 4.71-4.63 (1H, m), 2.58 (1H, t, *J* = 11.2 Hz), 2.48- 2.34 (1H, m), 2.36 (1H, t, *J* = 13.3 Hz), 2.17-2.06 (2H, m), 2.04 (3H, s), 2.02 (3H, s), 1.93-1.76 (3H, m), 1.71-1.39 (7H, m), 1.29-1.17 (2H, m), 1.13-1.05 (1H, m), 1.10 (3H, s), 0.79 (3H, s); ^{13}C{^{1}H} NMR (100 MHz, $CDCl_3$): 208.5, 170.7, 170.4, 93.0 (d, *J* = 184.3 Hz, C15), 78.3 (d, *J* = 2.6 Hz, C17), 72.5, 54.6, 49.9 (d, *J* = 18.1 Hz, C14), 48.6, 45.8, 45.6, 44.1 (d, *J* = 5.2 Hz, C13), 36.8, 36.6, 36.0, 35.8, 35.7, 33.7, 27.0, 21.3, 21.1, 21.0, 13.5, 11.7; ^{19}F NMR (282 MHz, $CDCl_3$): -167.6 (1F, dm, *J* = 53.3 Hz); υ_{max} (ATR- IR): 1735 (br), 1717 cm^{-1}; HRMS (ESI) m/z $C_{23}H_{35}FO_5Na^+$: calc 431.221209, observed 431.220332.

Table 3. Compound 12.

The reaction was run according to the general procedure, and both diastereomers were isolated. Regiochemical assignment was made on the basis of 1) chemical shift in the ^{19}F NMR spectrum that indicates a secondary fluoride, 2) $^{2}J_{HF}$- coupling in the ^{1}H and ^{19}F NMR spectra that indicates cyclopentane ring fluorination (>50 Hz), and 3) identification of $^{2}J_{CF}$- and $^{3}J_{CF}$-coupling to distinguishable peaks in the ^{13}C NMR spectrum, i.e. C8, C13, C14, C16, and C17 *vide infra*. Stereochemical assignment for the major diastereomer was made on the basis of X-ray crystallography. Stereochemical assignment for the minor diastereomer was made on the basis of X-ray crystallography.

(*Major Diastereomer*) White solid; m.p. 154-155 °C. ^{1}H NMR (400 MHz, $CDCl_3$): 4.94-4.64 (3H, m), 2.56 (1H, t, *J* = 11.3 Hz), 2.37 (1H, t, *J* = 13.1 Hz), 2.17-2.11 (1H, m), 2.04 (3H, s), 2.02 (3H, s), 1.99-1.38 (14H, m), 1.37-1.22 (2H, m), 1.18 (3H, d, *J* = 6.1 Hz), 1.10 (3H, s), 0.68 (3H, s); ^{13}C{^{1}H} NMR (100 MHz, $CDCl_3$): 208.9, 170.4, 170.2, 94.4 (d, *J* =

181.7 Hz, C15), 72.5, 71.5 (d, *J* = 1.5 Hz, C17), 54.8, 54.0 (d, *J* = 17.3 Hz, C14), 51.6, 51.5, 48.5, 45.9, 45.7, 43.5 (d, *J* = 5.9 Hz, C13), 38.1, 35.9 (d, *J* = 23.6 Hz, C16), 35.1, 34.8, 33.7, 27.1, 21.5, 21.4, 19.8, 13.6, 11.6; ^{19}F NMR (282 MHz, $CDCl_3$): -167.4 (1F, dm, *J* = 55.1 Hz); υ_{max} (ATR-IR): 1729, 1708 cm^{-1}; HRMS (ESI) m/z $C_{25}H_{37}FO_5Na^+$: calc 459.251724, observed 459.252169.

(*Minor Diastereomer*) White solid; m.p. 170-171 °C. ^{1}H NMR (400 MHz, $CDCl_3$): 5.56 (1H, dm, *J* = 55.9 Hz), 5.02-4.92 (1H, m), 4.75-4.64 (1H, m), 2.74 (1H, t, *J* = 11.6 Hz), 2.42 (1H, t, *J* = 12.6 Hz), 2.39-2.22 (1H, m), 2.12-2.07 (1H, m), 2.04 (3H, s), 2.03 (3H, s), 1.97-1.87 (1H, m), 1.85-1.77 (2H, m), 1.73-1.41 (9H, m), 1.36-1.27 (1H, m), 1.23- 1.17 (1H, m), 1.19 (3H, d, *J* = 6.1 Hz), 1.13 (3H, s), 1.10-1.04 (1H, m), 0.85 (3H, d, *J* = 2.1 Hz); ^{13}C{^{1}H} NMR (100 MHz, $CDCl_3$): 210.6, 170.5, 170.2, 93.3 (d, *J* = 176.9, C15), 72.6, 72.0, 55.0, 54.0, 53.3 (d, *J* = 20.3 Hz, C14), 46.4, 45.5, 44.9 (d, *J* = 3.7 Hz, C13), 41.9 (d, *J* = 1.8 Hz, C8), 39.1, 36.0, 35.7, 35.6 (d, *J* = 21.0 Hz, C16), 33.8, 27.0, 21.6, 21.4, 21.3, 19.8, 14.4 (d, *J* = 4.4 Hz, C18), 11.6; ^{19}F NMR (282 MHz, $CDCl_3$): -179.1 (1F, dddd, *J* = 57.9, 38.4, 37.3, 20.7 Hz).

Table 3. Compound 13.

The reaction was run according to the general procedure, and the major diastereomer was isolated. Regiochemical assignment was made on the basis of 1) chemical shift in the ^{19}F NMR spectrum that indicates a secondary fluoride on a cyclohexane ring and 2) identification of $^2J_{CF}$- and $^3J_{CF}$-coupling to distinguishable peaks in the ^{13}C NMR spectrum, i.e. C2, C3, C5, and C10 *vide infra*. Stereochemical assignment was made on the basis of 1) chemical shift and splitting in the ^{19}F NMR spectrum that indicates F_{eq} on a cyclohexane

ring and 2) identification of the two distinct *trans* diaxial $^{3}J_{HH}$-coupling constants (t, 10.8 Hz) in the ^{1}H NMR spectrum.

White solid; m.p. 189-192 °C. ^{1}H NMR (400 MHz, $CDCl_3$): 4.94 (1H, dtd, J = 48.2, 10.8, 5.5 Hz), 4.64 (1H, dd, J = 9.2, 7.8 Hz), 2.38 (1H, t, J = 10.0 Hz), 2.34 (1H, dd, J = 12.3, 4.5 Hz), 2.23-2.13 (2H, m), 2.07 (1H, t, J = 12.2 Hz), 2.04 (3H, s), 1.90-1.58 (6H, m), 1.55-1.14 (9H, m), 0.78 (3H, s), 0.73 (3H, s); ^{13}C{^{1}H} NMR (100 MHz, $CDCl_3$): 208.4, 171.1, 86.8 (d, J = 170.6 Hz, C4), 82.2, 63.4 (d, J = 15.8 Hz, C5), 54.4, 51.1, 46.7, 44.7 (d, J = 7.0 Hz, C10), 43.1, 38.6, 36.9 (d, J = 2.2 Hz, C1), 36.4, 31.5 (d, J = 18.8 Hz, C3), 27.3, 23.2, 21.1, 20.8, 19.3 (d, J = 12.2 Hz, C2), 14.0, 12.0; ^{19}F NMR (282 MHz, $CDCl_3$): -176.8 (1F, dm, J = 47.6 Hz); υ_{max} (ATR-IR): 1736, 1716 cm^{-1}; HRMS (ESI) m/z $C_{21}H_{31}FO_3Na^{+}$: calc 373.214944, observed 373.215192.

Table 3. Compound 14.

The reaction was run according to the general procedure, and both diastereomers were isolated. Regiochemical assignment was made on the basis of 1) chemical shift in the ^{19}F NMR spectrum that indicates a secondary fluoride on a cyclohexane ring, 2) identification of $^{4}J_{HF}$-coupling to the distinguishable C18 Me hydrogen atoms in the ^{1}H NMR spectrum, and 3) identification of $^{2}J_{CF}$- and $^{3}J_{CF}$-coupling to distinguishable peaks in the ^{13}C NMR spectrum, i.e. C11, C13, C17a, and C18 *vide infra*. Stereochemical assignment for the major diastereomer was made on the basis of 1) chemical shift and splitting in the ^{19}F NMR spectrum that indicates F_{ax} on a cyclohexane ring and 2) identification of the distinct *trans* diaxial $^{3}J_{FH}$-coupling constant (46.5 Hz) in the ^{19}F NMR spectrum. Stereochemical assignment for the minor diastereomer was made on the basis of 1) chemical shift, splitting,

and two "gauche" $^{3}J_{FH}$-coupling constants (t, 8.0 Hz) in the ^{19}F NMR spectrum that indicates F_{eq} on a cyclohexane ring and 2)

identification of the distinct *trans* diaxial $^{3}J_{HH}$-coupling constant (11.7 Hz) in the ^{1}H NMR spectrum.

(*Major Diastereomer*) White solid; m.p. 130-132 °C. ^{1}H NMR (400 MHz, $CDCl_3$): 5.08 (1H, dm, J = 47.1 Hz), 4.72-4.64 (1H, m), 2.50-2.41 (1H, m), 2.36-2.30 (1H, m), 2.01 (3H, s), 2.00-1.79 (6H, m), 1.73-1.61 (3H, m), 1.56-1.16 (9H, m), 1.10-1.02 (1H, m), 1.00 (3H, d, J = 1.1 Hz), 0.98-0.86 (1H, m), 0.81 (3H, s); ^{13}C{^{1}H} NMR (100 MHz, $CDCl_3$): 212.4, 170.6, 91.2 (d, J = 172.9 Hz, C12), 73.4, 51.4 (d, J = 18.4 Hz, C13), 46.5, 44.0, 42.1 (d, J = 1.5 Hz), 37.1, 36.1, 35.2, 34.5, 33.8, 30.7, 28.4, 27.2, 25.5 (d, J = 21.4 Hz, C11), 23.1, 21.8, 21.4, 16.4 (d, J = 7.0 Hz, C18), 11.9; ^{19}F NMR (282 MHz, $CDCl_3$): -184.7 (1F, td, J = 46.5, 10.3 Hz); υ_{max} (ATR-IR): 1732, 1712 cm^{-1}; HRMS (ESI) m/z $C_{22}H_{33}FO_3Na^{+}$: calc 387.230594, observed 387.230475.

(*Minor Diastereomer*) Viscous oil. ^{1}H NMR (400 MHz, $CDCl_3$): 4.91 (1H, ddd, J = 46.8, 11.7, 5.3 Hz), 4.71-4.63 (1H, m), 2.76-2.67 (1H, m), 2.22-2.18 (1H, m), 2.13-2.07 (1H, m), 2.05-1.96 (1H, m), 2.02 (3H, s), 1.87-1.79 (3H, m), 1.75 (1H, dt, J = 13.0, 3.5 Hz), 1.67-1.61 (1H, m), 1.58-1.22 (8H, m), 1.21 (3H, d, J = 1.3 Hz), 1.17-1.08 (2H, m), 1.06-0.98 (1H, m), 0.90-0.73 (2H, m), 0.83 (3H, s); ^{13}C{^{1}H} NMR (100 MHz, $CDCl_3$): 213.3 (d, J = 0.7 Hz, C17a), 170.6, 91.5 (d, J = 179.0 Hz, C12), 73.3, 53.1 (d, J = 15.5 Hz, C13), 50.8 (d, J = 4.1 Hz), 50.2 (d, J = 10.3 Hz), 43.9, 37.3, 36.4, 35.5 (d, J = 1.1 Hz), 34.3 (d, J = 1.5 Hz), 33.7, 30.9, 28.2, 27.3, 26.8, 26.7 (d, J = 18.4 Hz), 22.4 (d, J = 2.6 Hz), 21.4, 12.1, 11.1 (d, J = 5.2 Hz, C18); ^{19}F NMR (282 MHz, $CDCl_3$): -179.8 (1F, dt, J = 46.5, 8.0 Hz).

Table 3. Compound 15.

The reaction was run according to the general procedure, and the major diastereomer was isolated. Regiochemical assignment was made on the basis of 1) chemical shift in the ^{19}F NMR spectrum that indicates a secondary fluoride on a cyclohexane ring and 2) identification of $^{2}J_{CF}$- and $^{3}J_{CF}$-coupling to distinguishable peaks in the ^{13}C NMR spectrum, i.e. C11, C13, and C18 *vide infra*. Stereochemical assignment was made on the basis of 1) chemical shift and splitting in the ^{19}F NMR spectrum that indicates F_{ax} on a cyclohexane ring and 2) identification of the distinct *trans* diaxial $^{3}J_{FH}$- coupling constant (47.6 Hz) in the ^{19}F NMR spectrum.

White solid; m.p. 146-147 °C. ^{1}H NMR (400 MHz, $CDCl_3$): 7.79 (2H, dm, J = 8.3 Hz), 7.33 (2H, dm, J = 8.6 Hz), 4.87 (1H, dm, J = 49.4 Hz), 4.39 (1H, m), 2.46-2.36 (1H, m), 2.44 (3H, s), 2.18-2.06 (1H, m), 2.02-0.83 (18H, m), 0.81-0.79 (6H, m); $^{13}C\{^{1}H\}$ NMR (100 MHz, $CDCl_3$): 216.4, 144.4, 134.6, 129.7, 127.6, 90.3 (d, J = 173.6 Hz, C12), 81.8, 51.4 (d, J = 20.3 Hz, C13), 48.3, 44.7, 43.8, 36.4, 36.3, 35.0, 34.8, 34.4, 30.4, 28.1, 28.0, 26.4 (d, J = 21.8 Hz, C11), 21.6, 21.0, 13.3 (d, J = 7.4 Hz, C18), 11.9; ^{19}F NMR (282 MHz, $CDCl_3$): -187.5 (1F, td, J = 47.6, 11.5 Hz); υ_{max} (ATR-IR): 1743 cm^{-1}; HRMS (ESI) m/z $C_{26}H_{35}FO_4SNa^{+}$: calc 485.213230, observed 485.212970.

Table 3. Compound 16.

The reaction was run according to the general procedure, and the major diastereomer was isolated. Regiochemical assignment was made on the basis of 1) chemical shift in the ^{19}F NMR spectrum that indicates a secondary fluoride on a cyclohexane ring and 2) identification of $^{2}J_{CF}$- and $^{3}J_{CF}$-coupling to distinguishable peaks in the ^{13}C NMR spectrum,

i.e. C11, C13, and C18 *vide infra*. Stereochemical assignment was made on the basis of 1) chemical shift and splitting in the ^{19}F NMR spectrum that indicates F_{ax} on a cyclohexane ring and 2) identification of a *trans* diaxial $^{3}J_{FH}$-coupling constant in the ^{19}F NMR spectrum.

Viscous oil. ^{1}H NMR (400 MHz, $CDCl_3$): 4.94 (1H, dm, J = 48.1 Hz), 3.66 (3H, s), 2.62-2.44 (2H, m), 2.40-2.27 (2H, m), 2.25-1.98 (7H, m), 1.92-1.85 (1H, m), 1.80-1.53 (4H, m), 1.43-1.31 (1H, m), 1.13 (3H, s), 0.90 (3H, d, J = 0.9 Hz); $^{13}C\{^{1}H\}$ NMR (100 MHz, $CDCl_3$): 215.4 (d, J = 1.1 Hz), 212.9, 174.0, 89.6 (d, J = 175.1 Hz), 51.6, 51.3 (d, J = 19.9 Hz), 49.9, 43.3 (d, J = 1.5 Hz), 42.1, 37.6, 36.2, 34.0, 29.6, 29.3, 28.9, 26.6 (d, J = 22.1 Hz), 21.1, 20.3, 13.4 (d, J = 7.4 Hz); ^{19}F NMR (282 MHz, $CDCl_3$): -186.5 (1F, m); υ_{max} (ATR-IR): 1739, 1733, 1706 cm^{-1}; HRMS (ESI) m/z $C_{19}H_{27}FO_4Na^{+}$: calc 361.178559, observed 361.178146.

Scheme 1. Compound 17 and 18.

The reaction was run according to the general procedure, and the product was isolated as a mixture of regioisomers. Regio- and stereochemical assignments were confirmed by X-ray crystallography.

^{1}H NMR (400 MHz, $CDCl_3$): 5.74 (1H, s), 5.66-4.81 (1H, m), 3.10-2.72 (1H, m), 2.47-2.24 (4H, m), 2.20-2.14 (3H, m), 2.10-1.52 (10H, m), 1.50-1.23 (2H, m), 1.17 (3H, s), 1.15-1.02 (1H, m), 0.71-0.64 (3H, m); $^{13}C\{^{1}H\}$ NMR (100 MHz, $CDCl_3$): 209.4, 206.8, 199.6, 199.5, 170.6, 170.3, 124.54, 124.47, 95.1 (d, J = 175.8 Hz), 92.8 (d, J = 176.2 Hz), 71.5, 71.3, 55.30, 55.26, 53.70, 53.69, 48.2, 47.8, 47.3, 47.1, 45.3, 45.2, 38.9, 38.8, 38.3,

35.9, 35.8, 35.5, 35.2, 34.2, 34.1, 33.7, 33.5, 32.94, 32.89, 32.0, 31.9, 31.8, 31.3, 26.9, 26.7, 23.8, 22.6, 21.0, 17.6, 17.5, 14.8, 13.22, 13.16; ^{19}F NMR (282 MHz, $CDCl_3$): -172.0 (1F, dm, J = 53.3 Hz), -192.2 (1F, ddd, J = 48.2, 47.0, 12.1 Hz).

9.3 Experimental Details for Chapter 3.

General Ammoniofluorination Procedure. Selectfluor (354 mg, 1.0 mmol) was added to an oven-dried microwave vial equipped with a stir bar; the vial was then sealed with a cap with Teflon septum using a crimper and evacuated/refilled with N_2 multiple times. Anhydrous CH_3CN (8 mL) was added, followed by the alkene substrate (0.50 mmol) (if the substrate is a solid, it is added along with Selectfluor before sealing the vial) and then cyclohexenone (0.048 mL, 0.50 mmol). The reaction mixture was irradiated with 300 nm light while stirring. After 12 h, a 0.3 mL aliquot was taken for ^{19}F NMR yield determination. The rest of the reaction mixture was either subjected to the reduction (see below) or triturated with solvent to isolate the ammonium salt product. Note: We found it difficult to separate the Selectfluor-adduct products from the excess Selectfluor and Selectfluor byproducts, which are all cationic species. This is not a significant issue, as the Selectfluor-adducts are more typically reduced to piperazines before isolation, at which point separation from the Selectfluor byproducts is straightforward. However, if there is a desire to isolate the fluorinated Selectfluor-adduct, a typical procedure is as follows: The reaction mixture was diluted with a mixture of 1:1 hexanes/EtOAc (25 mL), causing the product to precipitate out of solution along with the Selectfluor byproducts. The solid precipitate/ oil was collected and washed with diethyl ether (25 mL × 3) to remove the nonpolar impurities (cyclohexenone and alkene starting material). The product can then be

further purified by recrystalliza- tion from EtOH and/or trituration (the adduct is dissolved using a 40:60 mixture of ACN−DCM (25 mL × 2), filtered, and concentrated to dryness. Figure S25 provides a labeled ^{1}H NMR to point out peaks derived from Selectfluor impurities.

General Procedure for the One-Pot Reduction of Selectfluor-Adducts. The following procedure was adopted from a previously reported method. After the aminofluorination reaction has completed (0.50 mmol scale, see above), a solution of saturated aq $Na_2S_2O_3$ (5.0 mL) was added to the microwave vial, followed by H_2O (5.0 mL) (for larger scale reactions, the reaction mixture was transferred to a pressure tube to accommodate the larger volume). The mixture was stirred in the sealed vial at 100 °C for 12−24 h. Upon cooling to room temperature, the reaction mixture was transferred to a separatory funnel and diluted with DCM (10 mL). Ethylene diamine (0.9 mL) was added, followed by 6 M NaOH (2.9 mL), and the mixture was shaken. The resulting emulsion was treated with brine (50 mL), and after shaking, the organic layer was separated. The aqueous layer was re-extracted with DCM (2 × 10 mL), and then the combined organic layers were extracted with 1 M HCl (2 × 10 mL). Ethylene diamine (2.9 mL) was added to the combined HCl extracts, followed by 6 M NaOH (4.7 mL). The basicified aqueous mixture was then extracted with DCM (3 × 10 mL), and the combined organic layers were dried with $MgSO_4$, filtered, and concentrated. The crude residue was used directly in the next step or purified on basic alumina, eluting with EtOAc/hexanes.

General Procedure for the Acylation of Fluoropiperazines. The piperazine (0.50 mmol) was dissolved in dichloromethane (5.0 mL) in a round-bottom flask equipped with a stir bar under N_2. The reaction mixture was cooled to 0 °C and treated with triethylamine (0.14 mL, 1.0 mmol) followed by benzyl chloroformate (0.108 mL, 0.75 mmol). The reaction was stirred overnight at room temperature under N_2 and then was diluted with DCM (50 mL) and transferred to a separatory funnel. The organic mixture was washed with saturated sodium bicarbonate (25 mL), then brine (25 mL), and then dried with $MgSO_4$ and concentrated. The crude residue was purified via column chromatography on basic alumina with EtOAc/hexanes to provide the Cbz-piperazine.

General Fluorination Procedure for Compounds 18−20. Selectfluor (354 mg, 1.0 mmol) and the alkene substrate (0.50 mmol) were added to an oven-dried microwave vial equipped with a stir bar. The vial was then sealed with a cap with a Teflon septum using a crimper and evacuated/refilled with N_2 multiple times. Anhydrous CH_3CN (8 mL) was added, and the reaction mixture was stirred at either room temperature (compound 18) or at 80 °C (compounds 19 and 20). After 12 h, a 0.3 mL aliquot was taken for ^{19}F NMR yield determination. The reaction mixture was transferred to a separatory funnel, diluted with water (50 mL), and extracted with DCM (3 × 25 mL). The combined organic layers were washed with brine, dried with $MgSO_4$, and concentrated. The crude residue was purified via column chromatography on silica gel with EtOAc/hexanes.

Characterization of Fluorinated Compounds.

Benzyl 4-(2- Fluoro-3,3-dimethylbutyl)piperazine-1-carboxylate (14)

Fluorination was run according to the general aminofluorination procedure, and the product was isolated via gradient column chromatography on basic alumina gel eluting with 15% EtOAc/hexanes.

Yellow oil (85 mg, 53% over 3 steps). ^{1}H NMR (400 MHz, $CDCl_3$): δ 7.39−7.29 (5H, m), 5.13 (2H, s), 4.37−4.22 (1H, m), 3.55−3.53 (4H, m), 2.63−2.48 (6H, m), 0.94 (9H, d, J = 1.27 Hz); $^{13}C\{^{1}H\}$ NMR (100 MHz, $CDCl_3$): δ 155.2, 136.7, 128.5, 128.0, 127.9, 98.6 (d, J = 175.81 Hz), 67.1, 58.7 (d, J = 21.75 Hz), 53.3, 43.8−43.6 (m), 34.1 (d, J = 19.53 Hz), 25.3 (d, J = 4.79 Hz); ^{19}F NMR (282 MHz, $CDCl_3$): δ −184.0 to (−184.4) (1F, m); HRMS (ESI-Orbitrap) m/z: $[M + H]^+$ Calcd for $C_{18}H_{28}O_2N_2F^+$323.2134; Found 323.2123.

Benzyl 4-(2-Fluoro-3-phenylpropyl)piperazine-1-carboxylate (15)

Fluorination was run according to the general aminofluorination procedure, and the product was isolated via gradient column chromatography on basic alumina gel eluting with 15% EtOAc/ hexanes.

Yellow oil (98 mg, 55% over 3 steps). ^{1}H NMR (400 MHz, $CDCl_3$): δ 7.37−7.29 (8H, m), 7.24−7.21 (2H, m), 5.13 (2H, s), 5.02−4.84 (1H, m), 3.56−3.54 (4H, m), 3.01−2.93 (2H, m), 2.65− 2.49 (6H, m); $^{13}C\{^{1}H\}$ NMR (100 MHz, $CDCl_3$): δ 155.1, 136.6, 136.6−136.5 (m), 129.3, 128.5, 128.5, 128.0, 127.9, 126.7, 92.4 (d, J = 173.13 Hz), 67.1, 61.1 (d, J = 21.27 Hz), 53.3, 43.6−43.4 (m), 39.6 (d, J = 21.27 Hz); ^{19}F NMR (282 MHz, $CDCl_3$): δ −177.4 to (−177.9) (1F, m); HRMS (ESI-Orbitrap) m/z: $[M + H]^+$ Calcd for $C_{21}H_{26}O_2N_2F^+$ 357.1978; Found 357.1964.

1-(2-Fluoro-3-phenylpropyl)piperazine (15b)

Fluorination was run according to the general aminofluorination procedure, and the product was isolated via gradient column chromatography on basic alumina gel eluting with 60% EtOAc/hexanes.

Yellow oil (93 mg, 84% over 2 steps). ^{1}H NMR (400 MHz, $CDCl_3$): δ 7.32−7.28 (2H, m), 7.25−7.21 (3H, m), 4.97−4.79 (1H, m), 3.00−2.97 (1H, m), 2.95− 2.89 (4H, m), 2.64−2.45 (7H, m); $^{13}C\{^{1}H\}$ NMR (100 MHz, $CDCl_3$): δ 136.9 (d, J = 4.77 Hz), 129.3, 128.4, 126.5, 92.6 (d, J = 173.13 Hz), 61.9 (d, J = 21.27 Hz), 54.6 (d, J = 1.10 Hz), 45.8, 39.7 (d, J = 21.27 Hz); ^{19}F NMR (282 MHz, $CDCl_3$): δ −177.6 to (−178.1) (1F, m); HRMS (ESI-Orbitrap) m/z: $[M + H]^+$ Calcd for $C_{13}H_{20}N_2F^+$ 223.1610; Found 223.1595.

Benzyl 4-(2-Fluoro-5-oxohexyl)piperazine-1-carboxylate (16)

Fluorination was run according to the general aminofluorination procedure, and the product was isolated via gradient column chromatography on basic alumina gel eluting with 20% EtOAc/ hexanes.

Yellow oil (71 mg, 42% over 3 steps). ^{1}H NMR (400 MHz, $CDCl_3$): δ 7.38−7.30 (5H, m), 5.13 (2H, s), 4.77−4.59 (1H, m), 3.54−3.52 (4H, m), 2.68−2.49 (8H, m), 2.16 (3H, s), 2.01−1.77 (2H, m); $^{13}C\{^{1}H\}$ NMR (100 MHz, $CDCl_3$): δ 207.7, 155.2, 136.7, 128.5, 128.0, 127.9, 91.4 (d, J = 169.83 Hz), 67.1, 62.2 (d, J = 21.27 Hz), 53.4, 43.7−43.6 (m), 38.6 (d, J = 3.67 Hz), 30.0, 27.2 (d, J = 20.91 Hz); ^{19}F NMR (282 MHz, $CDCl_3$): δ −182.5 to (−183.1) (1F, m); HRMS (ESI-Orbitrap) m/z: $[M + H]^+$ Calcd for $C_{18}H_{26}O_3N_2F^+$ 337.1927; Found 337.1914.

Benzyl 4-(6-(Diethylamino)-2-fluoro-6-oxohexyl)piperazine-1-carboxylate (17)

Fluorination was run according to the general aminofluorination procedure, and the product was isolated via gradient column chromatography on basic alumina gel eluting with 30% EtOAc/hexanes.

Yellow oil (67 mg, 33% over steps). ^{1}H NMR (400 MHz, CDCl): δ 7.36−7.30 (5H, m), 5.12 (2H, s), 4.79−4.61 3 (1H, m), 3.54−3.51 (4H, m), 3.38−3.26 (4H, m), 2.69−2.45 (6H, m), 2.33 (2H, t, J = 7.04 Hz), 1.82−1.61 (4H, m), 1.18−1.08 (6H, m); ^{13}C{^{1}H} NMR (100 MHz, CDCl3): δ 171.4, 155.1, 136.6, 128.4, 128.0, 127.8, 92.2 (d, J = 169.46 Hz), 67.1, 62.2 (d, J = 20.54 Hz), 53.3, 43.7−43.6 (m), 41.8, 40.1, 33.0 (d, J = 20.91 Hz), 32.4, 20.8 (d, J = 4.77 Hz), 14.3, 13.1; ^{19}F NMR (282 MHz, CDCl): δ −179.7 to (−180.2) (1F, m); HRMS (ESI-Orbitrap) m/z: [M + H] Calcd for C H O N F^{+} 408.2662; Found 408.2652.

Fluoride 18

Fluorination was run according to the general fluorination procedure for compounds 18−20, and the product was isolated via gradient column chromatography on silica gel eluting with a 96:2.5:1.5 mixture of DCM−MeOH−AcOH.

White solid (157 mg, 86%). Mp = 242−243 °C. ^{1}H NMR (400 MHz, CD CN): δ 6.43−6.40 (1H, m), 5.88−5.85 (1H, m), 4.62−4.07 (2H, m), 4.06 (1H, d, J = 3.52 Hz), 3.19 (1H, d, J = 7.24 Hz), 2.79 (1H, d, J = 7.24 Hz), 2.75−2.69 (1H, m), 2.28−2.21 (4H, m), 1.83−1.78 (1H, m), 1.53− 1.44 (3H, m), 1.23 (3H, s); ^{13}C{^{1}H} NMR (100 MHz, CD3CN): δ 215.5 (d, J = 3.32 Hz), 179.6, 174.0, 134.4, 131.4, 90.3, 84.6 (d, J = 167.33 Hz), 71.0, 56.4, 56.1, 53.4, 51.8, 51.1 (d, J = 1.11 Hz), 49.9, 49.7, 42.4 (d, J = 2.95 Hz), 29.8 (d, J = 6.27 Hz),

19.1 (d, J = 1.11 Hz), 14.7; ^{19}F NMR (282 MHz, CD_3CN): δ −229.7 (1F, t, J = 47.61 Hz); HRMS (ESI-Orbitrap) m/z: $[M + H]^+$ Calcd for $C_{19}H_{22}O_6F$ 365.1400; Found 365.1389.

Fluoride 19 (Major Diastereomer)

Fluorination was run according to the general fluorination procedure for compounds 18−20, and the product was isolated via gradient column chromatography on silica gel eluting with 10−15% EtOAc/hexanes.

White solid (117 mg, 51%). Mp = 257−258 °C. ^{1}H NMR (400 MHz, $CDCl_3$): δ 4.45−3.92 (2H, m), 3.84−3.78 (2H, m), 3.43 (1H, d, J = 7.92 Hz), 3.23−3.17 (1H, m), 1.75−1.69 (1H, m), 1.67−1.09 (23H, m), 0.97 (6H, s), 0.92 (6H, s), 0.84 (3H, s), 0.76 (3H, s), 0.72−0.68 (1H, m); $^{13}C\{^1H\}$ NMR (100 MHz, $CDCl_3$): δ 89.7 (d, J = 171.29 Hz), 82.0 (d, J = 3.67 Hz), 78.9, 71.4, 55.5, 51.1, 46.6, 41.7, 40.7, 40.6, 40.5, 38.9, 38.8, 37.3, 35.8, (d, J = 1.47 Hz), 34.1, 33.9, 28.0, 27.4, 26.5, 26.4, 26.3, 26.2, 20.9, 19.2 (d, J = 4.40 Hz), 18.2, 16.5, 15.7, 15.4, 13.5; ^{19}F NMR (282 MHz, $CDCl_3$): δ −229.6 (1F, t, J = 48.18 Hz); HRMS (ESI-Orbitrap) m/z: $[M + H]^+$ Calcd for $C_{30}H_{50}O_2F^+$ 461.3794; Found 461.3785.

Fluoride 20 (Major Diastereomer)

Fluorination was run according to the general fluorination procedure for compounds 18−20, and the product was isolated via gradient column chromatography on silica gel eluting with 10−15% EtOAc/hexanes.

White solid (187 mg, 79%). Mp = 215−217 °C. ^{1}H NMR (400 MHz, $CDCl_3$): δ 4.63−4.50(1H, m), 3.24−3.20 (1H, m), 2.18−2.06 (2H, m), 2.02−1.80 (4H, m), 1.75−1.53

(10H, m), 1.44−1.19 (10H, m), 1.11 (3H, s), 0.99 (6H, s), 0.90 (3H, s), 0.87 (3H, s), 0.78 (3H, s), 0.75−0.72 (1H, m); $^{13}C\{^{1}H\}$ NMR (100 MHz, $CDCl_3$): δ 179.3, 96.7 (d, J = 171.38 Hz), 88.0 (d, J = 25.80 Hz), 78.7, 55.0, 50.9, 44.6, 44.3, 41.9, 41.7, 38.9, 38.5, 36.4, 34.1, 33.5, 33.2, 31.5, 27.9, 27.4 (d, J = 10.32 Hz), 27.1, 25.8, 25.6, 23.7, 21.0, 18.3, 17.9 (d, J = 8.11 Hz), 17.6, 16.0, 15.3; ^{19}F NMR (282 MHz, $CDCl_3$): δ −179.3 to (−179.7) (1F, m); HRMS (ESI- Orbitrap) m/z: $[M + H]^+$ Calcd for $C_{30}H_{48}O_3F^+$ 475.3587; Found 475.3578.

Characterization of Selectfluor-Adducts.

Fluoride 1

Off-white solid (hygroscopic, quickly turning into an oil) (222 mg, 98%). ^{1}H NMR (400 MHz, CD_3CN): δ 5.06−4.83 (3H, m), 3.80−3.67 (14H, m), 1.47−1.34 (2H, m), 1.22−1.05 (3H, m), 0.72−0.67 (6H, m); $^{13}C\{^{1}H\}$ NMR (100 MHz, CD_3CN): δ 88.3 (d, J = 171.66 Hz), 69.6, 68.4−68.1 (m), 52.5−52.4 (m), 51.0, 33.4−33.3 (d, J = 4.03 Hz), 30.7−30.5 (m), 28.1, 22.4−22.2 (d, J = 15.41 Hz); ^{19}F NMR (282 MHz, CD_3CN): δ −181.2 to (−181.8) (1F, m); HRMS (ESI-Orbitrap) m/z: $[M - BF_4^-]^+$ Calcd for $C_{14}H_{28}N_2BClF_5^+$ 365.1954; Found 365.1940.

Fluoride 2

Off-white solid (214 mg, 92%). ^{1}H NMR (400 MHz, CD_3CN): δ 5.29−5.07 (3H, m), 4.06−3.80 (14H, m), 1.80−1.51 (3H, m), 1.43−1.26 (7H, m), 0.91 (3H, t, J = 6.85 Hz); $^{13}C\{^{1}H\}$ NMR (100 MHz, CD_3CN): δ 88.2 (d, J = 171.02 Hz), 69.8, 68.5−68.3 (m),

52.7−52.6 (m), 51.1, 32.9−32.6 (m), 32.0, 29.2, 24.6 (d, J = 4.05 Hz), 23.0, 14.1; ^{19}F NMR (282 MHz, CD CN): δ −181.3 to −(−181.9) (1F, m); HRMS (ESI-Orbitrap) m/z: [M − BF_4] Calcd for $C_{15}H_{30}N_2BClF_5^+$ 379.2110; Found 379.2096.

Fluoride 3

Off-white solid (197 mg, 90%). ^{1}H NMR (400 MHz, CD CN): δ 5.26 (2H, s), 4.94−4.73 (1H, m), 4.11−3.90 (14H, m), 0.95 (9H, s); C{ H} NMR (100 MHz, CD_3CN): δ 93.5 (d, J = 176.80 Hz), 69.5, 66.4−66.1 (m), 52.3−52.2 (m), 50.9, 35.2−35.0 (m), 24.5 (d, J = 4.77 Hz); ^{19}F NMR (282 MHz, CD_3CN): δ −184.8 to (−185.1) (1F, m); HRMS (ESI-Orbitrap) m/z: [M − BF_4^-]$^+$

Fluoride 4

Off-white solid (217 mg, 92%). ^{1}H NMR (400 MHz, 4.00−3.88 (14H, m), 3.13−2.93 (2H, m); C{ H} NMR (100 MHz, CD_3CN): δ 135.7 (d, J = 2.94 Hz), 130.5, 129.6, 128.2, 88.4 (d, J = 174.23 Hz), 69.9, 68.1−67.9 (m), 52.8−52.7 (m), 51.2, 38.8−38.6 (m); ^{19}F NMR (282 MHz, CD CN): δ −180.6 to (−181.1) (1F, m); HRMS (ESI-Orbitrap) m/z: [M − BF_4] Calcd for $C_{16}H_{24}N_2BClF_5$ 385.1641; Found 385.1625.

Fluoride 5

Off-white solid (238 mg, 98%). ^{1}H NMR (400 MHz, CD_3CN): δ 7.35−7.28 (2H, m), 7.27−7.18 (3H, m), 5.29−5.09 (3H, m), 4.05−3.81 (14H, m), 2.87−2.65 (2H, m), 2.06−1.95 (2H, m); ^{13}C{^{1}H} NMR (100 MHz, CD_3CN): δ 141.4, 129.5, 129.3, 127.2, 87.8 (d, J =

172.49 Hz), 69.9, 68.4−68.2 (m), 52.8−52.7 (m), 51.2, 34.7−34.5 (m), 30.8 (d, J = 4.42 Hz); ^{19}F NMR (282 MHz, CD_3CN): δ −182.1 to (−182.7) (1F, m); HRMS (ESI-Orbitrap) m/ z: $[M - BF_4^-]^+$ Calcd for $C_{17}H_{26}N_2BClF_5^+$ 399.1797; Found 399.1781.

Fluoride 6

Off-white solid (250 mg, 92%). ^{1}H NMR (400 MHz, CD_3CN): δ 8.04−8.01 (2H, m), 7.65−7.60 (1H, m), 7.52−7.47 (2H, m), 5.37−5.16 (3H, m), 4.39−4.26 (2H, m), 4.04−3.80 (14H, m), 1.92−1.73 (4H, m); $^{13}C\{^1H\}$ NMR (100 MHz, CD_3CN): δ 167.1, 134.0, 131.2, 130.1, 129.5, 88.0 (d, J = 172.40 Hz), 69.9, 68.4−68.2 (m), 64.6, 52.7−52.6 (m), 51.5, 29.6−29.4 (m), 24.3 (d, J = 4.03 Hz); ^{19}F NMR (282 MHz, CD_3CN): δ −182.4 to (−183.0) (1F, m); HRMS (ESI-Orbitrap) m/z: $[M - BF_4^-]^+$ Calcd for $C_{19}H_{28}O_2N_2BClF_5^+$ 457.1852; Found 457.1839.

Fluoride 7

Off-white solid (203 mg, 90%). ^{1}H NMR (400 MHz, CD_3CN): δ 5.30−5.07 (3H, m), 4.08−3.84 (14H, m), 2.70−2.58 (2H, m), 2.54−2.19 (2H, m), 2.11 (3H, s); $^{13}C\{^1H\}$ NMR (100 MHz, CD_3CN): δ 207.9, 87.7 (d, J = 171.66 Hz), 69.9, 68.3−68.1 (m), 52.8−52.7 (m), 51.2, 37.9 (d, J = 4.03 Hz), 29.9, 27.0−26.8 (m); ^{19}F NMR (282 MHz, CD_3CN): δ −181.8 to (−182.4) (1F, m); HRMS (ESI-Orbitrap) m/z: $[M - BF_4^-]^+$ Calcd for $C_{13}H_{24}ON_2BClF_5^+$ 365.1590; Found 365.1579.

Fluoride 8

Off-white solid (208 mg, 70%). ^{1}H NMR (400 MHz, CD_3CN): δ 7.78−7.76 (2H, m), 7.45−7.43 (2H, m), 5.30−5.09 (3H, m), 4.07−3.79 (16H, m), 2.43 (3H, s), 1.81−1.62 (4H, m); $^{13}C\{^{1}H\}$ NMR (100 MHz, CD_3CN): δ 146.2, 133.3, 130.8, 128.4, 87.6 (d, J = 171.66 Hz), 70.8, 69.6, 68.0−67.8 (m), 52.6−52.5 (m), 51.0, 28.9− 28.7 (m), 24.4 (d, J = 4.03 Hz), 21.4; ^{19}F NMR (282 MHz, CD_3CN): δ −182.2 to (−182.7) (1F, m); HRMS (ESI-Orbitrap) m/z: $[M - BF_4^-]^+$ Calcd for $C_{19}H_{30}O_3N_2BClF_5S^+$ 507.1678; Found 507.1663.

Fluoride 9

Off-white solid (204 mg, 78%). ^{1}H NMR (400 MHz, CD_3CN): δ 5.31−5.16 (3H, m), 4.05−3.90 (14H, m), 3.34−3.28 (4H, m), 2.39−2.30 (2H, m), 1.78−1.57 (4H, m), 1.15−1.02 (6H, m); $^{13}C\{^{1}H\}$ NMR (100 MHz, CD_3CN): δ 172.4, 88.0 (d, J = 170.93 Hz), 69.5, 68.2−68.0 (m), 52.5−52.4 (m), 51.0, 44.8, 32.3, 20.6 (d, J = 4.40 Hz), 14.2, 13.1; ^{19}F NMR (282 MHz, CD_3CN): δ −181.1 to (−181.7) (1F, m); HRMS (ESI-Orbitrap) m/z: $[M - BF_4^-]^+$ Calcd for $C_{17}H_{33}BClF_5N_3O^+$ 436.2325; Found 436.2297.

Fluoride 10

Off-white solid (240 mg, 81%). ^{1}H NMR (400 MHz, CD_3CN): δ 7.68−7.66 (2H, m), 7.42−7.40 (2H, m), 5.43−5.21 (3H, m), 4.11−3.71 (16H, m), 3.22−2.96 (2H, m), 2.68 (3H, s), 2.41 (3H, s); $^{13}C\{^{1}H\}$ NMR (100 MHz, CD_3CN): δ 144.8, 134.4, 130.6, 128.1, 86.0 (d, J = 172.03 Hz), 69.6, 68.0−67.7 (m), 52.6−52.5 (m), 51.0, 46.1 (d, J = 5.50 Hz), 35.5,

31.0−30.8 (m), 21.2; ^{19}F NMR (282 MHz, CD_3CN): δ −182.4 to (−182.9) (1F, m); HRMS (ESI- Orbitrap) m/z: $[M - BF_4^-]^+$ Calcd for $C_{19}H_{31}O_2N_3BClF_5S^+$ 506.1838; Found 506.1820.

Fluoride 11

Off-white solid (255 mg, 92%). ^{1}H NMR (400 MHz, CD CN): δ 7.86−7.79 (4H, m), 5.31−5.12 (3H, m), 4.02−3.69 (16H, m), 2.14−1.98 (2H, m); C{ H} NMR (100 MHz, CD_3CN): δ 169.2, 135.2, 133.1, 123.8, 86.5 (d, J = 172.03 Hz), 69.9, 68.0−67.8 (m), 52.8−51.2 (m), 45.2−45.1 (m), 33.9−33.8 (d, J = 5.14 Hz), 31.9−31.6 (m); ^{19}F NMR (282 MHz, CD_3CN): δ −183.4 to (−184.0) (1F, m); HRMS (ESI-Orbitrap) m/z: $[M - BF_4^-]^+$ Calcd for $C_{19}H_{25}O_2N_3BClF_5^+$ 468.1648; Found 468.1626.

Fluoride 12

Off-white solid (200 mg, 79%). ^{1}H NMR (400 MHz, CD_3CN): δ 5.37−5.31 (0.5H, m), 5.28−5.19 (2.5H, m), 4.33−4.19 (3H, m), 4.15−3.80 (13H), 2.75 (2H, t, J = 6.02 Hz), 2.58−2.42 (4H, m); ^{13}C{^{1}H} NMR (100 MHz, CD CN): δ 172.5, 118.9, 87.4 (d, J = 3 172.39 Hz), 69.9, 68.2−68.0 (m), 60.1, 52.8−52.7 (m), 51.2, 29.2 (d, J = 4.77 Hz), 28.2−28.0 (m), 18.4; ^{19}F NMR (282 MHz, CD_3CN): δ −183.2 to (−183.7) (1F, m); HRMS (ESI-Orbitrap) m/z: $[M - BF_4^-]^+$ Calcd for $C_{15}H_{25}O_2N_3BClF_5^+$ 420.1648; Found 420.1625.

Fluoride 13 (Mixture of Diastereomers)

White solid (290 mg, 63%). ^{1}H NMR (400 MHz, CD_3CN): δ 5.51−5.44 (1H, m), 5.32−5.21 (3H, m), 4.48−4.40 (1H, m), 4.11−3.90 (16H, m), 2.76−2.64 (1H, m), 2.49−2.28 (3H, m), 2.11−2.03 (3H, m), 1.98 (3H, s), 1.802−1.53 (9H, m), 1.44−1.35 (7H, m), 1.19−1.07 (12H, m), 0.86 (6H, s), 0.79 (3H, s); $^{13}C\{^{1}H\}$ NMR (100 MHz, CD_3CN): δ 201.6, 201.1, 176.9, 176.7, 171.5, 171.2, 128.4, 128.2, 86.7 (d, J = 59.05 Hz), 84.9 (d, J = 58.32 Hz), 80.9, 69.8, 69.7, 69.6, 69.4, 62.1, 62.0, 54.9, 52.8, 52.7, 52.6, 51.6, 51.1, 51.0, 49.6, 49.1, 46.0, 45.9, 44.6, 44.6, 44.5, 44.5, 44.0, 44.0, 43.9, 41.6, 39.1, 39.1, 38.5, 38.3, 38.1, 38.0, 37.6, 37.6, 37.5, 32.9, 32.4, 32.4, 31.2, 28.7, 28.6, 28.2, 28.1, 28.0 ; ^{19}F NMR (282 MHz, CD_3CN): δ −182.9-(−183.5) (1F, m), −186.8 to (−187.4)(1F, m); HRMS (ESI-Orbitrap) m/z: $[M - BF_4^-]^+$ Calcd for $C_{43}H_{68}O_5N_2BClF_5^+$ 833.4830; Found 833.4813.

Syntheses and Characterization of Starting Materials.

Pent-4-en-1-yl Benzoate (Starting Material for Compound 6)

4-Penten- 1-ol (0.5 mL, 4.85 mmol) was dissolved in dichloromethane (25 mL) in a round-bottom flask equipped with a stir bar under N_2. The reaction mixture was treated with triethylamine (1.4 mL, 9.7 mmol) and DMAP (60 mg, 0.485 mmol), followed by benzoic anhydride (2.19 g, 9.7 mmol). The reaction was stirred overnight at room temperature under N_2 and then was diluted with DCM (50 mL) and transferred to a separatory funnel. The organic mixture was washed with 1 M HCl (25 mL), saturated sodium bicarbonate (50 mL) then brine (50 mL), and then dried with $MgSO_4$ and concentrated. The crude residue was purified via column chromatography on silica gel,

eluting with 10% EtOAc/hexanes to provide pent-4-en-1-yl benzoate (0.84 g, 91%). NMR data matches previously reported spectra.

Pent-4-en-1-yl 4-Methylbenzenesulfonate (Starting Material for Compound 8)

4-Penten-1-ol (1.0 mL, 9.68 mmol) and DMAP (0.118 g, 0.968 mmol) were dissolved in dichloromethane (42 mL) in a round-bottom flask equipped with a stir bar under N_2. The reaction mixture was treated with TsCl (2.03 g, 10.6 mmol) and then triethylamine (1.48 mL, 10.6 mmol). The reaction stirred overnight at room temperature under N_2 and then was diluted with DCM (50 mL) and transferred to a separatory funnel. The organic mixture was washed with 1 M HCl (25 mL), saturated sodium bicarbonate (50 mL), then brine (50 mL), and then dried with $MgSO_4$ and concentrated. The crude residue was purified via column chromatog- raphy on silica gel, eluting with 10% EtOAc/hexanes to provide pent- 4-en-1-yl 4-methylbenzenesulfonate (2.16 g, 93%). NMR data matches previously reported spectra.

N,N-Diethylpent-4-enamide (Starting Material for Compound 9)

4-Pentenoic acid (0.817 g, 7.16 mmol) and diethylamine (1.48 mL, 14.32 mmol) were dissolved in dichloromethane (57 mL) in a round-bottom flask equipped with a stir bar under N_2. EDC-HCl (1.51 g, 7.87 mmol), HOBt (1.21 g, 7.87 mmol), and triethylamine (2.19 mL, 15.74 mmol) were added and the reaction and stirred overnight at room temperature under N_2. The reaction mixture was diluted with DCM (50 mL) and transferred to a separatory funnel. After washing with 1 M HCl (50 mL), saturated sodium bicarbonate (50 mL), and then brine (50 mL), the organic layer was dried with $MgSO_4$ and

concentrated. The crude residue was purified via column chromatography on silica gel, eluting with 30% EtOAc/hexanes to provide N,N-diethylpent-4-enamide (1.07g, 88%). NMR data matches previously reported spectra.

N-3-butenyl-N-methyl-p-toluenesulfonamide (Starting Material for Compound 10)

4-Bromo-1-butene (0.752 mL, 7.41 mmol) and p-toluenesulfonamide (2.53 g, 14.82 mmol) were dissolved in dry acetonitrile (22 mL) in a round-bottom flask equipped with a stir bar and a reflux condenser under N . The reaction mixture was treated with KI (0.123 g, 0.741 mmol) and K_2CO_3 (2.05 g, 14.82 mmol) and then stirred at reflux under N_2 overnight. The solvent was concentrated to dryness, redissolved in dichloromethane, washed with brine (100 mL), and then dried with $MgSO_4$ and concentrated. The crude material was purified via column chromatography on silica gel with EtOAc/hexanes to provide N-(but-3-en-1-yl)-4-methylben- zenesulfonamide (1.05 g, 63%). NaH (0.181 g, 4.52 mmol, 60%) was added to dry DMF (19 mL) in a round-bottom flask equipped with a stir bar under N_2 and the mixture was cooled to 0 °C. N-(But-3-en-1- yl)-4-methylbenzenesulfonamide (1.05 g, 4.66 mmol) in DMF (5 mL) was added dropwise at 0 °C and the mixture stirred for 30 min and warmed to room temperature. After cooling back down to 0 °C, MeI (0.352 mL, 5.66 mmol) was added dropwise and then the reaction was stirred overnight at room temperature under N_2. The reaction mixture was transferred to a separatory funnel, diluted with water (200 mL) and extracted with diethyl ether (50 mL × 3). The combined organic layers were washed with brine (100 mL × 3) and then dried with $MgSO_4$ and concentrated. The crude residue was purified via column chromatography on

silica gel, eluting with 20% EtOAc/hexanes to provide N-3-butenyl-N-methyl-p-toluenesulfona- mide (0.892 g, 80%). NMR data matches previously reported spectra.

2-(But-3-en-1-yl)isoindoline-1,3-dione (Starting Material for Compound 11)

Phthalimide potassium salt (1.46 g, 7.88 mmol) was dissolved in acetone (32 mL) in a round-bottom flask equipped with a stir bar and reflux condenser under N_2. 4-Bromo-1-butene (1.0 mL, 9.85 mmol) was added dropwise, and the reaction was stirred overnight at reflux. After cooling to room temperature, the solvent was removed in vacuo. The crude residue was dissolved in EtOAc (100 mL) and washed with water (50 mL), 1 M NaOH (50 mL), and then brine (50 mL). The organic layer was dried with $MgSO_4$ and concentrated, providing 2-(but-3-en-1-yl)isoindoline-1,3-dione, which was used without further purification (1.14 g, 72%). NMR data matches previously reported spectra.

2-Cyanoethyl Pent-4-enoate (Starting Material for Compound 12)

2-Cyanoethanol (0.372 mL, 5.44 mmol) was dissolved in dichloromethane (23 mL) in a round-bottom flask equipped with a stir bar under N_2. The reaction mixture was treated with triethylamine (0.95 mL, 6.80 mmol) and DMAP (55 mg, 0.453 mmol), and then 4-pentenoyl chloride (0.50 mL, 4.53 mmol) was added dropwise. The reaction stirred at room temperature under N_2 for 3 h, at which point the reaction was shown to be complete by TLC. The reaction mixture was diluted with DCM (50 mL) and transferred to a separatory funnel. The solvent was washed with 1 M HCl (25 mL), saturated sodium bicarbonate (50 mL), and then brine (50 mL) and then dried with $MgSO_4$ and concentrated. The crude residue was purified via column chromatography on silica gel using a gradient of 0−40%

EtOAc/hexanes to provide 2-cyanoethyl pent-4-enoate (0.583 g, 84%). Colorless oil. ^{1}H NMR (400 MHz, $CDCl_3$): δ 5.37−5.73 (1H, m), 5.07−4.97 (2H, m), 4.25 (2H, t, J = 6.26 Hz), 2.67 (2H, t, J = 6.36Hz),2.47−2.41(2H,m),2.39−2.32(2H,m);$^{13}C\{^{1}H\}$NMR (100 MHz, $CDCl_3$): δ 172.3, 136.1, 116.7, 115.7, 58.5, 32.3, 28.5, 17.9; HRMS (ESI-Orbitrap) m/z: $[M + H]^+$ Calcd for $C_8H_{12}O_2N^+$ 154.0868; Found 154.0856.

Starting Material for Enone 13

18β-Glycyrrhetinic acid (0.750 g, 1.59 mmol) was dissolved in pyridine (11 mL) in a round-bottom flask equipped with a stir bar under N_2. The reaction mixture was cooled to 0 °C and treated with acetic anhydride (7.5 mL) dropwise. The reaction stirred overnight at room temperature and then was poured into cold water (200 mL). The solid was washed with water (100 mL), then dissolved in dichloromethane, and dried with $MgSO_4$ and concentrated. Glycyrrhetinyl acetate (0.748 g, 1.46 mmol) was dissolved in dry DMF (15 mL), and then K_2CO_3 (0.243 g, 1.76 mmol) was added. 4-Bromo-1-butene (0.179 mL, 1.76 mmol) was added and the reaction stirred at room temperature for 4.5 h. The reaction mixture was poured into water (200 mL), filtered, and washed with water (100 mL). The solid was dissolved in dichloromethane, dried with $MgSO_4$, and concentrated. The crude residue was purified via column chromatography on silica gel, eluting with 10−15% EtOAc/hexanes to provide the desired product (0.457 g, 56% over two steps). White solid. Mp = 185−186 °C. ^{1}H NMR (400 MHz, $CDCl_3$): δ 5.80−5.68 (1H, m), 5.60 (1H, s), 5.11−5.02 (2H, m), 4.49−4.44 (1H, m), 4.17−4.05 (2H, m), 2.79−2.71 (1H, m), 2.39−2.29 (3H, m), 2.10−1.78 (8H, m), 1.68−1.51 (5H, m), 1.40−1.21 (8H, m), 1.17−0.90 (13H, m),

0.83 (6H, s), 0.75 (3H, s); $^{13}C\{^{1}H\}$ NMR (100 MHz, $CDCl_3$): δ 199.9, 176.2, 170.8, 169.1, 133.9, 128.3, 117.3, 80.4, 63.2, 61.6, 54.9, 48.1, 45.2, 43.9, 43.1, 40.9, 38.6, 37.9, 37.6, 36.8, 33.1, 32.6, 31.7, 30.9, 28.4, 28.3, 27.9, 26.3, 26.3, 23.4, 23.2, 21.2, 18.5, 17.2, 16.6, 16.3; HRMS (ESI-Orbitrap) m/z: $[M + H]^+$ Calcd for $C_{36}H_{55}O_5^+$ 567.4049; Found 567.4016.

9.4 Experimental Details for Chapter 4.

General Fluorination Procedure. Selectfluor (266 mg, 0.75 mmol, 1.5 equiv) and xanthone (9.8 mg, 0.05 mmol, 0.1 equiv) were added to an oven-dried microwave vial equipped with a stir bar; the vial was then sealed with a cap with Teflon septum using a crimper and evacuated/refilled with N_2 multiple times. The substrate (0.5 mmol, 1.0 equiv) was then added in a solution of anhydrous CH_3CN (8 mL) (on the other hand, if the substrate is a solid, it is added along with Selectfluor before sealing the vial). The reaction mixture was irradiated with visible light from two CFL bulbs while being stirred at room temperature. After 2−3 h, a 0.3 mL aliquot was taken for ^{19}F NMR yield determination (generally, ketals reacted for 2 h and carbamates for 3 h). The reaction mixture was triturated with 40 mL of 1:1 CH_2Cl_2/hexanes, filtered through Celite, and washed with CH_2Cl_2. After the crude mixture was concentrated in vacuo, the residue was purified via column chromatography on silica gel with EtOAc/hexanes.

Characterization of Fluorinated Compounds.

(3aR,5S,6S,6aR)-5-((4S)-5-Fluoro-2,2-dimethyl-1,3-dioxolan-4-yl)-2,2-dimethyltetrahydrofuro[2,3-d][1,3]dioxol-6-yl Acetate (Compound 1)

Fluorination was run according to the general procedure (1.5 equiv of Selectfluor, 2 h), and the major diastereomer was isolated via gradient column chromatography on silica gel eluting with 10−15% EtOAc/hexanes. Regiochemical assignment was made on the basis of (1) chemical shift in the ^{19}F NMR spectrum (δ −113.3 to −113.6 ppm) that indicates a secondary α-ethereal fluoride, (2) $^{2}J_{HF}$ coupling in the ^{1}H NMR spectrum consistent with a secondary fluoride (J = 68.2 Hz), (3) splitting pattern in the ^{19}F NMR spectrum with appropriate coupling constants (dd, $^{2}J_{FH}$ = 68.3 Hz, $^{3}J_{FH}$ = 16.6 Hz), and (4) identification of $^{2}J_{CF}$, $^{3}J_{CF}$, and $^{4}J_{CF}$ coupling to distinguishable peaks in the ^{13}C NMR spectrum; for example, the quaternary carbon of the fluorinated acetonide (δ 113.9 ppm, $^{3}J_{CF}$ = 2.9 Hz) and a methyl group of the fluorinated acetonide (δ 27.5 ppm, $^{4}J_{CF}$ = 3.3 Hz). Stereochemical assignment was made on the basis of ^{3}J coupling for the H−C−F proton in the ^{1}H NMR spectrum (J = 0.9 Hz for the major diastereomer, J = 2.4 Hz for the minor diastereomer): colorless oil (109 mg, 68%); ^{1}H NMR (400 MHz, $CDCl_3$) δ 6.05−5.87 (2H, m, H−C−F and anomeric C−H), 5.29− 5.28 (1H, m), 4.51 (1H, d, J = 3.7 Hz), 4.45−4.39 (1H, m), 4.20− 4.17 (1H, m), 2.11 (3H, s), 1.50 (6H, s), 1.48−1.30 (6H, m); $^{13}C\{^{1}H\}$ NMR (100 MHz, $CDCl_3$) δ 169.5, 113.9 (d, J = 2.9 Hz), 112.4, 110.6 (d, J = 225.2 Hz), 105.2, 83.2, 80.7 (d, J = 32.3 Hz), 78.2 (d, J = 8.1 Hz), 75.7, 27.5 (d, J = 3.3 Hz), 27.1, 26.7, 26. 1, 20.7; ^{19}F NMR (282 MHz, $CDCl_3$) δ −113.3 to −113.6 (1F, dd, $^{2}J_{FH}$ = 68.3 Hz, $^{3}J_{FH}$ = 16.6 Hz); HRMS (ESI-Orbitrap) m/z $[M + H]^+$ calcd for $C_{14}H_{22}O_7F^+$ 321.1350; found 321.1349.

((3aR,5R,5aS,8aS,8bS)-8b-Fluoro-2,2,7,7-tetramethyltetra-hydro-5H-bis([1,3]dioxolo)[4,5-b:4',5'-d]pyran-5-yl)methyl Acetate (Compound 2)

Fluorination was run according to the general procedure (1.5 equiv of Selectfluor, 2 h), and the major diastereomer was isolated via gradient column chromatography on silica gel eluting with 10−15% EtOAc/hexanes. Regiochemical assignment was made on the basis of (1) chemical shift in the ^{19}F NMR spectrum (δ −97.1 to −97.2 ppm) that indicates a tertiary α-ethereal fluoride, (2) lack of $^{2}J_{HF}$ coupling in the ^{1}H NMR spectrum consistent with a tertiary fluoride, (3) splitting pattern in the ^{19}F NMR spectrum with appropriate coupling constants (dd, $^{3}J_{FH}$ = 17.2 Hz, $^{3}J_{FH}$ = 2.9 Hz), (4) agreement with the calculated ^{19}F NMR shift (at B3LYP/6-311+ +G**), and (5) identification of $^{2}J_{CF}$ and $^{3}J_{CF}$ coupling to distinguishable peaks in the ^{13}C NMR spectrum; for example, the anomeric carbon (δ 97.2 ppm, $^{2}J_{CF}$ = 4.8 Hz). Stereochemical assignment of the major diastereomer was made on the basis of the chemical shift indicating the presence of the more deshielded cis-isomer, $^{3}J_{FH}$ coupling constants (described above), and the empirical preference for the cis-isomer that is observed during synthesis of the starting material: colorless oil (133 mg, 83%); ^{1}H NMR (400 MHz, $CDCl_3$) δ 5.53 (1H, d, J = 5.0 Hz, anomeric C−H), 4.50−4.45 (2H, m), 4.26−4.14 (3H, m), 2.09 (3H, s), 1.56 (6H, d, J = 8.3 Hz), 1.47−1.36 (6H, m); $^{13}C\{^{1}H\}$ NMR (100 MHz, $CDCl_3$) δ 170.8, 115.0 (d, J = 2.6 Hz), 113.9 (d, J = 237.3 Hz), 110.3, 97.2 (d, J =4.8Hz),79.5(d,J=31.2Hz),72.2(d,J=26.8Hz),67.7(d,J=7.3 Hz), 62.3 (d, J = 1.8 Hz), 27.7, 26.6 (d, J = 2.9 Hz), 25.9, 25.0, 20.8; ^{19}F NMR (282 MHz,

$CDCl_3$) δ −97.1 to −97.2 (1F, dd, $^3J_{FH}$ = 17.2 Hz, $^3J_{FH}$ = 2.9 Hz); HRMS (ESI-Orbitrap) m/z $[M + H]^+$ calcd for $C_{14}H_{22}O_7F^+$ 321.1350; found 321.1344.

(3a'S,4S,7'S,7a'S)-3a'-Fluoro-2,2,2',2'-tetramethyltetrahydrospiro[[1,3]dioxolane-4,6'-[1,3]dioxolo[4,5-c]- pyran]-7'-yl Acetate (Compound 3)

Fluorination was run according to the general procedure (1.5 equiv of Selectfluor, 2 h), and the major diastereomer was isolated via gradient column chromatography on silica gel eluting with 10−15% EtOAc/hexanes. Regiochemical assignment was made on the basis of (1) chemical shift in the ^{19}F NMR spectrum (δ −97.0 − (−97.1) ppm) that indicates a tertiary α- ethereal fluoride, (2) lack of $^2J_{HF}$ coupling in the ^1H NMR spectrum consistent with a tertiary fluoride, (3) splitting pattern in the ^{19}F NMR spectrum consisting of a doublet of triplets ($^3J_{FH}$ = 16.6 Hz, $^3J_{FH}$ = 3.7 Hz), and (4) identification of $^2J_{CF}$ and $^3J_{CF}$ coupling to distinguishable peaks in the ^{13}C NMR spectrum; for example, the quaternary carbon of the fluorinated acetonide (δ 114.7 ppm, $^3J_{CF}$ = 2.9 Hz) and the methylene α to the fluoride (δ 72.3 ppm, $^2J_{CF}$ = 26.8 Hz). Stereochemical assignment was made by analogy to compound 2: colorless oil (109 mg, 68%); ^1H NMR (400 MHz, $CDCl_3$) δ 4.51− 4.40 (3H, m), 4.13−4.08 (1H, m), 3.98 (1H, d, J = 11.8 Hz), 3.78− 3.73 (1H, m), 2.11 (3H, s), 1.58 (6H, d, J = 12.6 Hz), 1.47 (6H, d, J = 20.3 Hz); $^{13}C\{^1H\}$ NMR (100 MHz, $CDCl_3$) δ 170.0, 114.7 (d, J = 2.9 Hz), 113.6 (d, J = 237.3 Hz), 110.0, 103.2 (d, J = 5.5 Hz), 79.2 (d, J = 30.8 Hz), 72.3 (d, J = 26.8 Hz), 64.3, 63.3 (d, J = 7.0 Hz), 27.6, 26.6 (d, J = 2.9 Hz), 26.3, 25.2, 20.8; ^{19}F NMR (282 MHz, $CDCl_3$) δ −97.0 − (−97.1) (1F,

dt, $^{3}J_{FH}$ = 16.6 Hz, $^{3}J_{FH}$ = 3.7 Hz); HRMS (ESI-Orbitrap) m/z $[M + H]^{+}$ calcd for $C_{14}H_{22}O_7F^{+}$ 321.1350; found 321.1345.

(2R)-2-((4R)-5-Fluoro-2,2-dimethyl-1,3-dioxolan-4-yl)-5- oxo-2,5-dihydrofuran-3,4-diyl Diacetate (Compound 4)

Fluorination was run according to the general procedure (2.0 equiv of Selectfluor, 2 h), and the major diastereomer was isolated via gradient column chromatography on silica gel eluting with 10−20% EtOAc/ hexanes. Regiochemical assignment was made by analogy to compound 1. No stereochemical assignment was made: colorless oil (132 mg, 83%); ^{1}H NMR (400 MHz, $CDCl_3$) δ 6.09−5.92 (1H, m, H−C−F), 5.34 (1H, d, J = 1.6 Hz), 4.62−4.58 (1H, m), 2.32 (3H, s), 2.27 (3H, s), 1.49 (6H, d, J = 29.7 Hz); $^{13}C\{^{1}H\}$ NMR (100 MHz, $CDCl_3$) δ 166.1, 165.1, 164.7, 149.8 (d, J = 1.1 Hz), 122.5, 116.1 (d, J = 3.0 Hz), 111.1−108.9 (m), 80.5−80.2 (m), 74.4−74.2 (m), 27.3, 26.5, 20.5−20.4 (m), 20.1−20.0 (m); ^{19}F NMR (282 MHz, $CDCl_3$) δ −108.8 to −109.1 (1F, dd, $^{2}J_{FH}$ = 69.4 Hz, $^{3}J_{FH}$ = 17.8 Hz); HRMS (ESI-Orbitrap) m/z $[M + H]^{+}$ calcd for $C_{13}H_{16}O_8F^{+}$ 319.0829; found 319.0825.

(3aS,4R,6S,6aS)-6-((4S)-5-Fluoro-2,2-dimethyl-1,3-dioxo-lan-4-yl)-2,2-dimethyltetrahydrofuro[3,4-d][1,3]dioxol-4-yl Acetate (Compound 5)

Fluorination was run according to the general procedure (1.5 equiv of Selectfluor, 2 h), and the major diastereomer was isolated via gradient column chromatography on silica gel eluting with 10−15% EtOAc/hexanes. Regiochemical assignment was made by analogy to

compound 1. No stereochemical assignment was made: colorless oil (86 mg, 54%); ^{1}H NMR (400 MHz, $CDCl_3$) δ 6.16 (1H, s, anomeric C−H), 5.94 (1H d, J = 66.9 Hz, H−C−F), 4.89−4.86 (1H, m), 4.71 (1H, d, J = 5.9 Hz), 4.63−4.57 (1H, m), 3.93−3.90 (1H, m), 2.07 (3H, s), 1.57−1.35 (12H, m); $^{13}C\{^{1}H\}$ NMR (100 MHz, $CDCl_3$) δ 169.2, 114.2 (d, J = 2.9 Hz), 113.6, 110.7 (d, J = 227.1 Hz), 100.8, 84.9, 80.9 (d, J = 3.3 Hz), 80.7 (d, J = 20.9 Hz), 79.1, 27.7 (d, J = 3.3 Hz), 27.6, 25.8, 24.6, 21.0; ^{19}F NMR (282 MHz, $CDCl_3$) δ −113.6 to −113.8 (1F, dd, $^{2}J_{FH}$ = 67.1 Hz, $^{3}J_{FH}$ = 16.1 Hz); HRMS (LIFDI-TOF) m/z [M − CH_3]$^{+}$ calcd for $C_{13}H_{18}O_7F^{+}$ 305.1031; found 305.1043.

(3a'R,4R,5R,7a'R)-5-Fluoro-2,2,2',2'-tetramethyldihydrospiro[[1,3]dioxolane-4,6'-[1,3]dioxolo[4,5-c]- pyran]-7'(4'H)-one (Compound 6)

Fluorination was run according to the general procedure (1.5 equiv of Selectfluor, 2 h), and the major diastereomer was isolated via gradient column chromatography on silica gel eluting with 10−15% EtOAc/hexanes. Note that we were unsuccessful in isolating compound 6 in pure form, as we found it to be inseparable from the starting material. Chromatography on silica gel, Florisil, and alumina led only to a 1:1 mixture of starting material and product, due to significant streaking which we believe is caused by hydration of the unusually reactive ketone (see Figure S31 for the ^{19}F NMR spectrum of the major diastereomer and Figure S32 for the ^{1}H NMR spectrum of the 1:1 mixture): colorless oil (57 mg, 41%); ^{19}F NMR (282 MHz, $CDCl_3$) δ −120.9 (1F, d, $^{2}J_{FH}$ = 64.3 Hz).

Compound 7

Fluorination was run according to the general procedure (1.5 equiv of Selectfluor, 2 h), and the product was isolated via gradient column chromatography on silica gel eluting with 10− 20% EtOAc/hexanes. Regiochemical assignment was made on the basis of (1) chemical shift in the ^{19}F NMR spectrum (δ −105.9 to −106.0 ppm) that indicates a tertiary α-ethereal fluoride, (2) lack of $^{2}J_{HF}$ coupling in the ^{1}H NMR spectrum consistent with a tertiary fluoride, (3) disappearance of α-ethereal hydrogen atom in the ^{1}H NMR spectrum (see ^{1}H NMR spectrum of starting material in SI), and (4) identification of $^{2}J_{CF}$, $^{3}J_{CF}$, and $^{4}J_{CF}$ coupling to distinguishable peaks in the ^{13}C NMR spectrum; for example, C□O of the α-acetoxy ketone (δ 198.7 ppm, $^{3}J_{CF}$ = 1.5 Hz) and the quaternary carbon of the fluorinated acetonide (δ 112.6 ppm, $^{3}J_{CF}$ = 1.5 Hz): white solid (202 mg, 78%); ^{1}H NMR (400 MHz, $CDCl_3$) δ 6.92 (1H, d, J = 10.2 Hz), 6.29−6.26 (1H, m), 6.03 (1H, s), 5.55−5.52 (1H, m), 4.94−4.60 (2H, m), 2.57−2.49 (1H, m), 2.40−2.36 (1H, m), 2.26−2.10 (9H, m), 1.97−1.90 (3H, m), 1.49−1.44 (6H, m), 1.33−1.20 (6H, m), 1.04 (3H, s); $^{13}C\{^{1}H\}$ NMR (100 MHz, $CDCl_3$) δ 198.7 (d, J = 1.5 Hz), 185.8, 170.1, 169.7, 167.7, 153.9, 128.6, 124.1 (d, J = 259.0 Hz), 123.1, 112.6 (d, J = 1.5 Hz), 95.5 (d, J = 20.9 Hz), 70.7, 68.6, 53.7 (d, J = 1.1 Hz), 47.0 (d, J = 7.3 Hz), 45.8 (d, J = 2.6 Hz), 42.8, 37.3 (d, J = 29.3 Hz), 36.0, 33.7, 31.6, 30.2 (d, J = 1.5 Hz), 26.4 (d, J = 2.6 Hz), 26.2, 21.7, 20.7, 20.4, 16.3; ^{19}F NMR (282 MHz, $CDCl_3$) δ −105.9 to −106.0 (1F, m); HRMS (ESI-Orbitrap) m/z $[M + H]^+$ calcd for $C_{28}H_{36}O_8F^+$ 519.2394; found 519.2393.

Compound 8

Fluorination was run according to the general procedure (1.5 equiv of Selectfluor, 2 h), and the major diastereomer was isolated via gradient column chromatography on silica gel eluting with 10−15% EtOAc/hexanes. Regiochemical and stereochemical assignment was made by analogy to compound 1: white solid (170 mg, 49%); ^{1}H NMR (400 MHz, $CDCl_3$) δ 6.05−5.88 (2H, m), 5.28 (1H, d, J = 3.1 Hz), 4.72−4.64 (1H, m), 4.62−4.58 (1H, m), 4.52 (1H, d, J = 3.6 Hz), 4.46−4.40 (1H, m), 4.20−4.17 (1H, m), 2.70− 2.56 (4H, m), 2.19−2.10 (1H, m), 2.02 (3H, s), 1.83−1.79 (1H, m), 1.74−1.69 (2H, m), 1.65−1.60 (2H, m), 1.57 (3H, m), 1.50, (5H, m), 1.48 (3H, s), 1.42−1.37 (2H, m), 1.30 (3H, s), 1.29−1.23 (6H, m), 1.20−1.12 (2H, m), 1.07−0.99 (2H, m), 0.90−0.86 (2H, m), 0.82 (3H, s), 0.77 (3H, s), 0.69−0.62 (1H, m); $^{13}C\{^{1}H\}$ NMR (100 MHz, $CDCl_3$) δ 172.0, 171.1, 170.7, 113.9 (d, J = 2.6 Hz), 112.4, 110.7 (d, J = 225.6 Hz), 105.2, 83.2 (d, J = 29.7 Hz), 80.6 (d, J = 31.9 Hz), 78.2 (d, J = 8.4 Hz), 76.0, 73.6, 54.1, 50.6, 44.6, 42.8, 36.8 (d, J = 16.1 Hz), 35.5, 35.2, 34.0, 31.5, 29.0 (d, J = 3.7 Hz), 28.4, 27.5 (d, J = 3.3 Hz), 27.4 (d, J = 5.1 Hz), 27.2, 26.7, 26.2, 23.5, 21.4, 20.7, 12.2, 12.1; ^{19}F NMR (282 MHz, $CDCl_3$) δ −113.2 to −113.5 (1F, dd, $^{2}J_{FH}$ = 68.3 Hz, $^{3}J_{FH}$ = 16.6 Hz).

((Fluoro(phenyl)methoxy)carbonyl)-L-isoleucine (Compound 9)

Fluorination was run according to the general procedure (2.0 equiv of Selectfluor, 3 h), and the product was isolated via gradient column chromatography on silica gel eluting with 10−20% EtOAc/hexanes: colorless oil (95 mg, 67%); ^{1}H NMR (400 MHz, $CDCl_3$) δ 7.53−7.51 (2H, m), 7.46−7.44 (3H, m), 7.17 (1H, d, J = 56.3 Hz), 5.51 (1H, d, J = 8.7 Hz), 4.49−4.45 (1H, m), 2.03−1.96 (1H, m), 1.53−1.46 (1H, m), 1.23−1.19 (1H, m), 1.00−0.93

(6H, m); $^{13}C\{^{1}H\}$ NMR (100 MHz, $CDCl_3$) δ 175.9, 153.6 (d, J = 1.5 Hz), 134.7 (d, J = 24.2 Hz), 130.2 (d, J = 1.8 Hz), 128.6, 126.1 (d, J = 5.9 Hz), 102.8 (d, J = 222.3 Hz), 58.2, 37.9, 24.8, 15.4, 11.6; ^{19}F NMR (282 MHz, $CDCl_3$) (major diastereomer) δ −120.1 to −120.3 (1F, d, J = 56.8 Hz), (minor diastereomer) δ −119.2 to −119.4 (1F, d, J = 56.2 Hz); HRMS (ESI-Orbitrap) m/z $[M + H]^+$ calcd for $C_{14}H_{19}O_4NF^+$ 284.1298; found 284.1299.

3-Benzoyl-5-fluorooxazolidin-2-one (Compound 10)

Fluorination was run according to the general procedure (2.0 equiv of Selectfluor, 3 h), and the product was isolated through gradient column chromatography on silica gel eluting with 10−20% EtOAc/ hexanes. Regiochemical assignment was made by comparison to reported characterization data for gem-O and gem-N fluorinated oxazolidinones: white solid (59 mg, 56%); ^{1}H NMR (400 MHz, $CDCl_3$) δ 7.71−7.69 (2H, m), 7.62−7.58 (1H, m), 7.48−7.44 (2H, m), 6.76−6.59 (1H, m), 4.61−4.48 (2H, m); $^{13}C\{^{1}H\}$ NMR (100 MHz, $CDCl_3$) δ 167.9 (d, J = 2.2 Hz), 151.5 (d, J = 2.2 Hz), 133.2, 131.5, 129.3, 128.1, 92.4 (d, J = 215.3 Hz), 68.4 (d, J = 28.6 Hz); ^{19}F NMR (282 MHz, $CDCl_3$) δ −134.0 to −134.5 (1F, m); HRMS (ESI- Orbitrap) m/z $[M + H]^+$ calcd for $C_{10}H_9O_3NF^+$ 210.0567; found 210.0563.

1-Fluoroethyl Carbamate (Compound 11)

Fluorination was run according to the general procedure (2.0 equiv of Selectfluor, 3 h), and the product was isolated via gradient column chromatography on silica gel eluting with 15−25% EtOAc/hexanes: colorless oil (23 mg, 42%); ^{1}H NMR (400 MHz, $CDCl_3$) δ

6.50−6.32 (1H, m), 4.90 (2H, br s), 1.55−1.49 (3H, m); $^{13}C\{^{1}H\}$ NMR (100 MHz, $CDCl_3$) δ 154.2 (m), 102.1 (d, J = 219.7 Hz), 19.7 (d, J = 24.7 Hz); ^{19}F NMR (282 MHz, $CDCl_3$) δ −119.6 to −120.0 (1F, dq, $^{2}J_{FH}$ = 56.8 Hz, $^{3}J_{FH}$ = 20.7 Hz); HRMS (ESI-Orbitrap) m/z $[M + H]^+$ calcd for $C_3H_7O_2NF^+$ 108.0461; found 108.0462.

Syntheses and Characterization of Starting Materials.

Previously Reported Starting Materials.

Starting materials for compounds 1, 2, 3, and 5: Diacetonide esters of glucose, galactose, fructose, and mannose were prepared using previously reported methods. NMR data match previously reported spectra for glucose derivative 1, galactose 2, fructose 3, and mannose 5. Starting material for ketone 6 is commercially available; however, we observed higher yields with material that we synthesized, as described in Shi's original paper. Starting materials for compounds 9 and 10 were prepared using previously reported methods (NMR data matches reported spectra). Starting material for compound 11 is commercially available.

New Starting Materials

(R)-2-((S)-2,2-Dimethyl-1,3-dioxolan-4-yl)-5-oxo-2,5-dihydrofuran-3,4-diyl Diacetate (Starting Material for Compound 4)

Anhydrous $CuSO_4$ (4.49 g, 28.10 mmol, 1.65 equiv) was added to a mixture of L-ascorbic acid (3.0 g, 17.03 mmol) in dry acetone (70 mL). The reaction was stirred for 24 h; then another 1.65 equiv of anhydrous $CuSO_4$ was added and the reaction stirred

overnight. The mixture was filtered through Celite (washed w/acetone) and concentrated to dryness, yielding pure ascorbic acid acetonide. DMAP (85 mg, 0.693 mmol, 0.1 equiv) was added to ascorbic acid acetonide (1.5 g, 6.93 mmol, 1.0 equiv) in acetic anhydride (15 mL). The reaction was stirred at room temperature for 24 h, and then Ac_2O was removed via vacuum distillation with mild heat. The crude mixture was purified via column chromatography on silica gel with EtOAc/hexanes to provide (R)-2- ((S)-2,2-dimethyl-1,3-dioxolan-4-yl)-5-oxo-2,5-dihydrofuran-3,4-diyl diacetate (1.41 g, 68%): white solid; ^1H NMR (400 MHz, $CDCl_3$) δ 5.14 (1H, d, J = 2.4 Hz), 4.41−4.37 (1H, m), 4.21−4.08 (2H, m), 2.30 (3H, s), 2.27 (3H, s), 1.39 (3H, s), 1.36 (3H, s); $^{13}C\{^1H\}$ NMR (100 MHz, $CDCl_3$) δ 166.2, 165.5, 164.8, 150.8, 122.2, 110.9, 75.2, 72.9, 65.2, 25.7, 25.4, 20.5, 20.1; HRMS (ESI-Orbitrap) m/z $[M + H]^+$ calcd for $C_{13}H_{17}O_8^+$ 301.0923, observed 301.0920.

Desonide Diacetate (Starting Material for Compound 7)

Acetic anhydride (0.88 mL, 9.28 mmol, 4.0 equiv) was added to a mixture of desonide (0.97 g, 2.32 mmol, 1.0 equiv), DMAP (28 mg, 0.232 mmol, 0.1 equiv), and triethylamine (0.78 mL, 5.57 mmol, 2.4 equiv) in CH_2Cl_2 (23 mL) at room temperature. The mixture was stirred overnight and then was transferred to a separatory funnel (dilute with CH_2Cl_2) and washed with 1 M HCl, saturated aqueous sodium bicarbonate, and then brine. The organic layer was dried over Na_2SO_4, filtered, and concentrated to dryness. The crude white solid was recrystallized from boiling MeOH, yielding pure desonide diacetate (0.95 g, 82%): colorless crystals; ^1H NMR (400 MHz, $CDCl_3$) δ 6.93 (1H, d, J = 10.1 Hz), 6.28−6.25 (1H, m), 6.03 (1H, t, J = 1.5 Hz), 5.56−5.54 (1H, m), 5.02−4.64 (3H, m),

2.56−2.47 (1H, m), 2.39−2.34 (1H, m), 2.21−2.14 (4H, m), 2.13−2.06 (4H, m), 1.99−1.87 (2H, m), 1.74−1.69 (1H, m), 1.64−1.54 (2H, m), 1.42 (3H, s), 1.27−1.12 (8H, m), 0.82 (3H, s); $^{13}C\{^{1}H\}$ NMR (100 MHz, $CDCl_3$) δ 203.6, 185.9, 170.1, 169.8, 168.1, 154.1, 128.5, 123.0, 111.4, 97.3, 81.7, 71.1, 67.4, 53.8, 49.6, 45.5, 42.9, 36.5, 33.8, 33.7, 31.8, 30.8, 26.5, 25.5, 21.8, 20.8, 20.4, 16.5; HRMS (ESI-Orbitrap) m/z $[M + H]^+$ calcd for $C_{28}H_{37}O_8^+$ 501.2488, observed 501.2485.

Glycosteroid Derivative (Starting Material for Compound 8)

Acetic anhydride (2.11 mL, 22.3 mmol, 2.0 equiv) was added to a mixture of dehydroepiandrosterone (3.22 g, 11.15 mmol, 1.0 equiv), DMAP (136 mg, 1.11 mmol, 0.1 equiv), and triethylamine (1.95 mL, 13.94 mmol, 1.25 equiv) in CH_2Cl_2 (111 mL) at room temperature. The mixture was stirred overnight and then was transferred to a separatory funnel (dilute with CH_2Cl_2) and washed with 1 M HCl, saturated aqueous sodium bicarbonate, and then brine. The organic layer was dried over Na_2SO_4, filtered, and concentrated to dryness. The crude white solid was used in the next step without further purification. The crude material from the previous step was dissolved in MeOH (80 mL), and 5−10 mL of EtOAc was added the mixture required mild heat for the compound to fully dissolve. After being cooled back to rt, Pd/C (593 mg, 0.05 equiv, 10% Pd/C) was carefully added, and then the mixture was hydrogenated at 1 atm (via H_2 balloon) for 8 h. The mixture was filtered over Celite, washed with CH_2Cl_2, and concentrated to dryness. The crude white solid was used in the next step without further purification. The crude material from the previous step (11 mmol) was dissolved in MeOH (75 mL) and cooled to 0 °C in an ice bath. Sodium borohydride (530 mg, 13.9 mmol, 1.25 equiv) was added in

three portions. The mixture stirred at 0 °C for an additional 30 min and then slowly warmed to room temperature and continued to stir for 4 h. The reaction was quenched with 1 M HCl, and then MeOH was removed in vacuo. The mixture was diluted with water and transferred to a separatory funnel. After the aqueous layer was extraced with CH_2Cl_2 (50 mL × 3), the organic layer was washed with brine, dried over Na_2SO_4, filtered, and concentrated to dryness. The crude solid was recrystallized from boiling MeOH, yielding 1.452 g of colorless crystals. Succinic anhydride (0.868 g, 8.68 mmol, 2.0 equiv), triethylamine (0.76 mL, 5.43 mmol, 1.25 equiv), and DMAP (53 mg, 0.43 mmol, 0.1 equiv) were added to a solution of 1.452 g (4.34 mmol, 1.0 equiv) of the alcohol from the previous step in CH_2Cl_2 (45 mL). After being stirred overnight, an additional 0.5 g of succinic anhydride and 50 mg of DMAP were added, and the mixture was allowed to stir overnight again. The mixture was transferred to a separatory funnel (diluted with CH_2Cl_2) and washed with 1 M HCl, followed by brine, dried over Na_2SO_4, filtered, and concentrated to dryness. The crude mixture was purified via column chromatography on silica gel with EtOAc/ hexanes to provide the succinate derivative as a white solid (1.49 g, 79%). Glucose diacetonide (0.98 g, 3.76 mmol, 1.1 equiv), EDC−HCl (0.754 g, 3.93 mmol, 1.15 equiv), triethylamine (1.15 mL, 8.21 mmol, 2.4 equiv), and DMAP (0.460 g, 3.76 mmol, 1.1 equiv) were added to the succinate derivative from the previous step (1.49 g, 3.42 mmol, 1.0 equiv) in CH_2Cl_2 (35 mL) at rt. The reaction was stirred at rt overnight, and then an additional 0.5 g of EDC−HCl, 0.25 mL of Et_3N, and 0.25 g of DMAP were added. After being stirred for an additional 14 h, the mixture was transferred to a separatory funnel (dilute with CH_2Cl_2) and washed with water and then brine. The organic layer was dried over Na_2SO_4, filtered, and concentrated to dryness. The crude mixture was purified via

column chromatography on silica gel with EtOAc/hexanes to provide the glycosteroid derivative as a white solid (1.435 g, 62%): ^{1}H NMR (400 MHz, $CDCl_3$) δ 5.85 (1H, d, J = 3.7 Hz), 5.23 (1H, d, J = 2.5 Hz), 4.71− 4.63 (1H, m), 4.61−4.57 (1H, m), 4.49 (1H, d, J = 3.7 Hz), 4.24− 4.18 (2H, m), 4.09−4.06 (1H, m), 4.03−3.99 (1H, m), 2.68−2.56 (4H, m), 2.17−2.08 (1H, m), 2.01 (3H, s), 1.83−1.77 (1H, m), 1.74−1.65 (3H, m), 1.64−1.56 (2H, m), 1.54−1.25 (20H, m), 1.21− 0.93 (5H, m), 0.91−0.84 (1H, m), 0.82 (3H,s), 0.76 (3H,s), 0.68− 0.61 (1H, m); $^{13}C\{^{1}H\}$ NMR (100 MHz, $CDCl_3$) δ 172.0, 171.0, 170.7, 112.2, 109.3, 105.0, 83.3, 83.2, 79.7, 76.4, 73.6, 72.4, 67.2, 54.1, 50.6, 44.6, 42.7, 36.9, 36.7, 35.5, 35.2, 33.9, 31.4, 29.2, 29.1, 28.4, 27.5, 27.4, 26.8, 26.7, 26.2, 25.2, 23.5, 21.4, 20.6, 12.2, 12.1; HRMS (ESI-Orbitrap) m/z $[M + H]^+$ calcd for $C_{37}H_{57}O_{11}^+$ 677.3901, observed 677.3897.

9.5 Experimental Details for Chapter 5.

General 400 nm Fluorination Procedure. Selectfluor (177 mg, 0.50 mmol), benzil (5.0 mg, 0.025 mmol), and the substrate (0.25 mmol) were added to an oven-dried μω vial equipped with a stir bar; the vial was then sealed with a cap with a septum using a crimper and evacuated/refilled with N_2 multiple times. Anhydrous MeCN (4 mL) was added, and the reaction mixture was irradiated with a cool white LED work light while stirring. After 14 h, a 0.3 mL aliquot was taken for ^{19}F NMR yield determination. Then the reaction mixture was diluted with EtOAc, filtered through Celite, and concentrated. The crude reaction mixture was purified via gradient column chromatography on silica gel eluting with EtOAc/hexanes.

General 300 nm Fluorination Procedure. Selectfluor (97 mg, 0.28 mmol) and the substrate (0.13 mmol) were added to an oven-dried μω vial equipped with a stir bar; the vial was then sealed with a cap with a septum using a crimper and evacuated/refilled with N_2 multiple times. Anhydrous CH_3CN (6 mL) was added, and the reaction mixture was irradiated at 300 nm in a Rayonet reactor while stirring. After 4 h, a 0.3 mL aliquot was taken for ^{19}F NMR yield determination, and the rest of the reaction mixture was poured over Et_2O, filtered through Celite, and concentrated. The crude reaction mixture was purified initially via gradient column chromatography on silica gel eluting with EtOAc/hexanes. Analytical purity was obtained via subsequent HPLC purification.

Intermolecular Competition Procedure for $^{13}C/^{12}C$. Selectfluor (153 mg, 0.43 mmol), diphenylethanedione (7.5 mg, 0.036 mmol), and diphenylethanedione-$^{13}C_2$ (7.6 mg, 0.036 mmol) were added to an oven-dried microwave vial equipped with a stir bar. Then, the vial was sealed via crimper with a cap with septum; it was evacuated and refilled with N_2 multiple times. Anhydrous CH_3CN (3 mL) was added via syringe under N_2. The reaction mixture was stirred in front of LEDs overnight. Remaining starting material ratios were determined by mass spectrometry analysis; NMR ratios/yields were carefully determined to be in agreement with mass spectrometry analysis. The reaction was run in triplicate (1.05, 1.06, and 1.06) and averaged 1.06 (see Table S1; calculations for a single experiment).

Electrolysis Procedure. A mixture of Selectfluor (106 mg, 0.30 mmol), 1-chloromethyl-4-aza-1- azoniabicyclo[2.2.2]octane tetrafluoroborate (168 mg, 0.675 mmol), steroid

substrate **4** (104 mg, 0.25 mmol), and tetrabutylammonium hexafluorophosphate (3.14 g, 8.10 mmol) were added to a flame-dried round-bottom flask equipped with a stir bar; the flask was then evacuated/refilled with N_2 multiple times. Anhydrous CH_3CN (81 mL) was added, and the reaction mixture was stirred vigorously before being transferred to the bulk electrolysis glass cell vial. Working electrode (reticulated vitreous carbon - anode), the vial cap equipped with reference electrode (silver wire submersed in 0.01 M $AgNO_3$/0.1M n-Bu_4NPF_6 in anhydrous MeCN) and auxiliary electrode (coiled platinum - cathode) were all inserted into the mixture. The reaction mixture was electrolyzed at a constant potential of 1.8 V for 6 hours. After the reaction, a 2.0 mL aliquot was taken for ^1H NMR yield determination. The rest of the reaction mixture was concentrated in vacuo, diluted with Et_2O, and filtered through Celite. The crude reaction mixture was purified via gradient column chromatography on silica gel eluting with EtOAc/hexanes. A BASi® Bulk Electrolysis Cell Kit was used.

Cyclic Voltammetry General Procedure. The oxidation potential was measured for a 2.5 mM solution of the substrate in 0.1 M electrolyte $TBABF_4$ in MeCN. A conventional three-electrode configuration was used, platinum disk (working electrode), platinum wire (counter electrode), and Ag/$AgNO_3$ reference electrode. The cycling was performed by applying a linear potential scan at a sweep rate of 10 mV s^{-1}, and it was repeated until a reproducible cyclic voltammetry curve was obtained before the measurement curves were recorded. Nitrogen was purged through the solution for several minutes before the tests were performed. Potentials are reported relative to the Ag/Ag+ redox couple (0.00 V) against which the Fc/Fc+ couple was measured to be 0.221 V.

Borane Initiation Procedure. Selectfluor (133 mg, 0.375 mmol) was added to an oven-dried microwave vial equipped with a stir bar under N_2. Then, anhydrous CH_3CN (3.0 mL) was added to the reaction flask, and the solution was stirred vigorously at room temperature. Steroid substrate **1** (78.0 mg, 0.187 mmol) was added followed by a 1.0 M triethylborane solution in hexanes (0.05 mL, 0.034 mmol). The reaction mixture was stirred overnight. After the reaction, an aliquot was taken for ^{19}F NMR yield determination.

Ferrioxalate Actinometry Procedure. A 0.15 M solution of ferrioxalate was prepared by dissolving 2.20 g of potassium ferrioxalate hydrate in 30 mL of 0.05 M H_2SO_4. A buffered solution of phenanthroline was prepared by dissolving 50 mg of phenanthroline and 11.2 g of sodium acetate in 50 mL of 0.5 M H_2SO_4. The two solutions were wrapped in foil and stored until further use. To determine the photon flux of the spectrophotometer, 3.5 mL of the ferrioxalate solution was placed in a cuvette and irradiated for 90.0 seconds at λ = 436 nm with an emission slit width at 10.0 nm. Thereafter, 0.61 mL of the phenanthroline solution was added. The solution was then wrapped in foil and sat for 1 h to allow the ferrous ions to completely coordinate to the phenanthroline. The absorbance of the solution was measured at 510 nm. Also, a non-irradiated sample was prepared and the absorbance at 510 nm was measured. Moles of Fe^{2+} were calculated using Equation 1.

Note: V is the total volume (0.00411 L) of the solution after addition of phenanthroline, ΔA is the difference in absorbance at 510 nm between the irradiated and non-irradiated solutions, l is the path length (1.000 cm), and ε is the molar absorptivity at 510 nm (11,100 L mol^{-1} cm^{-1}). The photon flux can be calculated using Equation 2.

Where Φ is the quantum yield for the ferrioxalate actinometer (1.01 for a 0.15 M solution at λ = 436 nm), t is the time (90.0 s), and f is the fraction of light absorbed at λ = 436 nm (0.998, *vide infra*). The photon flux was calculated to be 9.61 x 10^{-9} einstein s^{-1}.

The absorbance of the above ferrioxalate solution at 436 nm was measured to be 2.72. The fraction of light absorbed (f) by this solution was calculated using Equation 3, where A is the measured absorbance at 436 nm.

Substrate **6** (0.25 mmol, 1 equiv), Selectfluor (0.50 mmol, 2 equiv), and benzil (0.025 mmol, 10 mol%) were added to a dry cuvette. The cuvette was then capped with a PTFE stopper and flushed with nitrogen gas. Then, 4.0 mL of degassed MeCN was added and the sample was stirred and irradiated (λ = 436 nm, slit width= 10.0 nm) for 2400 s. The yield of product formed was determined by ^{19}F NMR based on a 4-bromobenzotrifluoride standard. The quantum yield was determined using Equation 4. The fraction of light absorbed (f) was found to be 0.08 at the aforementioned reaction conditions.

Experiment example: 104 mg (0.25 mmol) substrate **6**, 177 mg (0.50 mmol) Selectfluor, 5 mg (0.025 mmol) benzil, 4.0 mL MeCN after 2400 s yielded 13% of the desired fluorinated product and Φ(13%) = 18.

Competition Experiment: Selectfluor vs. Compound 13-b. In separate oven-dried μω vials equipped with stirs bars, the fluorinating reagent (0.172 mmol), benzil (0.0006 mmol), and substrate **4** (0.030 mmol) were added. The vial was then sealed with a cap with septum using a crimper and evacuated/refilled with N_2 multiple times. Anhydrous MeCN (3 mL) was added, and the reaction mixture was irradiated with a cool white LED work light while

stirring. After an allotted amount of time, a 0.3 mL aliquot was taken for ^{19}F NMR yield determination.

Intermolecular Competition Procedure for 2-Ethyl-cyclohexan-1-one H/D. Selectfluor (133 mg, 0.375 mmol), 2-ethyl-cyclohexan-1-one (164.5 mg, 1.25 mmol), 2-ethyl-D5 cyclohexan-1-one (158.1 mg, 1.25 mmol), and benzil (5.0 mg, 0.025 mmol) were added to an oven-dried microwave vial equipped with a stir bar. Then, the vial was sealed via crimper with a cap with septum; it was evacuated and refilled with N_2 multiple times. Anhydrous CH_3CN (5 mL) was then added and the reaction mixture was stirred in front of LEDs for 48 h. Product ratios ([PH]/[PD]) were determined by ^{19}F NMR analysis of a sample composed of a 0.3 mL aliquot from the reaction flask and 0.2 mL of a dilute solution of 3-chlorobenzotrifluoride (internal standard) dissolved in CD_3CN. The reaction was run in duplicate (3.3 and 3.5); KIE average: 3.4.

Wurster's Blue Experiment. *N*,*N*,*N*',*N*'-Tetramethyl-p-phenylenediamine (50 mg, 0.304 mmol) was added to an oven-dried microwave vial equipped with a stir bar under N_2. Then, anhydrous CH_3CN (2.0 mL) was added to the reaction flask, and the solution was stirred at room temperature. Selectfluor (119 mg, 0.335 mmol) in CH_3CN (2.0 mL) was added dropwise and the reaction mixture immediately turned deep blue. After stirring for 30 minutes an aliquot was taken and analyzed via ^{1}H NMR.

Syntheses

15S-fluoro-7-keto-cholesteryl acetate

Cholesteryl acetate (4.0 g, 9.3 mmol) was dissolved in a mixture of acetone (475 mL) and acetic acid (50 mL) in a round-bottom flask equipped with a stir bar and reflux condenser under N_2. The reaction mixture was treated with *N*-hydroxysuccinimide (10.7 g, 93.0 mmol) and $K_2Cr_2O_7$ (11.0 g, 37.2 mmol), and then the reaction mixture was stirred at 40 °C for 48 h. The reaction mixture was cooled to rt, quenched with 10% aqueous sodium metabisulfite solution, filtered through Celite, and extracted into Et_2O. The combined organic layers were washed with saturated $NaHCO_3$ and brine, and then dried with $MgSO_4$ and concentrated. The crude residue was recrystallized in MeOH to provide 3β-acetoxy-cholest-5-en-7-one (compound **6**) (3.28 g, 80%). The aforementioned product was subjected to general 400 nm fluorination conditions.

White solid. ^{1}H NMR (400 MHz, $CDCl_3$): δ 5.85 (d, *J* = 2.0, 1H), 5.30 (dm, *J* = 53.4 Hz, 1H), 4.80-4.72 (m, 1H), 2.66-2.60 (m, 1H), 2.53-2.46 (m, 1H), 2.33 (t, *J* = 11.0, 1H), 2.22-2.10 (m, 1H), 2.8 (s, 3H), 2.05-1.86 (m ,4H), 1.77-1.60 (m, 4H), 1.56-1.45 (m, 3H), 1.43-1.28 (m, 5H), 1.20-1.05 (m, 7H), 0.95 (d, *J* = 6.5 Hz, 3H), 0.89 (d, *J* = 6.5 Hz, 3H), 0.88 (d, *J* = 6.7 Hz, 3H), 0.74 (s, 3H). $^{13}C\{^1H\}$ NMR (100 MHz, $CDCl_3$): δ 198.5, 170.2, 164.6, 127.4, 94.8, 93.1, 71.8, 58.4, 58.2, 52.6, 50.5, 45.2, 45.1, 43.1, 39.3, 39.1, 38.0, 37.7, 37.7, 37.6, 36.0, 35.6, 34.8, 29.6, 27.9, 27.3, 23.7, 22.7, 22.5, 21.2, 21.2, 18.5, 17.8, 13.0. ^{19}F NMR (282 MHz, $CDCl_3$): δ -160.5 - (-161.0) (m). HRMS (ESI-Ion Trap) m/z: [M + H]+ calcd for 461.3431, found 461.3424.

2-Ethyl-D5-cyclohexan-1-one

A solution of cyclohexanone (7.0 mL, 72 mmol) and pyrrolidine (12 mL, 143 mmol) in benzene (33 mL) was refluxed overnight with azeotropic removal of water. Benzene and

excess pyrrolidine were removed under reduced pressure. To the resultant residual yellow oil were added ethyl bromide (5.9 mL, 79 mmol) and ethanol (9 mL) at room temperature. After heating under reflux overnight, ethanol was removed under reduced pressure, and the resultant was heated under reflux with water (27 mL) for 3 h. After cooling, the mixture was extracted into Et_2O. The combined organic phases were washed with brine, and then dried with anhydrous sodium sulfate, filtered and concentrated. The crude reaction mixture was purified initially via gradient column chromatography on silica gel eluting with EtOAc/hexanes. Analytical purity was obtained via multiple HPLC purifications (10%, 1.0 g).

Colorless oil. ^{1}H NMR (400 MHz, $CDCl_3$): δ 2.40-2.34 (m,1H), 2.31-2.23 (m, 1H), 2.19-2.14 (m, 1H), 2.13-2.06 (m, 1H), 2.04-1.98 (m, 1H), 1.88-1.81 (m,1H), 1.73-1.59 (m, 2H), 1.42-1.32 (m, 1H). $^{13}C\{^{1}H\}$ NMR (100 MHz, $CDCl_3$): δ 213.0, 51.8, 41.7, 33.1, 27.8, 24.6, 21.2 (p, J = 19.5 Hz, 1C), 10.3 (hpt, J = 19.1 Hz, 1C). HRMS (ESI-Ion Trap) m/z: [M + H]+ calcd for 132.1437, found 132.1431.

Diphenylethanedione-$^{13}C_2$

To a flame-dried round-bottom flask equipped with a stir bar was added benzoic acid (0.50 g, 4.1 mol), DMF (1 drop), and DCM (10 mL) under N_2. Ethanedioyl dichloride (0.70 mL, 8.1 mmol) was added dropwise while stirring at 0 ^{o}C. After addition, the reaction mixture was stirred overnight and let gradually warm to rt. The reaction mixture was then concentrated, and the crude (~4.1 mmol) dissolved in THF (2.0 mL). Then, 81.2 mL of freshly made 0.1 M samarium (II) iodide in THF was added to the reaction mixture. The reaction mixture turned yellow after a few minutes. The mixture was purged with air before

adding dilute HCl and diethyl ether. The organic layer was separated, and the aqueous layer was extracted with diethyl ether. All organic layers were washed with water and brine, dried over sodium sulfate and concentrated. Purification by recrystallization with ethanol afforded the title compound as a yellow solid (150 mg, 35% yield).

Yellow solid. ^{1}H NMR (400 MHz, $CDCl_3$): δ 8.00-7.96 (m, 2H), 7.69-7.65 (m, 1H), 7.55-7.50 (m, 2H). $^{13}C\{^{1}H\}$ NMR (100 MHz, $CDCl_3$): δ 194.5, 134.9, 132.9 (t, *J* = 34.2 Hz, 1C), 129.9 (t, *J* = 1.9 Hz, 1C), 129.0 (t, *J* = 2.2 Hz, 1C). HRMS (ESI-Ion Trap) m/z: [M + H]+ calcd for 213.0826, found 213.0819.

*1-(2,4-difluorobenzyl)-4-fluoro-1,4-diazabicyclo[2.2.2]octane-1,4-ditrifluoromethanesulfonate (compound **13-b**)*

DABCO (1.3 g, 12 mmol) dissolved in 20 mL EtOAc, was added to a solution of 2,4-difluorobenzyl bromide (1.6 mL, 13 mmol) in 20 mL EtOAc and stirred for 20 h. The salt was isolated by filtration, thoroughly washed with ether and dried in vacuo. The aforementioned crude bromide salt (3.5 g, 10 mmol) was dissolved in 75 mL MeCN followed by the addition of an equimolar amount of silver tetrafluoroborate and stirred for 4 h. The precipitate of silver halide was removed by filtration. The filtrate was concentrated in vacuo and recrystallized with Et_2O/MeCN to afford a white solid in 81% over 2 steps (3.2 g). A solution of tetrafluoroborate salt (2.9 g, 8.9 mmol) and sodium tetrafluoroborate (0.97 g, 8.9 mmol) in acetonitrile (0.02 M) was prepared in a small PTFE reactor. The mixture was purged with argon and cooled to -40 °C. Elemental F_2 as a homogenous 1:19 (v/v) mixture with N_2 was introduced at a flow rate of approx. 10 mL/min into the rapidly stirred mixture via PTFE tubing at -40 °C (Caution: Poison, corrosive, toxic). The mixture

was purged with argon and warmed to room temperature before filtration to remove sodium fluoride, and the solution was evaporated under reduced pressure. Purification by recrystallization with Et_2O/MeCN afforded the title compound as a white solid (2.9 g, 75 % yield).

White solid. ^1H NMR (400 MHz, $CDCl_3$): δ 7.69-7.63 (m, 1H), 7.26-7.20 (m, 2H), 4.82 (s, 2H), 4.72-4.67 (m, 6H), 4.27-4.23 (m, 6H). $^{13}C\{^1H\}$ NMR (100 MHz, $CDCl_3$): δ 167.8, 167.7, 165.5,165.2, 165.1, 165.0, 162.6,162.5, 137.73,137.69, 137.62,137.58, 114.39,114.35, 114.2, 114.1, 110.52, 110.48, 110.4, 110.3, 106.5, 106.2, 106.0. 19F NMR (282 MHz, $CDCl_3$): δ 48.9 (bs), -104.2 - (-104.3) (m), -108.4 - (-108.5) (m), -150.6 - (-150.7) (m). HRMS (ESI-Ion Trap) m/z: calcd for 258.1332, found 258.1294 (observed without BF_4 counter ions; also, rapid decomposition gave rise to a large peak corresponding to a defluorinated species at 239.1355).

2'-fluoro-[1,1'-biphenyl]-2-carbonyl fluoride (compound 7)

Selectfluor (97 mg, 0.28 mmol) and 9-fluorenone (0.13 mmol) were added to an oven-dried μω vial equipped with a stir bar. The vial was then sealed with a cap with septum using a crimper and evacuated/refilled with N_2 multiple times. Anhydrous CH_3CN (6 mL) was added, and the reaction mixture was irradiated at 400 nm with LEDs overnight while stirring. Upon completion, a 0.3 mL aliquot was taken for ^{19}F NMR yield determination, and the rest of the reaction mixture was poured over Et_2O, filtered through Celite and concentrated. The crude reaction mixture was purified initially via gradient column chromatography on silica gel eluting with EtOAc/hexanes. Analytical purity was obtained via recrystallization with hexanes.

White solid. ^{1}H NMR (400 MHz, $CDCl_3$): δ 8.10 (dd, *J* = 7.9, 1.4 Hz, 1H), 7.73 (td, *J* = 7.6, 1.4 Hz, 1H), 7.55 (tt, *J* = 7.6, 1.0 Hz, 1H), 7.45-7.37 (m, 2H), 7.33 (dm, *J* = 2.0 Hz, 1H), 7.31 (dm, *J* = 2.0 Hz, 1H), 7.29 (dm, *J* = 2.0 Hz, 1H), 7.26-7.22 (m, 1H), 7.16-7.11 (m, 1H). $^{13}C\{^{1}H\}$ NMR (100 MHz, $CDCl_3$): δ 160.72, 160.71, 158.5, 158.28, 158.26, 155.1, 139. 13, 139.09, 134.5, 132.32, 132.30, 132.22, 132.19, 130.5, 130.4, 130.2, 130.1, 128.5, 128.0, 127.8, 125.22, 125.21, 124.64, 124.63, 124.4, 124.3, 115.6, 115.4. ^{19}F NMR (282 MHz, $CDCl_3$): δ 29.8, -115.7 - (-115.8) (m).

*(3S,8R,9S,10R,13S,14S,17S)-10,13-dimethyl-7-oxo-2,3,4,7,8,9,10,11,12,13,14,15,16,17-tetradecahydro-1H-cyclopenta[a]phenanthrene-3,17-diyl-15-d diacetate (compound **17**)*

Dehydroepiandrosterone (3.0 g, 10.4 mmol, 1.0 equiv.) was dissolved in a mixture of DMF (28 mL) and pyridine (12 mL). The mixture was cooled to 0 °C in an ice bath and stirred under N_2, then TMSCl (3.3 mL, 26 mmol, 2.5 equiv.) was added dropwise. The mixture stirred at 0 °C for 10 minutes and then was allowed to warm to room temperature and stir for 2 h. Water (150 mL) was added to quench the reaction, and the resulting mixture was extracted with Et_2O (50 mL x 3). The combined ether extracts were washed with H_2O (150 mL x 2), brine (100 mL) and then were dried over Na_2SO_4. The solvent was removed in vacuo to provide TMS-protected DHEA in quantitative yield, which was used without further purification in the next step.

The TMS-protected DHEA (1.71 g, 4.75 mmol, 1.0 equiv) was dissolved in anhydrous THF (10 mL) and added dropwise to a solution of freshly prepared LDA in 10 mL THF (9.975 mmol, 2.1 equiv.) at -78 °C under N_2. The solution stirred at -78 °C for 35 min to which TMSCl (1.22 mL, 9.5 mmol, 2.0 equiv.) was added dropwise. The reaction stirred

for a few minutes at -78 °C, then slowly warmed up to room temperature and stirred for 1.5 h. The solution was carefully quenched with brine (100 mL) then extracted with EtOAc (50 mL x 3). The combined organic layers were then washed with sat. sodium bicarbonate (50 mL) followed with brine (100 mL). The solvent was dried over Na_2SO_4 and then concentrated to dryness to provide the silyl enol ether of the TMS-protected DHEA in quantitative yield, which was used without further purification in the next step.

The material from the previous step (1.93 g, 4.45 mmol, 1.0 equiv.) was dissolved in anhydrous MeCN (70 mL) and stirred under N_2. $Pd(OAc)_2$ (1.0 g, 4.67 mmol, 1.05 equiv.) was added in one portion and the mixture stirred overnight at room temperature. The mixture was diluted with Et_2O (50 mL) and filtered through a small silica plug, which was then washed with DCM. The combined solvents were concentrated to dryness, in vacuo, to provide the enone in quantitative yield, which was used without further purification in the next step.

The enone from the previous step (1.58 g, 4.4 mmol, 1.0 equiv.) was dissolved in 60 mL of a 7:1 mixture of MeOH:EtOAc in a round-bottom flask. After degassing the mixture with N_2, Pd/C (100 mg, 0.02 equiv.) was carefully added in one portion. Deuterium gas (Cambridge Isotope Laboratories, Inc.) was introduced into the flask via balloon, after briefly placing the mixture under vacuum. The mixture stirred vigorously under D_2 for 1 h, at which time a crude NMR aliquot determined that the D-ring enone had been fully deuterated, while the B-ring olefin remained intact. The mixture was filtered through a short plug of Celite and concentrated to dryness, providing the desired di-deuterated intermediate in quantitative yield, which was used without further purification in the next step.

The di-deutero ketone from the previous step (1.60 g, 4.4 mmol, 1.0 equiv.) was dissolved in 20 mL of 1:1 THF/MeOH and catalytic Na_2CO_3 (17 mg, 0.035 equiv.) was added in 10 mL of DI water. The mixture was stirred vigorously for 24 h at room temperature. After quenching with 2 M HCl (6 mL), the mixture stirred for 30 min then most of the solvent was removed in vacuo. The mixture was extracted with DCM (50 mL x 3), then the combined organic layers were washed with brine and dried over Na_2SO_4. The solution was concentrated to dryness in vacuo, providing the mono-deutero intermediate in quantitative yield, which was used without further purification in the next step.

The material from the previous step (1.27 g, 4.4 mmol, 1.0 equiv.) was dissolved in MeOH (35 mL) and cooled to 0 °C in an ice bath and stirred under N_2. $NaBH_4$ (218 mg, 5.5 mmol, 1.25 equiv.) was carefully added in three portions; the mixture stirred at 0 °C for 30 min and then slowly warmed up to room temperature and stirred for 3 h. The mixture was concentrated to dryness and used crude in the subsequent step to avoid a difficult isolation of the insoluble product via an aqueous workup (quantitative yield).

The diol prepared in the previous step (1.28 g, 4.4 mmol, 1.0 equiv.) was dissolved in pyridine (8 mL) and MeCN (8 mL) and catalytic DMAP (25 mg) was added. The mixture was stirred under N_2 and cooled to 0 °C in an ice bath; Ac_2O (6 mL) was then added dropwise. The mixture slowly warmed up to room temperature and stirred for 1 h then was heated at 100 °C for 12 h. After concentrating down the solvent in vacuo, the mixture was quenched with H_2O (150 mL), and then extracted with Et_2O (50 mL x 3). The combined organic extracts were successively washed with 100–150 mL of H_2O, 1 M HCl, sat. sodium bicarbonate and brine then were dried over Na_2SO_4 and concentrated to dryness —

providing the diacetylated product in quantitative yield, which was used without further purification in the next step.

The material from the previous step (1.65 g, 4.4 mmol, 1.0 equiv.) was dissolved in acetone (75 mL) and stirred in a round-bottom flask under N_2. $K_2Cr_2O_7$ (5.4 g, 17.6 mmol, 4.0 equiv.) and *N*-hydroxysuccinimide (1.6 g, 13.2 mmol, 3.0 equiv.) were added in one portion followed by glacial acetic acid (7.5 mL). The mixture was heated at 55 °C for 24 h. An additional 1.5 g $K_2Cr_2O_7$ and 0.5 g NHS was then added and the mixture was heated overnight at the same temperature. The mixture was cooled to room temperature, diluted with Et_2O and filtered through a small silica plug, which was then washed with DCM. The combined organic solvents were concentrated under vacuo to remove most of the acetone then diluted with H_2O (150 mL). The water layer was extracted with DCM (50 mL x 3), and the combined organic layers were then successively washed with sat. sodium bicarbonate and brine then dried over Na_2SO_4. The solvent was removed in vacuo to provide crude deuterium labeled steroid **19**, which was recrystallized from MeOH to give pure material.

White solid (1.6:1.0 isotopomeric mixture). ^{1}H NMR (400 MHz, $CDCl_3$): δ 5.71 (d, *J* = 1.8 Hz, 1H), 4.75-4.67 (m, 1H), 4.64-4.61 (m, 1H), 2.59-2.54 (m, 1H), 2.50-2.39 (m, 1.7H), 2.27 (t, *J* = 10.9 Hz, 1H), 2.17 (t, *J* = 9.2 Hz, 0.7 H), 2.05 (s, 3H), 2.04 (s, 3H), 2.02-1.94 (m, 2.7H), 1.78-1.73 (m, 1H), 1.70-1.62 (m, 1.7H), 1.58-1.46 (m, 3H), 1.44-1.36 (m, 1H), 1.31-1.24 (m, 1H), 1.23-1.13 (m, 4.6H), 0.82-0.77 (m, 3H); $^{13}C\{^1H\}$ NMR (100 MHz, $CDCl_3$): δ 201.1, 171.1, 170.2, 164.3, 126.5, 81.9, 72.1, 49.8, 49.7, 45.0, 44.9, 44.7, 43.1, 43.0, 38.4, 37.8, 36.0, 35.8, 27.3, 21.2, 21.1, 20.7, 17.3, 12.1, 12.0; ^{2}H NMR (400 MHz,

$CDCl_3$): δ 2.25 (d, *J* = 12.6 Hz, 0.38D), 1.47 (s, 0.62D); HRMS (ESI-FTICR-MS) m/z: [M + Na]+ calcd for 412.2210, found 412.2203.

9.6 Experimental Details for Chapter 6.

General Fluorination Procedure. The substrate (1.0 mmol) was added to an oven-dried round-bottom flask equipped with a stir bar and then dissolved in anhydrous acetonitrile (20 mL). Selectfluor (2.0 mmol, 2.0 equiv) was added, and the reaction mixture stirred at room temperature overnight (12−24 h) and was monitored by ^{19}F NMR. For the ketone products, an additional 1.0 equiv of Selectfluor was added after the fluorination transpired, and the reaction mixture was stirred for 2−4 h. The reaction was quenched with 1 M HCl (50 mL), and the reaction mixture was transferred to a separatory funnel, diluted with H_2O, and extracted into CH_2Cl_2 (3×). The combined organic layers were washed with brine, dried with Na_2SO_4, and concentrated to dryness. The crude reaction mixture was purified via gradient column chromatography on silica gel with EtOAc/hexanes.

Fluorinated Product Characterization Data.

Compound 3

Fluorination was run according to the general procedure, and the product was isolated via gradient column chromatography on silica gel with EtOAc/hexanes: white solid (236 mg, 58%); ^{19}F NMR (282 MHz, $CDCl_3$) δ −203.70 (d, J = 48.2 Hz); ^{1}H NMR (400 MHz, $CDCl_3$) δ 5.73−5.69 (1H, m), 5.51−5.33 (1H, m), 5.30−5.22 (1H, m), 4.65 (1H, t, J = 8.7 Hz), 2.47 (1H, t, J = 11.6 Hz), 2.28−2.18 (2H, m), 2.06 (3H, s), 2.05−2.02 (4H, m), 1.89−1.73 (2H, m), 1.59−1.42 (4H, m), 1.34 (3H, s), 1.28−1.09 (4H, m), 0.94−0.76 (4H,

m); $^{13}C\{^{1}H\}$NMR (100 MHz, $CDCl_3$) δ 202.6 (d, $^{2}J_{C-F}$ = 13.9 Hz), 171.0, 170.5, 143.0 (d, $^{3}J_{C-F}$ = 11.4 Hz), 119.6 (d, $^{2}J_{C-F}$ = 13.9 Hz), 91.6 (C−F, d, $^{1}J_{C-F}$ = 199.9 Hz), 81.7, 69.7 (d, $^{4}J_{C-F}$ = 1.5 Hz), 53.3, 47.2, 43.3 (d, $^{4}J_{C-F}$ = 1.8 Hz), 42.4, 37.7 (d, $^{4}J_{C-F}$ = 2.9 Hz), 35.5, 35.1 (d, $^{4}J_{C-F}$ = 1.1 Hz), 27.5, 24.7, 24.0, 21.2, 21.1, 20.8, 19.0, 12.1; HRMS (ESI-Orbitrap) m/z $[M + H]^+$ calcd for $C_{23}H_{32}O_5F^+$ 407.2235, found 407.2224.

Compound 5

Fluorination was run according to the general procedure, and the product was isolated via gradient column chromatography on silica gel with EtOAc/hexanes: white solid (331 mg, 72%); ^{19}F NMR (282 MHz, $CDCl_3$) δ −203.44 (d, J = 48.8 Hz); ^{1}H NMR (400 MHz, $CDCl_3$) δ 5.71−5.68 (1H, m), 5.49−5.33 (1H, m), 5.30−5.23 (1H, m), 2.41 (1H, t, J = 11.7 Hz), 2.24−2.14 (1H, m), 2.09−2.00 (5H, m), 1.96−1.89 (1H, m), 1.87−1.80 (1H, m), 1.56−1.40 (5H, m), 1.36−1.31 (5H, m), 1.21−1.07 (7H, m), 1.05− 0.89 (6H, m), 0.88−0.85 (7H, m), 0.68 (3H, s); $^{13}C\{^{1}H\}$NMR (100 MHz, $CDCl_3$) δ 203.3 (d, $^{2}J_{C-F}$ = 13.9 Hz), 170.6, 143.5 (d, $^{3}J_{C-F}$ = 11.4 Hz), 119.2 (d, $^{2}J_{C-F}$ = 14.3 Hz), 91.7 (C−F, d, $^{1}J_{C-F}$ = 198.8 Hz), 69.9 (d, $^{4}J_{C-F}$ = 1.1 Hz), 54.9, 53.4, 48.2 (d, $^{4}J_{C-F}$ = 1.5 Hz), 47.5, 42.4, 39.4, 38.3, 37.7 (d, $^{4}J_{C-F}$ = 2.9 Hz), 36.1, 35.6, 35.1 (d, $^{4}J_{C-F}$ = 1.1 Hz), 28.3, 28.0, 24.7, 24.5, 23.7, 22.8, 22.5, 21.3, 21.2, 19.0, 18.7,$_{+}$12.0; HRMS (ESI-Orbitrap) m/z $[M + H]^+$ calcd for $C_{29}H_{46}O_3F$ 461.3432, found 461.3421.

Compound 7

Fluorination was run according to the general procedure, and the product was isolated via gradient column chromatography on silica gel with EtOAc/hexanes: white solid (298 mg, 61%); ^{19}F NMR (282 MHz, $CDCl_3$) δ −203.53 (d, J = 48.8 Hz); ^{1}H NMR (400 MHz, $CDCl_3$) δ 5.73−5.68 (1H, m), 5.52−5.35 (1H, m), 5.29−5.22 (1H, m), 4.54−4.45 (1H, m), 3.50−3.44 (1H, m), 3.37 (1H, t, J = 10.9 Hz), 2.63−2.54 (2H, m), 2.09−2.03 (4H, m), 1.86−1.72 (4H, m), 1.64−1.59 (3H, m), 1.56 (3H, s), 1.51−1.38 (3H, m), 1.35 (3H, s), 1.24−1.11 (4H, m), 0.98 (3H, d, J = 6.9 Hz), 0.81−0.76 (6H, m); ^{13}C{^{1}H}NMR (100 MHz, $CDCl_3$) δ 202.7 (d, $^{2}J_{C-F}$ = 13.9 Hz), 170.6, 143.1 (d, $^{3}J_{C-F}$ = 11.4 Hz), 119.5 (d, $^{2}J_{C-F}$ = 13.9 Hz), 109.3, 91.7 (C−F, d, $^{1}J_{C-F}$ = 199.2 Hz), 80.6, 69.8 (d, $^{4}J_{C-F}$ = 1.1 Hz), 66.8, 61.1, 53.3, 47.8 (d, $^{4}J_{C-F}$ = 1.5 Hz), 46.8, 41.5, 40.2, 38.3, 37.7 (d, $^{4}J_{C-F}$ = 2.9 Hz), 35.1, 31.8, 31.4, 30.3, 28.8, 24.7, 21.2, 21.0, 19.0, 17.1, 16.4, 14.5; HRMS (ESI-Orbitrap) m/z $[M + H]^+$ calcd for $C_{29}H_{42}O_5F^+$ 489.3017, found 489.3008.

Compound 8

Fluorination was run according to the general procedure (quenched with saturated aq. $NaHCO_3$ instead of HCl and using 1.5−2.0 equiv Selectfluor), and the product was isolated via gradient column chromatography on silica gel with EtOAc/hexanes: white solid (478 mg, 76%); ^{19}F NMR (282 MHz, $CDCl_3$) δ −189.28 (d, J = 47.6 Hz); ^{1}H NMR (400 MHz, $CDCl_3$) δ 7.87−7.83 (2H, m), 7.33−7.29 (2H, m), 5.73−5.45 (2H, m), 5.35−5.27 (1H, m), 2.48− 2.39 (4H, m), 2.29−2.19 (2H, m), 2.11−2.00 (6H, m), 1.87−1.74 (2H, m), 1.67−1.48 (5H, m), 1.40−1.24 (6H, m), 1.21 (3H, s), 1.18−1.08 (5H, m), 0.93 (3H, d, J = 6.5 Hz), 0.89−0.86 (6H, m), 0.71 (3H, s); ^{13}C{^{1}H}NMR (100 MHz, $CDCl_3$) δ 170.5, 167.7, 144.8,

142.9 (d, $^{3}J_{C-F}$ = 12.8 Hz), 135.3, 129.4, 128.5, 121.7 (d, $^{2}J_{C-F}$ = 15.8 Hz), 90.7 (C−F, d, $^{1}J_{C-F}$ = 201.0 Hz), 70.0, 55.1, 50.0, 43.8, 42.7, 39.5, 38.3, 37.4 (d, $^{4}J_{C-F}$ = 2.6 Hz), 36.1, 35.6, 35.1, 28.1, 28.0, 24.9, 24.6, 24.3, 23.7, 22.8, 22.5, 21.6, 21.2, 21.0, 19.1, 18.8, 12.0; HRMS (ESI-Orbitrap) m/z $[M + H]^+$ calcd for $C_{36}H_{54}O_4N_2FS^+$ 629.3789, found 629.3806.

Syntheses and Characterization of Starting Materials.

Compound 2

Dehydroepiandrosterone (2.5 g, 8.67 mmol) was dissolved in MeOH (55 mL), and the mixture was cooled to 0 °C in an ice bath. Sodium borohydride (410 mg, 10.84 mmol, 1.25 equiv) was added in three portions. The mixture was stirred at 0 °C for an additional 30 min and then slowly warmed to room temperature, where it continued to stir for 4 h. The reaction was quenched with 1 M HCl (25 mL), and then most of the MeOH was removed in vacuo. The precipitate was filtered, washed with water, and dried overnight under vacuum.

The crude solid was suspended in pyridine (10 mL); cat. DMAP was added (50 mg), then acetic anhydride (7 mL) was added dropwise. The mixture was heated at 95 °C for 24 h with a heating mantle. After cooling to room temperature, the reaction was quenched with water (150 mL), and the resulting precipitate was filtered and washed with water. This solid was then dissolved with DCM (100 mL) and washed in a separatory funnel with 1 M HCl, followed by brine. The solvent was dried over Na_2SO_4 and then concentrated to dryness.

The crude material from the previous step (8.5 mmol) was dissolved in acetone (140 mL). N-Hydroxysuccinimide (2.93 g, 25.5 mmol, 3.0 equiv) was added, followed by $K_2Cr_2O_7$ (10.0 g, 34 mmol, 4.0 equiv) and glacial acetic acid (14 mL). The mixture was stirred at 50 °C for 48 h with a heating mantle and then cooled to room temperature. The mixture was diluted with Et_2O and filtered through Celite (washed with Et_2O). Most of the acetone was removed in vacuo, and the mixture was diluted with more Et_2O and washed with water, then saturated sodium bicarbonate, and finally brine. The organic layer was dried over Na_2SO_4, concentrated to dryness, and then purified via column chromatography on silica gel (EtOAc/ hexanes), providing the diacetoxy enone of DHEA as a white solid (2.1 g, 62% from DHEA).

The product from the previous step (2.1 g, 5.4 mmol) was dissolved in anhydrous THF (60 mL). Tosyl hydrazide (2.51 g, 13.5 mmol, 2.5 equiv) was added, and the mixture was refluxed for 24 h with a heating mantle. After cooling to room temperature, the reaction mixture was diluted with EtOAc and washed with saturated sodium bicarbonate, followed by brine. The organic layer was dried over Na_2SO_4, concentrated to dryness, and purified via column chromatography on silica gel (EtOAc/hexanes), providing the hydrazone of DHEA as a white solid (2.3 g, 78%).

The hydrazone from the previous step (2.3 g, 4.2 mmol) was dissolved in CH_2Cl_2. Et_3N (1.2 mL, 8.4 mmol, 2.0 equiv) and cat. DMAP (0.1 equiv) were added, followed by acetic anhydride dropwise (0.8 mL, 8.4 mmol, 2.0 equiv). The reaction mixture was stirred overnight at room temperature, then was diluted with more DCM and transferred to a separatory funnel. The solution was washed with saturated sodium bicarbonate, followed by brine. The organic layer was then dried over Na_2SO_4 and concentrated to dryness.

Purification via column chromatography on silica gel (EtOAc/ hexanes) provided compound 2 as a white solid (2.1 g, 86%): ^{1}H NMR (400 MHz, $CDCl_3$) δ 7.88−7.84 (2H, m), 7.35−7.31 (2H, m), 6.34 (1H, br. s), 4.76−4.59 (2H, m), 2.67−2.47 (3H, m), 2.44 (3H, s), 2.42−2.33 (1H, m), 2.22−2.11 (1H, m), 2.06 (3H, s), 2.05 (3H, s), 2.04 (3H, s), 2.02−1.91 (2H, m), 1.83−1.75 (1H, m), 1.71−1.40 (8H, m), 1.30−1.23 (1H, m), 1.21 (3H, s), 0.86 (3H, s); $^{13}C\{^{1}H\}$- NMR (100 MHz, $CDCl_3$) δ 180.0, 171.2, 170.1, 169.4, 160.0, 144.9, 135.2, 129.4, 128.7, 116.7, 81.9, 72.3, 48.9, 44.9, 42.7, 40.4, 39.0, 38.2, 36.1, 35.3, 27.3, 27.2, 27.0, 24.4, 21.7, 21.2, 21.1, 20.3, 17.6, 12.2; HRMS (ESI-Orbitrap) m/z [M + H]$^{+}$ calcd for $C_{32}H_{43}O_7N_2S^{+}$ 599.2792, found 599.2782.

Compound 4

Cholesterol (2.5 g, 6.47 mmol) was dissolved in CH_2Cl_2. Et_3N (1.8 mL, 12.94 mmol, 2.0 equiv) and cat. DMAP (0.1 equiv) were added, followed by acetic anhydride dropwise (1.22 mL, 12.94 mmol, 2.0 equiv). The reaction mixture was stirred overnight at room temperature, then diluted with more DCM and transferred to a separatory funnel. The solution was washed with 1 M HCl, then saturated sodium bicarbonate, and finally brine. The organic layer was then dried over Na_2SO_4 and concentrated to dryness.

The crude material from the previous step (6.4 mmol) was dissolved in acetone (105 mL). N-Hydroxysuccinimide (2.21 g, 19.2 mmol, 3.0 equiv) was added, followed by $K_2Cr_2O_7$ (7.53 g, 25.6 mmol, 4.0 equiv) and glacial acetic acid (10.5 mL). The mixture was stirred at 50 °C for 48 h with a heating mantle, then cooled to room temperature. The mixture was diluted with Et_2O and filtered through Celite (washed with Et_2O). Most of

the acetone was removed in vacuo, and the mixture was diluted with more Et_2O and washed with water, then saturated sodium bicarbonate, and finally brine. The organic layer was dried over Na_2SO_4, concentrated to dryness, and purified via column chromatography on silica gel (EtOAc/hexanes), providing the acetoxy enone of cholesterol as a white solid (2.03 g, 71% from cholesterol).

The product from the previous step (2.03 g, 4.59 mmol) was dissolved in anhydrous THF (51 mL). Tosyl hydrazide (2.14 g, 11.475 mmol, 2.5 equiv) was added, and the mixture was refluxed for 24 h with a heating mantle. After cooling to room temperature, the reaction was diluted with EtOAc and washed with saturated sodium bicarbonate, followed by brine. The organic layer was dried over Na_2SO_4, concentrated to dryness, and purified via column chromatography on silica gel (EtOAc/hexanes), providing the hydrazone of DHEA as a white solid (1.91 g, 68%).

The hydrazone from the previous step (1.91 g, 3.12 mmol) was dissolved in CH_2Cl_2. Et_3N (0.87 mL, 6.24 mmol, 2.0 equiv) and cat. DMAP (0.1 equiv) were added, followed by acetic anhydride dropwise (0.6 mL, 6.24 mmol, 2.0 equiv). The reaction mixture stirred overnight at room temperature, then diluted with more DCM and transferred to a separatory funnel. The solution was washed with saturated sodium bicarbonate and brine. The organic layer was dried over Na_2SO_4 and concentrated to dryness. Purification via column chromatography on silica gel (EtOAc/hexanes) provided compound 4 as a white solid (1.67 g, 82%): ^{1}H NMR (400 MHz, $CDCl_3$) δ 7.88−7.85 (2H, m), 7.32−7.29 (2H, m), 6.32 (1H, br. s), 4.74−4.64 (1H, m), 2.59−2.44 (3H, m), 2.41 (3H, s), 2.40−2.33 (1H, m), 2.03 (3H, s), 2.00 (3H, s), 1.99−1.88 (2H, m), 1.86−1.77 (1H, m), 1.70− 1.46 (6H, m), 1.39−1.21 (5H, m), 1.19−1.07 (9H, m), 0.95−0.91 (3H, m), 0.87−0.84 (6H, m), 0.83−0.74 (2H, m),

0.71 (3H, s); $^{13}C\{^{1}H\}$NMR (100 MHz, $CDCl_3$) δ 180.6, 170.0, 169.5, 159.5, 144.7, 135.3, 129.2, 128.7, 116.8, 72.4, 54.6, 50.0, 42.8, 40.7, 39.4, 38.9, 38.1, 38.0, 36.1, 35.5, 28.2, 27.9, 27.3, 27.2, 26.8, 24.3, 23.7, 22.7, 22.5, 21.6, 21.1, 20.7, 18.9, 17.4, 12.0; HRMS (ESI-Orbitrap) m/z $[M + H]^+$ calcd for $C_{38}H_{57}O_5N_2S^+$ 653.3989, found 653.3974.

Compound 6

Diosgenin (2.5 g, 6.03 mmol) was dissolved in CH_2Cl_2. Et_3N (1.7 mL, 12.06 mmol, 2.0 equiv) and cat. DMAP (0.1 equiv) were added, followed by acetic anhydride dropwise (1.14 mL, 12.06 mmol, 2.0 equiv). The reaction mixture was stirred overnight at room temperature, then was diluted with more DCM and transferred to a separatory funnel. The solution was washed with saturated sodium bicarbonate and then brine. The organic layer was then dried over Na_2SO_4 and concentrated to dryness.

The crude material from the previous step (6.0 mmol) was dissolved in EtOAc (50 mL), and 3 Å activated molecular sieves were added (2.0 g). tert-Butyl hydroperoxide in decane (5.48 mL, 5.0 equiv) was added. After stirring for 5−10 min, $Mn(OAc)_3$ was added (186 mg, 0.1 equiv), and the reaction mixture was stirred for 24 h at room temperature. The mixture was filtered through Celite and concentrated to dryness. Purification via column chromatography on silica gel (EtOAc/hexanes) provided the enone as a white solid (2.07 g, 73% from diosgenin).

The product from the previous step (2.07 g, 4.4 mmol) was dissolved in anhydrous THF (50 mL). Tosyl hydrazide (2.05 g, 11.0 mmol, 2.5 equiv) was added, and the mixture was refluxed for 24 h with a heating mantle. After cooling to room temperature, the reaction was diluted with EtOAc and washed with saturated sodium bicarbonate, followed by brine.

The organic layer was dried over Na_2SO_4, concentrated to dryness, and purified via column chromatography on silica gel (EtOAc/hexanes), providing the hydrazone of diosgenin as a white solid (1.80 g, 64%).

The hydrazone from the previous step (1.80 g, 2.82 mmol) was dissolved in CH_2Cl_2. Et_3N (0.79 mL, 5.64 mmol, 2.0 equiv) and cat. DMAP (0.1 equiv) were added, followed by acetic anhydride dropwise (0.53 mL, 5.64 mmol, 2.0 equiv). The reaction mixture was stirred overnight at room temperature, then was diluted with more DCM and transferred to a separatory funnel. The solution was washed with saturated sodium bicarbonate and then brine. The organic layer was dried over Na_2SO_4 and concentrated to dryness. Purification via column chromatography on silica gel (EtOAc/ hexanes) provided compound 6 as a white solid (1.69 g, 88%): ^{1}H NMR (400 MHz, $CDCl_3$) δ 7.88−7.84 (2H, m), 7.35−7.31 (2H, m), 6.32 (1H, br. s), 4.76−4.66 (1H, m), 4.43 (1H, q, J = 7.6 Hz), 3.52− 3.45 (1H, m), 3.38 (1H, t, J = 11.0 Hz), 2.85−2.78 (1H, m), 2.75− 2.64 (1H, m), 2.59−2.53 (1H, m), 2.51−2.46 (1H, m), 2.43 (3H, s), 2.04 (3H, s), 1.99 (3H, s), 1.91−1.86 (1H, m), 1.80−1.55 (11 H, m), 1.52−1.36 (3H, m), 1.31−1.12 (6H, m), 1.00 (3H, d, J = 7.0 Hz), 0.83 (3H, s), 0.79 (3H, d, J = 6.3 Hz); ^{13}C{^{1}H}NMR (100 MHz, $CDCl_3$) δ 180.2, 170.1, 159.6, 144.8, 135.3, 129.4, 128.7, 116.9, 109.2, 80.5, 77.2, 72.4, 66.8, 61.1, 49.7, 48.7, 41.5, 40.8, 40.1, 39.1, 38.2, 38.1, 36.0, 34.7, 31.4, 30.2, 28.8, 27.2, 24.3, 21.7, 21.2, 20.5, 17.5, 17.1, 16.6, 14.7; HRMS (ESI-Orbitrap) m/z $[M + H]^+$ calcd for $C_{38}H_{53}O_7N_2S^+$ 681.3574, found 681.3565.

Compound 9

Steps 1−3 were performed identically to those for the synthesis for compound 4. The hydrazone of cholesterol (0.83 g, 1.36 mmol) was then dissolved in anhydrous THF (20 mL), and to the solution were added K_2CO_3 (0.3 g, 2.17 mmol, 1.6 equiv) and PPh_3 (96 mg, 0.36 mmol, 0.27 equiv). Methyl iodide (0.17 mL, 2.72 mmol, 2.0 equiv) was added dropwise, and the mixture was stirred at room temperature for 36 h. The reaction was quenched with water, transferred to a separatory funnel, and extracted with Et_2O (3×). The combined organic layers were washed with brine, dried over Na_2SO_4, and concentrated to dryness. Purification via column chromatography on silica gel (EtOAc/hexanes) provided compound 9 as a white solid (0.67 g, 79%): ^{1}H NMR (400 MHz, $CDCl_3$) δ 7.76−7.73 (2H, m), 7.32−7.29 (2H, m), 6.61 (1H, d, J = 1.6 Hz), 4.73−4.64 (1H, m), 2.67 (3H, s), 2.59−2.52 (1H, m), 2.50−2.35 (5H, m), 2.32−2.23 (1H, m), 2.05 (3H, s), 2.03−1.87 (3H, m), 1.77−1.68 (1H, m), 1.59−1.49 (3H, m), 1.39−1.25 (6H, m), 1.18−1.04 (10H, m), 0.92 (3H, d, J = 6.6 Hz), 0.89−0.87 (6H, m), 0.86−0.76 (2H, m), 0.68 (3H, s); ^{13}C{^{1}H}NMR (100 MHz, $CDCl_3$) δ 174.7, 170.3, 156.5, 143.7, 131.2, 129.7, 128.9, 117.0, 72.7, 54.7, 50.0, 49.1, 42.8, 40.0, 39.5, 39.4, 38.7, 38.3, 38.0, 36.2, 36.2, 35.6, 28.2, 28.0, 27.4, 26.9, 23.7, 22.8, 22.6, 21.6, 21.3, 20.7, 18.9, 17.5, 12.2; HRMS (ESI- Orbitrap) m/z $[M + H]^+$ calcd for $C_{37}H_{57}O_4N_2S^+$ 625.4040, found 625.4033.

9.7 Experimental Details for Chapter 7.

General Amination Procedure. The arene substrate (1.0 mmol, 1.0 equiv) was added to an oven-dried round-bottom flask equipped with a stir bar and then dissolved in anhydrous acetonitrile (25 mL). The nitrogen heterocycle (2−4 equiv; yields reported with 3.5 equiv unless otherwise stated) was then added, and the solution was stirred at room temperature.

Selectfluor (1.2 mmol, 1.2 equiv) was then added, and the reaction mixture was stirred for 3−6 h. The reaction was monitored by ^{1}H NMR (0.3 mL reaction aliquot + 0.2 mL of CD_3CN). Yields for the aryl-fluoride byproducts were determined by ^{19}F NMR spectroscopy of the crude reaction mixture via the integration of product signals relative to an internal standard. The reaction can be driven further to completion by adding an additional amount of Selectfluor relative to the amount of the unreacted arene substrate and stirring for an additional 2−5 h. After the reaction, most of the solvent was removed in vacuo, and the mixture was diluted with 1 M NaOH. The mixture was extracted with CH_2Cl_2 (×3); the combined organic layers were then washed with 2 M NaOH (to remove the excess nitrogen heterocycle), followed by brine. The organic solution was finally dried over Na_2SO_4 and concentrated to dryness. The residue was purified by gradient flash chromatography on silica gel.

Characterization of Amination Products.

1-(3,4- Dimethoxyphenyl)-1H-benzo[d]imidazole (Compound 1)

The amination was run according to the general procedure using 1,2- dimethoxybenzene as the arene substrate and benzimidazole as the nitrogen heterocycle. The product was isolated via gradient column chromatography on silica gel with EtOAc/hexanes: white solid (173 mg, 68%); ^{1}H NMR (400 MHz, $CDCl_3$): δ 8.07 (1H, s), 7.91−7.85 (1H, m), 7.50−7.45 (1H, m), 7.36−7.30 (2H, m), 7.07−6.99 (3H, m), 3.97 (3H, s), 3.93 (3H, s); $^{13}C\{^{1}H\}$ NMR (100 MHz, $CDCl_3$): δ 149.9, 148.9, 142.6, 129.3, 123.6, 122.6, 120.5,

116.7, 111.7, 110.3, 108.2, 56.2, 56.1; HRMS (ESI-Orbitrap) m/z $[M + H]^+$ calcd for $C_{15}H_{15}N_2O_2^+$ 255.1128, found 255.1125.

1-(3,4-Dimethoxyphenyl)-1H-benzo[d][1,2,3]triazole (Compound 2)

The amination was run according to the general procedure using 1,2-dimethoxybenzene as the arene substrate and benzotriazole as the nitrogen heterocycle. The product was isolated via gradient column chromatography on silica gel with EtOAc/ hexanes: white solid (138 mg, 54%); spectral data match the previously reported characterization.

5-(tert-Butyl)-2-(3,4-dimethoxyphenyl)-2H-tetrazole (Compound 3, Major Isomer)

The amination was run according to the general procedure using 1,2-dimethoxybenzene as the arene substrate and 5-tBu tetrazole as the nitrogen heterocycle. The product was isolated via gradient column chromatography on silica gel with EtOAc/hexanes: white solid (194 mg, 74% for both regioisomers); ^{1}H NMR (400 MHz, $CDCl_3$): δ 7.65−7.58 (2H, m), 6.93 (1H, d, J = 8.6 Hz), 3.96 (3H, s), 3.92 (3H, s), 1.47 (9H, s); $^{13}C\{^1H\}$ NMR (100 MHz, $CDCl_3$): δ 174.3, 149.7, 149.4, 130.6, 112.1, 111.0, 103.6, 56.2, 56.1, 31.6, 29.5; HRMS (ESI-Orbitrap) m/z $[M + H]^+$ calcd for $C_{13}H_{19}N_4O_2^+$ 263.1503, found 263.1502.

1-(3,4-Dimethoxyphenyl)-1H-imidazole (Compound 4)

The amination was run according to the general procedure using 1,2-dimethoxybenzene as the arene substrate and imidazole as the nitrogen heterocycle using the following

modifications: 4.0 equiv of imidazole, 4.0 equiv $NaHCO_3$, and 3.5 equiv of Selectfluor. The product was isolated via gradient column chromatography on silica gel with EtOAc/hexanes: white solid (84 mg, 41%); spectral data match the previously reported characterization.

4,5-Dibromo-1-(3,4-dimethoxyphenyl)-2-methyl-1H-imidazole (Compound 5)

The amination was run according to the general procedure using 1,2-dimethoxybenzene as the arene substrate and 4,5-dibromo-2-methylimidazole as the nitrogen heterocycle. The product was isolated via gradient column chromatography on silica gel with EtOAc/hexanes: white solid (275 mg, 73%); ^{1}H NMR (400 MHz, $CDCl_3$): δ 6.96 (1H, d, J = 8.5 Hz), 6.82−6.77 (1H, m), 6.69 (1H, d, J = 2.4 Hz), 3.95 (3H, s), 3.89 (3H, s), 2.26 (3H, s); $^{13}C\{^1H\}$ NMR (100 MHz, $CDCl_3$): δ 150.0, 149.5, 146.6, 128.4, 120.0, 115.7, 111.0, 110.7, 104.2, 56.2, 56.1, 14.5; HRMS (ESI-Orbitrap) m/z $[M + H]^+$ calcd for $C_{12}H_{13}Br_2N_2O_2^+$ 374.9338, found 374.9338.

2-((1-(3,4-Dimethoxyphenyl)-1H-benzo[d]imidazol-2-yl)-methyl)isoindoline-1,3-dione (Compound 6)

The amination was run according to the general procedure using 1,2-dimethoxybenzene as the arene substrate and 2-methylphthalimidobenzimidazole as the nitrogen heterocycle. The product was isolated via gradient column chromatography on silica gel with EtOAc/hexanes: white solid (322 mg, 78%); ^{1}H NMR (400 MHz, $CDCl_3$): δ 7.85−7.81 (2H, m), 7.76−7.70 (3H, m), 7.28−7.19 (2H, m), 7.13−7.09 (1H, m), 7.06− 7.02 (1H, m),

7.00−6.93 (2H, m), 5.04 (2H, s), 3.93 (3H, s), 3.87 (3H, s); $^{13}C\{^{1}H\}$ NMR (100 MHz, $CDCl_3$): δ 167.5, 149.8, 149.6, 148.6, 137.1, 134.1, 132.1, 127.8, 123.5, 123.2, 122.6, 119.8, 119.7, 111.4, 110.6, 110.1, 56.1, 56.1, 34.9; HRMS (ESI-Orbitrap) m/z $[M + H]^+$ calcd for $C_{24}H_{20}N_3O_4^+$ 414.1448, found 414.1440.

1-(Chloromethyl)-4-(3,4-dimethoxyphenyl)-1,4-diazabicyclo[2.2.2]octane-1,4-diium (Compound 7)

The amination was run according to the general procedure with the following modification: no nitrogen heterocycle was added. The product was precipitated with the addition of 50% EtOAc in hexane, filtered, and washed with more EtOAc/hexane. The product was dissolved in acetone and concentrated to dryness: white hygroscopic solid (448.8 mg, 95%); ^{1}H NMR (400 MHz, $CDCl_3$): δ 7.31−7.26 (2H, m), 7.13−7.09 (1H, m), 5.36 (2H, s), 4.42−4.36 (6H, t, J = 7.3 Hz), 4.16−4.10 (6H, t, J = 7.3 Hz), 3.92 (3H, s), 3.88 (3H, s); HRMS (ESI-Orbitrap) m/z $[M - BF_4]^+$ calcd for $C_{15}H_{23}N_2O_2ClBF_4^+$ 385.1472, found 385.1465. The product was inseparable from the Selectfluor byproducts, namely the DABCO monocation, as it was also a BF_4 salt and had similar properties. The ^{1}H NMR spectrum shows the product along with the Selectfluor-derived amine in a 1.0:1.1 ratio.

1-(3,4-Dimethoxyphenyl)piperazine (Compound 8)

The amination was run according to the procedure for compound 7. The DABCO adduct was reduced to a piperazine using a previously reported procedure. After the amination had completed, a solution of saturated aq $Na_2S_2O_3$ (10.0 mL) was added to the mixture,

followed by H_2O (10.0 mL). The mixture was stirred in the sealed flask or tube at 100 °C for 12−24 h using a heating mantle with sand. Upon cooling to room temperature, the reaction mixture was transferred to a separatory funnel and diluted with DCM (20 mL). Ethylene diamine (2 mL) was added, followed by 6 M NaOH (6 mL), and the mixture was shaken. The resulting emulsion was treated with brine (50 mL), and the organic layer was separated after shaking. The aqueous layer was re-extracted with DCM (2 × 20 mL), then the combined organic layers were extracted with 1 M HCl (2 × 20 mL). Ethylene diamine (6 mL) was added to the combined HCl extracts, followed by 6 M NaOH (10 mL). The basified aqueous mixture was then extracted with DCM (3 × 20 mL), and the combined organic layers were dried with Na_2SO_4, filtered, and concentrated: yellow oil (157.8 mg, 71%); spectral data match the previously reported characterization.

1-(2,5-Dimethoxyphenyl)-1H-benzo[d]imidazole (Compound 9)

The amination was run according to the general procedure using 1,4-dimethoxybenzene as the arene substrate and benzimidazole as the nitrogen heterocycle. The product was isolated via gradient column chromatography on silica gel with EtOAc/hexanes: white solid (142 mg, 56%); ^{1}H NMR (400 MHz, $CDCl_3$): δ 8.09 (1H, s), 7.88−7.85 (1H, m), 7.37−7.29 (3H, m), 7.06 (1H, d, J = 8.9 Hz), 7.02−6.96 (2H, m), 3.82 (3H, s), 3.74 (3H, s); $^{13}C\{^1H\}$ NMR (100 MHz, $CDCl_3$): δ 153.7, 148.0, 143.8, 143.3, 134.2, 125.3, 123.3, 122.4, 120.3, 114.2, 113.6, 113.1, 110.7, 56.3, 55.9; HRMS (ESI- Orbitrap) m/z $[M + H]^+$ calcd for $C_{15}H_{15}N_2O_2^+$ 255.1128, found 255.1129.

1-(3,4,5-Triethoxyphenyl)-1H-benzo[d]imidazole (Compound 10)

The amination was run according to the general procedure using 1,2,3-triethoxybenzene as the arene substrate and benzimidazole as the nitrogen heterocycle. The product was isolated via gradient column chromatography on silica gel with EtOAc/ hexanes: white solid (232 mg, 71%); ^{1}H NMR (400 MHz, $CDCl_3$): δ 8.07 (1H, s), 7.89−7.84 (1H, m), 7.55−7.50 (1H, m), 7.35−7.29 (2H, m), 6.67 (2H, s), 4.16−4.06 (6H, m), 1.46 (6H, t, J = 7.0 Hz), 1.41 (3H, t, J = 7.1 Hz); $^{13}C\{^{1}H\}$ NMR (100 MHz, $CDCl_3$): δ 153.8, 143.9, 142.4, 137.6, 133.9, 131.6, 123.6, 122.7, 120.6, 110.5, 103.1, 69.1, 65.0, 15.6, 14.8; HRMS (ESI-Orbitrap) m/z $[M + H]^+$ calcd for $C_{19}H_{23}N_2O_3^+$ 327.1703, found 327.1703.

N-(5-(1H-Benzo[d]imidazol-1-yl)-2,3-dimethoxybenzyl)-acetamide (Compound 11)

The amination was run according to the general procedure using N-(2,3-dimethoxybenzyl)acetamide as the arene substrate and benzimidazole as the nitrogen heterocycle. The product was isolated via gradient column chromatography on silica gel with EtOAc/hexanes: white solid (195 mg, 60%); ^{1}H NMR (400 MHz, $CDCl_3$): δ 8.02 (1H, s), 7.86−7.81 (1H, m), 7.50−7.46 (1H, m), 7.34−7.28 (2H, m), 7.03 (1H, d, J = 2.5 Hz), 6.95 (1H, d, J = 2.5 Hz), 6.37−6.20 (1H, m), 4.51 (2H, d, J = 6.1 Hz), 3.94 (3H, s), 3.90 (3H, s), 2.00 (3H, s); $^{13}C\{^{1}H\}$ NMR (100 MHz, $CDCl_3$): δ 170.1, 153.4, 146.5, 143.7, 142.1, 133.7, 133.6, 131.9, 123.6, 122.7, 120.3, 116.5, 110.4, 107.8, 60.7, 56.0, 38.5, 23.1; HRMS (ESI- Orbitrap) m/z $[M + H]^+$ calcd for $C_{18}H_{20}N_3O_3^+$ 326.1499, found 326.1499.

1-(6,7,9,10,17,18,20,21-Octahydrodibenzo[b,k]-[1,4,7,10,13,16]hexaoxacyclooctadecin-2-yl)-1H-benzo[d]-imidazole (Compound 12)

The amination was run according to the general procedure using dibenzo-18-crown-6 as the arene substrate and benzimidazole as the nitrogen heterocycle. The product was isolated via gradient column chromatography on silica gel with DCM/ hexanes with 1.5% Et_3N: white solid (305 mg, 64%); ^1H NMR (400 MHz, $CDCl_3$): δ 8.03 (1H, s), 7.88−7.84 (1H, m), 7.47−7.42 (1H, m), 7.34−7.27 (2H, m), 7.02−6.98 (3H, m), 6.91−6.86 (4H, m), 4.26−4.22 (2H, m), 4.21−4.15 (6H, m), 4.08−4.01 (8H, m); $^{13}C\{^1H\}$ NMR (100 MHz, $CDCl_3$): δ 149.6, 148.7, 148.7, 148.6, 143.8, 142.5, 134.1, 129.5, 123.5, 122.5, 121.3, 121.3, 120.4, 117.0, 113.9, 113.6, 113.6, 110.3, 110.1, 70.0, 69.7, 69.6, 69.2, 69.1, 68.7, 68.6; HRMS (ESI-Orbitrap) m/z $[M + H]^+$ calcd for $C_{27}H_{29}N_2O_6^+$ 477.2020, found 477.2018.

Synthesis and Characterization of New Starting Materials.

N-(2,3-Dimethoxybenzyl)acetamide (Starting Material for Compound 11)

2,3-Dimethoxybenzylamine (335 mg, 2.0 mmol, 1.0 equiv) was dissolved in 20 mL of CH_2Cl_2 in a round- bottom flask. Triethylamine (0.56 mL, 4.0 mmol, 2.0 equiv) and cat. DMAP (25 mg, 0.2 mmol, 0.1 equiv) were added. Acetic anhydride (0.2 mL, 2.1 mmol, 1.05 equiv) was added dropwise, and the solution was stirred at room temperature overnight (12 h). The reaction mixture was diluted with more CH_2Cl_2 and transferred to a separatory funnel. The solution was washed successively with aq 1 M HCl, saturated aq $NaHCO_3$, and finally brine. The organic layer was dried over anhydrous Na_2SO_4 and then concentrated to dryness. The product was isolated via gradient column chromatography on

silica gel with EtOAc/hexanes: white solid (390 mg, 93%); ^{1}H NMR (400 MHz, $CDCl_3$): δ 7.02 (1H, t, J = 7.9 Hz), 6.91−6.85 (2H, m), 5.92 (1H, br. s), 4.44 (2H, d, J = 5.7 Hz), 3.87 (3H, s), 3.86 (3H, s), 1.97 (3H, s); $^{13}C\{^{1}H\}$ NMR (100 MHz, $CDCl_3$): δ 169.7, 152.6, 147.2, 131.8, 124.2, 121.4, 111.9, 60.6, 55.7, 39.0, 23.2; HRMS (EI) m/z +· +[M] calcd for CHNO 209.1052, found 209.1078.

Vita

Joseph Capilato was born in Voorhees, New Jersey to Philadelphia natives Patricia and Joseph Capilato in 1992. He grew up in Cherry Hill, NJ and completed his early education at Horace Mann Elementary School and Beck Middle School. After graduating from Cherry Hill East high school in 2010, he studied at Rowan University in Glassboro, NJ—receiving a bachelor's degree in biochemistry in 2014. While at Rowan, Joseph performed research in organic chemistry and medicinal chemistry with Professor Lark Perez., which proved to be a life-changing experience. He continued working in the Perez lab and received a master's degree in pharmaceutical sciences in 2015. Throughout his college years, he worked numerous part-time jobs including as a buser at Cescaphe Ballroom, and a stocker at Roger Wilco's Wine Warehouse. In the summer of 2016, Joseph arrived at Johns Hopkins University and joined the Leckta group later that year. During his doctoral work, he studied organic chemistry with a focus on regioselective fluorination and amination methodologies using Selectfluor. His research led to the publication of at least seven articles in peer-reviewed scientific journals, which have facilitated grant renewal for the lab. Following completion of a PhD in chemistry in the summer of 2021, Joseph will be applying for jobs in the New Jersey-Pennsylvania-Delaware tri-state area.